Annual World
IMA Warsaw
CONFERENCE '08

65th Annual World Magnesium Conference

CONFERENCE PROCEEDINGS

Hilton Warsaw
Hotel & Convention Centre

Warsaw, Poland

May 18–20, 2008

intlmag.org

65th Annual
World Magnesium Conference
PROCEEDINGS

Table of Contents

continued on next page

Status and Potentials of Magnesium Production in China: Life Cycle Analysis Focusing on CO2eq Emissions

Simone I. Ehrenberger, Stephan A. Schmid, Shaobo Song, and Horst E. Friedrich, German Aerospace Center (DLR)

Financial Benefits from SF6 Emission Reductions

Adi Dishon, Eco Traders

Superplastic Forming of Magnesium Alloys

Mathias Liewald, Jens Kappes and Robert Pop, Institute for Metal Forming Technology

Development of the Magnesium Die Cast Motorcycle Chassis

Takaharu Suzuki, Junichi Inami, and Toshikatsu Koike, Yamaha Motor Company

Recycling of Post-Consumer Mg Scrap

Dr. Adam J. Gesing, Gesing Consultants, Inc., Dr. Alain Dubreuil, Natural Resources Canada

Heat Treatment of Magnesium Alloys – Opportunities and Limitations

Frank Czerwinski, Husky Injection Molding Systems Ltd.

China’s Magnesium Industry Development Status in 2007

Mr. Meng Shukun, Mr. Wu Xiuming and Mr. Xu Jinxiang

May 18, 2008

[Abstracts] This article will release the output of primary magnesium, with magnesium alloys and powders/chips/granules included, and the domestic consumption in China in 2007.

Insisting on its own innovative way, the China’s magnesium industry has adopted clean energy resources and high-temperature heat-storage air combustion technology, which help it to save energy up to 40%. A part of smelters in China has increased their competence with the aid of the mode of circular economy.

In China, the flourishing development of deep-processing magnesium products is promoting the whole industry to optimize its structure. In 2007, the domestic consumption in China breaks through 263 kt and China will continue its efforts to expand the magnesium applications. The domestic consumption is set to rise quickly and the exports of primary magnesium & alloys will be reduced further.

Key Words: China’s magnesium industry, heat-storage, circular economy, optimization and upgrades to the industry structure

1. Magnesium Output, Exports, Consumption to Grow Further in China

1.1 Output to Grow Continuously

In 2007, China produces 659.3 kt of primary magnesium, 25.44% higher than last year. The magnesium alloy output reaches 226.2 kt, rising by 7.20% year on year. The output of magnesium powders/granules/chips is 110.8 kt, rising by 11.24% year on year. These data are list in the Table 1 below. China’s primary magnesium output in 2007 is 5.36 times of that in 1998, with annual average growth rate of 20.5%.

Table 1 Primary Magnesium Output in 2007 and Comparisons with 2006

Unit: kt

Product / Year	Primary magnesium output	Magnesium alloy output	Granule magnesium output
2006	525.6	211.0	99.6
2007	659.3	226.2	110.8
Growth rate/y-o-y/%	25.44	7.20	11.24

In 2007, there are totally 15 primary magnesium producers with their individual output above 10 kt, whose accumulative output reaches 403.7 kt, 61.23% of the total in China. In the Table 2, the updated list of Top 10 in China is given, whose accumulative output is 346.3 kt, 18.27% higher than last year and accounting for 52.53% of the total output in China. Scale production has been going forward further.

Table 2 Top 10 Largest Magnesium Smelters and Their Output in China in 2007

Unit: kt

No.	Company	Output
1	Taiyuan Tongxiang Magnesium Co., Ltd.	106.0
2	Taiyuan Yiwei Magnesium Co., Ltd.	53.9
3	Shanxi Wenxi Yinguang Magnesium (Group) Co., Ltd.	47.2
4	Ningxia Huiye Magnesium Co., Ltd.	40.0
5	Shanxi Gold Trust Yiwei Magnesium Co., Ltd.	20.0
6	Ningxia Huayuan Metallurgy Industry Co., Ltd.	19.6
7	Shanxi Wenxi Hongfu Magnesium Co., Ltd.	16.3
8	Shanxi Jinxing Magnesium Co., Ltd. (Former Shanxi Qizhen Magnesium Co., Ltd.)	15.6
9	Shaanxi Yulin Tianlong Magnesium Co., Ltd.	15.3
10	Shanxi Wenxi Bada Magnesium Co., Ltd.	12.4

1.2 More Magnesium Exported but Degree of Dependence on Exports to Continue to Go Down

In 2007, China has totally exported 408 kt of magnesium products, rising by 16.64% year on year. Among them, totally 207.7 kt of pure magnesium ingots are exported, 19.92% higher than last year; Magnesium alloy exports rise by 24.39% year on year to 106.6 kt; Magnesium scrap exports decreases by 42.1% to 1.1 kt; For the exports of magnesium chips, powders and granules, it rises little, by about 0.13% to 79.9 kt; Magnesium alloy profile exports reach 5.5 kt, 19.57% higher than last year; The exports of magnesium and magnesium alloy articles are 7.2 kt in total, representing a 56.52% rise to last year.

In 2007, Chinese magnesium products are exported to more than 70 countries and regions in the world. Europe, North America and Asia are still the top three destinations. For China's pure magnesium exports, Europe, Asia and N.A. absorb 52.05%, 27.97% and 11.08% respectively; For magnesium alloy exports, Europe and Asia take 72.90% and 23.43% respectively; For granule magnesium exports, Europe, N.A. and Asia take 40.47%, 38.88% and 16.88% respectively. U.S.A. only imports 26 kt of granular magnesium from China in 2007.

Figure 1 Exports Destination of China's Magnesium Products in 2007

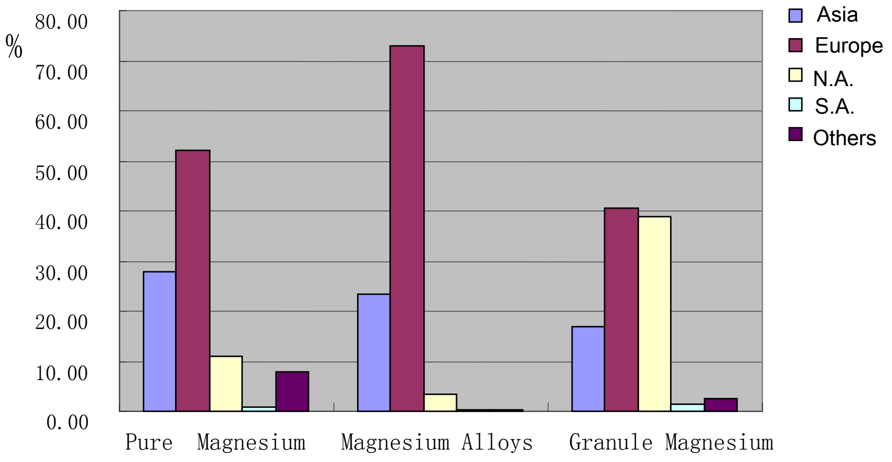

Figure 2 Exports Destination of China's Primary Magnesium in 2007

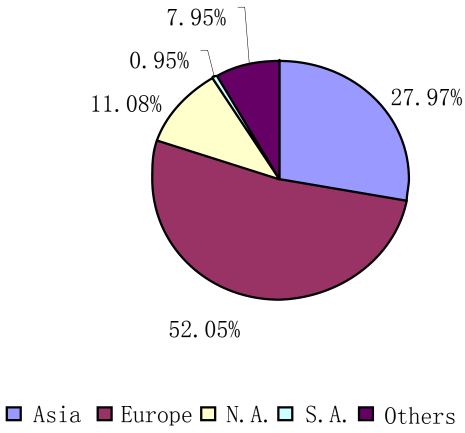

In 2007, the capacity of primary magnesium in the western world is reduced by 60 kt, most of which will turn to rely on supplies from China. In recent years, the world primary magnesium production structure has been characterized by continuous reduction in the western world and gradual increases from China. The trend will continue in the future. Therefore, market demands outside China have to rely on more exports from China. However, when China is exporting its magnesium output in great volume, resources and energy have been wasted with serious pollution left within China. So the Chinese government has now begun to control the exports of resource products with intensive energy consumption and high pollution. As a result, China is reducing its exports of primary magnesium products and increasing its deep-processing products such as magnesium die castings tremendously. Even now, most of the deep-processing products will be used within China and a small part will be exported.

In the Figure 3, you could see that the degree of dependence on exports for the Chin's magnesium products has been descending in the past several years.

Figure 3 Degree of Dependence on Exports for the China's Magnesium Products to Continue to Descend in the Past Several Years

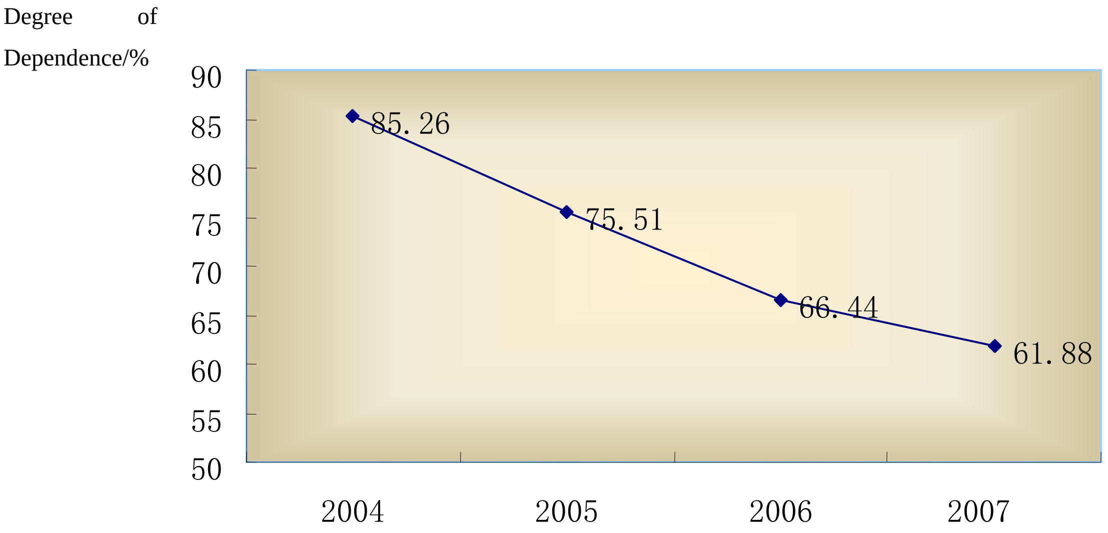

From the above Figure 3, we know that from 2004 through 2007, the degree of dependence has been falling from 85.26% to 61.88%. It is the third consecutive year for the degree of dependence to go down in 2007, 23.28 percentage points lower than in 2004. The decrease shall be attributed to the macro-controls by the Chinese government, including the cancellation of exports rebates and improvement of exports tariffs, and fast rise of domestic consumption.

1.3 Domestic Consumption to Reach 263 kt

Challenged by the continuous deterioration of major nonferrous metals resources, the advantage of magnesium resources and its excellent performance have widely been recognized. Most people are turning their attention to magnesium. In recent years, magnesium alloy accessories made with casting technology, especially die casting process, have widely been used. The basic researches and industrialization of the processes, technologies and equipment for magnesium alloy plates & sheets have made some substantial progress in China. The researches and innovations of applications for them are gestating great breakthroughs. Therefore, in 2007, the domestic consumption of magnesium in China surges to 263 kt, which makes China a big power for magnesium consumption.

The domestic consumption in 2007 is 68.05% higher than in 2006. Aluminum alloy sector consumes 65 kt, 92 kt for magnesium castings, die castings and profiles, 30 kt for steel desulphuration, 13 kt for nodular iron, 40 kt for metal reduction, 10 kt for rare earth magnesium alloys and 13 kt for other industries. Their proportions of the total consumption are respectively 24.71%, 34.98%, 11.41%, 4.94%, 15.21%, 3.80% and 4.94%. The former three sectors are major consumers, accounting for 71.10% of the total. In 2007, the metal reduction sector consumes 40 kt of magnesium, rising by 433%, which is due to the sharp rise of 30 kt in the sponge titanium industry.

Magnesium is now finding more and more uses in China. Besides aerospace, aviation and military sectors, magnesium has been used in China’s automotive industry, trains, motorcycles, bicycles, 3Cs products, manual tools and power tools industry. In automotive industry, magnesium is used for transmission systems, engines, car body and chassis systems. For trains, magnesium is used for braking part valves and magnesium plates have been used in quasi-high speed trains. Some electric bicycles are also adopting more magnesium alloys. The 3Cs products which have used magnesium alloys include shells for digital cameras, cell phones, DVD, optical system brackets for projectors and so on. Now even in building industry, for some small hardware, sports products and PS plates for printing, etc. are also begin to use magnesium and magnesium alloys. The changes of product structure in China have effectively promoted the domestic consumption in the recent years.

2 Insisting on Self-Innovation, the China’s Magnesium Industry Saves Up to 40% of Energy by Adopting Clean Energy and High-temperature Heat-storage Air Combustion Technology. Circular Economy Mode Helps Some Enterprises to Improve Their Competence

2.1 Clean Energy to Be Used to Save 40% Energy Consumption. Competence Improved with Reduced Energy Consumption, Lower Emission and Costs.

Traditionally, solid coal is the major fuel for the silicon thermal process, in which more than 60% of combustion heat is taken away by the waste gas. In the past two years, in order to solve the problem of energy waste and environmental pollution, more than half of smelters have begun to adopt clean coke gas(semi-coke gas or coal gas) after being washed as fuel for the magnesium production. Some smelters are using the heat-storage technology as well as the waste heat recycling technology. The combustion-supporting air is pre-heated to near 1150 , the temperature within the reduction furnace and the waste gas temperature is lowered to be lower than 100 . Heat losses taken away by the waste gas is reduced from the former 60% to only around 5% now. In this way, the heat efficiency of reduction furnaces is increased and energy consumption is reduced by about 40% compared with the traditional way. It is an effective way for the heat-storage reduction furnaces to solve the problem of tense energy supply and high energy consumption in the magnesium smelting industry. Meanwhile, because the clean energy used has been treaded environmentally, harmful gas emission is reduced accordingly. To conclude, the use of clean energy can not only save the energy and reduce emissions, but increase the economy benefits of smelters.

2.2 Circular Economy Mode to Help Some Smelters to Increase Their Competence

Currently, there are totally 7 smelters in China already adopting the circular economy mode. Most of them have their own ferrosilicon plants, coke(semi-coke) plants and power plants together with their magnesium facilities. Even some others have their own coal mines, dolomite mines and retort plants. For these complexes, magnesium production is combined organically with ferrosilicon and coke production. Products or by-products from the former process become the fuel or raw materials for the downstream process, which extends the inner industry chains of these group companies. We concluded three characteristics for such connections. First, the synthetic uses of resources can reduce the energy consumption obviously and costs as a result. Second, the origins of pollutant are controlled to realize clean production. Third, the productivity and resource utilization rate are both improved.

From practices of these 7 complexes, a new way with higher technology contents, better economic benefits, lower resources consumption and environment pollution is made. It is a circular way for the magnesium smelting industry to minimize the waste discharge and increase resource utilization rate by using resources to their utmost from origin of production and in the full process. The circular economy mode will promote the sustainable development of the whole industry.

3. To Optimize the Industry Structure by Vigorously Developing Deep Processing Products

China is not only producing pure magnesium, alloys and powders for the whole world, and now it is paying great attention to the deep processing products. In 2007, nearly 100 kt of magnesium castings, die casting and profiles are consumed domestically and half of the final products are exported. It is a trend in a long run for the whole industry to optimize its structure by developing more deep processing products.

3.1 Some Smelters Adding Deep Processing Product Lines to Change Their Economic Growth Mode

Some magnesium smelters such as Shanxi Wenxi Yinguang Magnesium (Group) Co.,Ltd., Shanxi Guangling Jinghua Magnesium Co., Ltd. And Taiyuan Tongxiang Yuejin Magnesium Co., Ltd., has set up their own magnesium deep-processing lines besides primary magnesium production. To take Shanxi Wenxi Yinguang as an example, it has set up a continuous casting and rolling magnesium alloy plate production line together with North West University. It is a new technology that melt magnesium is cast directly into rollers to make alloy plates, which is world leading and characterized by short flow, low cost, fine grains, high strength and high extensibility. Now the company is offering 0.5-0.6 mm thick magnesium alloy sheets for domestic and overseas customers. Furthermore, the company also has its own die casting and extrusion lines. It is now supplying large size magnesium alloy semi-continuous casting rods for the aerospace, aviation and military industry.

3.2 Magnesium Specialty Enterprise Offering High-end Products

Chalco Luoyang Copper Co., Ltd. is dedicated to the magnesium plate production and now supplying new types of deformed magnesium alloys to Boeing. European auto giant, VW is also seeking partnership with the company to produce deformed magnesium alloy products.

3.3 Universities and Institutes Supporting the Deep Processing Industry Technically

There are 13 research institutes and universities in China to carry out comprehensive research work in the magnesium alloy melting, anti-combustion, molding, surface treatment and recycling. Many fruits have come true from them and laid a solid technical foundation for the magnesium and magnesium alloy development and applications in China. To take Shanghai Jiaotong University as an example, a research center is located on campus and another trail production basis is set up in Jiuting Town of Shanghai. The base is taking the engineering and industrialization work for newly developed magnesium alloys combined with new technologies(in the Table 3 below) in their research center. The base has produced tens of products for civil and military uses with enormous economic benefits made in defense and auto industry. The university has developed three heat-resistance magnesium alloys for auto transmission systems with its own intellectual property rights. They have very good high strength and creep-resistance performance under high temperatures, auto parts made from them could work long under the temperature of 250 . Now the university is working together with a world famous auto maker to make engine blocks for automobiles.

Alloy	Technology	Typical Products
High strength casting alloys	Coat transfer+low pressure sand casting	Aerospace and military products
	Gravity casting	Auto wheels
	Squeeze casting	Engine brackets
High strength deformed alloys	Isothermal forging	Engine blocks
	Squeeze casting	Engine brackets
Heat-resistance alloys	Low pressure sand casting	Engine valve cover
	High pressure casting	Auto transmission cases
	Vacuum casting	Air conditioner compressor head
High temperature alloys	Low pressure sand casting	Helicopter casings
High plasticity alloys	Isothermal rolling	Magnesium alloy plates
	Differential extension	Magnesium alloy stampings
Anti-combustion alloys	High pressure casting	3Cs products
High damp alloys	Sand casting	Magnesium alloy dampings

Data Source: Shanghai Jiaotong University

3.4 More Foreign Capitals Coming in to Push and Affect the Deep Processing Industry in China

Looking at the enormous potential market and abundant raw material supplies in China, many companies from western developed countries come to China to set up magnesium die casting plants in eastern coastal cities such as Shenzhen, Dongguan, Xiamen, Shanghai, Suzhou, Nanjing and Qingdao. They supply magnesium die castings for auto and 3Cs industry in the international market, or send them back to customers in their own countries or sold a small part in China. These companies include world leading ones such as Meridian Technology Inc., George Fisher, Lunt, Laukoetter Dessau, Husky, etc.

Besides, due to good industrial atmosphere within China, some enterprises in Taiwan Province, Japan, N.A. and Europe have moved or are moving their production bases to China to enlarge their capacities.

3.5 Initial Scale Production of Deep Processing Industry Formed, to Push Forward the Optimization of the Industry Structure and Upgrades

Nowadays in China, there are more than 90 die casting specialty plants for transportation and 3Cs sectors, and another 50 more companies involved in the production of deformed alloy products including profiles, plates and other innovative products. Several magnesium industry bases and industry clusters have been formed in China with their own special traits. They are respectively located in Jiaodong Peninsula, Yangtze Delta in the East China, Pearl River Delta in South China, Chongqing, Ningxia and Qinghai in the West China and Heilongjiang in the North China. A comparatively integrated magnesium alloy technology innovation industry chain has been formed preliminarily in China, which occupies whole China and whole industry chain from raw material production, equipment manufacturing, product development and industrialization. The formation of such an integrated chain can greatly promote the optimization and upgrades of the Chinese magnesium industry. One day, China will for sure turn into the world largest high added-value magnesium deep processing base.

INTERNATIONAL MAGNESIUM ASSOCIATION
1000 N. Rand Road, Suite 214
Wauconda, IL 60084 USA
Tel: 847-526-2010; Fax: 847-526-3993
E-mail: info@intlmag.org

65th Annual World Magnesium Conference
PROCEEDING PAPER

Status, Potential & Challenges for Automotive Magnesium Applications from the Point of View of an OEM

Status, Möglichkeiten und Herausforderungen für Magnesium im Automobilbau aus Sicht der Produktion Volkswagen

Hans-Helmut Becker, Volkswagen AG, Werk Kassel

Abstract

The reduction of CO2 emission caused by car traffic is a significant and important aim for all car manufactures. The CO2 emission is directly correlated to the consumption of fossil fuels. Therefore cars must be developed which need less fuel. One way to reduce the fuel consumption consists in reduction of the car weight by the means of lightweight design and the use of light metals. Magnesium alloys with the low density of about 1.8 kg/dm3 offer a high level of weight reduction in comparison with conventional construction materials.

There are several methods to produce magnesium or magnesium composite parts. In addition to the application of extrusion and sheet metal processes die casting is an established method. Some usual parts are gearbox housing, cylinder block or thin-walled and highly integrative vehicle structure components.

This paper discusses the different kinds of production and magnesium products in automotive applications from the Volkswagen point of view starting in history with the beetle till his day. Furthermore a foresight will be given.

1. Introduction - Status

The greenhouse effect is necessary for the human being at earth. In the atmosphere of the earth greenhouse gases as steam, carbon dioxide, methane and ozone have a significant influence to the climate history and todays climate.

Since about two hundred years happens an unbalance in the global climatic cycle influenced among other things by human activities especially the industrialization. The phenomenon of the global warming means an approved fact. Several parameters are important for the global warming. One parameter means the drastic increase of the part of greenhouse gases in the last 100 years (C02 about 35 %, methane about 150 %).

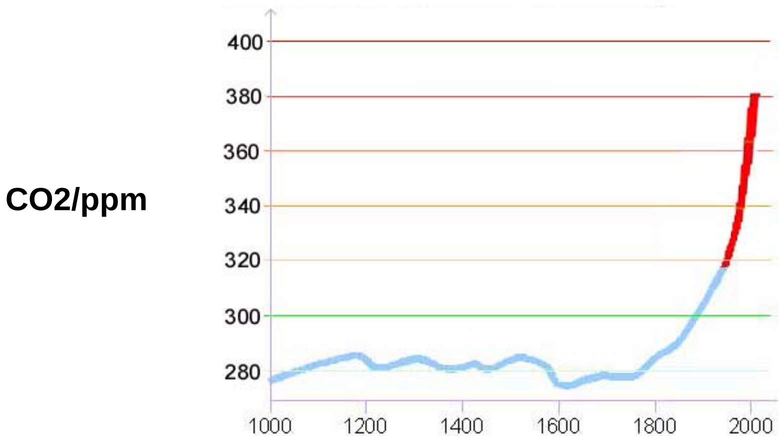

Fig 1.: CO2 increase during the past 1000 years
(red line, measurements Global Atmosphere Watch Mauna Loa, Hawaii)

Figure 1 demonstrates the rapid increase of the part of CO2 in the earth atmosphere. CO2 will be emitted by natural and human (anthropogen) sources. The human part of CO2 emission is about 4 % (Figure 2):

- on top to natural emission
- rapid increase.

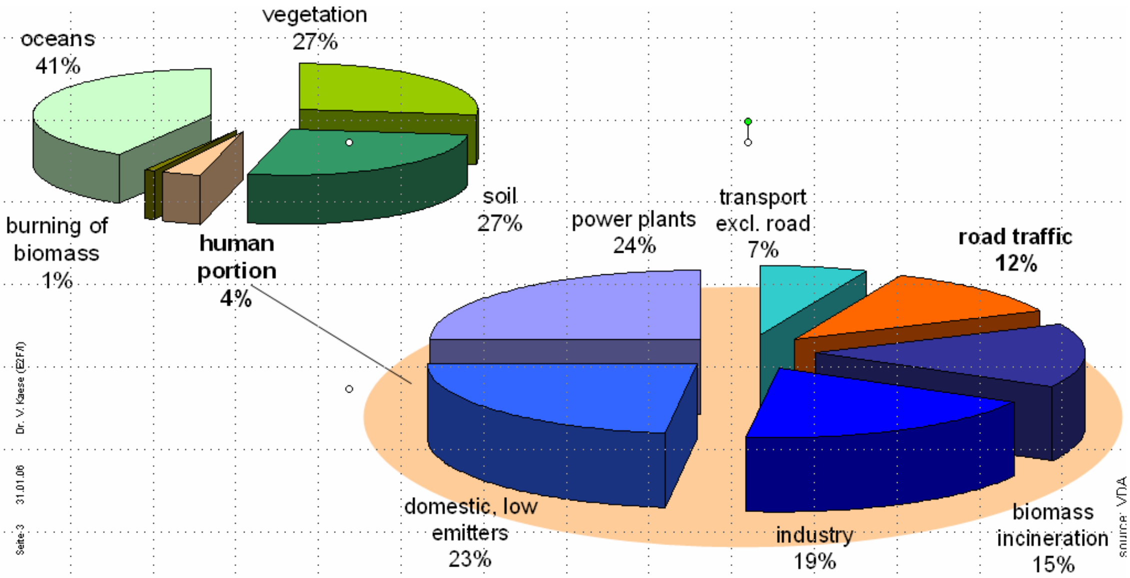

Fig. 2: CO2-Emission – Share of Transportation [1]

Therefore a reduction of human CO2 emission is most urgent. In view of a car manufacturer it is necessary to reduce the fuel consumption of car because less fuel consumption causes less CO2 emission. One liter gasoline burns to about 2400 gram CO2. The following aspects are important for reducing the fuel consumption of a car [2]:

- rolling resistance,
- aerodynamic resistance,
- combustion-, powertrain efficiency,
- vehicle weight.

The vehicle weight can be reduced by using light metals especially Magnesium alloys for several applications as body in white, chassis, gearbox housing, seat and interior components and so on. Figure 3 shows some examples of light metal use and weight reduction in comparison to steel components.

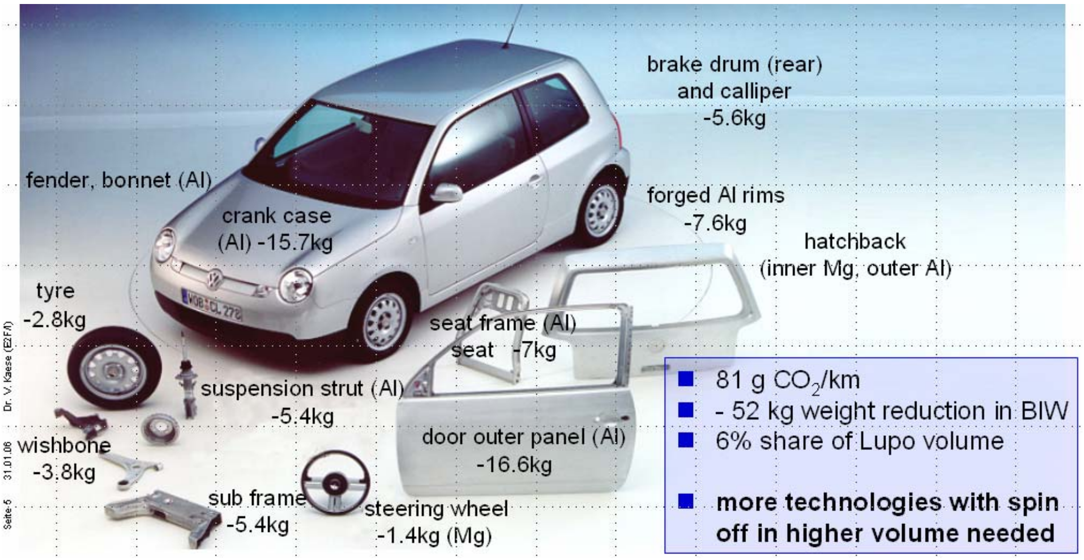

Fig. 3: 3l-Lupo; weight reduction since 2002 [1]

2. Magnesium Overview - Potential

The application of magnesium has a long history at the Volkswagen group. Already the historic beetle has had magnesium gearbox housings and engine components (Fig. 4).

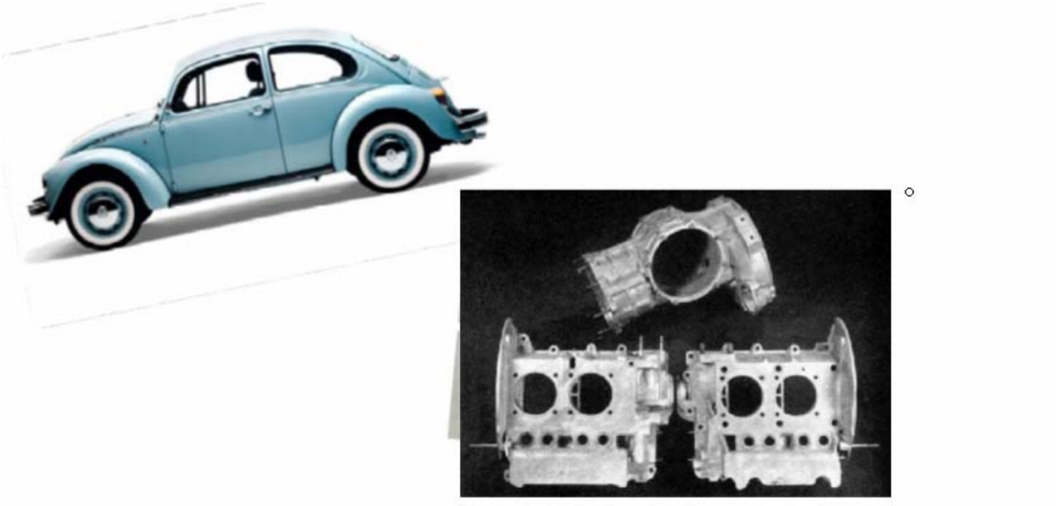

Fig. 4: Historic beetle with gearbox housing and engine components

The use of magnesium in motor vehicles today and in the future depends on numerous technical and economical factors. Obviously the price of magnesium means a vitally factor. On the other hand the reduction of fuel consumption becomes more and more important in aspect to the high fuel prices and the future strict legal regulations with regards to fuel consumption respective CO2 emission. Furthermore it is relevant where one can reduce the car weight. In most cases is an urge, especially on front-wheel drive vehicles, to save weight at the front axle. Weight distribution influences handling and braking behaviour. Lightweight design at the front of the vehicle or in the roof area (lowering the centre of gravity) is therefore especially effective from a vehicle technology point of view. In contrast, weight reductions at the rear only impact on overall weight, i.e. less value is placed on the benefit of these.

Schumann et al. [3] have described already the limiting conditions of the lightweight design with magnesium. The components have to be evaluated with regards to their lightweight design benefit (position of the component in the vehicle) and the cost situation. Third the use of lightweight design depends on the type of vehicle and their unit number and demonstrates a technological leadership.

Up to now the main focus of the current magnesium applications can be seen in the drive train and in the interior. Developments relate to thin-walled integrative structural components.

2.1 Drive Train Applications

Mg-components in drive train have long tradition at Volkswagen. Since 1930 first Mg components for this application have been realized. The use of magnesium decreased rapidly with the end of production of the original beetle. As already described especially on front-wheel drive vehicles one aim consists in saving weight at the front axle.

There was a renaissance of magnesium at VW/Audi with the B80 gearbox housing in 1996. Several magnesium gearbox housings for longitudinal and transverse installation in vehicles have been designed with the aim of weight reduction. The VL 300 was the first CVT gearbox (continuous velocity transmission) with a magnesium housing installed in a series production vehicle. By this way a weight reduction about 8 kg was realized compared to an aluminium version [4].

Figure 5 shows magnesium parts of the MQ 350 gearbox. The gearbox housing and clutch housing are produced at the Volkswagen plant Kassel by die-casting process. The gearbox MQ 350 is installed in several vehicles. Prototypes of magnesium crankcase have been produced by the means of die-casting. The engine block has a modular structure with an aluminium cylinder inserts – Mg-Hybrid cylinder block [5]. Several different Mg alloys have been tested. The successful manufacturing has been proved.

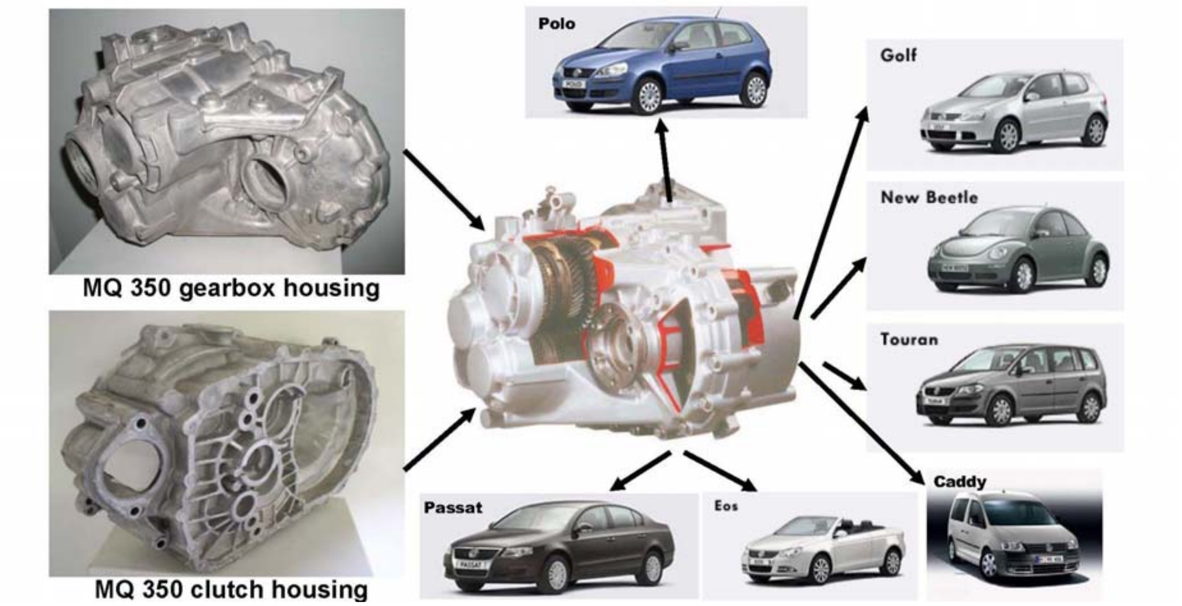

Fig. 5: Products in Magnesium produced at the Volkswagen plant Kassel

2.2 Interior Applications

Magnesium has been discussed as interior material for a long term because of low corrosion attack and a moderate temperature load. There is a competition with the lightweight materials aluminium and plastics. Sometimes the high demands for safety–related components such as steering wheel and seats are difficult to fulfill for magnesium (Fig. 6).

Fig. 6: Steering Wheel (VW/Audi), Seat (Alfa Romeo)

Low demands consists for various trim and small parts. More and more the use of magnesium becomes attractive compared to plastics because of higher temperature stability and his strength. As already described the demands on the components are very different. A special knowledge of material properties and lightweight design is necessary.

2.3 body, structural components

Integrative functional die casting components are of increasing importance particularly for automotive application. Compared to traditional fabrication of light metal chassis the magnesium die casting process is an efficient an economical technology which provides the fabrication of complex parts with closer tolerances. A new type of structural components has been established by means of this manufacturing technique and its rapid advances in the last years. Figure 7 shows magnesium hatchback of the 3l-Lupo. This hatchback was a demonstrator of the feasibility. A series production has not been intended because of weight problems at the front axle and not at the rear axle.

Fig. 7: Hatchback of 3l-Lupo

Another example of structural parts means the instrument panel. Mainly US vehicles are equipped with magnesium instrument panels up to now. Some European car manufacturer do it the same way.

3. Magnesium Challenges

<u>Magnesium Material Properties</u>. The material magnesium itself has to fulfill several requirements e. g.

- crash performance
- producibility
- creep behavior
- corrosion resistance.

Especially new high temperature die-casting magnesium alloys for power train applications have been developed with participation of volkswagen [4]. Improvements of corrosion resistance could be reached by the modern surface technology and the development of material-specific joining techniques for magnesium body structures [6].

Nevertheless the attempts to improve the mechanical and technological properties of magnesium have to be carried on.

Magnesium Recycling. As described pressure die-casting is a suitable process for manufacturing magnesium gearbox housings, hybrid cylinder blocks and complicated structural components. Pressure die-casting belongs to the near-net-shape fabrication methods. The product has nearly the requested geometry after casting. Stamping and some cutting processes of local areas of the product are necessary. Rest material accrues by theses processes mainly the stamping and has to be recycled. Figure 8 demonstrates the weight of the part after casting and after the following stamping and cutting.

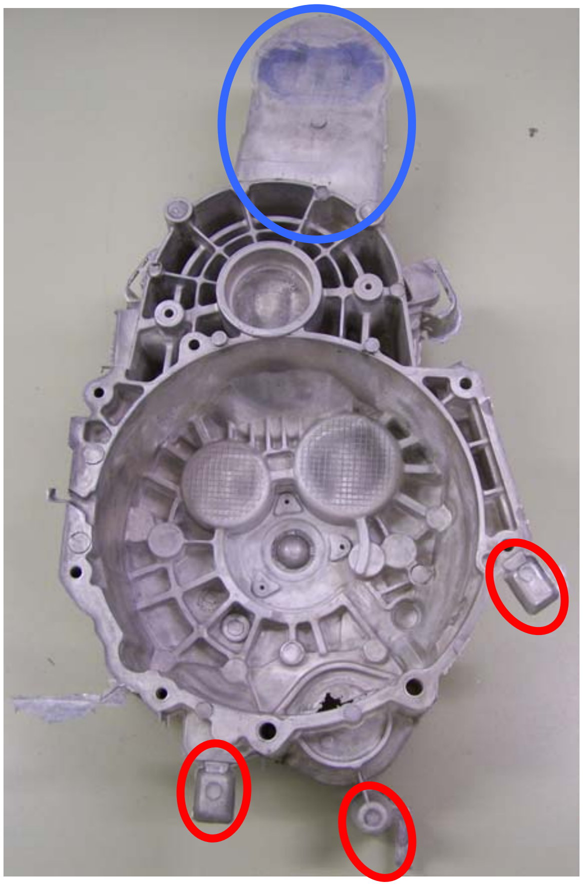

Fig. 8: Clutch Housing MQ 350, weight of the part after casting about 11 kg, after stamping about 7 kg

The gate system has to be recycled. Therefore the Volkswagen plant Kassel built up its own recycling center (Fig. 9). Environmental aspects were taken already into account. That way Volkswagen Kassel generates its own magnesium secondary cycle.

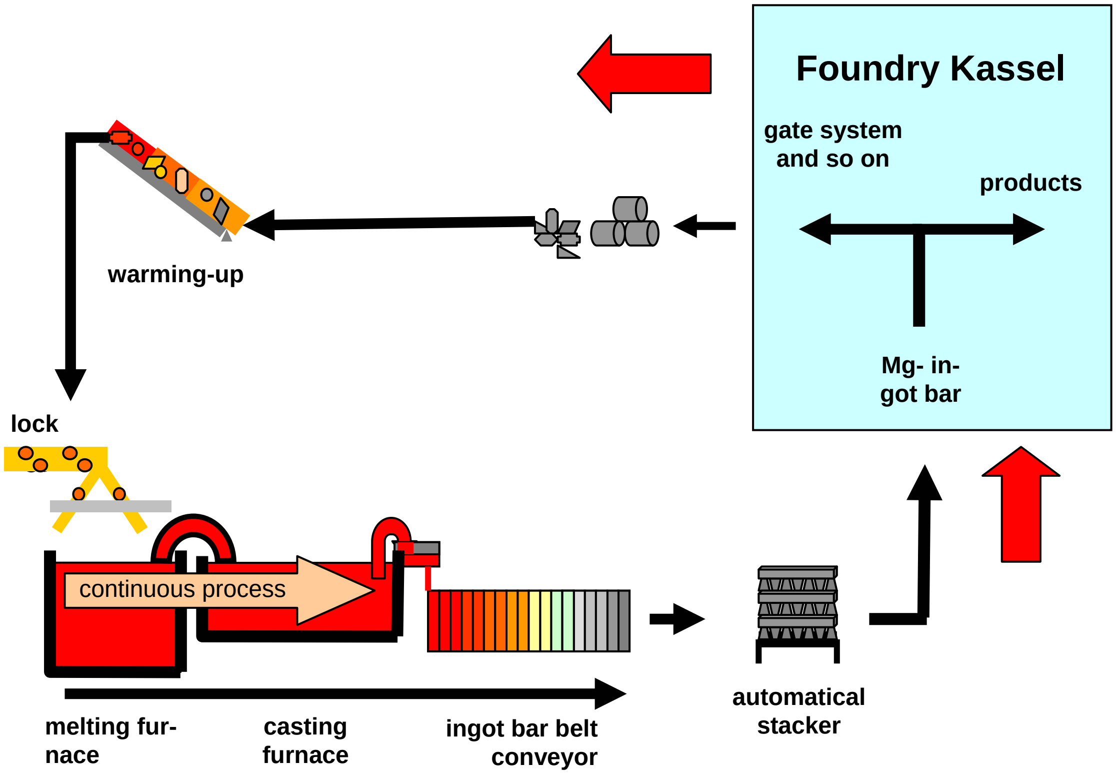

Fig. 9: Magnesium Recycling center at Volkswagen plant Kassel

Magnesium Thixomolding as a new casting process will be established at the Volkswagen plant Kassel. Magnesium molding is the high-speed injection molding of metal alloys in a semi-solid state (solid alloy particles suspended in molten alloy). This process reduces complexity in the manufacturing process, increases productivity and enhances the properties of parts [7]. Magnesium's unique properties, coupled with the benefits of thixomolding technology, opens new possibilities for the production of lightweight metal components:

- lower component costs (e. g. faster cycle times),
- better qualitity (e. g. higher ductility, lower porosity),
- environmentally aspects (e. g. elimination of toxic cover gases, energy efficient).

A magnesium thixomolding machine functions much like a plastics injection molding machine, except chipped metal alloys are used rather than plastic pellets. These chips are melted on demand in a reciprocating screw injection unit, under a blanket of an inert argon gas. The screw meters a precisely controlled ratio of solid and liquid alloy slurry increasing its fluidity and its ease of injection molding [7]. Figure 10 shows a schematic layout of a thixomolding machine.

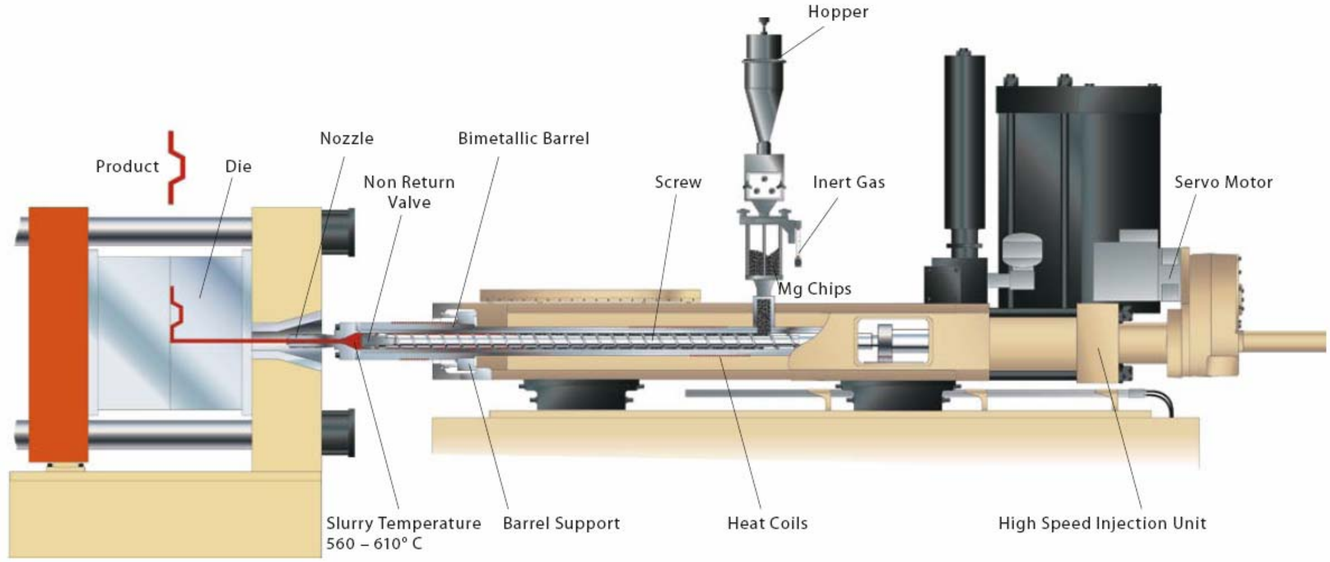

Fig. 10: schematic layout of a thixomolding machine [7]

The thixomolding process is predestinated for thin walled and high precision applications. This molding process is already established in consumer electronic components. Thixomolding in automotive application means a new territory. Therefore it is a challenge to manufacture automotive parts as

- steering wheels,
- seating,
- shifter housings,
- instrument panels,
- roof structures,
- structural chassis components

using the thixomolding process.

4 Conclusions

Magnesium component adoption in automobiles is growing at an annual rate of 12–15% [7]. The main drivers for conversion are cost and weight reduction in order to reduce emissions and improve fuel efficiency. Applications in powertrain, drivetrain, safety systems and seating are taking advantage of the enhanced mechanical properties possible through magnesium molding to mold thinner walls and further reduce weight. The decision to use magnesium or not depends on three factors mainly:

1. CO2 emission and fuel efficiency of motor vehicles
2. cost situation
3. material properties respective the application.

Volkswagen has a long tradition and know how in manufacturing magnesium casting parts. Furthermore Volkswagen feels to be in charge for environmental aspects, sustainability of products and processes.

Literature

[1] Käse, V; Boundary Conditions For High Volume Light Weight Vehicles; Alu-Form Congress, Senlis, France, 2006

[2] Friedrich, H. E.; Herausforderungen der Werkstofftechnik für Fahrzeugkonzepte des Niedrigstverbrauchs; DGM-Tagung, Aachen 2002

[3] Schumann, S; Friedrich, H.; The Route from the Potential of Magnesium to increased Application in Cars, 60th Annual World Magnesium Conference, Stuttgart, 2003

[4] Buch, F.; Schumann, S.; Friedrich, H.; New high Temperature Die-Casting Magnesium Alloys for Power-Train Applications; Sinomag Magnesium Seminar, Beijing, 2002

[5] Böhme, J.; Doerr, J. et al.; Audi Hybrid Magnesium Technology – A new approach to the lightweight engine block; 61st Annual World Magnesium Conference, New Orleans, 2004

[6] Hahn, O.; Schumann, S. et al.; Material-specific joining techniques for Magnesium Body Structures; Int. Conf. on Magnesium, Beijing, 2004

[7] HyMET Systems; HyMET brochure, Husky, Canada, 2006

Accelerated corrosion tests for magnesium alloys: Do they really simulate field conditions?

Martin Jönsson and Dan Persson

ABSTRACT

Magnesium is a very un-noble metal, therefore corrosion properties are an important issue which has to be considered when magnesium alloys are used in corrosive environments. To evaluate and compare magnesium alloys accelerated corrosion tests, such as salt spray tests, is commonly use by the industry to simulate real conditions.

However, the corrosion rates after different types of accelerated corrosion tests often show a wide scatter, and the corrosion behaviour is poorly correlated with the results obtained in the field. In the present study magnesium alloy AZ91D was exposed in three different types of atmospheric environment, viz. urban, rural and marine exposure sites. Corrosion rates, corrosion products formed, and the influence of the microstructure on the corrosion behaviour of the alloy were investigated. The results were compared with the behaviour observed previously in laboratory exposure. The differences between the laboratory and the field are considered and the implications for the design of accelerated corrosion tests of magnesium alloys are discussed.

Keywords: Magnesium alloys, Field exposure, Atmospheric corrosion, Microstructure, Corrosion rate, Corrosion product

INTRODUCTION

Magnesium alloys have the lowest density of the structural metals, and this has made magnesium interesting for the automotive industry and other industries where weight is of importance. But since magnesium is a very un-noble metal, its corrosion properties are an issue which has to be considered, when magnesium alloys are used in corrosive environments. For evaluation and comparison of magnesium alloys accelerated corrosion tests are commonly used in industrial research to simulate real conditions. However, in order to design corrosion tests that mimic the working environment of a magnesium component, a better understanding of the corrosion mechanisms in the field of magnesium alloys is needed. Few studies (1-11) have been dedicated to the atmospheric corrosion of magnesium alloys in the field. Corrosion behaviour in the atmosphere differs considerably from exposure in solution (9, 12).

Godard (1) refers to field studies where two magnesium alloys (AZ80A and ZK61A) together with several other structural metals were exposed at different field sites. The corrosion resistance of AZ80A was at many of these exposure sites superior to that of steel. However, the corrosion rate of both these magnesium alloys was high at industrial sites with severe SO_2 pollution. The authors, in previous papers (13-16), have reported on studies of the corrosion rate, the corrosion products and the influence of the microstructure on the atmospheric corrosion of the magnesium alloys AZ91D and AM50 in a laboratory environment. The corrosion rate (13) was higher for the AM50 alloy compared to that of the AZ91D alloy. The corrosion rate was also strongly influenced by the amount of NaCl applied on the samples and it was accelerated when the relative humidity was increased. The corrosion product formed in the laboratory during the NaCl-induced atmospheric corrosion process resulted in the formation of corrosion products that mainly consisted of magnesium carbonate (14). Hydromagnesite ($Mg_5 (CO_3)_4 (OH)_2 4H_2O$) and Nesquehonite ($MgCO_3 3H_2O$) were the main corrosion products identified. During the initiation of the atmospheric corrosion on AZ91D the α-phase in larger grains was attacked (15, 16). It was shown that the initiation points of the attacks were located at the boundary between the α-phase and the eutectic α-/β-phase. In the work reported on in the present study the magnesium alloys AZ91D and AM50 were exposed at three different field-exposure sites with different types of atmospheric environments: urban, rural and marine. The aim was to investigate the corrosion behaviour of these alloys with particular emphasis on corrosion rate, corrosion product composition and the influence of the microstructure and to compare and validate these results with the authors' earlier findings under laboratory exposure conditions.

EXPERIMENTAL

Materials and Exposure Conditions

Corrosion test panels (130x100x3 mm) of die-cast AZ91D and AM50 were supplied by Hydro Magnesium. The composition of each magnesium alloy is given in Table 1.

Table 1: Nominal composition (weight %) of magnesium alloys AZ91D and AM50

	Al	Zn	Mn	Si	Ni	Cu	Fe	ppm Be	Mg
AZ91D	9	0.79	0.23	0.02	0.0007	0.0027	0.0014	5	remainder
AM50	5	0.013	0.28	0.016	0.0004	0.0016	0,0008	6	remainder

The samples had a geometrical area of approximately 130 cm^2 and were sequentially polished down to 1200 grit. The samples were exposed for 2 weeks, 1 month, 3 months and 12 months, respectively, at three different field stations with different types of atmospheric environment: urban, rural and marine. The urban test site is located in Stockholm on the roof of the Corrosion and Metals Research Institute (KIMAB). The rural field station is located in Ruda, 100 km west of Stockholm, and the marine field station 3-5 meters from the Atlantic shore in Brest, France, at the facilities of Institute de la Corrosion. For each exposure time 3 replicas were used. The panels were mounted on racks with a 45° declination facing south. At the marine field station both AZ91D and AM50 were exposed, whereas at the rural and urban field stations only AZ91D was studied. Climatic data for the field stations are given in Table 2.

Table 2: Summary of climate data from the field exposure stations.

	Atmospheric Data			**Precipitation**		
	Month	Temperature (°C)	Relative humidity (%RH)	Rainfall. mm	pH	Cl^- mg/L
Marine	**Average 2006**	12.5	84	1087	6.1	42.5
Urban	**Average 2006**	8.3	76	547	5.2	2.2
Rural	**Average 1998**	4.8	85	542	4.6	0.3

and more detailed information is presented elsewhere (17). After the corrosion products had been investigated, the mass gain and the mass loss were determined gravimetrically.

For investigation of the corrosion products in the laboratory, the AZ91D samples were contaminated by 70 µg/cm^2 NaCl. When the influence of the microstructure on the corrosion behaviour was investigated in the laboratory, a lower NaCl concentration of 1 µg/cm^2 was used. Both types of samples were exposed in 95% relative humidity (RH) in a closed vessel. To achieve 95% RH, a saturated solution of K_2SO_4 was used (18). For the pickling procedure a solution of 200 g/L chromium trioxide (CrO_3) and 10 g/L silver nitrate ($AgNO_3$) was used.

Methods of Analysis

Corrosion products formed on the magnesium surface were analysed using FTIR spectroscopy. Samples were analysed using both the KBr pellet method and FTIR microspectroscopy. In the KBr pellet method a small mass, typically 1 mg, of reference minerals or corrosion products was mixed with a spectroscopic grade potassium bromide (KBr) powder. The mixture was then grinded in a mortar and pressed to pellets in a die. The FTIR spectrometer used in this study was a model Bio-Rad 175C, equipped with a DTGS detector. Reference spectra were obtained from reference minerals, magnesite ($MgCO_3$), nesquehonite ($MgCO_3$ $3H_2O$) and hydromagnesite (Mg_5 $(CO_3)_4$ $(OH)_2$ $4H_2O$) that were acquired from the Swedish Museum of Natural History. The Confocal microscope used in this experiment was "LEXT OLS3000”, manufactured by Olympus. The light source in this instrument is a blue laser with a wavelength of 408 nm. Element and line analysis was performed using an electron microscopy model JSM6400 (SEM), equipped with an Energy Dispersive Spectrometer (EDS). The acceleration voltage was set at 20 KeV.

RESULTS AND DISCUSSION

Corrosion rates at different field exposure sites

The corrosion rates at the different field exposure sites are displayed in Figure 1.

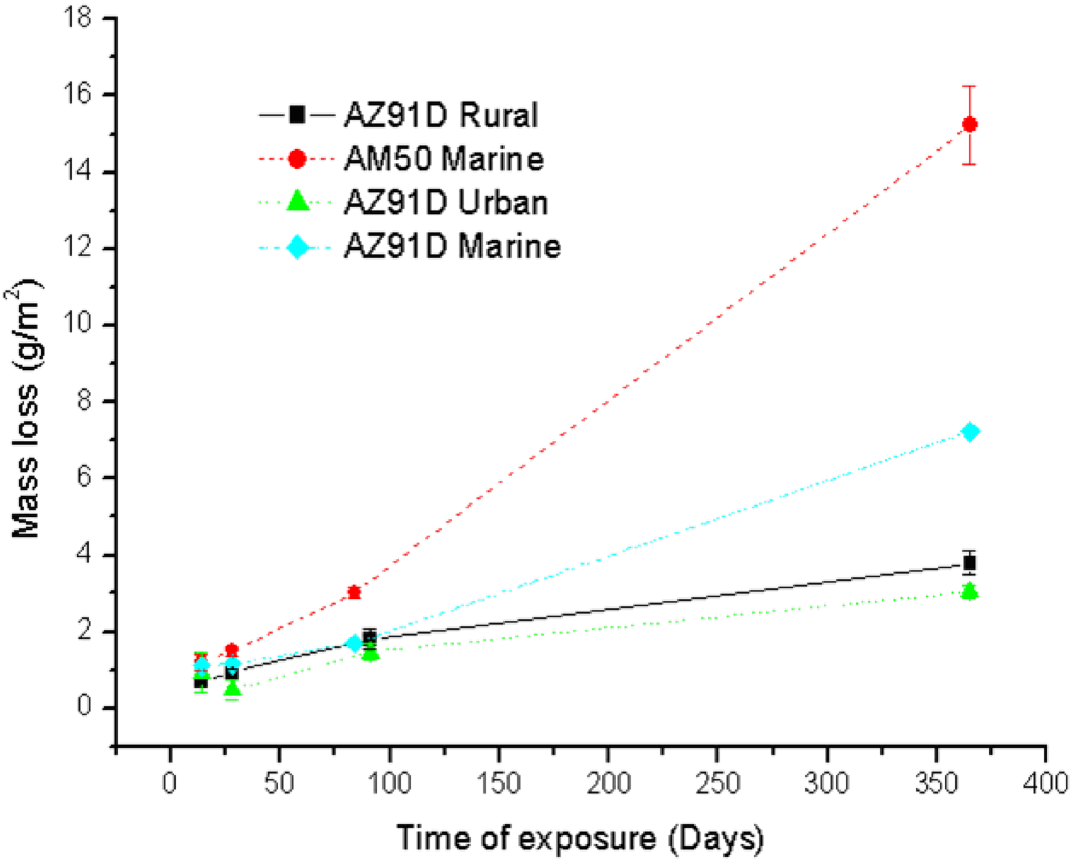

Figure 1: The mass loss given in g/m^2 for magnesium alloys AZ91D and AM50 exposed for 2 weeks, 1 month, 3 months and 12 months at three different field-exposure stations.

The highest corrosion rate was displayed by the marine environment where the AM50 alloy was exposed, which had a corrosion rate of 8.8 µm/year. The corrosion rate of AZ91D, measured in µm/year, was after 12 months exposure 4.2, 2.2 and 1.8 at the marine, rural and urban sites, respectively. In all, the results suggest the formation of corrosion products with poor protective properties under a broad range of exposure conditions. As can be seen, the weight loss of the magnesium alloys is linear with time. This was also observed in the laboratory (14) and has been reported in the literature (1, 11). This indicates that the layer of corrosion products works poorly as a physical barrier against corrosion attacks. Table 3 the corrosion rates AZ91 exposed in different corrosion tests, both field tests and accelerated tests, is compiled. The different test shows a wide scatter. The strong acceleration of the corrosion hints that the corrosion mechanism in the field may be different from that in the accelerated corrosion tests. This difference is discussed further down.

Table 3: Corrosion rates of magnesium alloy AZ91 and AZ61, given in μm/year, of different corrosion tests, both accelerated tests and corrosion rates obtained in the field.

	Rural	Industrial	Marine	Urban	Acc. Tests
This study	2,18		4,15	1,75	
Godard (1)	4,3	15,7	22		
Southwell et al.[a] (7)	12,6		19,2		
Lunder[b] (19)					2307,47
Wei[c] (20)					62,9
Isacsson[d] (21)					49,95
Le Bozec[e] (13)					112,9

[a] Magnesium alloy AZ61X

[b] 3 days exposure in 5%NaCl saturated with $Mg(OH_2)$

[c] 10 days exposure NaCl spray test in accordance with ASTM B117

[d] 6 weeks exposure in climatic chamber with cyclic RH immersion in 1% NaCl 5min twice a week.

[e] 4 weeks exposure 95% RH with 70 μg/cm^2 NaCl

Also included in the table are corrosion rates, found in the literature (1, 7) of field-exposed magnesium alloys. The weight gain was measured before the pickling of the panels. The panels had in many cases a weight below the initial weight, i.e. the corrosion product had been removed by rainfall, wind and sea spray from the waves.

Corrosion products

On all the field-exposed panels with both of the AZ91 and AM50 alloys the corrosion product consisted of magnesium carbonate, hydromagnesite ($Mg_5 (CO_3)_4 (OH)_2 4H_2O$) On some of the panels traces of nesquehonite ($MgCO_3 3H_2O$) could be found.

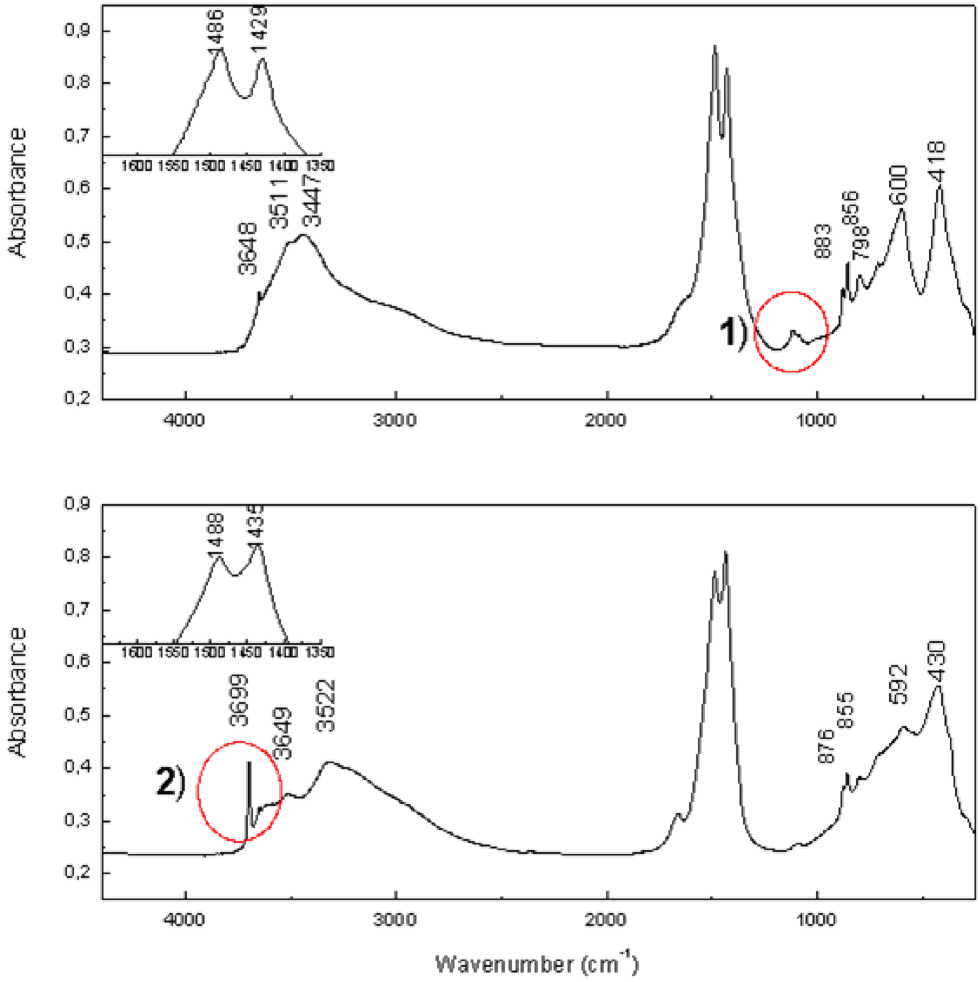

Figure 2A: Infrared adsorption spectra of the corrosion product formed on AZ91D after 12 months exposure at the marine field station. Top left shows a blow-up of the CO_3^{-2} asymmetric stretching peaks.

B: Infrared adsorption spectra of the corrosion product formed on AZ91D after 4 weeks exposure in 95% RH, in the presence of 70 µg/cm^2. Top left shows a blow-up of the CO_3^{-2} asymmetric stretching peaks.

Figure 2A shows the infrared spectra of the corrosion product obtained from an AZ91D panel exposed in the marine field-exposure site for 12 months. In Figure 2B the infrared spectra of the corrosion product obtained after 1 month atmospheric conditions (i.e. 95% RH) in the laboratory can be seen. Comparing the spectra from the field with the one previously obtained in the laboratory, it appears that the main corrosion product is the same, i.e. all the main peaks can be assigned to hydromagnesite (14). However, two differences can be noted between the corrosion product formed in the field and the corrosion product formed in the laboratory:

Firstly: On the field-exposed panels there are minor bands around 1100 cm^{-1}, which are due to sulphate ions, marked with (1) in Figure 2A . In the literature sulphur- containing corrosion products, such as $MgSO_4$ $6H_2O$, have been reported to form on magnesium at urban industrial sites (1) and under laboratory conditions (22, 23). Since only minor bands could be found caused by sulphate under current field conditions, the results suggest that SO_2-induced corrosion did not have any large impact on the exposed panels, probably due to too low SO_2 levels in the atmosphere at the exposure sites.

Secondly. Peaks that originated from brucite ($Mg(OH_2)$) could not be found on any of the field-exposed samples. In the laboratory brucite ($Mg(OH_2)$) could be detected after six days of exposure (14). The brucite peaks are marked with (2) in Figure 2B. A closer investigation (14) of the corrosion product formed in the laboratory showed that brucite had developed in the pits under a lid of hydromagnesite that hindered the transport of species such as CO_2 and O_2 through the corrosion product crust. The low CO_2 content in the pits beneath the hydromagnesite layer explains why brucite was not transformed into magnesite during the laboratory exposure. The formation of brucite indicates that the pH was higher in the pits than on the surface. Since aluminium is passive in neutral solutions but active in alkaline solutions (19, 24), the higher pH in the pits was unfavourable for the corrosion resistance of aluminium-containing phases. In contrast, in the field the corrosion products consisted exclusively of magnesium carbonates indicating that CO_2 penetrates more easily through the whole layer of corrosion products.

With the exception of the two differences mentioned above there are considerable similarities between the corrosion products formed on magnesium samples in the laboratory and those formed in the field. This indicates that the sequence found in the laboratory (14), according to which $Mg(OH)_2$ will react with CO_2 in the surrounding air to form magnesite ($MgCO_3$) and magnesite together with water will form hydromagnesite or nesquehonite, also applies to the field-exposed samples.

In addition Figure 3 shows the infrared adsorption spectra of the corrosion products formed after 24h immersion in 5% NaCl. Comparing Figure 2 and Figure 3 clear differences can be seen between the corrosion products formed in the field and the ones formed in solution. In solution the corrosion products mainly consists of brucite $Mg(OH_2)$ and MgO. Bands that originates from carbonates (1443 cm^{-1}) are considerable smaller than is the case for field exposed samples. The formation of brucite indicates that the pH was high in solution and that the access of CO_2 is limited.

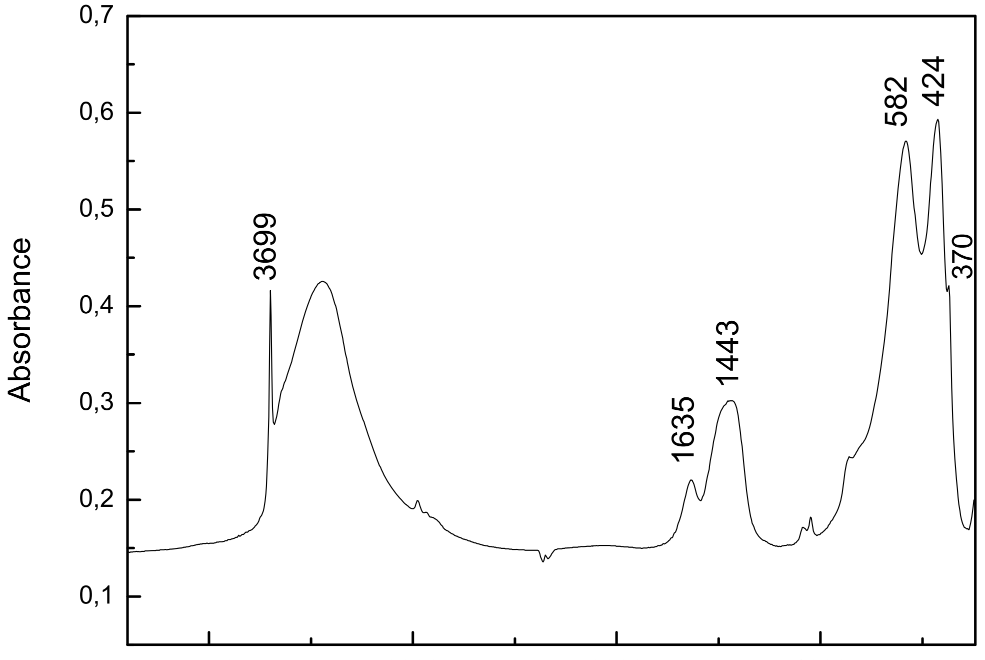

Figure 3: Infrared adsorption spectra of the corrosion product formed on AZ91D formed after 24h immersion in 5% NaCl solution.

Influence of the microstructure on the corrosion behaviour

It has earlier been shown in the laboratory that the microstructure is of vital importance for the atmospheric corrosion behaviour of magnesium alloys (15, 16, 25). The microstructure of unexposed AZ91D can be seen in the SEM image in Figure 4B.

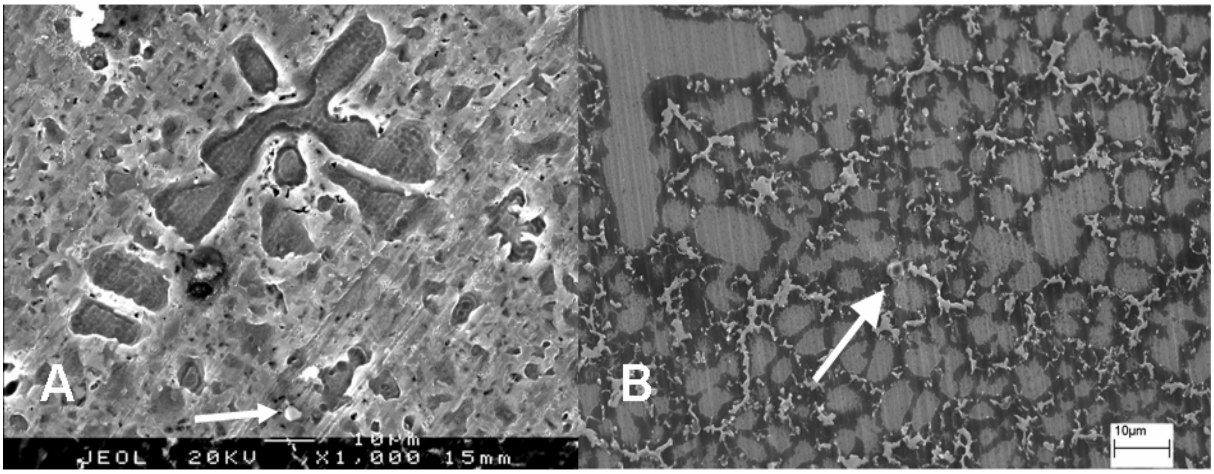

Figure 4A: SEM image of the corroded AZ91D surface exposed for 3 months in the marine environment. Marked with the arrow is an intermetallic Al-Mn particle with the composition Al 47.1%, Mn 51.2%, and Fe 1.8%.

B: SEM image of an unexposed AZ91D surface. Marked with the arrow is an intermetallic Al-Mn particle with the composition Al 56.3%, Mn 39.5% and Fe 1.2%. The β-phase ($Mg_{17}Al_{12}$) can be seen as white areas and the eutectic α-/β phase as dark grey areas at the grain boundaries.

The AZ91D has a microstructure typically consisting of a matrix of primary α-phase grains with an aluminium content of around 6 wt%. At the grain boundaries the β-phase ($Mg_{17}Al_{12}$) can be found (seen as white areas in Figure 4B). The composition of the β-phase has previously been reported to have approximately 71 at% Mg and 27 at% Al (15). In between these two phases is a zone consisting of a eutectic mixture of the α-phase and the β-phase (seen as dark grey areas in Figure 4B). The aluminium content of the eutectic phase varies between that of the β-phase (~27%) and that of the α-phase (~6%). The width and the variation of the aluminium content of the eutectic zone are dependent on the solidification rate. The AZ91D alloy also contains intermetallic Al-Mn phases. These Al-Mn intermetallics are often of the type Al_8Mn_5. The nobility of the different phases has earlier (15) been shown to decrease in the following order in atmospheric environments: Al_8Mn_5 > β-$Mg_{17}Al_{12}$ > α-Mg.

Influence of Mg-Al phases on the corrosion behaviour

For investigation of the influence of the microconstituents on the corrosion performance of AZ91D both SEM and confocal microscopy have been utilised. Figure 4A shows a SEM image of an AZ91D sample that was exposed in the marine environment for 3 months. In order to compare a field and a laboratory exposed sample, the AZ91D sample in Figure 4B was exposed in 95% relative humidity in the laboratory for four days in the presence of 1 µg/cm^2 NaCl. After the exposure the corrosion products were removed through pickling. The areas observed in Figure 4A and 3B were then identified and analysed using confocal microscopy. These images can be seen in Figure 5A (field) and 4B (lab).

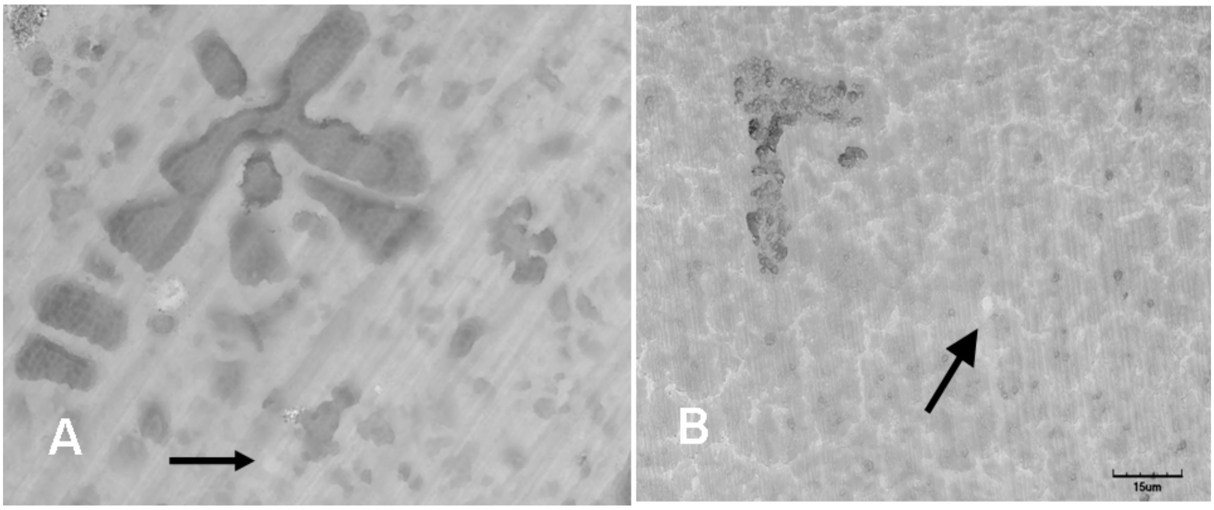

Figure 5A: Confocal image of the same area as seen in Figure 4A. Marked with the arrow is the Al-Mn particle.

B: Confocal image of the same area as seen in Figure 4B after 4 days exposure in 95% RH, in the presence of 1 µg/cm^2 NaCl. Marked with the arrow is the Al-Mn particle.

As can be inferred form Figure 5A and 4B, both in the field-exposed sample and the laboratory-exposed sample, the most severe corrosion attacks can be found in large α-phase grains. In order to further investigate the role of the magnesium-aluminium phases, i.e. β-phase, eutectic α-/β-phase and α-phase, in the corrosion process, the aluminium content of the microstructure was examined using SEM-EDS. Figure 6 is a line scan of the surface showing the depth profile, measured with confocal microscopy, as well as the aluminium content along the same line, measured with EDS in the SEM.

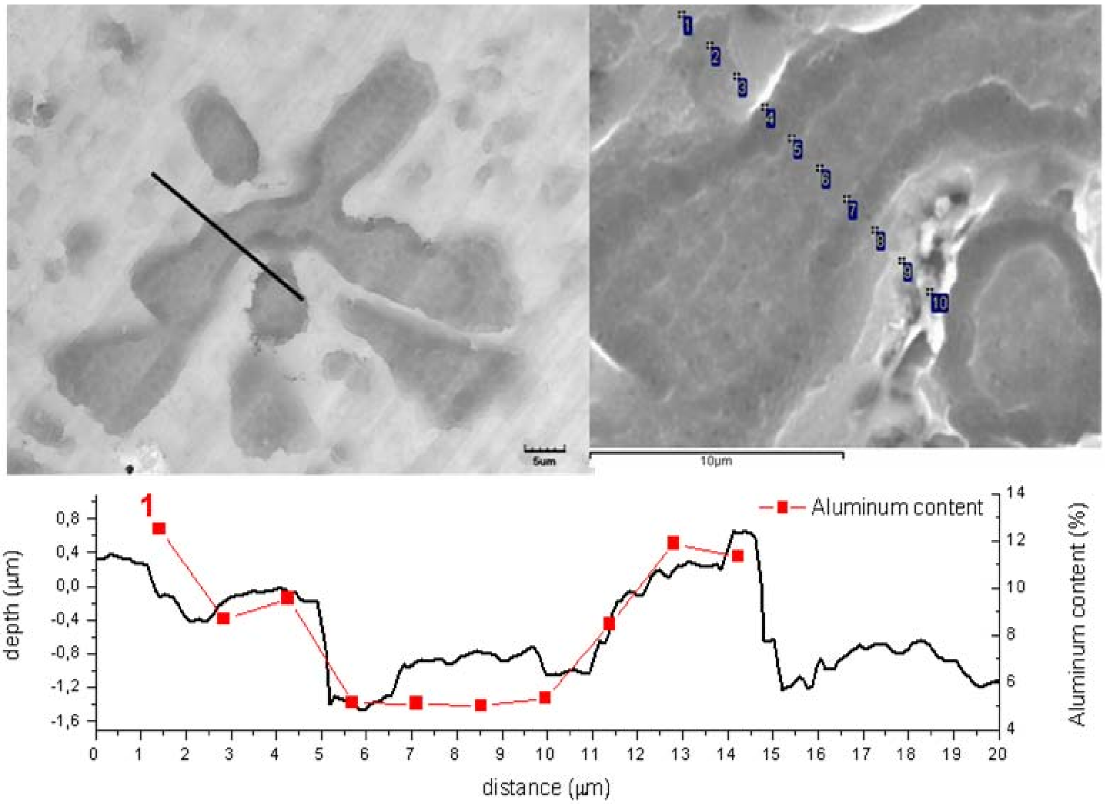

Figure 6: Surface profile and aluminium content of part of the AZ91D surface exposed for 3 months in the marine environment shown in Figure 4A and Figure 5A

In addition, a sample was exposed for 6 days in 95% RH in the presence of 1 µg/cm^2 NaCl in the laboratory (Figure 7).

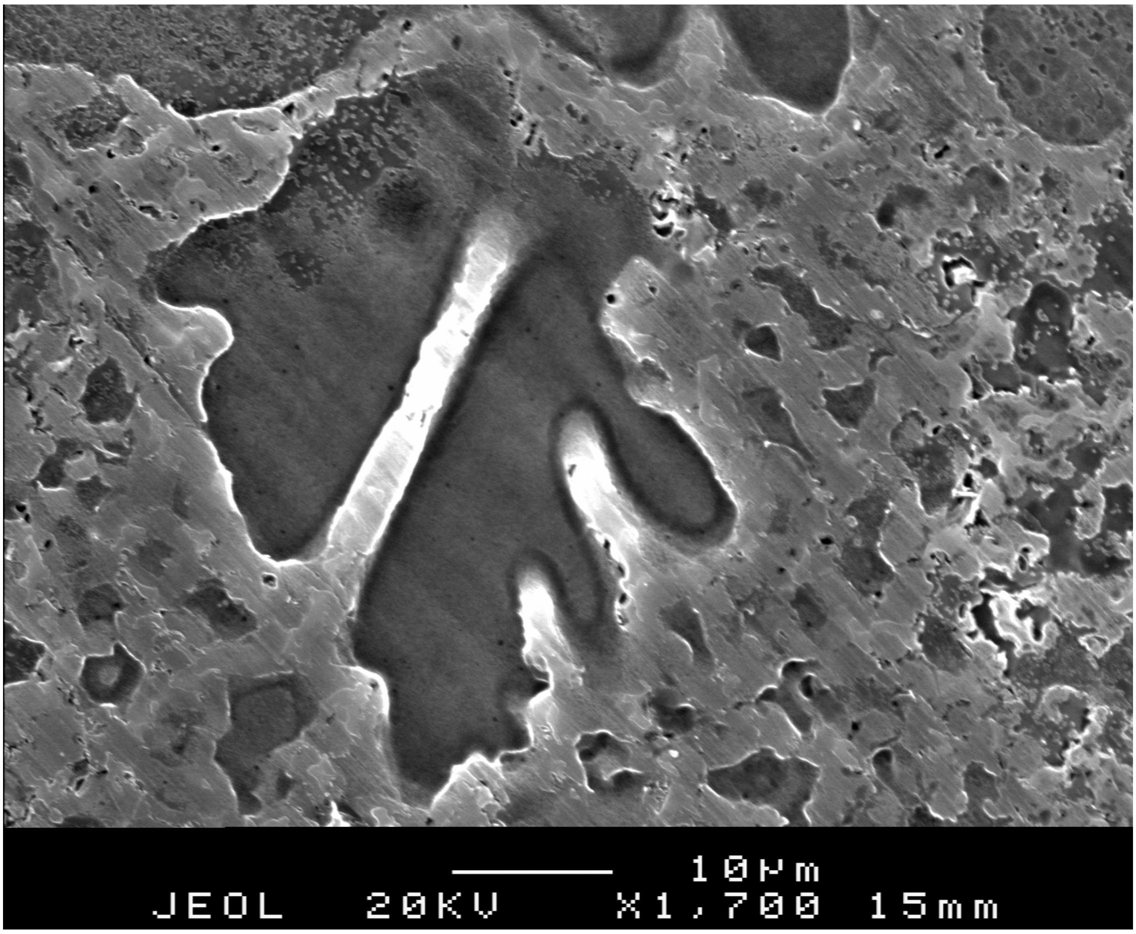

Figure 7: SEM image of the corroded AZ91D surface after 6 days exposure in 95% RH, in the presence of 1 µg/cm^2 NaCl.

The same line scan, using both SEM-EDS and confocal microscopy, was performed on the laboratory-exposed AZ91D sample (Figure 8).

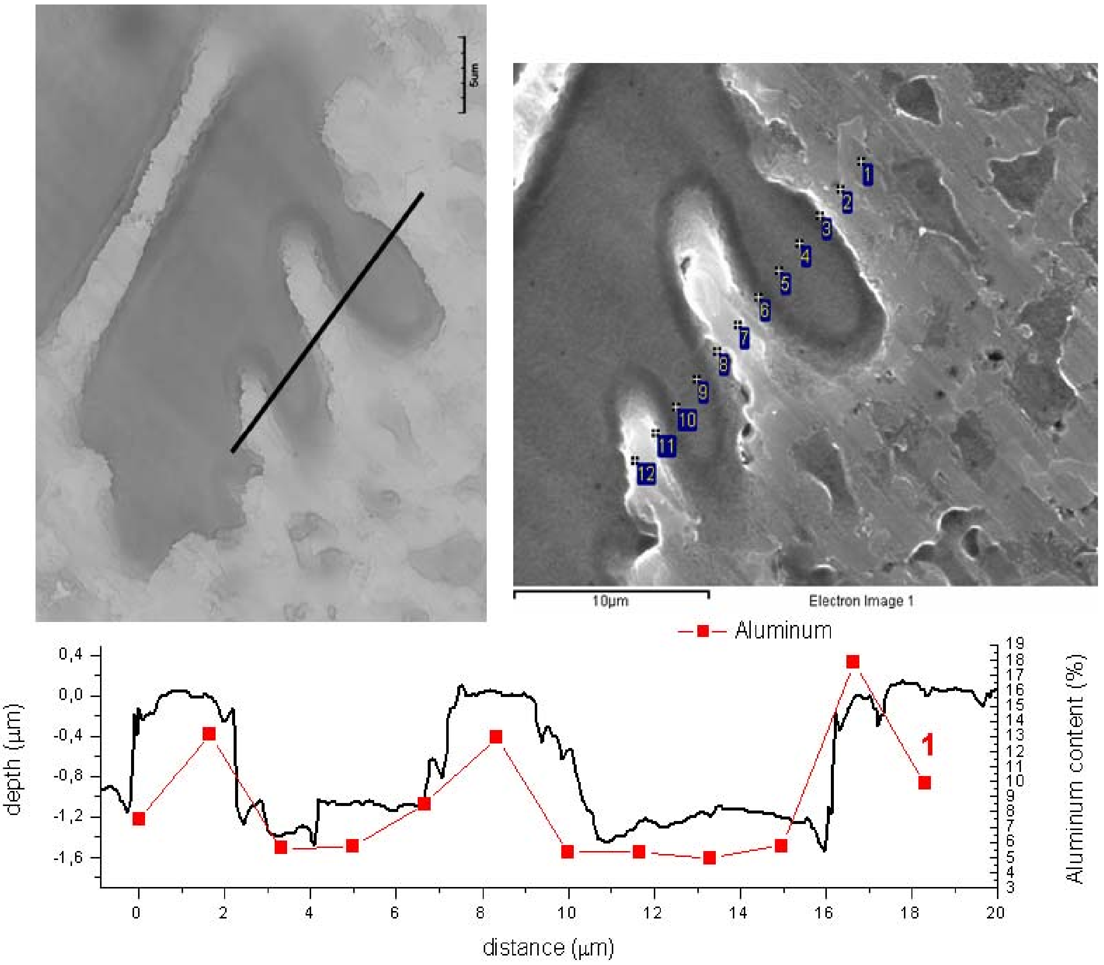

Figure 8: Surface profile and aluminium content of part of the AZ91D surface seen in Figure 7. The sample was exposed for 6 days in 95% RH, in the presence of 1 µg/cm^2 NaCl.

As can be inferred from Figure 6 and Figure 8, the field and the samples exposed in 95% RH in the laboratory samples show close similarities. The depth profile, from the confocal measurements, follows the aluminium content, in both types of samples. In the field-exposed sample trenches have formed in the vicinity of the eutectic α-/β phase, where the aluminium content increases. For both the samples the most severe corrosion effect can be seen in areas that contain around and below 6% aluminium. In the eutectic area the aluminium content increases above 6% and so does the corresponding depth profile line. In the field-exposed sample (Figure 6) trenches have formed in the α-phase, where the aluminium content is 5-6%. Just outside the trench the aluminium content is over 10% and the area is not as affected by corrosion. The same trenches, but not so pronounced, can be seen in the sample exposed in the laboratory (Figure 8). The formation of the trenches suggests that a galvanic coupling operates between areas with a high and a low aluminium content. Areas with an aluminium content below 6% are anodic and areas with a higher aluminium content (>6%) primarily cathodic.

An interesting feature can be seen to the right in the diagram in Figure 8 (points 1 and 2), where the aluminium content is 10% and 18%, respectively. The corresponding profile line does not change accordingly. This indicates that an aluminium content of around 10% plays a similar cathodic role in the initial stages of a corrosion attack as areas with a higher Al-content. This is in accordance with our previous findings (16) that the Volta potential increases rapidly up to a 10-12% Al content in the eutectic α-/β phase. Above that Al content the Volta potential seems to be more or less constant. This was previously explained by the accumulation of aluminium in the surface layer of the magnesium-aluminium-containing phases, which results in the formation of a protective aluminium oxide film that is present on the surface of the different aluminium-containing phases.

Influence of Al-Mn particles

As can be inferred from Figure 5A and 4B, no corrosion attack could be seen in the vicinity of the Al-Mn particles, nor was this the case on the field-exposed sample or the sample exposed in the laboratory. These particles have been reported to have the highest Volta potential of the different microconstituents present in the AZ91D alloy (15), and the driving force for the initiation of the corrosion attack at these locations could therefore be expected to be high. The reason why no corrosion attack could be seen has been declared (16) to be the surrounding of the Al-Mn particles. Both of the Al-Mn particles in Figure 4A and 3B are embedded in areas with a high aluminium content, i.e. the eutectic α/β-phase or the β-phase, and the Al-Mn particles are not located in the vicinity of a more un-noble α-Mg phase. In fact, due to the solidification process the majority of the Al-Mn particles can be found in the areas of a eutectic α-/β-phase (26, 27). Thus, due to the higher aluminium content in the eutectic α-/β-phase, the driving force is not strong enough for the initiation of corrosion attacks at these locations. Therefore the Al-Mn particles seem to play a minor role at least under early field or laboratory exposure conditions.

Some differences between the field and the accelerated corrosion testing

The processes in atmospheric corrosion in the field is complex and influenced by a number of factors, such as gaseous constituents, e.g. SO_2, CO_2, NO_2 HNO_3, pollutants, e.g. Cl^-, as well as climatic factors, e.g. humidity, temperature (28). In the laboratory the number parameters can to some extent be controlled. To evaluate magnesium alloys both immersion and saltspray tests are often used. Table 3 shows corrosion rates obtained after different types of accelerated corrosions test taken from the literature (13, 19, 21, 29). The corrosion rates show a wide scatter.

The electrolyte layer is an important factor differentiates the laboratory from the field. To accelerate the corrosion in the laboratory, high relative humidity, bulk electrolyte or salt spray are used, often together with high amounts of NaCl and elevated temperatures. A higher relative humidity results in a thicker electrolyte layer and similarly higher amounts of NaCl applied on the surface increases the thickness and the hence the ability to provide a conductive path between anodic and cathodic regions on the surface, which of course will have influence on the corrosion behaviour. The thicker electrolyte also results in a higher conductivity on the surface. A better ability to support current through the electrolyte layer allows a greater separation between the local anode and cathode on the surface. In a bulk electrolyte, galvanic coupling is possible without any larger ohmic potential drop in the solution. Hence the various micro constituents, such as the β phase and the Al-Mn phases, will play a more important roll as cathodes in the corrosion process. In contrast during field conditions a larger ohmic potential drop will be formed in the thin water layer on the surface. This decreases the possibility of galvanic coupling of alloy constituents located at larger distances from each other.

The thickness of the electrolyte layer influence both the anodic and cathodic processes. Rozenfeld (9) have shown that with a decreasing thickness of the electrolyte film the passivity region increase both for aluminium and magnesium. This is related to the easy access to oxygen, and consequently the ability to withstand active corrosion attack increases under thin electrolyte layer. Also the cathodic processes are affected by a thinner electrolyte layer (9). If there is an easy access to oxygen, as is the case under thin electrolyte layers, oxygen reduction will be the preferred cathodic reaction, whereas hydrogen evolution is dominating in solution and with very thick electrolyte layers. This is probably of importance for the corrosion behaviour of magnesium in the atmosphere and during immersed conditions. For instance, it is well known that the corrosion of magnesium in solution is strongly dependent on impurities, especially elements with a low hydrogen overvoltage, such as Fe, Cu and Ni.

Another factor that is of importance for the corrosion properties of Mg-Al alloys is the pH of the electrolyte. It's been shown that the pH have a profound effect on the activity of the Mg-Al phases (19, 24, 30). Corrosion potential data shows that Mg is stabile in alkaline solutions and exhibits an increasing corrosion rate in decreasing pH, while aluminium is passive in neutral solutions but active and suffers a high corrosion rate in alkaline solutions (19, 24). Ambat et al.(30) tested the corrosion rate of AZ91 in three different pH, 2.00, 7.25 and 12.00 respectively, the corrosion rate increase in the following order, pH 7.25 < pH 12.00 < pH 2.00. One the other hand it's been reported that pure magnesium has a corrosion rate 26 times lower at pH 12 compared to pH 8.5 (19), due to the passivation of magnesium in alkaline environments. Hence, the pH influence the corrosion rate in completely different ways depending on the proportion of magnesium and aluminium in the material tested. Measuring the corrosion properties of magnesium alloys in solutions in a closed vessel the pH will increase to 10.5 within hours (31). This is due to the release of $Mg(OH)_2$ that is the main corrosion product in the absence of CO_2 (22). The high pH is detrimental to the protective aluminium-oxide containing surface layer resulting in a selective dissolution of aluminium in the outermost layers of the surface (19, 32). In contrast, during atmospheric conditions the electrolyte layer is thin and the corrosion products consist of magnesium carbonates, such as nesquehonite and hydromagnesite (14). The dissolution of CO_2 in the surface electrolyte causes a decrease in the pH (22). The surface film on Mg-Al alloys, that contains a high Al content (16, 33, 34), will be more stable due to the more neutral pH, thus increasing the corrosion protective properties of the film.

Thus, accelerated corrosion test performed in solution, salt spray or under conditions with very thick electrolyte layers on the surfaces may result in corrosion behaviour which differs considerably form magnesium alloys exposed under field conditions. Care has to be taken to design accelerated test methods for magnesium in order to reproduce the corrosion behaviour under field conditions.

CONCLUDING REMARKS

The corrosion behaviour of the AZ91D alloy was investigated at three different exposure sites and was compared with the behaviour observed previously in laboratory exposure with predeposited NaCl. Just as in the earlier laboratory exposure, the microstructure was found to play a vital role for the initiation of the corrosion attack in the field, which here, too, was initiated in the less noble α-phase, with the more noble eutectic α-/β phase close to the α-phase acting as the cathodic site. The Al content of different phases was closely related to the extent of the corrosion attack: the higher the Al content the lesser the corrosion effect. Hydromagnesite ($Mg_5 (CO_3)_4 (OH)_2 4H_2O$) was the main corrosion product at all the field sites, just as in the earlier laboratory exposure. This product possesses poor protective properties shown by a constant corrosion rate throughout the first year of exposure; 4.2, 2.2 and 1.8 µm/year at the marine, rural and urban sites, respectively. Two parameters that has to be considered when comparing magnesium aluminium alloys exposed in accelerated tests with samples exposed in the field is the difference in pH and the thickness of the electrolyte layer.

ACKNOWLEDGMENTS

The authors would like to thank Dominique Thierry and Nathalie LeBozec at Institute de la Corrosion for helping with the exposure at the marine field site.

REFERENCES

1. H. P. Godard, W. B. Jepson, M. R. Bothwell and R. L. Lane, The Corrosion of Light MetalsWiley and Sons, New York, 1967.
2. Y. Mikhailovskii, A. Skurikhin, M. Czerny, R. Wellesz and M. Zaydel, Atmospheric corrosion of metallic systems III. Corrosion behavior of aluminium and magnesium alloys in various atmospheric conditions., Prot. Met., 15, (1979) 419-426.
3. F. Pearlstein and L. Teitell, Corrosion of aluminium and magnesium in the tropics, Materials Performance, 13, (1974) 22-27.
4. D. V. Vy, A. A. Mikhajlov, Y. N. Mikhajlovskij, P. V. Strekalov and T. B. Do, Composition and microstructure of corrosion products of aluminum and MA2-1 magnesium alloy in wet tropical climate of Vietnam, Zashchita Metallov, 30, (1994) 578-581.
5. Y. N. Mikhajlovskij, P. V. Strekalov and V. V. Agafonov, A model of atmospheric corrosion of metals allowing for meteorological and aerochemical characteristics, Zashchita Metallov, 16, (1980) 396-413.
6. Y. Mikhailovskii and N. A. Sokolov, Predicting the corrosion resistance of metals and alloys in industrial atmospheres, Zashchita Metallov, 17, (1981) 431-436.
7. C. R. Southwell, A. L. Alexander and C. W. Hummer, Corrosion of metals in tropical environments - Aluminium and Magnesium, Materials Protection, 4, (1965) 30-35.
8. J. E. Hillis and R. W. Murray, in 14th International die casting congress and expo., paper no. G-T87-003, Toronto, Canada (1987)
9. I. L. Rozenfeld, Atmospheric corrosion of metalsNACE, Huston, 1972.
10. P. V. Strekalov, Atmospheric corrosion of metals in the tropics and subtropics. II. The corrosion resistance of various metals and alloys, Protection of metals, 29, (1993) 673-706.
11. L. Gruss, F. Pearlstein and L. Teitell, in *Atmosperic corrosion*, W. H. Ailor Editor, John Wiley and Sons, New York (1982).
12. N. D. Tomashov, Theory and protection of metals: The science of corrosionThe Macmillan company, New York, 1966.

13. N. Le Bozec, M. Jönsson and D. Thierry, Atmospheric Corrosion of Magnesium Alloys: Influence of Temperature, Relative Humidity and Chloride deposition, Corrosion, 60, (2004) 356-361.

14. M. Jonsson, D. Persson and D. Thierry, Corrosion product formation during NaCl induced atmospheric corrosion of magnesium alloy AZ91D, Corrosion Science, 49, (2007) 1540-1558.

15. M. Jönsson, D. Thierry and N. LeBozec, The influence of microstructure on the corrosion behaviour of AZ91D studied by scanning Kelvin probe force microscopy and scanning Kelvin probe, Corrosion Science, 48, (2006) 1193-1208.

16. M. Jönsson, D. Persson and R. Gubner, The initial atmospheric corrosion of magnesium alloy AZ91D, Journal of the Electrochemical Society, 154, (2007) C684-C691.

17. L. Tuvesson-Carlström and K. Altros, Miljö och korrosivitetsdata 2006, in, Corrosion and Metals Research Institute, Stockholm (2006).

18. J. F. Young, Humidity control in the laboratory using salt solutions-a reveiw, J. Applied Chemistry, 17, (1967) 241-245.

19. O. Lunder, J. E. Lein, T. K. Aune and K. Nisancioglu, The role of Mg17Al12 phase in the corrosion of mg alloy AZ91, Corrosion, 45, (1989) 741-748.

20. L.-Y. Wei, H. Westengen, T. K. Aune and D. Albright, in Magnesium Technology 2000, TMS Annual Meeting, 153-160, Nashville, TN, United States (2000)

21. M. Isacsson, M. Strom, H. Rootzen and O. Lunder, in Proceedings of the 1997 International Congress and Exposition, Feb 24-27 1997, SAE Special Publications, 43-55, Detroit, MI, USA (1997)

22. R. Lindström, L.-G. Johansson and J.-E. Svensson, in 15th international corrosion congress, Granada, Spain (2002)

23. D. Blücher Bengtsson, Carbon dioxide: the unknown factor in the atmospheric corrosion of light metals A laboratory study, in *Department of Chemical and Biological Engineering*, Chalmers University of Technology, Göteborg (2005).

24. S. Mathieu, C. Rapin, J. Steinmetz and P. Steinmetz, A corrosion study of the main constituent phases of AZ91 magnesium alloys, Corrosion Science, 45, (2003) 2741-2755.

25. M. Jonsson and D. Persson, The difference between magnesium alloy AZ91D and AM50 from a microstructural perspective,

26. V. Y. Gertsman, J. Li, S. Xu, J. P. Thomson and M. Sahoo, Microstructure and second-phase particles in low- and high-pressure die-cast magnesium alloy AM50, Metallurgical and Materials Transactions A: Physical Metallurgy and Materials Science, 36, (2005) 1989-1997.

27. C. J. Simensen, B. C. Oberlander, J. Svalestuen and A. Thorvaldsen, Phase diagram for magnesium-aluminium-manganese above 650 °C, Zeitschrift fuer Metallkunde, 79, (1988) 696-699.

28. C. Leygraf, in *Corrosion mechanisms in theory and practice*, P. Marcus Editor, p. 529-563, Marcler Dekker, New York (2002).

29. L.-Y. Wei, Development of microstructure in cast magnesium alloys, in, p. 217 (1990).

30. R. Ambat, N. N. Aung and W. Zhou, Studies on the influence of chloride ion and pH on the corrosion and electrochemical behaviour of AZ91D magnesium alloy, Journal of Applied Electrochemistry, 30, (2000) 865-874.

31. O. Lunder, K. Nisancioglu and R. S. Hansen, in International Congress and Exposition, Mar 1-5 1993, SAE Special Publications, 117-126, Detroit, MI, USA (1993)

32. C. D. Lee, C. S. Kang and K. S. Shin, Effect of Mg-rich matrix on the corrosion behavior of as-cast magnesium-aluminium alloys, Metals and Materials, 6, (2000) 441-448.

33. J. H. Nordlien and K. Nisancioglu, in European Symposium on Modification of Passive Films, Paris (1993)

34. J. H. Nordlien, O. Sachiko, M. Noburo and K. Nisancioglu, Morphology and structure of oxide films formed on MgAl alloys by exposure to air and water, Journal of Electrochemical Society, 143, (1996) 2564-2571.

Development of new low-cost Mg-Al-Zn based casting magnesium alloys with high strength and high ductility

Y. Xie[1,2], S.M. Liang[1,2], Y.Q. Ma[1], R.S. Chen[1*], E.H. Han[1]
[1]Environmental Corrosion Center, Institute of Metal Research, Chinese Academy of Sciences
[2]Graduate School of the Chinese Academy of Sciences
[*]Corresponding author: rschen@imr.ac.cn

Abstract

Magnesium based alloys with excellent properties as well as low cost have great potential for substituting their heavier aluminum and steel based counterparts. This investigation focused on the effects of carbon inoculation by adding magnesite particles, antimony element, and heat treatment on the microstructure and room temperature mechanical properties of Mg-Al-Zn alloys with compositions within the high zinc castable domain. Thus, a system study for improving both strength and ductility of Mg-Al-Zn based magnesium alloys was carried out and series of low-cost casting magnesium based alloys possessing mechanical properties superior to AZ91 were obtained. For example, excellent tensile properties (Y.T.S.≈160MPa, U.T.S.≈313MPa and Elongation≈6.0%) were obtained in AZ64-0.1Sb-C magnesium based alloy under T6 condition. These excellent tensile properties are higher than those of existing Mg–Al–Zn series casting magnesium alloys and promising for the application to automotive load-bearing parts.

1. Introduction

As a lightweight metallic material, magnesium alloys are attracting increasing attention from the automotive industry due to increasing demands for weight reduction and fuel efficiency. However, the low strength and/or ductility of magnesium alloys, relative to aluminum alloys, have greatly restricted their applications, such as application on the wheels of lightweight vehicles, where high strength and high ductility are both required. Therefore, it is of significance to develop new magnesium based alloys with excellent mechanical properties as well as low cost.

It has been reported that proper antimony (Sb) addition can improve both strength and ductility of the commonly used alloy AZ91 by refining grain size and the secondary phase of the alloy [1,2]. Likewise, carbon inoculation by carbon-contained agents such as magnesite is also an efficient way to refine the grain size [3]. Magnesium based alloys with medium aluminum and medium zinc content, which are also within castable domain of Mg-Al-Zn system [4], have been reported to have superior creep resistance than AZ91 while much lower tensile properties at ambient temperature in the as-cast condition [5]. However, the tensile properties of those alloys are promising to be greatly improved by carbon inoculation and/or Sb addition. And appropriate heat treatment can further improve its mechanical properties. In previous papers, we reported some achievement in developing low cost Mg-Al-Zn alloys [6， 7]. In this paper, we present a profoundly technology to develop the low-cost Mg-Al-Zn based casting magnesium alloys with high strength and high ductility and keys to improving strength and ductility.

2. Selection of content of the main alloying element

Table 1 shows the composition of the alloys studied in this work, and Fig. 1 shows the typical as-cast microstructures of the studied alloys, which consist of dendritic primary phase α-phase and the secondary phases of lamellar and block shape distributed in interdendritic spacing area and along grain boundaries. Besides the typical secondary phase γ-phase as in the commonly used alloys AZ91, AZ31, other three kinds of secondary phases occur, i.e. φ-phase, τ-phase and the quasi-crystalline I-phase. Table 1 also lists the obtained results with combination of SEM/EDAX, XRD, and thermal analysis showing the phase constituents, the forming temperatures of the corresponding phases, and the solidus of the alloys [7]. For example, the alloy AZ64 contains three phases, i.e. primary α-phase, forming at 605.7 ℃ and two secondary phases i.e. γ-phase and φ-phase,forming at 383 ℃ and 361 ℃ respectively, and the solidification ends at temperature 351 ℃. It should be noticed that these data of temperatures are crucial to the design of heat treatment procedures, which would be discussed in the following part about the heat treatment of these alloys. Fig.2 clearly illustrates the relationship between phase constituents and compositions of the alloys with medium Al and Zn contents. Roughly, the secondary phases vary, in sequence, from γ-phase to φ-phase, τ-phase and the quasi-crystalline I-phase with the Zn/Al ratio increasing. However, owing to the particularity of the quasi-crystalline I-phase, that is, the forming of the I-phase is beyond the common sense that the quasi-crystalline phase usually would not occur in the as-cast microstructures obtained under the normal casting conditions of non-extremely rapid cooling rates and it is related with the crystalline τ-phase[9], the zone of α+I is surrounded by the zone of α+τ, which supposes that we should not be able to judge the phase constituents of certain alloy just only based on its Zn/Al ratio, additional conditions such as the specific content of Al or Zn are required.

Table 1 Phase constituents, corresponding forming temperatures and solidus of the examined alloys (Unit :℃)

Alloys	Primary Phase	Secondary Phases				Solidus
	α-phase	γ-phase	φ-phase	τ-phase	I-phase	
AZ60	624.0	434				428
AZ62	615.3	404	404			399
AZ64	605.7	383	361			351
AZ65	604.5	375	357			351
AZ66	602.6	371	357			351
ZA62	625.0				344	330
ZA64	609.7			351		343
ZA65	606.3		361			351
ZA74	606.2				354	343
ZA84	610.3				354	343

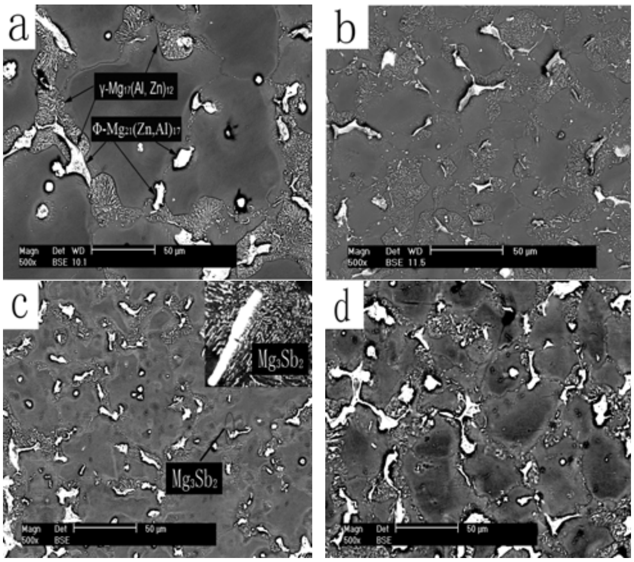

Fig. 1 Microstructures of the as-cast AZ64 alloys with and without carbon inoculation and Sb addition: (a) AZ64; (b) AZ64-C; (c) AZ64-0.5%Sb; (d) AZ64-0.5%Sb-C.

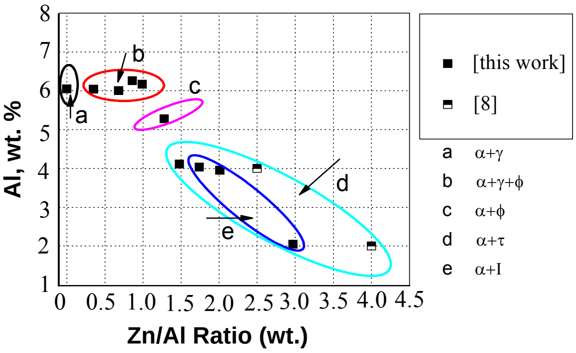

Fig. 2 The diagram of phase constituents of the as-cast alloys with variation in Zn/Al and Al content.

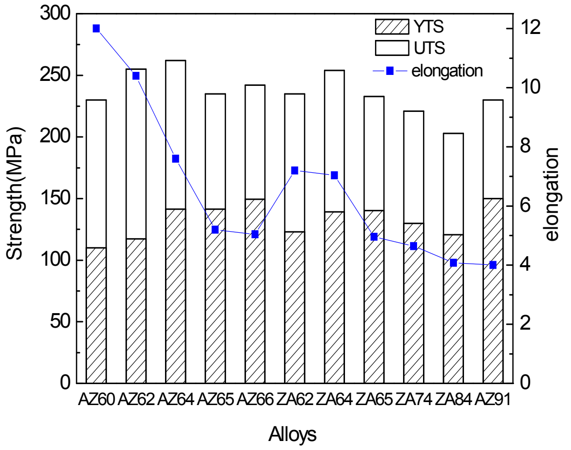

Fig. 3 Tensile properties of the experimental alloys with carbon inoculation.

As it can be seen in Fig. 3, the studied alloys (AZ64 and ZA64) have comparative strength with AZ91 while with higher ductility. It seems that the mechanical properties is related to the total content of Zn and Al; UTS increases while elongation decreases with the total content increasing and the UTS achieve its peak with total amount of Zn and Al content of 10%.

3. Effect of carbon inoculation and/or Sb addition

Fig.1 and Fig.4 illustrate the influence of carbon inoculation and/or Sb addition on the as-cast microstructures and the tensile properties of the alloy AZ64. As reported by many researchers [3, 4], the carbon inoculation greatly refines the grains as shown in Fig. 1b, indicating both strength and ductility would improve according to the strengthening theory, which right explains the results of the tensile tests. The result also shows that the carbon inoculation greatly refine the grain size only when the Al content is more than 4%. Unlike carbon inoculation, the effect of Sb addition is complicated. On one hand, as shown in Fig.1c, the Sb addition significantly decreases the grain size and simultaneity refines the lamellar secondary phase, leading to the increase in strength and ductility. On the other hand, low solubility of Sb in magnesium matrix which suggests that Sb primarily exist in its compound, i.e. Mg_3Sb_2 as shown in Fig.1c, means Sb would improve the strength through precipitation hardening while decrease the ductility. At the same time, the Mg_3Sb_2 precipitate, a needle-shaped precipitate inserting in the lamellar secondary phase as seen in Fig. 1c, has increasing possibility to become crack initiation area with its coarsening, which means that excessive Sb addition would instead lead to the decrease in strength. Therefore, optimum Sb content should be chosen to achieve the optimum mechanical properties. The results of tensile tests, in accordance with the results of SEM observation, shows that compared with the alloy without Sb addition, 0.1%Sb increases both strength and ductility of the alloy AZ64 and when the content of Sb reaches 0.5%, its strength decreases slightly with ductility increasing. Fig. 1d and Fig. 4 show the influence of carbon inoculation together with Sb addition on the as-cast microstructure and tensile properties of the alloy AZ64. The results indicate that carbon inoculation and Sb addition are not mutually exclusive and the alloy AZ64-0.5 Sb-C has the optimal tensile properties.

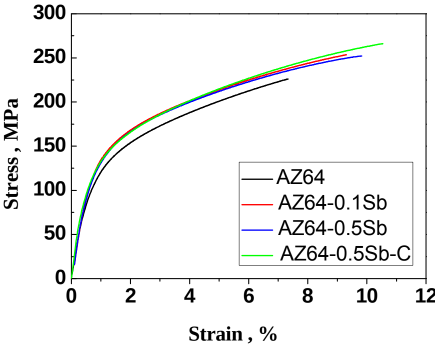

Fig. 4 Influence of carbon inoculation together Sb addition on tensile properties

4. Optimized T6 treatment

T6 treatment (solid solution followed by aging), the commonly used heat treatment in magnesium alloys, is adopted to improve the mechanical properties of the studied alloys to reshape and redistribute the secondary phases. Commonly, T4 treatment (solid solution) during which dissolving of the secondary phases into the α-Mg matrix leads to the increase in ductility is carried out at the temperature 10~20℃ lower than the practical solidus temperature in case inclusive liquid which deteriorates the properties. In addition, when the Zn contents of the alloys exceed 2%, multi-step solid solution is needed to avoid the occurrence of liquid, which indicating that the highest temperature of solid solution could be reached by multi-step treatment. Therefore, for the alloys AZ64~AZ66 with two peaks corresponding with the forming of secondary phases, the temperature ranging between the two peaks may be feasible. Thus, two kinds of solid solution treatment for the alloys AZ64~AZ66 are available: the normal one with the highest solid solution temperature10~20 ℃ lower than the solidus temperature, denoted as T4, and the optimized one with that 10~20℃ lower than the temperature where the secondary phase begins to form while maybe higher than the solidus temperature, denoted as T4-I. Accordingly, there are two kinds of T6 treatment, denoted as T6 and T6-I respectively.

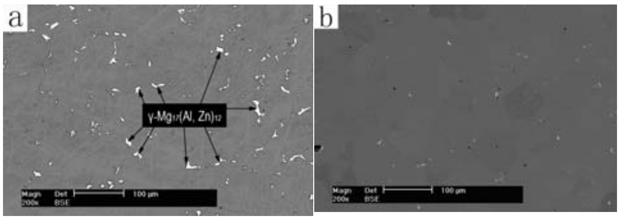

Fig. 5 Influence of different T4 heat treatment on the microstructures of AZ64: (a) microstructure under T4; (b) microstructure under T4-I.

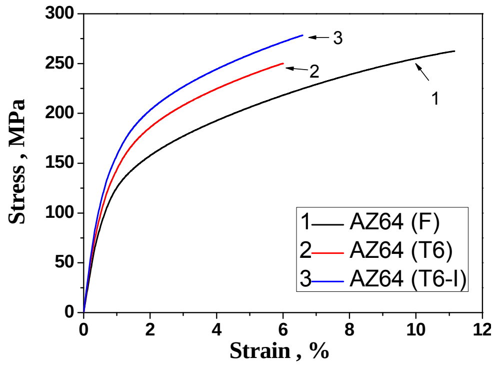

Fig. 6 Influence of different T6 heat treatment on tensile treatment of AZ64

Here, the processing of T6/T6-I and their influence on the mechanical properties of the alloy AZ64 are discussed. Moreover, for convenience of comparison, the total time of the solid solution is 16h and the alloys are heated at 180℃ for 20h during aging as a rule. According to the concerned typical temperatures of the alloy AZ64, i.e. 351℃ and 383 ℃ shown in Table 1, the T6 and T6-I heat treatment are designed as follows:(1) T6 300℃, 320℃, and 340℃ each for 2h; 345℃ for 10 and 180℃ for 20h, and (2) T6-I 300℃, 320℃, and 340℃ for each 2h; 350℃ and 360℃ each for 4h; 370℃ for 2h and 180 ℃ for 20h. As seen in Fig.6, T6-I treatment is more efficient in improving strength and ductility. The results of Fig. 6 can be well explained by Fig.5 which illustrates that T4-I treatment more completely dissolve the secondary phases into the magnesium matrix, leading to better ductility after solid solution and then better strength after aging because of larger amount of precipitate. Furthermore, the rules of T6-I heat treatment are also adapted to the other concerned Mg-Al-Zn alloys.

5. Summary of the technologies for new Mg-Al-Zn based alloys with high strength and ductility

Based on the above analysis, four keys to achieving high strength and ductility of the magnesium based Mg-Al-Zn alloys with medium Al and Zn contents are summarized: (1) advisable selection of the content of the main alloying element, especially the total amount of Al and Zn, (2) carbon inoculation to refine primary grains greatly and disperse the second phases of the alloys with Al content more than 4 wt.%, (3) optimum Sb content to obtain an improved combination of strength and ductility, and (4) an optimized T6-I heat treatment of high efficiency to improve the mechanical properties.

(1) Thus, a technology combining those four keys is carried out to confirm new Mg-Al-Zn based casting alloys with high strength and ductility. The technology consists of respects as follows:

(2)

Selection of alloying element: the alloys are comprised of 3~9 wt.% of aluminum, 3.5~9 wt.% of zinc, 0.15~1 wt.% of manganese, 0.01~2 wt.% of antimony, and balanced magnesium.

Controlling of the smelting and casting procedures: the smelting and casting procedures of the alloy were as following:

(3) Set the temperature of the crucible to 700~750 ℃ and start heating. Preheat the raw materials in a furnace at 140~200℃, and dry the covering flux at the same time. The quantity of the flux is 0.6~4 wt% of total weight of the alloy. Preheat the casting mold in another furnace at 200~400 ℃;

(4) When the temperature of the crucible rise up to 280~320℃, introduce the CO_2 gas into the crucible to replace the air, put 30%~50% of the preheated covering flux into the bottom of the crucible, then put the preheated pure magnesium ingot into the crucible;

(5) After the melting of the pure magnesium ingot, while the temperature of the melting rise up to 700~750℃, introduce other preheated raw materials into the melting in turn from high melting point one to low melting point one, and then stir the melting for 8~10 minutes; In this step, put some of the residual preheated covering flux onto the top of the melting to prevent burning of the melting;

(6) Stir the melting for 8-10 minutes and at the same time scatter the refining agent to the melt. The magnesite particles, with a size of about 0.5mm and wrapped up with aluminum foil, are introduced in a bell jar to the melt after refining. And the amount of $MgCO_3$ in magnesite particles is more than 98 wt.% and the addition of magnesite particles to the melt accounts for 1.5 wt.% of the total weight of raw materials.

(7) After stabilizing the melting at 700~750℃ for 4~6 minutes, remove the scum from the top of the melting; In this step, introduce the mixed protective gases, which has composition of 99~99.5vol% air or CO_2 plus 0.5~1vol%SF_6, to prevent the melting from burning;

(8) After scumming, while maintaining the temperature of the melting at 700~750℃, cast the melting into the preheated mold under the protection of mixture protective gases, which has composition of 99~99.5vol% air or CO_2 plus 0.5~1vol%SF_6.

(9) Optimized T6 treatment: unlike the normal T6 treatment, the normal one is characterized by the highest solid solution temperature which is lower than the solidus temperature, while the optimized treatment may be higher than the solidus temperature, as a multi-step solid

solution has been adopted to avoid inclusive liquid during thermal treatment.

According to the above mentioned technologies, a series of low-cost casting magnesium based alloys possessing mechanical superior to AZ91 were obtained as shown in Table 2.

Table 2 New developed alloys with high strength and high ductility

Alloys	Heat treatment	Mechanical Properties		
		YTS (MPa)	UTS (MPa)	Elongation (%)
AZ64-0.1%Sb-C	300℃, 320℃ and 340℃, each 2h; 350℃ and 360℃, each 4h; 370℃, 2h ; 180℃, 20h	160	313	6
AZ64-0.5%Sb-C	300℃, 320℃ and 340℃, each 2h; 350℃ and 360℃, each 4h; 370℃, 2 h ; 180℃, 20h	150	308	6.7
AZ65-C	300℃, 2h; 340℃, 10 h; 370℃, 2 h ; 180℃, 18h	150	302	7.0

The advantages of the present technology can be summarized as follows:

(1) High strength and high ductility at room temperature. Especially meet with the demands in lightweight, high strength, and high ductility structural applications.
(2) High performance at low cost. The alloying elements are easily attainable. The cost of the production is low, so it is suitable for mass production.
(3) Melting and casting processes are easily controlled. No by-products due to little unwanted reactions between alloying elements and crucible wall or flux materials.
(4) Suitable for most of the casting processes, such as permanent casting, sand casting, special die casting, squeeze casting.

Acknowledgement

Thanks should be given to National Basic Research Program of China (973 Program) for its financial support through project No.2007CB613704.

References

[1] Q. D. Wang, W. H. Chen, W.J. Ding, Y. P. Zhu, M. Mabuchi, Metall. Mater. Trans, A 32A (2001) 787.
[2] G. Y. Yuan, Y. S. Sun, W.J. Ding, Scr. Mater. 43 (2000) 2009.
[3] Shi-Jun Zhang, Wen-Xian Li, Kun Yu, Dun-Qiang Tan, Foundry 50 (2001) 373 (in Chinese).
[4] G. S. Foerster, in Proceedings of the IMA 33rd Annual Meeting, Montreal, Quebec, Canada, 23–25 May 1976, (1976) 35.
[5] Z. Zhang, A. Couture, A. Luo, Scr. Mater. 39 (1998) 45.
[6] Y. Q. Ma, R. S. Chen, E. H. Han， Materials Letters, 61 (2007) 2527.
[7] S.M. Liang, Y.Q. Ma, R.S. Chen, E.H. Han, The 2008 TMS Annual Meeting & Exhibition, Symposium on Magnesium Technology 2008, March 9-13, 2008, New Orleans, Louisiana，USA
[8] Zhang. Jing et al, Mater. Sci. Eng., A 415 (2007) 43
[9] M. Vogel, O. Kraft, G. Dehm, E. Arzt, Scr. Mater., 45, (2001) 517

Improved magnesium alloys for automotive powertrain applications and extrusion: AM-SC1™, AM-HP2plus™ and AM-EX1™

Gordon Dunlop and Morris Murray, Advanced Magnesium Technologies, Australia
Mark Gibson, Mark Easton, Aiden Beer, Matthew Barnett and Chris Davies CAST CRC, Australia

Abstract

In order to be truly competitive in critical automotive applications, magnesium alloys need to have properties that are similar to, or better than, their aluminium alloy counterparts and they need to be readily manufacturable. For high temperature powertrain applications, AM-SC1 is an excellent alloy for sand casting and permanent mould casting with properties that have been proven in engine applications. AM-HP2plus has been tailored specifically to provide good castability for high pressure diecasting while delivering similar high temperature mechanical properties. These two magnesium alloys have similar creep strengths to aluminium alloys used in powertrain components. The newly developed extrusion alloy, AM-EX1, can be extruded at rates similar to 6xxx series aluminium alloys and has mechanical properties that are also comparable to aluminium alloys.

Introduction

Rapidly rising concerns for global warming and the cost of fuel are putting increased pressure on the development of light weight magnesium alloys that can reduce the weight of automobiles and thus reduce both fuel consumption and exhaust emissions.

The key competitor material for magnesium is aluminium. There are well established aluminium alloys for both powertrain and body applications and, while magnesium is attractive by virtue of its lower density, magnesium alloys need to have mechanical properties and processing capabilities that are comparable with aluminium in order to be considered. The relative cost of magnesium and aluminium alloys is also an important consideration.

Two new magnesium alloys (AM-SC1 and AM-HP2plus) have been developed for high temperature powertrain applications, such as engine blocks and automatic transmission housings. These alloys have similar mechanical properties to the aluminium alloys that are commonly used in powertrain applications. AM-SC1 is a heat treatable alloy that can be cast by either sand casting or permanent mould casting processes and has similar properties to aluminium alloys such as A319 and A380. AM-HP2plus is a high pressure diecasting alloy that has similar properties but which has been tailored to have considerably improved diecastability. This improved diecastability overcomes a problem inherent in most high creep strength magnesium alloys that have a strong tendency for hot cracking and the formation of other defects during diecasting.

Wrought magnesium alloys are generally significantly more difficult to process than aluminium alloys and therefore magnesium alloys have only made very small inroads into potential markets for extrusions, sheet and forgings. The main issue for magnesium extrusion alloys has been to increase the rate of extrusion, while retaining good mechanical properties, so that the cost of processing can be reduced to levels comparable to aluminium alloys. The new magnesium extrusion alloy, AM-EX1, was specially developed to be capable of similar extrusion rates as 6xxx series aluminium alloys and has comparable mechanical properties to these aluminium alloys.

New powertrain alloys

There are a number of magnesium alloys containing aluminium that have been developed for improved high temperature properties for use in automotive powertrain applications. Examples of these are AJ62, AS31, AE42 and AE44. None of these alloys have equivalent high temperature creep properties to aluminium alloys and, with current trends of increased performance at higher temperatures, the use of magnesium alloys containing aluminium will become increasingly less competitive because of their relatively poor creep properties.

The Mg/Al composite crank case for BMW's in-line 6 cylinder engine uses an aluminium alloy open deck insert with the magnesium alloy AJ62, that contains aluminium and strontium, as the outer shell [1]. A fully magnesium alloy crank case would require an alloy with considerably improved creep properties compared to AJ62. Magnesium alloys that have rare earth elements as their major alloying components are well recognised as having the potential to fill this role.

Both AM-SC1 and AM-HP2plus are rare earth containing alloys with outstanding creep properties. As shown in Fig 1 the creep strength of these two alloys is similar to aluminium alloy A380 (and also A319) and under some circumstances is even better than their aluminium counterparts.

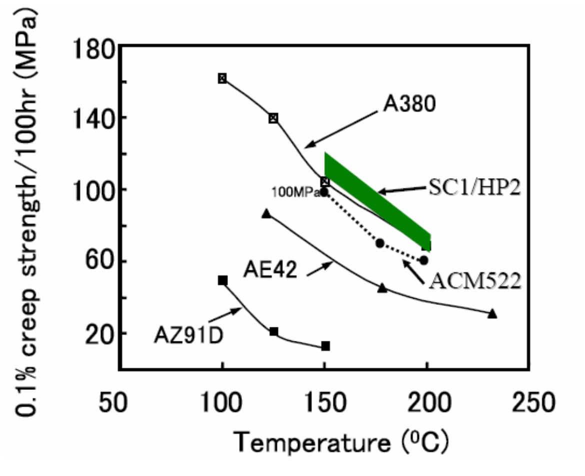

Figure 1. Comparison of 0.1% creep strength of AM-SC1 and AM-HP2 with aluminium alloy A380 and a number of other magnesium alloys. After [2].

AM-SC1: creep resistant alloy for sand casting and permanent mould casting

AM-SC1 [3, 4] was developed by AMT in collaboration with MEL, VAW (now Hydro Aluminium), AVL List, and the Australian research organisation CAST. It is a lean alloy that has been designed to give excellent performance in the heat treated condition at a reasonable cost. The alloy was first used in the crank case of the Genios turbo-diesel engine that was designed and manufactured by AVL List (Fig 2). This engine was subjected to extensive bench testing and was road tested in a Volkswagen Lupo vehicle for 65 000km over a two year period. Subsequent diagnostics on the engine demonstrated that AM-SC1 had performed very well [5].

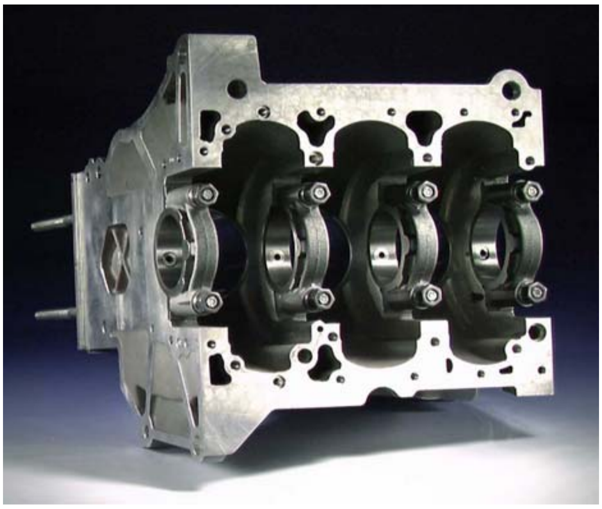

Figure 2. Sand cast AM-SC1 crank case of Genios turbo-diesel engine.

Since then AM-SC1 has been selected for the engine block of a magnesium V6 petrol engine developed in the USCAR MPCC development project. This engine has now been built and is currently undergoing bench trials [6].

Recently an extensive study of the properties of permanent mould cast AM-SC1 has been undertaken in collaboration with BMW. This work has highlighted the excellent combination of thermophysical properties and mechanical properties of this alloy [7].

For example, Fig 3 compares the heat capacity of permanent mould cast AM-SC1 with diecast magnesium alloy AJ62 and permanent mould cast aluminium alloy AlSi8Cu3Fe0.4 (A319). The heat capacity of AM-SC1 lies between that of AJ62 and A319 and tends towards the latter at higher temperatures. Also, as shown in Fig 4, the thermal conductivity of AM-SC1 is very similar to aluminium alloy A380 and is significantly higher than AJ52x and AZ31. Thus AM-SC1 has a similar ability to conduct heat as aluminium alloys and the thermal conductivity is much greater than other competing magnesium alloys.

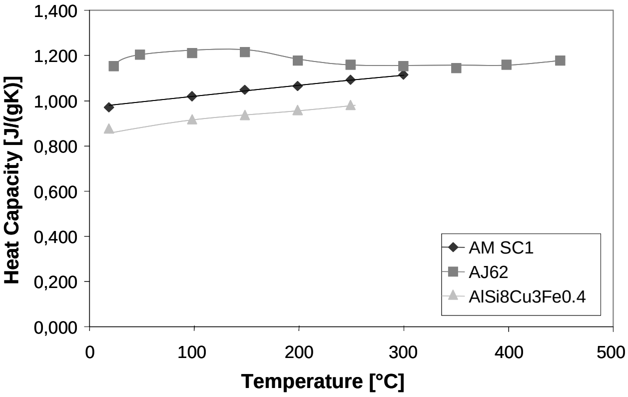

Figure 3. Heat capacity as a function of temperature. Permanent mould cast AM-SC1 compared with diecast AJ62 and permanent mould cast aluminium alloy A319 [7].

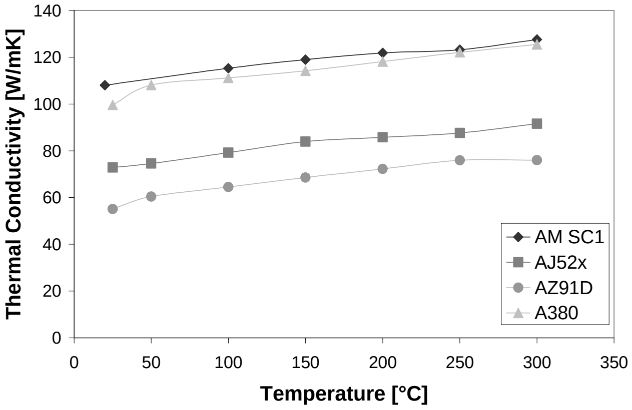

Figure 4. Thermal conductivity as a function of temperature. Permanent mould cast AM-SC1 compared with diecast AJ52x, diecast AZ91D and diecast aluminium alloy A380 [7].

The creep properties of AM-SC1 are similar to aluminium A380 and A319 alloys. While sand cast AM-SC1 has good tensile strength and fatigue properties these properties can be further improved by permanent mould casting. This is probably a result of casting quality with fewer casting defects and a refined microstructure in the more rapidly solidified permanent mould castings. Fig 5 shows the similarity of creep behaviour between permanent mould cast and sand cast AM-SC1 at temperatures of 150ºC and 200ºC. The vast improvement in creep performance compared to AJ62 is shown in Fig 6 which shows results for creep testing where the load was increased in stepwise increments.

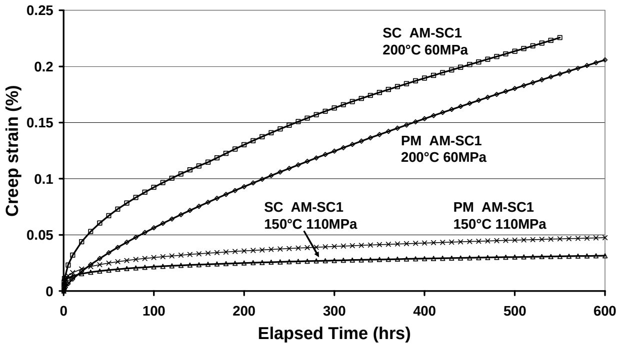

Figure 5. Comparison of creep behaviour of permanent mould cast (PM) and sand cast (SC) AM-SC1 at 150ºC and 200ºC [7].

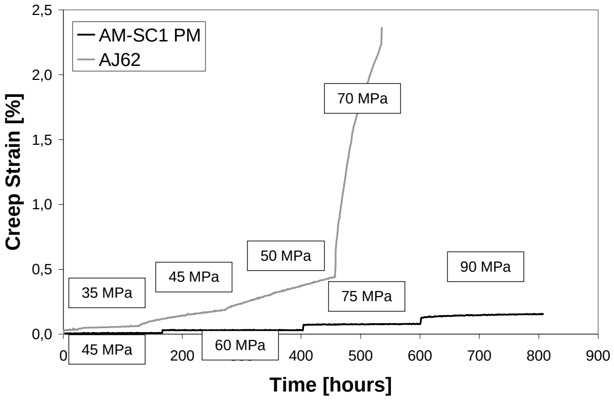

Figure 6. Creep performance of permanent mould cast AM-SC1 compared with diecast AJ62 in multi-load testing at 175ºC [7].

AM-HP2plus: creep resistant alloy for diecasting

AMT has been working with its research partner, CAST, for some time to develop an alloy that has the excellent properties of AM-SC1 but which can be satisfactorily high pressure diecast. The extremely rapid rate of filling of dies combined with high rates of heat extraction from the solidifying casting put very significant demands on both alloy and process if complex castings of high integrity are to be produced. Good diecastability in an alloy requires a combination of high fluidity in order to cast complex and thin walled sections, resistance to soldering, oxidation resistance to enhance welding of merging flows, and resistance to both hot and cold cracking. It is difficult to meet these requirements which are often in conflict with the need for good high temperature creep resistance. Indeed it is common for magnesium alloys with good creep resistance to be prone to hot cracking in parts of castings that are highly constrained during solidification and cooling.

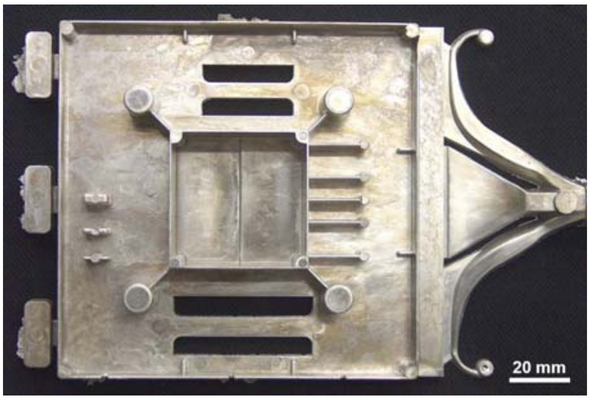

Figure 7. Part made in diecastablity test die with runner system and overflows intact.

Through manipulation of the alloy composition, the solidification characteristics of AM-HP2plus have been tailored to substantially reduce the tendency for hot cracking while retaining high fluidity, resistance to soldering, oxidation resistance and, of course, good mechanical properties at high temperatures. Fig 7 shows the part and runner system for a special diecastability test die that was developed for this work [8]. This die was developed to purposely enhance sensitivity to hot and cold cracking as well as maximising the need for high fluidity in complex thin sections. The complexity of the die enables all of the key aspects of diecastability to be tested in a single casting and comparisons can be readily made between the performance of alloys of different compositions.

Fig 8 shows a comparison of the casting quality between two alloys in a particular section of the diecastability test die. These two alloys have very similar high temperature creep properties but modifications to the second alloy (AM-HP2plus) resulted in considerably improved solidification characteristics and consistently better quality castings.

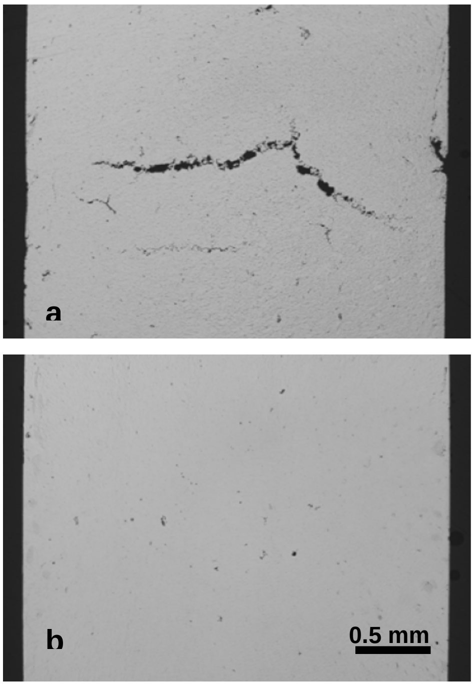

Figure 8. Comparison of casting quality between two alloys in a 3mm thick section of the diecastability test die. (a) Alloy A, (b) AM-HP2plus

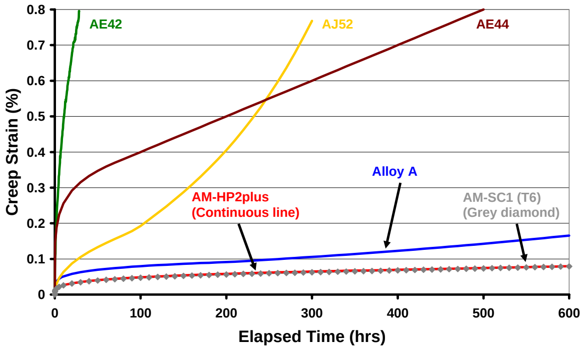

Figure 9. Comparison of creep properties at 177ºC and 90 MPa for AM-HP2plus with AM-SC1 and a number of other diecast magnesium alloys. Alloy A is the same alloy as shown in (a) of Fig 8.

The excellent creep properties of AM-HP2plus are demonstrated in Fig 9 and compared with AM-SC1 and a number of other competing creep resistant magnesium alloys. Full property evaluation of AM-HP2plus is now in progress in association with large scale industry beta trials.

AM-EX1: new improved extrusion alloy

The main problem in growing the market for magnesium extrusions is the high cost of extrusion for existing magnesium alloys compared with aluminium alloys. The problem for the most common magnesium extrusion alloy, AZ31, is illustrated graphically in the extrusion limit diagram of Fig 10. This diagram shows the limits on extrusion ram speed for AZ31, aluminium alloy AA6063 and the new alloy AM-EX1. The lines in this diagram indicate the fastest extrusion speed that can be used to produce extrusions of reasonable quality at a particular temperature.

For AA6063 there is a wide “window” of operating conditions between 300 and 600ºC where good quality extrusions can be produced. The operating window for AZ31 is considerably reduced and the maximum allowable speed is very slow by comparison. Thus, production output from an extrusion press is severely limited for AZ31 and the cost is high. The new alloy AM-EX1 has similar extrusion limits to AA6063 and therefore the cost of extrusion can be expected to be similar to the aluminium alloy. Some of the metallurgical principles that have been used in the development of AM-EX1 are described in [9].

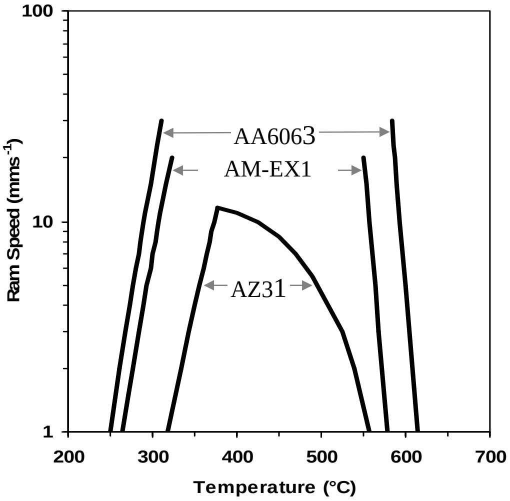

Figure 10. Extrusion limit diagram for aluminium alloy AA6063, magnesium alloy AZ31 and AM-EX1.

The data for Fig 10 was obtained in small scale laboratory tests. These results are supported by industrial scale extrusion trials that have demonstrated, for the same billet temperature, AM-EX1 can be extruded at speeds more than twice that possible for AZ31.

Another requirement for a competitive magnesium alloy is that its mechanical properties should be at least as good as comparable aluminium alloys. As shown in Table 1 AM-EX1 in the as-extruded condition has a similar yield strength and ultimate tensile strength to both T6 heat treated AA6063 and AZ31. However, by virtue of its lower density, the specific strength of AM-EX1 is considerably better than AA6063. AM-EX1 also has excellent tensile ductility which is considerably better than AZ31.

Alloy	0.2% Proof Strength (MPa)	Specific Strength (kN.m/kg)	Ultimate Tensile Strength (MPa)	0.2% Proof Strength Anisotropy ($YS_{comp}/YS_{tension}$)	Tensile ductility (%)
AA6063-T6	195	72	258	1	24.6
AZ31	203	112	247	0.4	14.4
AM-EX1	184	102	259	0.7	29.8

Table 1. Mechanical properties of T6 heat treated aluminium alloy AA6063, magnesium alloy AZ31 and AM-EX1.

Another parameter of importance is the anisotropy between the compressive yield stress and tensile yield stress. This has considerable bearing on the uniformity of deformation in post extrusion forming operations and the performance of structural components. The compressive yield strength of AZ31 is only 40% of the tensile yield strength – which is far from desirable. For AM-EX1 this parameter is vastly improved at 70%. These properties indicate that AM-EX1 should be an excellent alloy for post extrusion forming operations and for service performance.

The prime reason for the excellent performance of AM-EX1 is that it is a very dilute alloy with a fine stable grain size. This is generally difficult to achieve but the composition of the alloy has been specifically tailored for this purpose. Figure 11 shows the typical microstructure of extruded AM-EX1. The microstructure is typified by fine equiaxed grains with no second phase particles visible at this magnification. The stability of this microstructure is illustrated in Fig 12 which shows the evolution of grain size in both AM-EX1 and AZ31 after compression at 350ºC to a strain of 1.5 followed by annealing at the same temperature. After 1000h of annealing the grain size of AZ31 increases from 6µm to 25µm while the grain size of AM-EX1 stays virtually constant during this time.

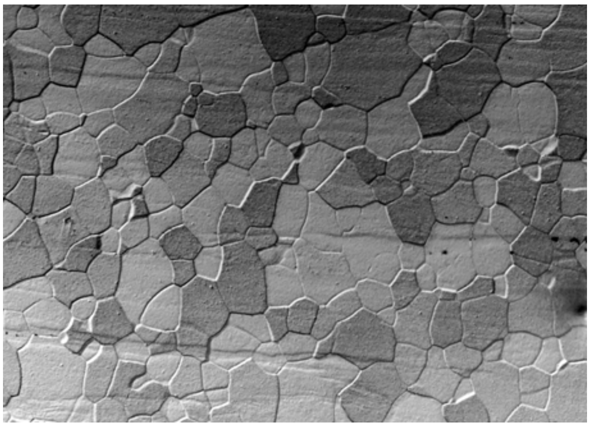

Figure 11. Typical microstructure of extruded AM-EX1. Note the fine equiaxed grains with no visible second phase particles.

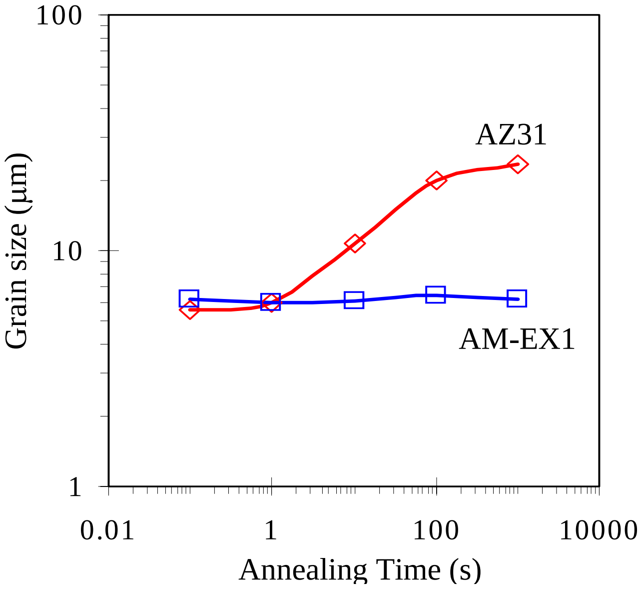

Figure 12. Evolution of grain size after compression at 350ºC to a strain of 1.5 followed by annealing at the same temperature.

Conclusions

1. The properties of two new creep resistant magnesium alloys (AM-SC1 and AM-HP2plus) compare well with aluminium alloys currently used for automotive powertrain components.

2. The performance of sand cast AM-SC1 has been demonstrated in the Genios turbo-diesel engine developed by AVL List and more recently in the USCAR MPCC project V6 petrol engine

3. Recent work has demonstrated that even better properties are obtained when AM-SC1 is permanent mould cast.

4. AM-HP2plus has been specially tailored to provide good diecastability while retaining excellent mechanical properties at high temperatures.

5. AM-EX1 is a new magnesium extrusion alloy that can be extruded at similar extrusion speeds to aluminium 6xxx series alloys and has comparable mechanical properties to those alloys.

References

1. A Fischersworrings-Bonk, S.Thalmair, M.Eibl, M. Kunst and A Dietsche, Mater. Sci. Tech. 23 (12) 2007, 1389-1395

2. S. Koike, K. Washizu, S. Tanaka, T. Baba and K. Kikawa, SAE Trans.: J. Mater. Manuf., 109 (2000) 560-566.

3. C.J. Bettles, C.T. Forwood, D.S. Jones, J.R. Griffiths, M.T. Frost, D.H. StJohn, Ma Qian, G-L. Song, J.F. Nie, SAE Technical paper 2003-01-1365.

4. C.J. Bettles, C.T. Forwood, D. StJohn, M.T. Frost, D.S. Jones, M. Qian, G-L. Song, J.R. Griffiths, J.F. Nie, Magnesium Technology 2003, TMS

5. W. Schoeffmann, F. Beste, M. Atzwanger and R.Marquard, Auto tech. 5. 2002, 50-53

6. J.A. Hines, R.C. McCune, J.E. Allison, B.R.Powell, L.J.Ouimet, W.L.Miller, R. Beals, L. Kopka, P.P. Reid, SAE Technical Paper series 2006-01-0522

7. M. Kunst, A. Fischersworrings-Bonk, M. Gibson, G. Dunlop, SAE Technical Paper Series 2008-01-0375

8. M. Gibson, M. Easton, V.Tyagi, M. Murray and G. Dunlop, TMS New Orleans, 2008

9. D. Atwell and M. R. Barnett, Metallurgical and Materials Transactions A **38** (12) 2007, 3032-3041

Development of a new AZ based secondary magnesium alloy

C. Blawert, E. Morales and K.U. Kainer
GKSS Forschungszentrum Geesthacht GmbH
C. Scharf, P. Živanović and A. Ditze
TU Clausthal

The increasing use of magnesium in various sectors will result in a rising quantity of scrap and there is a clear trend towards recycling of magnesium alloys visible. However, so far post consumer scrap has not been used for magnesium alloy production. Two major problems in this regard are on the one hand the entry of impurities and on the other hand the use of feedstock from mixed alloys. Removal of the impurities by melt cleaning is difficult, expensive or even impossible. To address this problem new secondary magnesium alloys are required with a much higher tolerance limit against impurities and variations of concentrations compared to the available conventional magnesium alloys.

Such a new AZ based secondary magnesium alloy with a high tolerance limit against impurities and similar corrosion properties as AZ91D was successfully developed. The various development steps included the alloy development combined with a microstructural characterisation and casting from lab scale gravity die casting to final industrial high pressure die casting of real components. Microstructure, mechanical and corrosion properties were determined and compared to the standard AZ91D alloy, revealing quite similar property profiles. The major draw back of the secondary alloy is the reduced ductility.

Introduction

Although on the one hand the use of magnesium alloys in the transport sector has the potential to reduce weight of vehicles and therefore reduce fuel consumption and CO_2 emission, on the other hand the energy consumption of primary magnesium production is rather high. A positive CO_2 balance in the average life time of a car can only be obtained if the Mg components of a car are predominantly produced from secondary Mg alloys. Recycling of magnesium requires only a fraction of energy compared to primary magnesium production [1].

However, in spite of this benefit real Mg secondary alloys are generally not used and even more there are no secondary alloys defined. Up to now, recycling of Mg is most of the time only the re-melting of pure scrap and of larger components which can be easily separated or cleaned from contaminations and sorted by the different alloys. If the impurity level is too high the re-melted material will be blended with primary alloys to fulfil the standard requirements. The reason for this practise is the problem that the presently used standard Mg alloys are only corrosion resistant if the impurity level of heavy metals such as Cu, Ni, Co and Fe is kept extremely low. These metals are part of standard scrap fractions, alloying elements in other light metals or are even used as coatings on Mg alloys. They can contaminate Mg alloys during the re-melting process if they are not completely removed from the scrap fraction. Because this is almost impossible and melt refining is difficult and expensive no used magnesium scrap (shredder or dismantling scrap) or coated (Ni, Cu) waste will be recycled up to date.

The use of secondary magnesium alloys is an essential step for the wide-spread use and acceptance of magnesium. It will give an important contribution to the reduction of CO_2–emission during life cycle of Mg-parts. Among all magnesium alloys the alloy AZ91 is the most commonly used alloy, thus the content of AZ in a scrap fraction can be expected to be relatively high. Therefore a new secondary magnesium alloy was developed based on the AZ system which is able to tolerate higher levels and fluctuations of typical impurities. This new alloy

AZC1231 contains higher levels of Al (12%) and Zn (3%) which modifies the microstructure and makes it more corrosion resistant, thus tolerating up to 1% copper having still similar corrosion rates as AZ91D [2-9]. The present paper will give some details about the castability, microstructure and properties (corrosion and mechanical) of the new alloy, suggesting that this alloy group may offer a suitable secondary alloy for Mg similar as the widely used AlSiCuNi system for aluminium.

Microstructure and composition

It is well known that the β-phase in AZ based alloys can either enhance or decrease the corrosion of the alloy. It all depends on the distribution of the β-phase. If it is uniformly distributed at the grain boundaries, covering the whole grains and forming a dense network, it works as a corrosion barrier and improves the corrosion resistance of the alloy remarkably. However, in AZ91D this beneficial β-phase network forms only under certain casting conditions. The alloy content is on the lower level for forming a sufficient amount of β-phase allowing the network to form under various casting conditions. Due to the much nobler character of the β-phase compared to the Mg matrix, separated β-phase precipitates in the matrix cause localised galvanic corrosion and enhance the corrosion rate. Therefore the ideas involved in increasing the Al, Mn and Zn content to improve the corrosion resistance are the following:

- grain refinement (by addition of Al, Zn and Mn)
- higher amount and continuity of the β-phase network (acting as corrosion barrier)
- setting of impurities in intermetallic phases (Fe and Ni are incorporated by Al_8Mn_5 phase, which is partly embedded in β and Cu is forming the τ-phase together with Mg, Al and Zn)
- critical more noble precipitates are embedded in β-phase and τ-phase (isolation from matrix)
- higher Al and Zn content should prevent the formation of corrosion detrimental Mg-Cu binary phases.
- stabilisation of passive layers

Comparing the microstructure of AZ91D and the new secondary AZC 1231 alloy clearly shows that the above mentioned ideas were successfully implemented (Fig. 1). In gravity die casting the AZ91D alloy shows only isolated single β-phase precipitates, while the new alloy forms the intended network. Furthermore the grain refinement is obvious with a reduction from about 700 µm to 100 µm. A detailed analysis of the phases present in the two alloys at the same impurity level of 0.5 % Cu, 0.008% Fe and 0.0035% Ni reveals the advantage of the new alloy (Tab. 1). The binary Mg-Cu phases are suppressed and Cu is forming in combination with Mg, Al and Zn the τ-phase. The β-phase and the τ-phase are embedding other more noble and therefore critical precipitates, isolating them from a direct contact with the matrix, thus reducing galvanic effects. The β-phase as the dominating phase is also embedding the τ-phase to a large extent. It is interesting to note that increasing only the Al, Zn or Mn content is not sufficient to reach the improved corrosion resistance and tolerance against higher impurity levels. This indicates that the formation of τ-phase is at least as important as the barrier function of the β-phase and only the combination of both mechanisms results in the intended positive effects. The composition of the new alloy and the tolerable impurity levels are shown in Tab. 2.

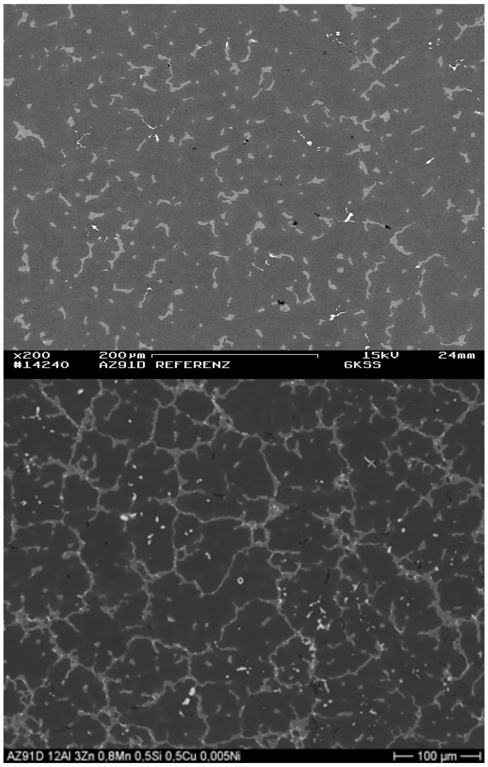

Fig. 1: SEM micrograph of the typical microstructure of AZ91D (top) and AZC1231 (bottom) showing the β-phase distribution

Tab. 1: Phases identified in alloys AZ91D, contaminated AZ91, pure AZM1231 and AZC1231

Phase	AZ91D	AZ91	AZM1231	AZC1231
α-phase	x	x	x	x
β-phase	x	x	x	x
Mg_2Si	x	x	x	x
Al_8Mn_5	x	x	x	x
$Mg_6Cu_3Al_7$	-	x	-	x
Mg_2Cu	-	x	-	-
$MgCu_2$	-	x	-	-
MgZn	-	-	x	-
τ-phase	-	-	-	x

Tab. 2: Composition of AZ91D, contaminated AZ91, pure recycling alloy AZM1231 and AZC1231 (all concentrations given in wt%, Mg remainder)

Alloy	Al	Zn	Mn	Si	Cu	Fe	Ni
AZ91D	8.75	0.67	0.2	0.054	0.008	0.0022	0.00061
AZ91	7.79	0.74	0.23	0.13	0.5	0.0085	0.0037
AZM1231	12.3	2.9	0.21	0.002	0.004	0.0017	0.00039
AZC1231	11.7	3.04	0.48	0.39	0.47	0.0087	0.0032

Casting

Casting behaviour

After changing the composition of the AZ91 alloy by increasing the contents of Al, Zn and Mn as well as the content of impurities the effect on the castability had to be checked and the possibility to process the new secondary alloy with various casting processes requires an additional evaluation. On the one hand for an alloy with a good casting behaviour the casting velocity can be kept low with positive effects on the lifetime of the casting dies and on the other hand the intended microstructure should be obtained independent from the casting process. Therefore the pouring characteristics were determined by casting trials using a pouring helix.

The evaluation of the pouring characteristics is only possible on a qualitative base as no standard test proceeding exists. For that reason the pouring characteristic of the new alloy was compared with the well known commercial high pressure die cast alloy AZ91D using the same helix and casting parameters (700°C melt temperature, helix preheated to 200°C and release agent Demotex S). During the casting trials the average temperature of the helix was maintained at 160°C. The results for the two alloys are displayed in Table 3.

Tab. 3 **:** Parameters and results of the helix castings trials for the two alloys AZC1231 und AZ91D

Alloy	T_{helix} [°C]	angle [°]	filled length of the helix [cm]	completely filled length of the helix [cm]
AZ91D	159.0 ± 5.7	256.8 ± 36.1	48.6 ± 7.4	23.0 ± 1.8
AZC1231	158.8 ± 2.5	408.8 ± 28.4	66.1 ± 5.6	39.5 ± 6.0

The results indicate clearly that the pourability and the mould filling capacity of the new secondary alloy are better compared to the AZ91D alloy. Therefore it can be concluded that the new alloy can be used with the same casting processes suitable for AZ91D which will be demonstrated later.

Influence of various casting processes

As demonstrated above the pouring capability of the new alloy is better compared to AZ91, thus it is no surprise that the new alloy has no restrictions regarding the processing routs. Gravity die casting, semi-solid processing (new rheo-casting) and high pressure die casting tests were successfully performed, casting test specimens from melts ranging from 10 to 150 kg AZC1231 alloy. Moreover the β-phase network as well as the presence of the τ-phase can be obtained under all casting conditions (Fig. 2) (cooling rates) thus the good corrosion resistance of the new secondary alloy is maintained almost independent of the processing route.

Industrial casting trials

More detailed information about the industrial casting trials which were performed in co-operation with Norsk Hydro Magnesiumgesellschaft (now Magontec) and Schweizer & Weichand can be found elsewhere [11]. Two aspects, melt handling of a larger amount of AZC1231 and casting of a real component were addressed by these trials. One ton of the alloy AZC1231 was produced from scrap at Norsk Hydro Magnesiumgesellschaft (now Magontec) and cast as ingots. The ingots were re-melted at Schweizer & Weichand and housings of a navigation device (Fig. 3) was cast with a Weingarten cold chamber high pressure die casting machine. The casting behaviour and the properties of the final housing were compared with the standard AZ91D alloy. The whole melt handling of the AZC1231 was similar to AZ91. Re-melting, casting and mould filling and the surface quality of the final housing were good. At some of the housing the cooling fins showed some minor casting defects (Fig. 4).

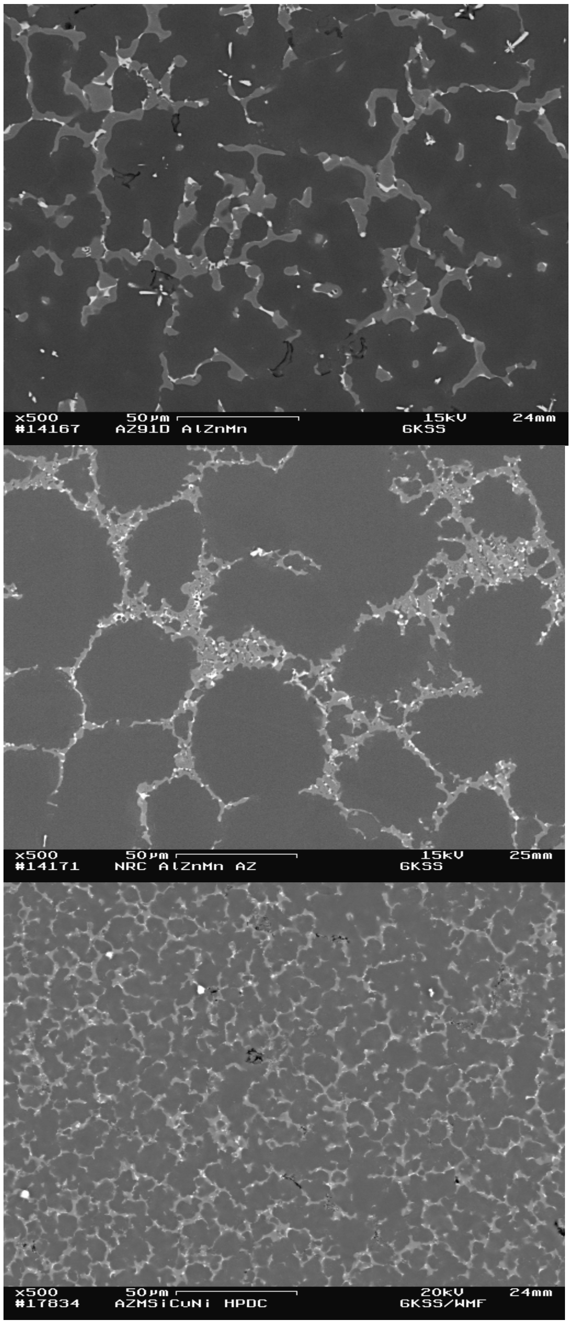

Fig. 2: SEM micrographs of the AZC1231 microstructure after gravity die casting (top), new rheo-cast semi-solid processing (center) and high pressure die casting (bottom)

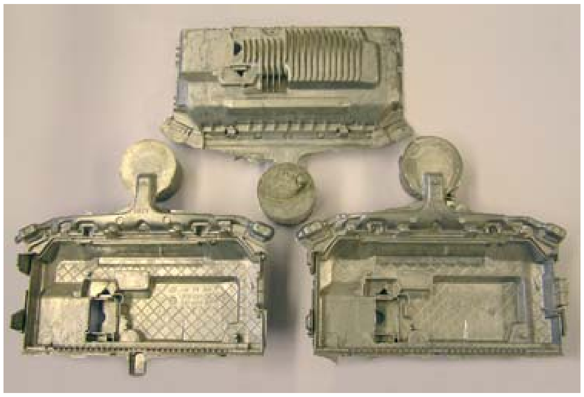

Fig. 3: Housing cast by cold chamber high pressure die casting using the newly developed secondary alloy AZC1231

Fig. 4: Casting defects on cooling fins produced from alloy AZC1231

The microstructure as a main indicator for a good corrosion resistance was very fine and the β-phase showed the formation of the required corrosion barrier network (Fig. 5). Although the amount of β-phase is higher for the AZC1231 the amount in the AZ91D alloy is sufficiently high to form a dense network as well. This is consistent with the general finding that HPDC AZ91D is able to develop the corrosion barrier network which is claimed to be responsible for the good corrosion resistance of AZ91 [13]. However, the increasing amount in the AZC1231 alloy seems to increase the processing window for forming the network especially if some of the impurities form additional precipitates in combination with aluminium (and other alloying elements), reducing the amount of β-phase.

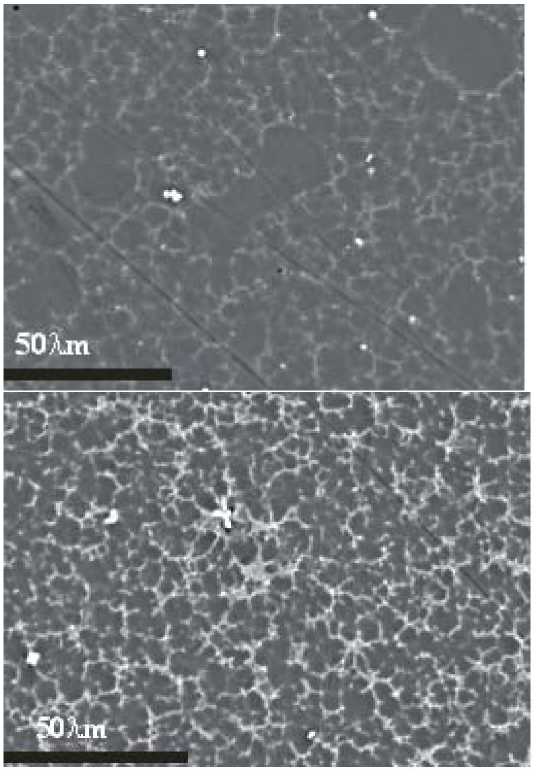

Fig. 5: SEM micrograph of the microstructure of alloy AZ91D (top) and AZC1231 (bottom) taken from the housings.

Properties

The primary aim of the alloy development was an improved tolerance limit for impurities combined with a corrosion resistance similar to AZ91D offering the possibility to use recycled magnesium alloys without an extensive melt cleaning or diluting with high purity grade. As mentioned above this aim could only be obtained by increasing simultaneously the Al, Zn and Mn content of the alloy. Figure 6 shows this effect for 5 alloys with the same level of impurities in comparison to the pure AZ91D alloy. Only the alloy with increased contents of Al, Zn and Mn has a similar corrosion resistance in salt spray test as the high purity AZ91D alloy. Regarding the corrosion rates the other alloys were even worse compared to the contaminated AZ91 alloy. The good corrosion resistance of the new secondary alloy was tested and compared to AZ91D under various conditions and the results are summarised in Tab. 4.

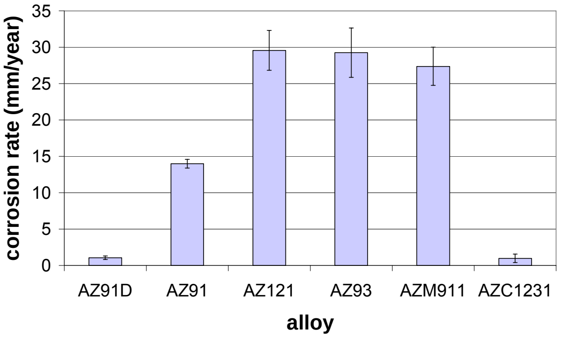

Fig. 6: Salt spray (5% NaCl, 48 h) corrosion rates of various AZ based alloys contaminated with 0.5%Cu, 0.5% Si and 0.005% Ni

Tab. 4: Corrosion properties of AZ91D and AZC1231 determined in various corrosion tests (gravity die casting except * HPDC housing)

Corrosion test condition	AZ91D	AZC1231
Pot.dyn. polarisation (after 1h in 5%NaCl, pH11)	0.43 ± 0.04 mm/year	1.81 ± 0.59 mm/year
Lin. polarisation resistance (after 24h in 5%NaCl, pH11)	247 Ωcm^2	80 Ωcm^2
Impedance (after 36h in 3.5%NaCl, pH7)	263 Ωcm^2	149 Ωcm^2
Saltspray (after 48h in 5%NaCl, pH7)	1.07 ± 0.23 mm/year	0.99 ± 0.58 mm/year
Immersion* (average after 400 h in 3.5%NaCl, pH6)	1.49 mm/year	1.42 ± 0.26 mm/year

It is obvious that the corrosion performance of the new alloy is comparable to AZ91 in spite of the much higher content of impurities. However, the results indicate that short term tests (<2 hours) are not suitable to identify the real potential of the secondary alloy. The development of the barrier function of the β-phase requires some time, in which enhanced dissolution of the matrix occurs, thus short term test will show higher corrosion rates.

The long term corrosion resistance (up to 700 hours) of AZC1231 and AZ91D (specimens taken from the HPDC housings) was studied using an automated immersion test (3.5% NaCl, pH 6 kept constant by HCl addition). The amount of hydrogen produced by the corrosion process of magnesium was measured as a function of the immersion time (Fig. 7), from which the corrosion rate was calculated (Fig. 8). One AZ91 and six AZC1231 housings were tested and the results indicate that the corrosion rates are all in the same order. This demonstrates that the good corrosion resistance of the secondary alloy is maintained even in an industrial type of processing.

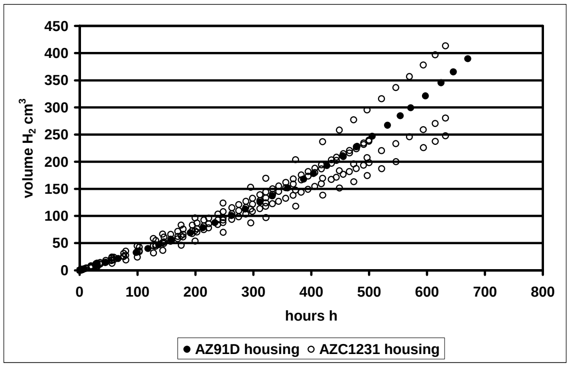

Fig. 7: Hydrogen development during immersion testing of HPDC housing specimens (specimens size: 25x25 mm, h=2 mm, 3,5% NaCl, pH=6, V=1,9 l, T=25°C, p=715 Torr)

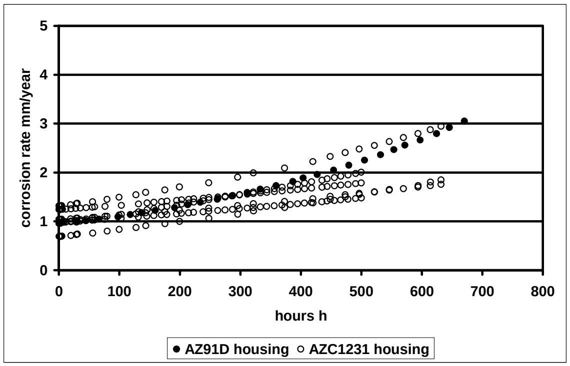

Fig. 8: Immersion test corrosion rates calculated from the hydrogen development shown in Fig. 7

However, not only the corrosion resistance was improved. Due to the higher content of β-phase compared to AZ91, the hardness of the alloy increases which has a positive effect on the wear resistance (Tab. 5). The coefficient of friction against steel under dry conditions is lower and the wear volume is markedly reduced (air, 10N load, 6 mm steel ball, 5 mm/s, 23°C, 25% humidity) [12].

The other mechanical properties of the new alloy show a sufficiently good property profile as well (Tab. 5). In spite of the higher fraction of β-phase the creep resistance (compression creep, 135°C, 70 MPa) is much better than for AZ91 and close to MRI153 alloy. A possible explanation for this behaviour might be the increase in copper content in the matrix and the β-phase as well as the large fraction of τ-phase. However, one important negative effect is the reduced ductility of the alloy. Tensile tests were performed on specimens tooled from the housing cast in the industrial trials and compared to AZ91D. The results clearly indicate that yield (R_p) and tensile strength (R_m) of the secondary alloy are comparable to AZ91D, but the strain (A5) is much lower. However, a strain of about 1% can be expected for a magnesium alloy containing 12% Al [10].

Tab. 5: Comparison of the mechanical properties of the new alloy AZC1231 and AZ91D

Property	AZ91	AZC1231
Hardness (HV5)**	83,2 ± 3,3	104,9 ± 2,8
Friction coefficient**	0.27	0.23
Wear volume** (mm^3/N/m)	11.5 * 10^{-4}	6.7 * 10^{-4}
R_m* (MPa)	263±14	246±17
R_p* (MPa)	198±15	187±27
A5* (%)	2.1±0.5	0.7±0.5
Creep rate ** (s^{-1})	4,38 * 10^{-8}	1,74 * 10^{-8}
SCC threshold stress*** (MPa)	90	130

* HPDC housing, ** HPDC test specimen, *** gravity die cast

Another concern regarding the use of magnesium alloys is the stress corrosion cracking behaviour. This was tested under slow strain rate conditions (strain rate: 10^{-7} s^{-1}, environment: air, distilled water and 0.5% NaCl solution) using gravity die cast specimens. The observed failure mechanism under a corrosive environment for both alloys is cracking of the passive film by straining, followed by anodic dissolution and most likely hydrogen development at the crack tip. This may result in hydrogen embrittlement and a reduced ductility. Due to the higher yield strength of the secondary alloy in the gravity die cast condition (AZ91: 81 MPa and AZC1231: 152 MPa) a critical strain level that results in cracking of the passive film is reached at a higher stress level. This results in a higher threshold stress against stress corrosion cracking. However, for HPDC material with similar yield stress levels a similar susceptibility can be expected.

Summary and conclusions

The newly developed secondary alloy AZC1231 has a similar corrosion resistance than conventional high purity alloys such as AZ91D. However, this advantage is combined with microstructural changes which cause a larger loss of ductility at similar strength levels compared to AZ91D. Therefore applications which require a certain level of ductility are not suitable for this secondary alloy. Nevertheless a large range of application, such as housings for mobile phones, computers, tools and automotive components outside of crash relevant areas do not require too much ductility and are suitable applications for the new alloy.

Thus it can be concluded, that with this new alloy the existing gap in the recycling of magnesium alloys can be closed to a large extent. Now it is possible to recycling magnesium post-consumer scrap and magnesium alloys contaminated with copper and/or nickel by simple re-melting. The advantages can be summarised as following:

- same recycling process as AZ91D
    - only re-melting which adjustment of the composition
    - same energy consumption compared to recycling of standard alloys
    - no expensive alloying elements
    - all scrap alloys can be re-melted to the new alloy (depending on the scrap the composition has to adjusted by alloying element additions or diluting with high purity Mg or alloys)
    - same equipment can be used (crucible, melt protection, gas, salt)
    - same melt handling
- similar corrosion resistance as AZ91D (immersion, salt spray)
- similar strength as AZ 91 (but much lower ductility)
- good casting properties (better than AZ91), thus suitable for high pressure die casting, semi-solid processing, sand casting or gravity die casting
- lower cost as AZ91D, because of cheaper raw materials (scrap and Cu + Ni contaminated components)
- large potential to save energy resources as reduced amount of primary magnesium is required
- reduction of CO_2–emission during life cycle of Mg-parts

Acknowledgements

The development of the new corrosion resistant magnesium secondary alloy is a joint project of the Institut für Metallurgie of the Technische Universität Clausthal and the GKSS Forschungszentrum Geesthacht GmbH and is supported by the Deutsche Forschungsgemeinschaft within the Schwerpunktprogramme 1168 “InnoMagTec” Project-Nr. EN370/9-1, DI492/9-2, KA 1053/9-2. The authors acknowlegde the financial support of the Deutschen Forschungsgemeinschaft.

Literature

[1] Ditze, A., Scharf, C.: World of Metallurgy – Erzmetall 57 (2004), pp. 251-257.

[2] Scharf, C., Ditze, A., Shkurankov, A., Morales, G. E. D., Blawert, C., Dietzel, W., Kainer, K. U.: Advanced Engineering Materials 7, No.12 (2005), pp. 1134-1142.

[3] Blawert, C., Morales, G. E. D., Dietzel, W., Kainer, K. U., Scharf, C. and Ditze, A.: SAE paper 2006-01-0254, 2006.

[4] Blawert, C., Morales, G. E. D., Dietzel, W., Hort, N., Kainer, K. U., Scharf, C., Ditze, A. and Endres, F.: Corrosion properties of secondary AZ91 alloys, N. R. Neelamegghan, H. I. Kaplan, B. R. Powell (Eds.), Proc. of Conf. Magnesium Technology 2005, The Minerals, Metals & Materials Society (TMS), 13. – 17.2.2005, San Francisco, California, USA, pp. 447-450.

[5] Blawert, C., Morales, G. E. D., Dietzel, W., Kainer, K. U., Scharf, C., Ditze, A.: 7th int. conference on magnesium alloys and their applications, Dresden, Nov. 2006.

[6] Ditze, A. Scharf, C.: 14th Magnesium Automotive and User Seminar 28./29. September 2006 Aalen.

[7] Scharf, C., Živanović, P., Ditze, A.: European Metallurgy Conference 2007 Düsseldorf, Vol. 3, ISBN 978-3-940276-06-3, pp. 1405-1412.

[8] Ditze, A. Scharf, C., Blawert, C., Kainer, K. U., Morales, G.E.D.: Magnesiumsekundärlegierung. DE 10 2005 033835 A1, 2005.

[9] Ditze, A., Scharf, C., Blawert, C., Kainer, K. U., Morales, G. E. D.: Magnesium Alloy. WO 2007/009435 A1, 2006.

[10] Beck, A.: Magnesium und seine Legierungen. Springer-Verlag 1939 und 2001, ISBN 3-540-41675-7.

[11] Scharf, C., Zivanovic, P., Ditze, A., Horny, K., Franke, G., Blawert, C., Kainer, K.U., Morales, E., Gießerei, Vol. 94, 11, 2007, pp. 38 - 50

[12] Srinivasan, P.B.; Blawert, C.; Dietzel, W., Wear, to be submitted:

[13] Blawert, C.; Morales, E.; Wiese, G.; Kree, V.; Dietzel, W.; Jin, S.; Ghali, E.: Correlations of microstructure and corrosion properties in HPDC AZ91. In: Pekguleryuz, M.O.; Mackenzie, L.W.F. (Eds.): Magnesium Technology in the Global Age, Conference of Metallurgists, COM 2006. Montreal (CDN), 01.-04.10.2006, 2006. 295 - 314. (ISBN: 1-894475-66-6)

Using Magnesium to Reduce Weight in Aviation Industry- Magnesium Rudder Pedal Assembly for passenger jet aircraft.

I. Reich, A. Wirthiem, O. Wertheim, Ortal Diecasting, Israel
H. Rosenson, Y. Aviav, Israel Institute of metals, Technion Israel

Abstract: Today the majority of all parts in aircrafts are made of aluminum alloys. Replacement of Al by Mg would therefore reduce the weight of parts up to 35%. The mechanical properties of magnesium, high specific strength, castability and energy absorption properties makes the magnesium a preferred material for weight saving applications, especially in the aviation industry.

The subject of this work is replacement of 7075 aluminium alloy rudder pedal assembly produce by machining with an AZ91D magnesium alloy die-cast assembly. The 3 parts magnesium assembly was developed by Ortal in cooperation with the customer. The complicated development involved stress analyses under static and dynamic loads, casting simulations, designing and producing dies and improving and upgrading these dies.

All the 3 parts of the magnesium assembly underwent strict mechanical, corrosion and quality tests, required by the aviation standards and passed these tests successfully.

This innovative design, utilizing magnesium for pedal assembly for the aviation industry will lead to development of additional parts for this field.

Introduction: Ortal Die-casting Company, part of TG Group, is leading a research and development project for replacing aluminum alloy pedals assemblies produced by machining with magnesium alloy die-casting components. Magnesium is the lightest of all commonly used metals and is thus very attractive for transportation applications. It also has other desirable features including good ductility, better damping characteristics than aluminum and excellent castability. Magnesium can be joined by riveting or any commonly used welding methods, it can be machined faster and has the best strength-to-density ratio of any of the commonly used structural metals. Clearly, the low density of magnesium is its major asset. All of these characteristics make magnesium attractive to the aerospace industry. The steering wheels in Boeing aircraft, for example, have historically been made of magnesium alloys and these alloys have been also suggested as substitute for aluminum alloys in seats structure, as well as other applications, due to the potential for weight savings. Magnesium is currently used in aerospace systems but at low capacity. It is, therefore, very important to define what needs to be done to lead to increased aerospace use of magnesium, both in the commercial and military segments of aerospace, and suggest how that increased use can be achieved. In the past, corrosion used to be a problem in magnesium related alloys, but in the last decades, due to the development of high purity alloys and the new coating technologies, corrosion in magnesium alloys is a resolved issue.

Procedure: The Pedal assembly consists of two symmetrical apparatuses (left and right). Each apparatus contains three components: long arm, short arm and pedal. Fig.1 illustrates the general view of the original aluminum assembly.

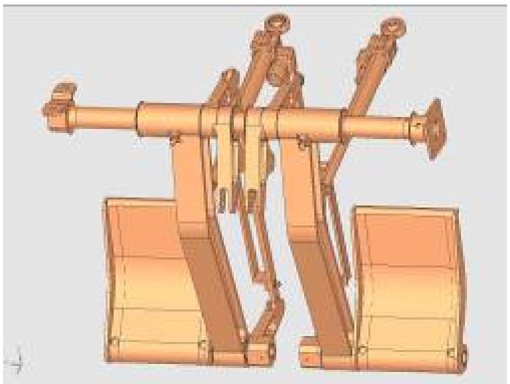

Fig 1: A schematic view of the original aluminum assembly.

The procedure of replacement of machined aluminum 7075 alloy assembly by cast magnesium AZ91D alloy assembly was based on these stages: 1.Feasibility check of the project. 2.Definition of the requirements (loads, environment). 3.Selection of alloys. 4.Specification and verification of alloys properties. 5.Engineering drawing and preliminary design. 6.Simulations and stress analyses (see fig. 2-4). 7.Final design. 8.Equipment and tools production. 9.Production of prototypes. 10.Testing the prototypes. 11.Production of improved components. 12.Coating definition. 13.Qualification tests process.

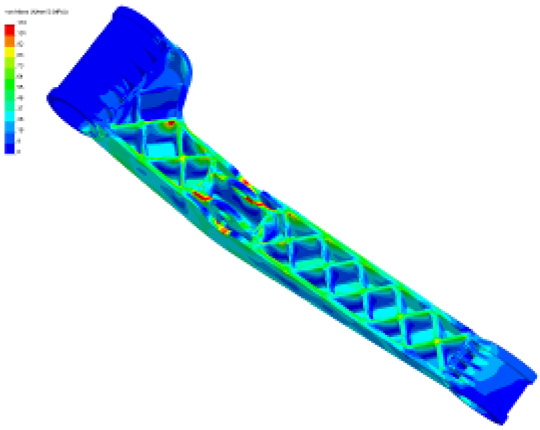

Fig 2: Stress analyses simulation of the long arm.

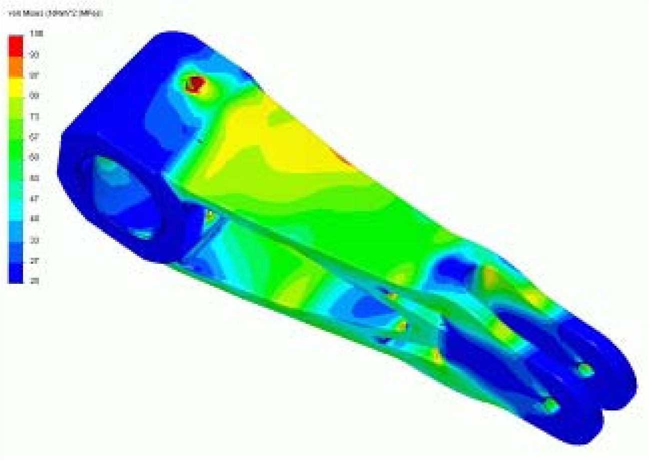

Fig 3: Stress analyses simulation of the short arm.

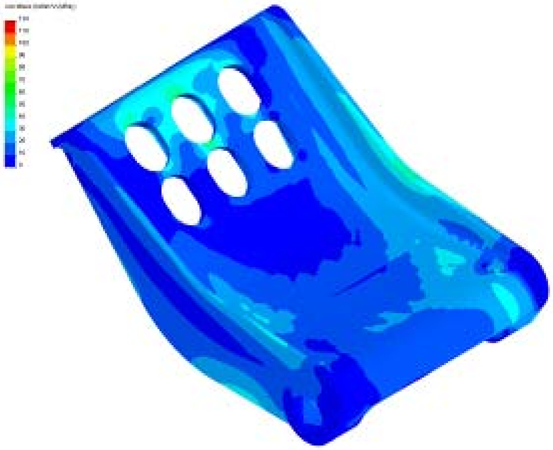

Fig 4: Stress analyses simulation of the pedal.

The assembly components were cast by high pressure die casting machines of two categories. The long arms (left and right) components were cast in 840 tons locking force cold chamber machine, and the short arm and pedal were cast in 500 tons locking force hot chamber machine. Fig. 5 shows the magnesium cast assembly.

Within this development procedure, a designated qualification tests program has been held. The qualification test plan was based on three modes of tests: 1.Mechanical tests. 2.Corrosion substantiation. 3.Flammability substantiation.

Fig 5: The magnesium cast assembly.

Results:

Mechanical tests: Two types of mechanical tests were conducted: 1.Destructive tests which were carried out on samples that were taken from the production sequence of all the assembly components, and 2.Non-distructive tests that were conducted on all the assembly components as a part of an acceptance procedure tests.

Destructive tests

Four types of destructive tests were applied: 1.Application of loads on critical points and positions in order to define the elastic and plastic strains, maximum loads and strain in the elastic zone. The applied load on the long arm is illustrated in Fig. 6 and the obtained displacement-load curves are presented in Fig. 7. The applied load on the short arm and the pedal are illustrated in Fig. 8 and 9. 2.Tension tests of specimens that were cut from critical points of the components (Fig. 10), 3. Microstructure examinations of specimens that were taken from critical points of the components, 4.Endurance tests were applied according duty-cycle procedure (Fig. 11).

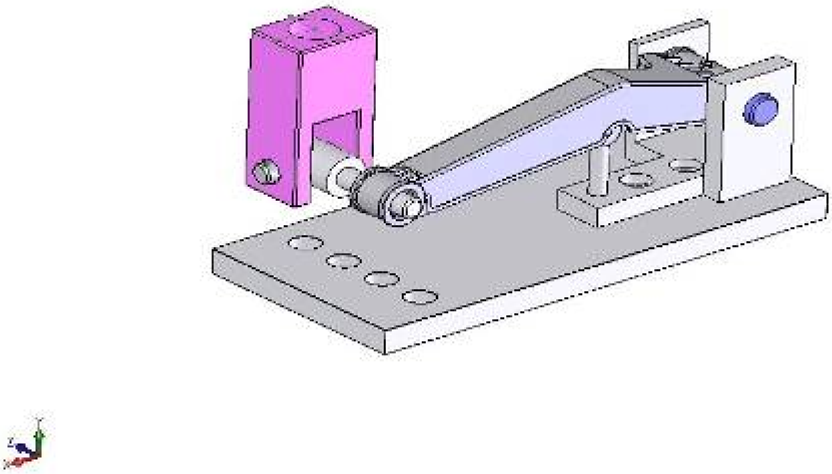

Fig 6: Illustration of the applied load on the long arm.

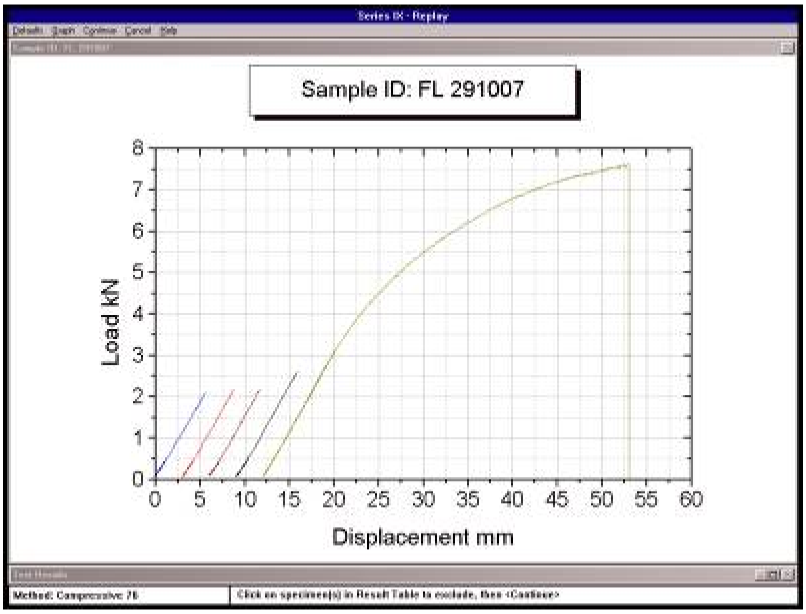

Method: Compressive 78

Click on specimen(s) in Result Table to exclude, then <Continue>

Fig. 7: The obtained displacement-load curves of the long arm.

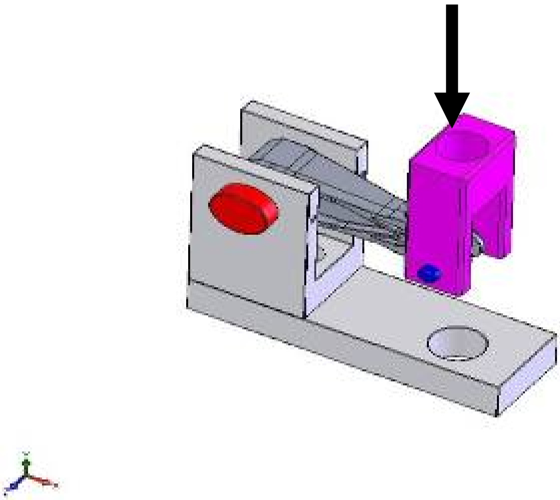

Fig 8: Illustration of the applied load on the short arm.

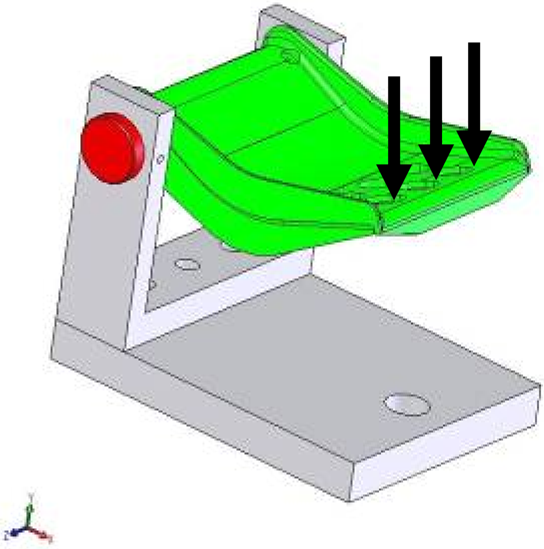

Fig 9: Illustration of the applied load on the pedal.

The qualification test process requirements and some of the quantitative results are presented in Table1.

The long arm was loaded four times until the ultimate load without deformation (see Fig. 3.1. a), and thus was loaded until failure. The short arm and the pedal were loaded until failure of the mounting pins, without any damage of the magnesium components.

***Table 1**. Examined parts, qualification test process requirements and testing results*

Part	qualification test process requirements: loading without deformation, kN		
	Nominal	Ultimate	Obtained
Long arm	1.36	2.04	3.25
Short arm	2.35	3.53	3.25
pedal	1.36	2.04	1.80

It may be seen that the long arm had obtained plastic deformation at a load significantly higher than the ultimate load required by the qualification test process. The behavior of the short arm and the pedal can not be properly discussed based on the obtained results, since the pins of the mounting facility had failed. It may be noted only, that these parts surely demonstrated mechanical properties higher than the nominal one required by the qualification test process.

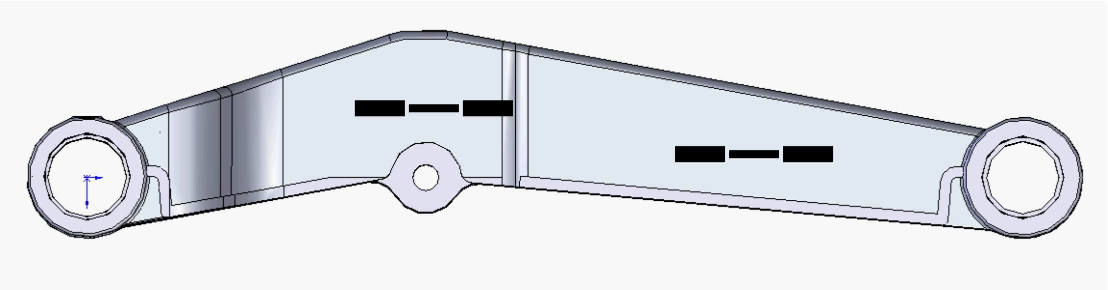

Fig 10: Specimens that were cut from critical points of the components for tension tests.

All the specimens that were cut from the magnesium components and were taken for tension tests, showed good mechanical properties, higher then required by the qualification test process. The microstructure examinations that were performed on specimens that were cut from the sampled components presents a die-cast typical structure without any significant evident.

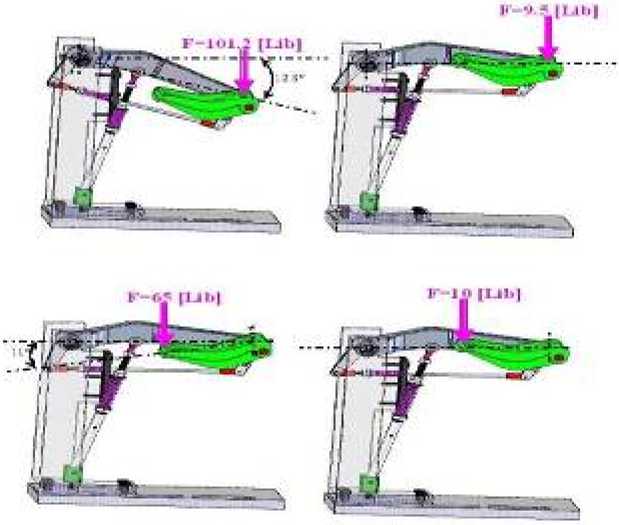

Fig 11: Modes of endurance tests that were applied according duty-cycle procedure.

Non-destructive tests

The following non-destructive tests were applied on every product: 1.Radiographic examinations, and 2. Application of the nominal load (300 Lbs) on the critical points of every one of the magnesium components. The critical points are shown in fig. 6-8.

Corrosion substantiation

Coated and painted specimens were tested in salt spray cabin according to ASTM B117 standard. The specimens were scratched before the introduction into the salt spray cabin. First evaluation of corrosion resistance was performed after exposure of 1000 hours and final evaluation was performed after exposure of 2000 hours in the salt spray cabin. All the examined components withstand the both evaluation and showed good corrosion resistance.

Flammability substantiation.

All the magnesium components passed the flammability tests which were conducted according the requirements of FAR Part 25, Appendix F, Part I.

Summary: a successful rudder pedal assembly was developed from magnesium AZ91D alloy. The assembly components were cast by high pressure die casting machines of two categories. The long arms components were cast in 840 tons locking force cold chamber machine, and the short arms and pedals were cast in 500 tons locking force hot chamber machine. Replacing the contemporary aluminum 7075 alloy assembly is followed by 35% weight reduction (the weight of the aluminum assembly components was ….. while the magnesium components weight is….). All the parts of the magnesium assembly underwent strict mechanical, corrosion and quality tests, required by the aviation standards and by specific qualification test process and fulfil successfully all these requirements.

This successful development project, which demonstrate the potential of magnesium alloys of high mechanical properties and highly considerable weight saving, will lead to many innovative solutions in the aerospace and automobile industries, and will increase the awareness to weight saving potential of the magnesium in the aviation field.

Mobile with Magnesium Sheet

Peter Juchmann, Sébastien Wolff
Salzgitter Magnesium-Technologie GmbH, Salzgitter, Germany

Abstract
In Europe several R&D-activities concentrate on the development of new Magnesium wrought materials and process chains especially for automotive applications. Salzgitter Magnesium-Technologie GmbH is heading an ongoing joint research project in Germany called “**M**obil **m**it **M**agnesium”, in which among other partners leading automotive companies like Daimler and Porsche are involved. The following presentation shall give a brief overview of current material-, process and application developments.

Keywords: Magnesium sheet, AZ31, ZE10, Mobil mit Magnesium, sheet forming, automotive applications

INTRODUCTION

Magnesium sheet – how long will the breakthrough of this lightweight structural material take? Such a question seems to be justified, because worldwide growing R&D activities concerning Magnesium sheet production and application are still in extreme contrast to a limited series use. However, the intensified discussion about ecologically beneficial processes and natural resources create a basically fortunate climate for new lightweight metallic materials.

Mobile with Magnesium sheet

Report about some current R&D-activities in Germany with the accent on a joint BMBF-project “Mobil mit Magnesium”

Peter Juchmann, Sébastien Wolff
www.szmt.de

International Magnesium Association
65th Annual World Magnesium Conference, Warsaw, Poland, May 18-20, 2008

Illustration 1: Topic - Mobile with Magnesium sheet

In competition to Steel, Aluminium, reinforced plastics or Magnesium-diecastings especially Magnesium rolled products represent an universal semi-finished product group for ultralight and rigid sheet forming parts for automotive or aircraft use as well as for mass-reduced components of i.e. high performance machinery. Nevertheless, a breakthrough of Magnesium sheet metal in volume markets seems to be very difficult. On the one hand, this is due to insufficiently answered technical questions of part design, corrosion protection and assembly. On the other hand, Magnesium sheet is still comparatively expensive resulting from a limited infrastructure for high volume strip production, which goes together with a low and only slightly growing demand.

GERMAN R&D-PROJECT “MOBIL MIT MAGNESIUM”

Despite limited series applications the prototyping and testing of Magnesium sheet metal parts goes on in Asia, North America and Europe at high speed. Supported by the Ministry of Education and Research (BMBF) an ongoing German joint project called „**M**obil **m**it **M**agnesium“ is focused on technically and economically competitive process chains for Magnesium sheet applications in automotive. Special emphasis is laid on application orientated solutions for interior and car-body components. The cooperation is headed by Salzgitter Magnesium-Technologie GmbH and incorporates the following Magnesium-experienced partners:

Industrial partners:

Salzgitter Magnesium-Technologie GmbH, Salzgitter	(SZMT; leader)
ThyssenKrupp Umformtechnik GmbH, Ludwigsfelde	(TKU)
AIMT Holding GmbH, Kerpen	(AIMT)
GP Innovation GmbH, Lübbenau	(GPI)
Böllhoff Systemtechnik GmbH & Co.KG, Bielefeld	(Böllhoff)
Daimler AG, Sindelfingen	(Daimer)
Porsche Engineering Group GmbH, Weissach	(Porsche)

Research institutes:

GKSS Forschungszentrum GmbH, Geesthacht	(GKSS)
Institut für Werkstoffkunde, Universität Hannover	(IW)
Lehrstuhl für Umformtechnik und Gießereiwesen, TU-München	(utg)
Institut für Umformtechnik, Universität Stuttgart	(IFU)

Illustration 2 shows structure and work packages of the joint project „Mobil mit Magnesium“.

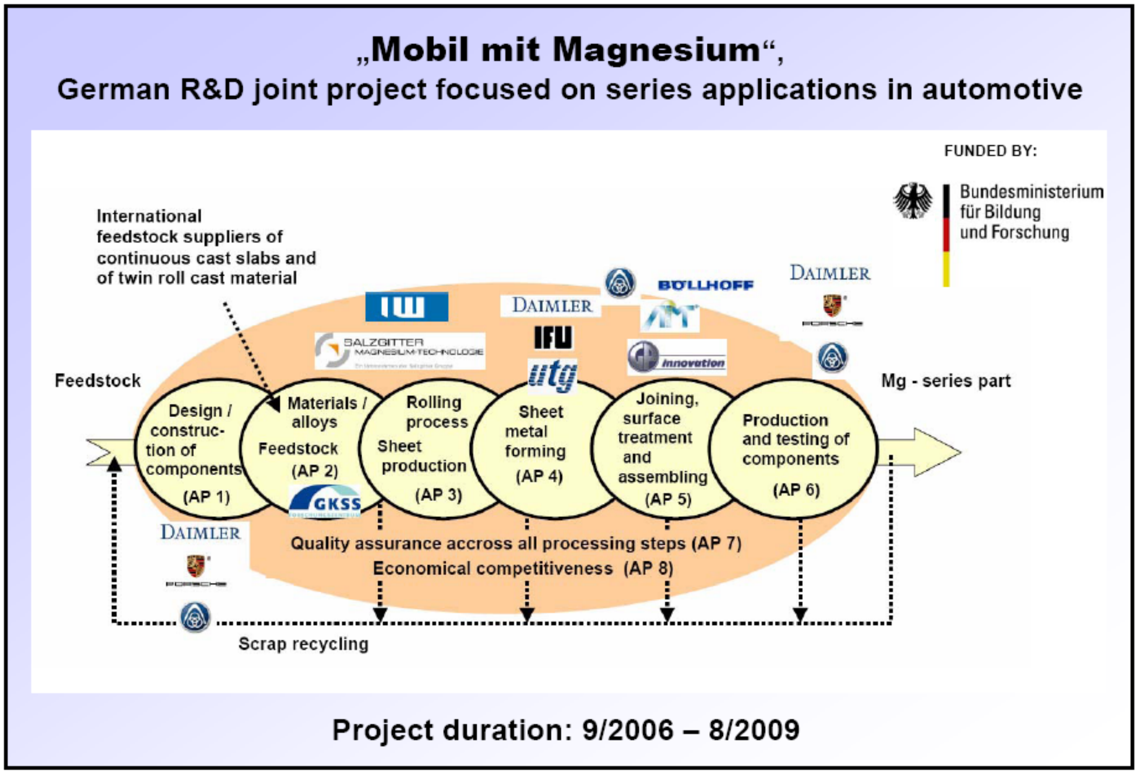

Illustration 2: Joint project „Mobil mit Magnesium“ – Structure and work packages

MATERIAL DEVELOPMENT AND SHEET FABRICATION

Supported by material research partners the development of sheet metal alloys, rolling processes and semifinished products takes place at Salzgitter Magnesium-Technologie GmbH (SZMT) using an industrial Magnesium rolling mill in Salzgitter, Germany. Meanwhile SZMT produces a wide range of tailor-made rolled products and also accompanies its customers as material and technology partner in downstream processing steps up to product solution and series production. With a maximal rolling width of nearly 2,000mm and a minimal thickness of 1.0mm nearly all sheet dimensions required by the automotive industry and many other transportation sectors can be fabricated. On the one hand, the single sheet production offers the opportunity for a flexible and demand-orientated qualification and production of tailor-made Magnesium sheet metal grades, dimensions and quantities. On the other hand, certain limitations concerning productivity and surface quality have to be accepted, which can only be overcome completely by strip processes. At present Salzgitter’s capabilities enable customers to get in touch with this new material group and to start testing first processing steps and applications.

Magnesium sheet alloy developments concentrate on an enlarged technological property profile [1-3]. The objective is to significantly increase the formability compared to the standard grade AZ31B, while reaching or ensuring best possible surface quality and acceptable corrosion resistance. This material qualification corresponds to improved sheet metal production capabilities based on DC cast- as well as on twin roll cast feedstock.

Looking at the mechanical and microstructural properties an interesting correlation between formability, strength and texture can be observed, which helps to draw conclusions for further material design. In illustration 3 micrographs show a more homogeneous and finer grain structure for AZ31B standard sheet metal compared to an alternative alloy ZE10. Both materials are examined in a finally annealed „O“- condition. In contrast to that AZ31B reveals a typical but strong basal texture in the rolling plane, which is basically unfavourable for sheet metal forming. Compared to that ZE10 sheets show a completely different texture profile of significantly lower intensity, which is characterized by an increased expansion perpendicular to the rolling direction. This microstructural characteristic of ZE10 i.e. corresponds with an extended sheet metal formability at lower temperatures and higher deformation speeds. The mechanical properties measured in a room-temperature tension test according to DIN-EN 10002 do not fully represent this behaviour. To optimize the isotropy of mechanical properties is one main aspect of further material qualifications.

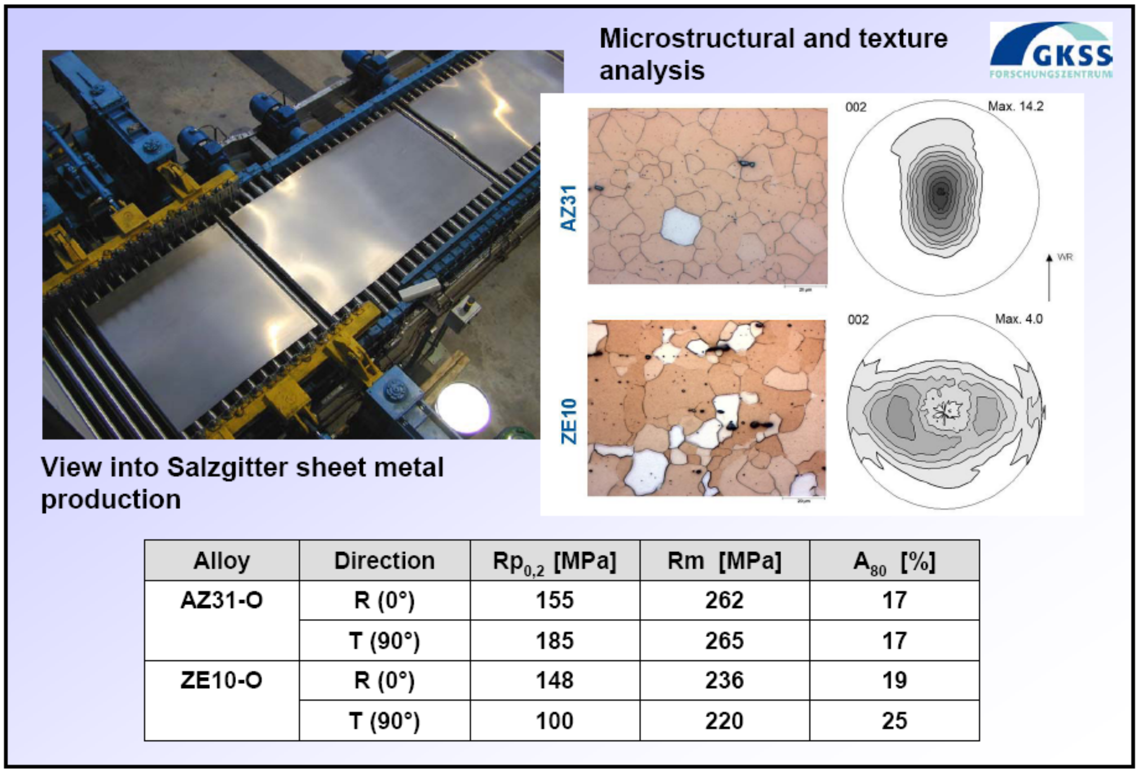

Microstructural and texture analysis

View into Salzgitter sheet metal production

Alloy	Direction	$Rp_{0,2}$ [MPa]	Rm [MPa]	A_{80} [%]
AZ31-O	R (0°)	155	262	17
	T (90°)	185	265	17
ZE10-O	R (0°)	148	236	19
	T (90°)	100	220	25

Illustration 3: View into Salzgitter’s sheet metal rolling and mechanical properties (SZMT): Alloy dependent texture analysis of hot rolled Mg-sheet metal (GKSS)

The quality of sheet metal products is documented in i.e. 3.1B standard certificates according to DIN-EN 10204 including selected mechanical and microstructural properties as well as chemical and surface specifications. For example annealed AZ31B-O sheet metal reaches a fully recrystallized grain structure with an average grain size of roughly 10µm. Due to high optical requirements the as rolled untreated surface shows a comparatively low roughness. The R_a-values normally range in the field of 0.3 to 0.5 µm.

SHEET PROCESSING AND APPLICATION DEVELOPMENT

Preferable application fields for Magnesium sheet metal include the 3C-market as well as the automotive sector. Here a variety of attractive interior and body components can be identified, where rolled Magnesium can point out its technical advantages. Typical for new materials Magnesium sheet will certainly be used at first in ready to be installed modules. Thus Magnesium sheet components may be divided into different categories according to a growing complexity of corrosion and optical requirements (illustration 4). The spectrum of parts which has already been prototyped to a large extend includes mechanically loaded interior components (category I) like a back-seat panel, design parts as well as crash-relevant bumper beams and hang-on reinforcements up to high-end outer-skin solutions. Related to the finally mentioned category III it has to be pointed out that exterior applications are in its very early stages of development. Questions like a powerful long-term corrosion protection especially in the case of surface damage (stoning, vandalism) as well as an integration of Magnesium sheet parts in hybrid structures protected against galvanic corrosion have to be answered.

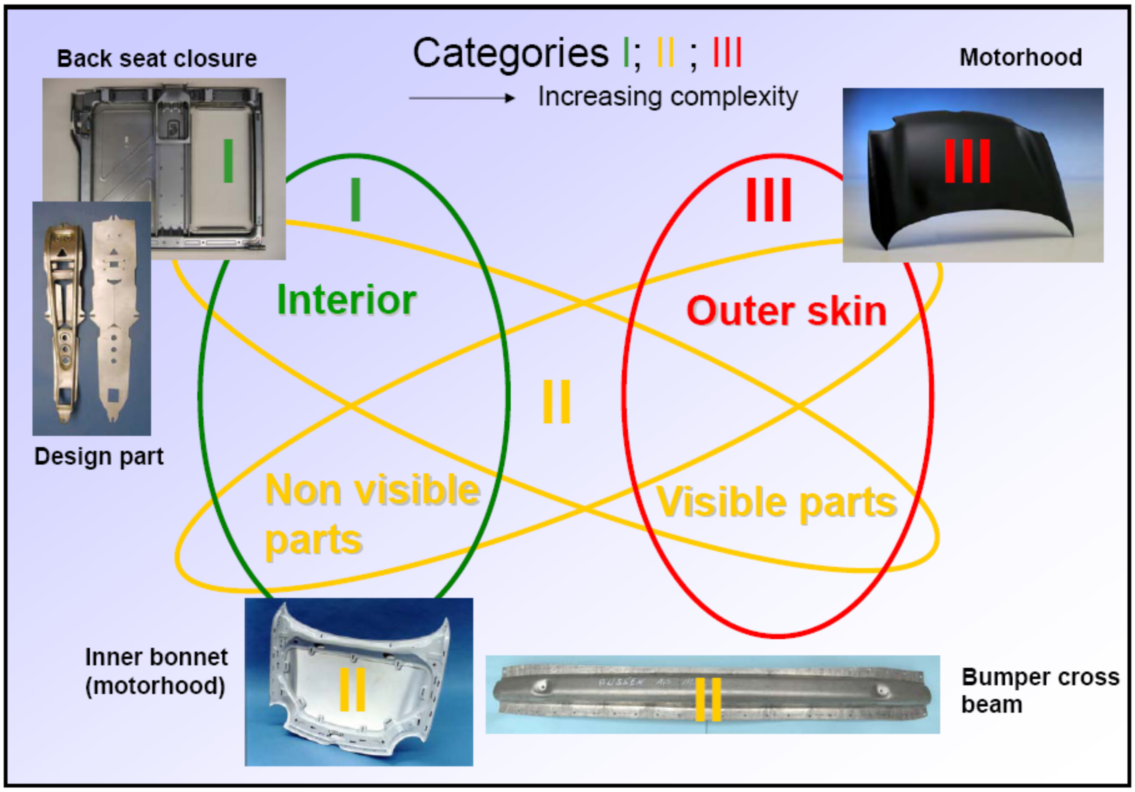

Illustration 4: Potential application areas for Magnesium sheet in automotive

R&D-projects like „Mobil mit Magnesium“ work at complete process and product solutions starting from alloy selection and semifinished products to the finally assembled and proved part [4, 5]. A retractable hard top represents one key demonstrator (illustration 5). Here overall advantages of weight saving can be ideally connected with a lowered gravity point of the car and an improved mobility of the roof system. Thus an AZ31B-O reinforcing inner bonnet was fabricated by hot deep drawing at roughly 200°C. Following operations like cutting and calibration steps were carried out at room-temperature with series tool equipment. Using the alternative sheet grade ZE10 geometrically acceptable parts could be produced at temperatures down to roughly 100°C.

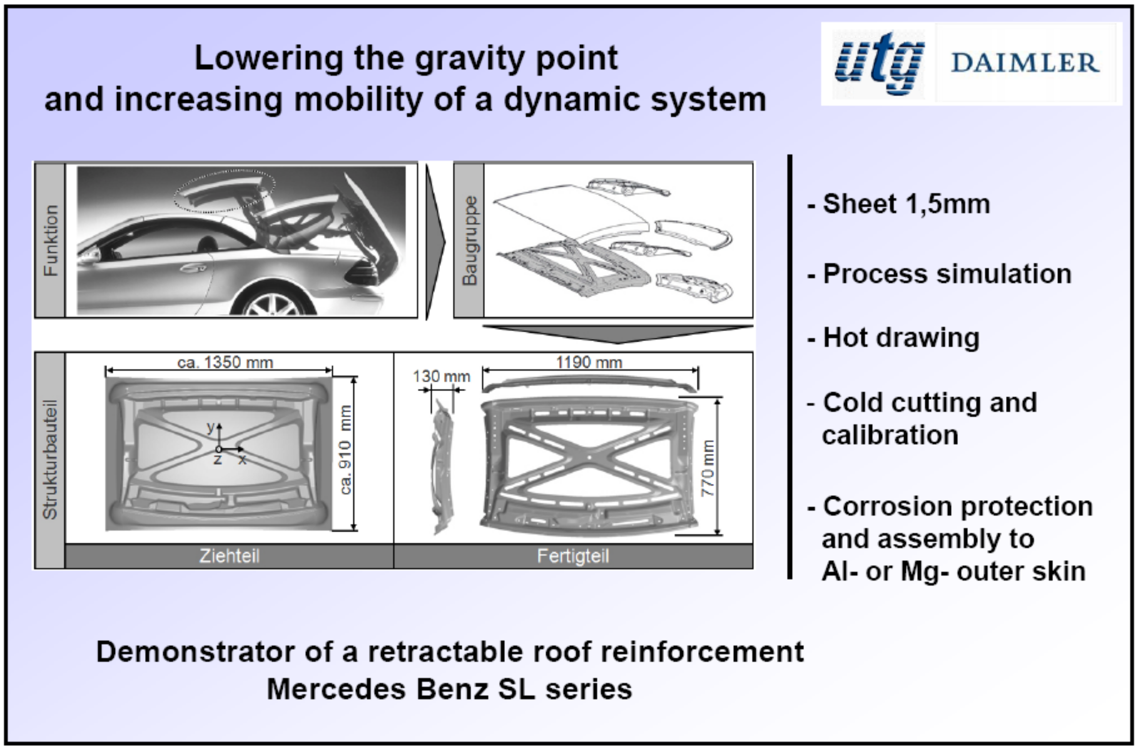

Lowering the gravity point and increasing mobility of a dynamic system

utg DAIMLER

- **Sheet 1,5mm**
- **Process simulation**
- **Hot drawing**
- **Cold cutting and calibration**
- **Corrosion protection and assembly to Al- or Mg- outer skin**

Demonstrator of a retractable roof reinforcement
Mercedes Benz SL series

Illustration 5: Demonstrator - reinforcing inner bonnet of a retractable roof, Mercedes Benz SL

In the past hot forming seemed to be a limiting factor for Magnesium sheet processing. It has been developed significantly and is even much more popular today for demanding Steel- and Aluminium alloys. For simulation a growing data base is available including temperature dependent limit forming diagrams. Nevertheless, the “virtual world” will remain an important R&D-topic for Magnesium sheet.

Furthermore, the example of a completely cold bended Magnesium profile may underline the general chance to form some smoothly shaped Magnesium parts without heating. On a 16-step rollform facility normally used for high strength steel coils well deformable Magnesium-sheets could be easily processed without any modifications (illustration 6). Orange skin and edge crack formation, which has to be expected for AZ31B standard material, did not occur. A first comparison of mechanical properties did not show a significant variation from sheet to profile. Microstructural effects of cold forming operations are under evaluation.

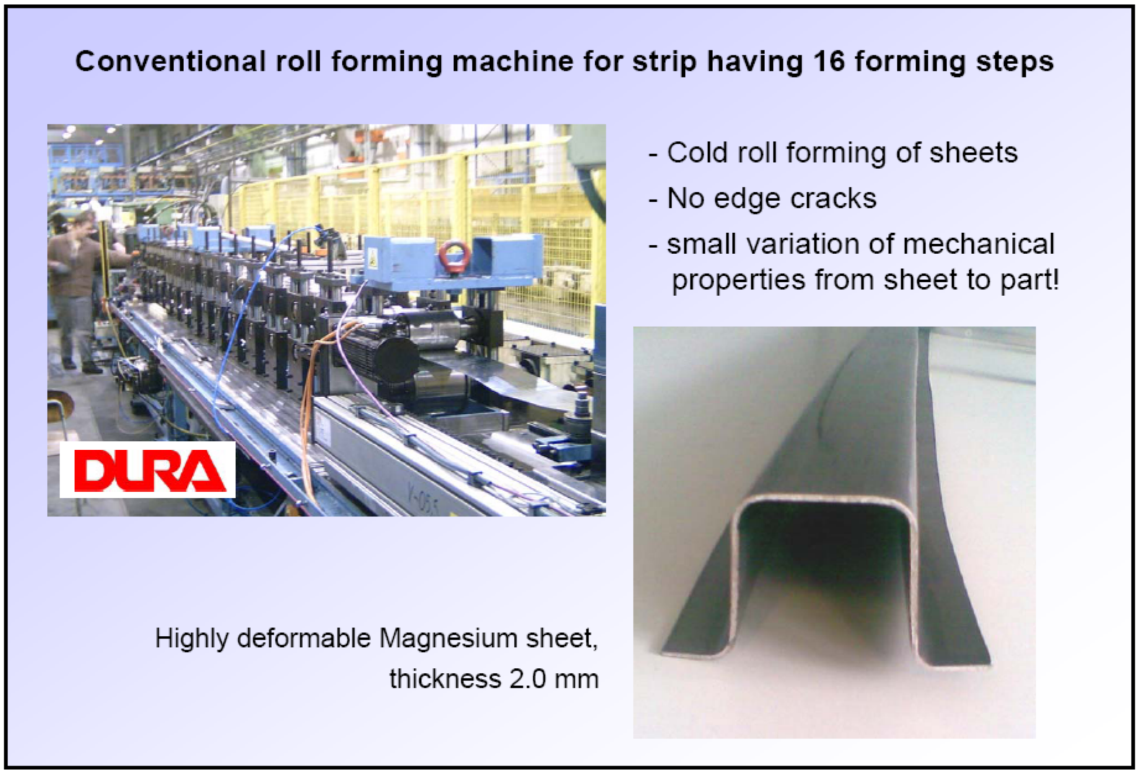

Conventional roll forming machine for strip having 16 forming steps

- Cold roll forming of sheets
- No edge cracks
- small variation of mechanical properties from sheet to part!

Highly deformable Magnesium sheet,
thickness 2.0 mm

Illustration 6: Cold roll-forming of Magnesium sheet profiles

At the same time further developments are focused on adequate solutions for joining, corrosion protection and assembly. Some aspects are shown looking at another prototyping example of a common project “ScaLight” of Salzgitter AG and Wilhelm Karmann, an established German manufacturer of niche cars.

Here an ultralight, dent-resistant Magnesium sheet front wall part was connected with an advanced Steel body in white structure. There, it contributes to an increased torsional stiffness of a cabrio vehicle (illustration 7). For prototyping 3mm AZ31B-sheets were preheated in a separate oven and pressed in a cold tool without blank-holder. The objective was to use their forming potential best possible. Unacceptable wrinkling was not observed. This successful drawing strategy also confirms experiences gained with large hang-on parts (like retractable roof), in which flat and elastic blank-holders were used to locally influence the sheet metal flow. Structural simulations show the mechanical stability of the Magnesium front wall even in case of a highly loaded roll-over.

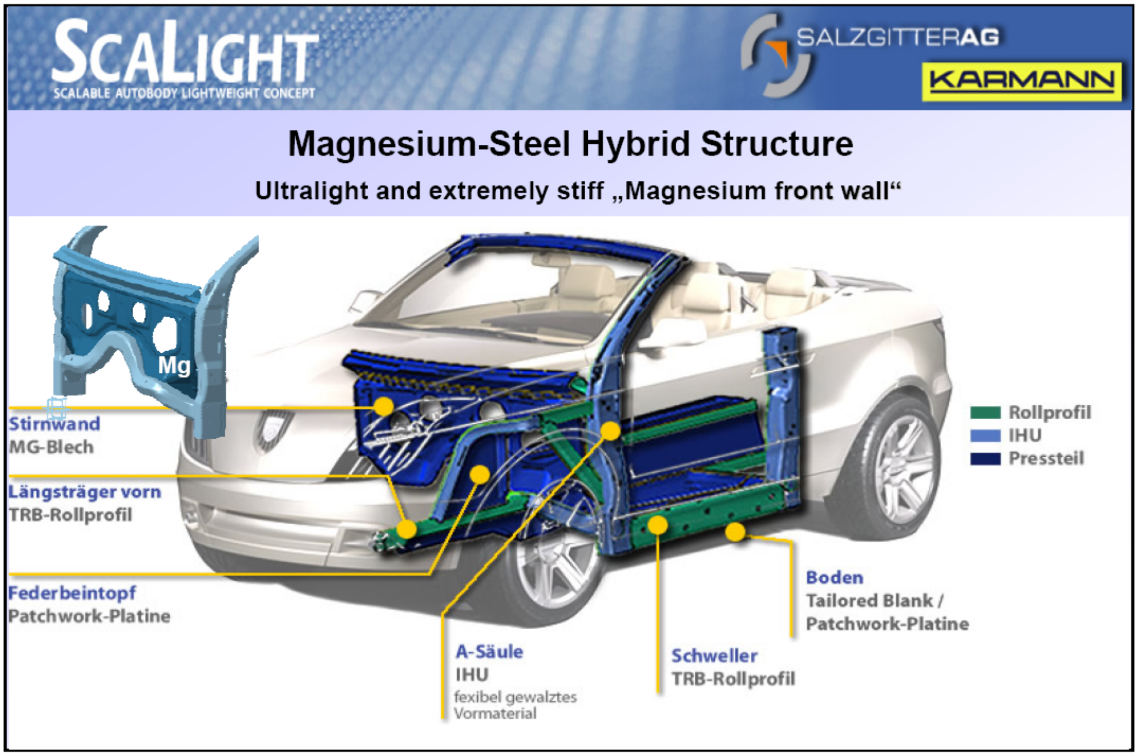

Magnesium-Steel Hybrid Structure

Ultralight and extremely stiff „Magnesium front wall“

Illustration 7: Lightweight design of cars using Steel-Magnesium hybrid structures (Project ScaLight)

Joining and corrosion protection methods have been selected with regard to specific assembly conditions and industrial process chains. After laser cutting the Magnesium front wall was chemically treated and powder coated. This pre-treatment will be the basis for an adhesive bonding to the Steel body in white frame. The Magnesium part will be additionally fixed with spread rivets made of plastics, until the conglutination is hardened. This hybrid joining technique completes the concept of an efficient galvanic material separation. Other components like pedal systems will be assembled using suitable Al-fastening elements. Ongoing laboratory corrosion tests will give a first clarification about the performance of this Steel/Mg hybrid strategy. Further experiences have to be gained in field tests.

CONCLUSIONS

For using Magnesium sheets in future automotive applications the following items could be summarized.

1. New Magnesium sheet products really open interesting perspectives for a metallic ultra-lightweight design of cars.
2. Series developments even for higher loaded interior and body components seem to be possible by using the present and continuously increasing state of the art.
3. The long-term corrosion protection for out-door components has not been achieved yet. Surface treatments are necessary, which prevent corrosion even in case of stoning or other damages.

4. Magnesium sheets have to face the hard competition of other structural materials and are still much more expensive in comparison to Steel and Aluminium.
5. By now series applications seem to be only realistic in high price niche vehicles.
6. Volume applications need a cooperative growth of demand and industrial sheet and strip production capabilities.
7. Among others Salzgitter Magnesium-Technologie GmbH is prepared to assist as experienced material supplier and technology partner for tailor-made Magnesium-sheet solutions.

ACKNOWLEDGEMENTS

The Government of Lower Saxony, the European Union, the German Ministry of Education and Research as well as its project coordinator ptj are gratefully acknowledged for funding our R&D-work.

Furthermore, many thanks to our project partners of “Mobil mit Magnesium”, DURA automotive as well as to our sister company Salzgitter Mannesmann Forschung GmbH for supporting this paper with results, data and helpful discussions.

LITERATURE

[1] Bohlen, J.; Nürnberg, M.R.; Senn, J.W., Letzig, D.; Agnew, S.R.;
The texture and anisotropy of magnesium-zinc-rare earth alloy sheets;
Acta Mater. 55 (2007) 2101-2112

[2] Liu, J.; Chen, Z.; Yan, H.; Chen, D.; Research of deformation characteristics in polycrystalline AZ31 Magnesium alloy at moderate temperatures;
Metall, 62. Jahrgang 1-2/2008, 43-46

[3] Hillis, J.; Chapter 7.2 Corrosion; Magnesium-Technology, Eds. Friedrich, H. and B.L. Mordike; Springer-Verlag 2006

[4] Juchmann, P.; Magnesiumblech – noch Chancen in der Karosserie der Zukunft?;
Proceedings: 26. Europäische Karosseriekonferenz, Strategische Fragen des Karosseriebaus heute für morgen, 26.02.2008, Bad Nauheim, Germany

[5] Juchmann, P.; Wolff, S.; Taron, R.; Leichtbauwerkstoff Magnesiumblech – wo bleibt der Durchbruch?; 28. EFB-Kolloquium Blechverarbeitung 2008, 03.04.2008 Dresden, Germany

Cost attractive lightweight solutions through new Mg-concepts for the vehicle structure

Prof. Dr. Horst E. Friedrich, DLR
Dipl. Ing. Gundolf Kopp, DLR
Dipl.Ing. Elmar Beeh, DLR
Tony Lawson, Meridian Technologies
Luca Zaffaina, Meridian Technologies

Contents

Abstract

The reduction of the vehicle mass is an important point in order to reach new milestones in reducing fuel consumption and emissions. Today's and future steel structure concepts still shows lightweight potential. But even more attractive potential for lightweight body in white structures could be realised by new multi material design concepts. The DLR (German Aerospace Center) Institute of Vehicle Concepts and Meridian Technologies Inc. are working on innovative and cost attractive magnesium A-pillar solutions. By using the topology optimisation a new design idea for the A-pillar area was found. This new design concept offers the possibility to integrate additional functions. The new design shows expedient crash behaviour. A developed solution has a weight benefit of more than 50% compared to a steel reference structure. Because of functional integration the magnesium part is very cost attractive. To achieve the requirements of corrosion prevention Magnesium parts need to be proper designed. Within the example of a serial production Front End Carrier (FEC) possible solutions will be shown.

1 Introduction

Worldwide CO_2 emission and therefore also the proportion attributable to traffic is considered to be one of the reasons of climate change. The Institute of Vehicle Concepts (DLR-FK) is working on the technology of low-emission vehicles of tomorrow. Research areas pursued by the Institute with the aim of achieving mobility with low or even zero CO_2 emission include:

Increasing energy efficiency:

- Secondary energy utilisation
- Alternative energy conversion

Reducing driving resistances:

- Lightweight construction strategies
- Multi-material design
- Hybrid design

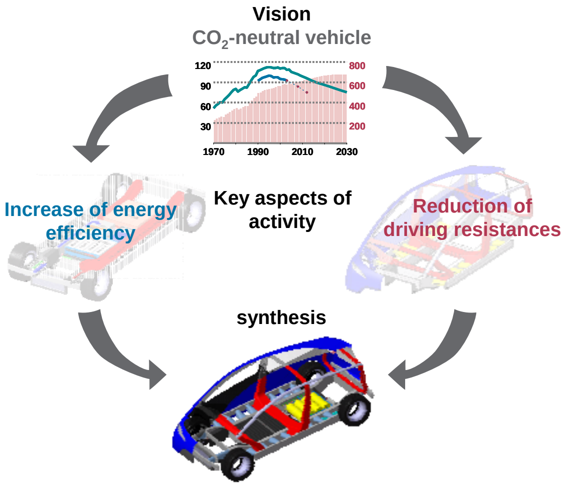

Fig 1: Vision: a CO_2 neutral vehicle

The results from the individual technologies make up a portfolio for a synthesis of new vehicle concepts primarily developed by the DLR-FK as a partner of the vehicle industry.

1.1 Potential of magnesium

Magnesium is a material with a great growth potential. The ‘Magnesium Vision 2020‘ study conducted by the United States Automotive Materials Partnership (USAMP) [1] demonstrates clearly that the magnesium components already implemented in vehicles today could be increased to cover a significantly higher proportion of vehicle parts. Every North American vehicle contains an average of approximately 5-6kg of magnesium at present. The weight of all the individual parts used however adds up to 190kg of magnesium. Examples of parts that have already been realised include seat structures, control panel mounting, gearbox casing and engine mounting systems. Obstacles nevertheless stand in the way of a broader utilisation of magnesium. At the moment one of these is the problem of magnesium extraction. The majority of crude magnesium is currently obtained in China. The method used is both energy intensive and environmentally damaging. A further challenge for successful utilisation of magnesium in vehicles is presented by the problem of corrosion of the material. In addition to this generally solvable criterion, there are other circumstances making it difficult for magnesium solutions to become widespread. The vehicle structures of today are often optimised for sheet metal shell constructions. New construction methods to suit the material are required to realise lightweight design using magnesium. Examples of structural parts made of magnesium conceived by the DLR Institute for Vehicle Concepts in conjunction with Meridian Technologies are presented below.

2 Topology optimisation of front end and concept design

2.1 Definition of design space requirements

The front end structure selected as a basis for development of a concept is a technologically challenging and particularly interesting area for lightweight construction. A topology optimisation was carried out based on the general requirements and load cases as well as the available design space. A lower middle range car was selected and the available design space was constructed using CATIA V5. In contrast to the standard practice in vehicles of today, the engine hood area was specified as potential load-bearing structure.

Fig 2: Constructed design space for topology optimisation

2.2 Topology optimisation

This 3D data record was then processed using the topology optimisation tool TOSCA. A total of 12 load cases (see below) were included in the optimisation.

Load cases:

- Torsion, left + right
- 1g compression (downward bend)
- Upward bend
- Curve motion, left + right
- Braking
- 40% front crash, left + right
- 30° inclined front crash, left + right
- Pole crash, front

Since today’s topology optimisation tools are not suitable for optimisation of dynamic load cases, crash load cases were assumed to be equivalent static load cases. Since the illustrated design space only represents one part of the vehicle structure, special attention was paid to reproduce the behaviour of the non-represented remaining structure as realistically as possible. An elastic rather than rigid support was specified for the design space shown above for this purpose. Using the 40% front crash load case, a prescribed load distribution was set by adjustment of the individual spring stiffness values.

- 2 x A-pillar: 12.5% each
- 2 x Rocker panel: 25% each
- Transmission tunnel 15%
- 2 x Base: 5% each

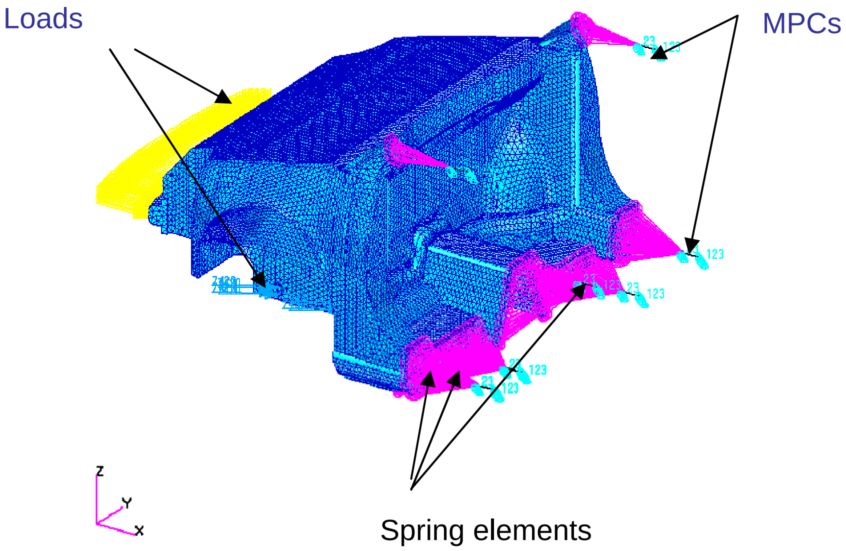

Fig 3: Loads and supports for topology optimisation

The importance of specification of the load distribution is clearly indicated by the table below. The first four columns show the respective absolute and percentage share of the load for the rigidly supported total model and the optimised result model. It becomes clear that 70% of the load is directed to the base during optimisation. The base of a real vehicle however takes up significantly smaller longitudinal forces. If the result was used for establishment of an optimal front end structure in this form, an incorrect result would be obtained. The four columns on the right of the table show the effect of the spring support. The optimisation allows allocation of realistic loads to the individual structural areas and thereby simulation of the stiffness of the missing residual vehicle structure.

	Bauraummodell, fest fixiert		Opt, 10 % Vol, fest fixiert		Bauraummodell, feder in x		Opt, 10 % Vol, feder in x	
	RFx	%	RFx	%	RFx	%	RFx	%
a-säule	-25588.623	12.79	-28427.1758	14.18	-24572.31	12.29	-25749.66	12.87
a-säule	-25399.9297	12.70	-28889.274	14.65	-24315.37	12.16	-22944.7	11.47
schweller	-16506.0645	8.25	-0.625537	0.00	-50697.52	25.35	-49971.93	24.99
schweller	-16237.5713	8.12	-11.536131	0.01	-50083.52	25.04	-50298.9	25.15
mitteltunnel	-19937.1484	9.97	-50.073971	0.02	-30119.36	15.06	-30795.89	15.40
boden	-47713.5664	23.86	-71310.75	35.57	-10144.56	5.07	-10049.2	5.02
boden	-48617.2813	24.31	-71310.75	35.57	-10067.55	5.03	-10189.91	5.09
Summe RFx	-200000.185		-200000.185		-200000.19		-200000.19	

Fig 4: Load distribution with and without spring support of the design space

The result of the structure optimisation is a structure with improved stiffness. This topology optimisation serves as a basis for further conceptual considerations. The aim of the project was to design a highly loaded magnesium structure with a high degree of functional integration. On closer inspection of the topology optimisation, it becomes evident that in contrast to the strut mounting concepts used today, no direct (in the direction of the spring effect) connection between strut mounting and the side member area is achieved. Instead a cantilever type of connection from the A-pillar forwards to the spring plate is obtained. This realisation gave rise to the idea of integrating the spring plate base in one large A-pillar cast node.

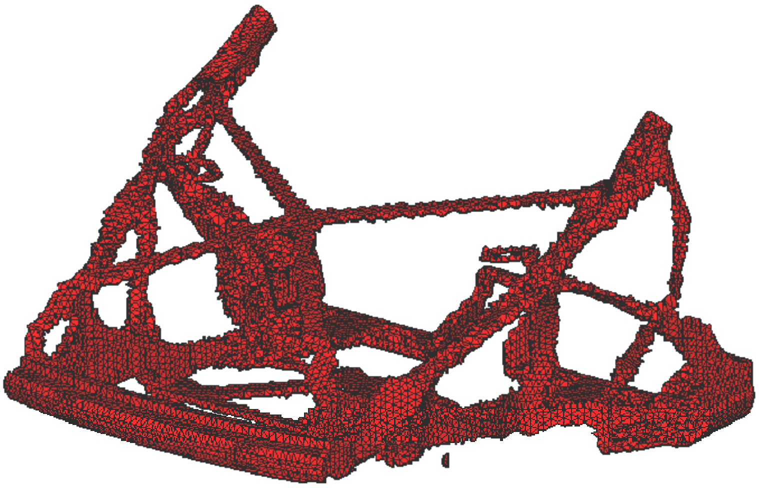

Fig 5: Result of topology optimisation – View 1

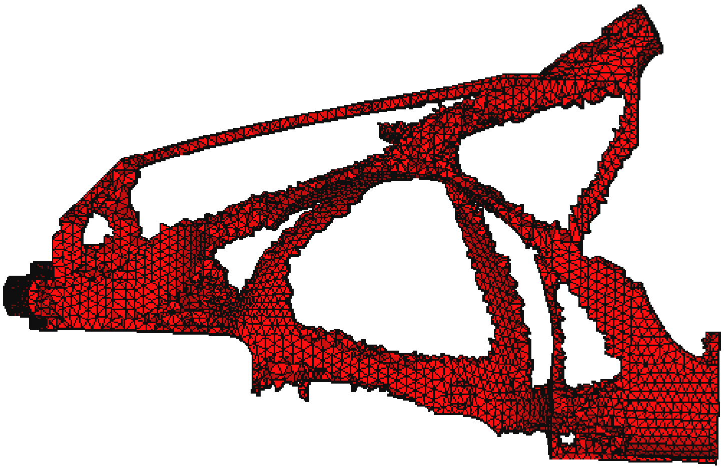

Fig 6: Result of topology optimisation – View 2

3 Detail development of the highly integrated cast Mg node

3.1 Construction and computed design of the A-pillar node

Starting with the topology optimisation results, a close-to-production preliminary development of the A-pillar node with integrated spring plate was carried out with the support of Meridian Technologies. The aim of this work was to determine the potential of magnesium for a highly loaded vehicle structure. Component specific load cases for this structural area were defined for this purpose. In addition to load cases at the strut mounting, door lowering load cases and a crash load case were included. The main load at the strut mounting was purposely exceeded by 1/3 in order to demonstrate scalability to higher vehicle classes.

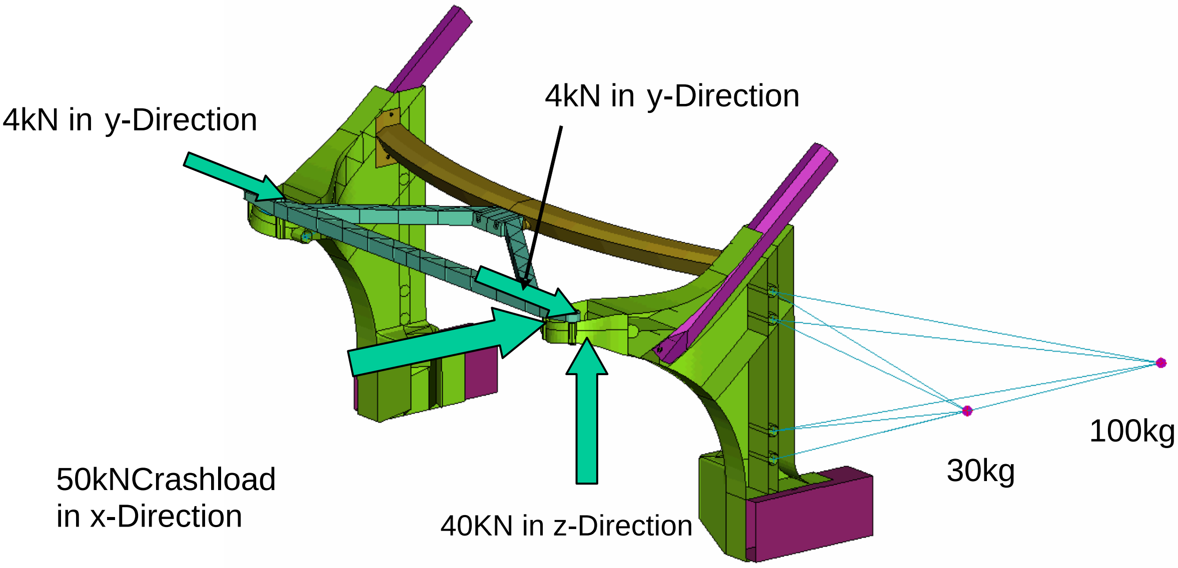

Fig 9: Design loads for the A-pillar node

A component specific topology optimisation in the available design space was carried out with the specified loads. This was then transformed into a rib pattern which was optimised by a topometry optimisation with reference to wall thicknesses. This work was conducted by Meridian Technologies in the European Development Centre in England.

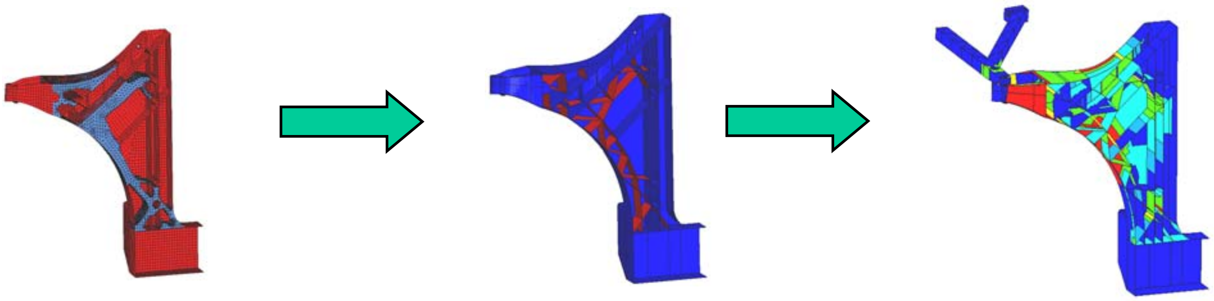

Fig 10: Component evolution by topology and topometry optimisation

A functional lightweight structure made of magnesium that meets the load case requirements including crash was developed using this procedure. Tensional forces of 130MPa are developed in the component during the crash load case. Component expansion remains below 6% so that no structural failure occurs.

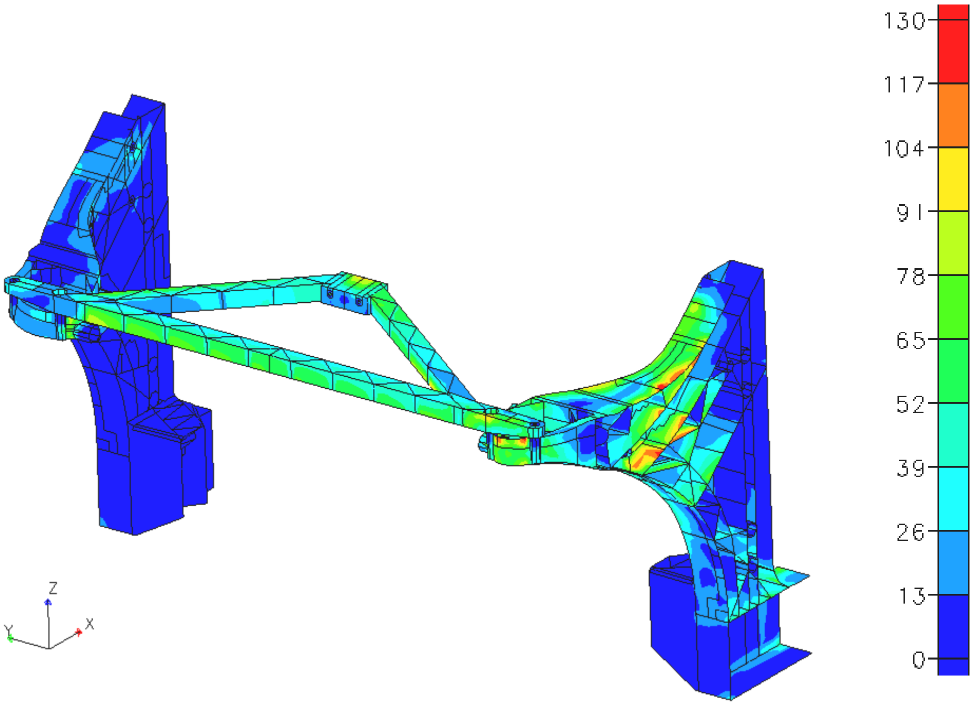

Fig 11: Computed result for the ODB crash load case

3.2 Cost and weight consideration

A weight saving of 43% was achieved with the developed design method in association with using magnesium as a material. With a modified two shell design of the part a weight saving of >55% have been achieved. Taking a lower middle range vehicle for comparison, 12 steel moulded parts were replaced with one casting. With regard to costs, it was estimated on the basis of data available at the Institute of Vehicle Concepts that production of a magnesium casting with the same degree of functional integration would be possible at the same price. The necessary corrosion protection is already taken into account here.

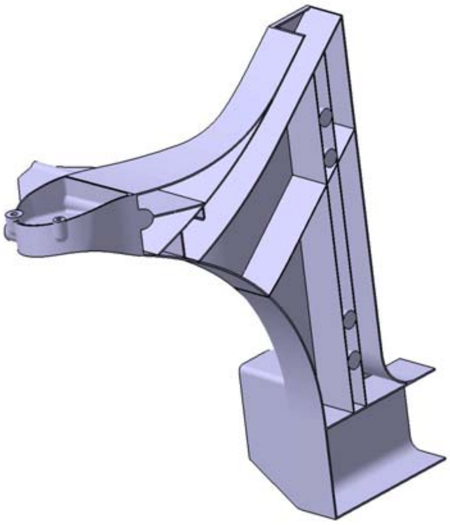

Fig 12: Detailed view of the A-pillar node

Summary:

- **Weight saving: 43% (5kg) proved by calculation**
- **Weight saving > 55% with a modified two shell design possible**
- **Component costs: Same than steel reference value**

4 Challenges and solutions for exterior magnesium applications

4.1 Example of a structural exterior magnesium application in serial production

Traditionally vehicle body structure front end modules have been either fabricated pressed steel assemblies, fabricated pressed aluminium assemblies or plastic / steel hybrids. Magnesium die cast technical solutions are now in series production (figure 1) which are either welded at the “BIW” stage or bolted in the body at the exterior trim stages of production.

The most evident advantage in using magnesium for a FEC is weight saving: a reduction of up to 9kg over steel system equivalent technology can be achieved [3]. Magnesium also offers good savings versus aluminium assemblies and in a minor extent over plastic steel hybrids. In addition to that, improvements to body structure performance and NVH can be achieved, together with enhanced geometric stability (fit and finish) advantages and integration opportunities (reduced complexity and cost) whilst satisfying durability, crash, corrosion and visual requirements. In addition, the reduced mass at the front of the vehicle triggers induced weight saving on the body in white.

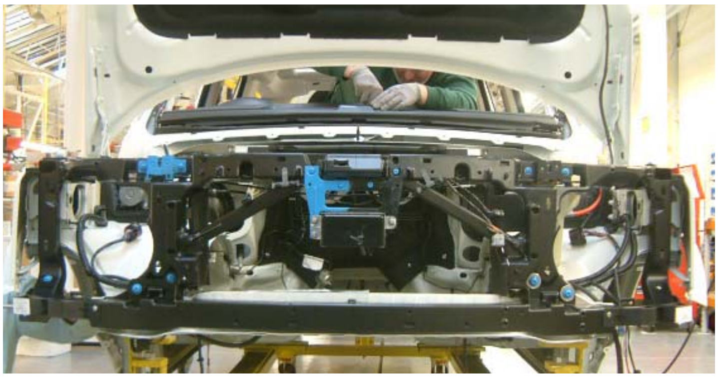

Fig.13: Magnesium FEC example

4.2 Corrosion prevention on exterior applications

The location of an FEC in automotive body structure results in the component experiencing a particularly harsh corrosive environment. In the past, the biggest issue facing the use of magnesium for exterior applications has been corrosion prevention and in particular galvanic corrosion.

Today galvanic and cosmetic corrosion requirements are achieved by proper design of component and fixings and proper choice of joint materials. Protection from galvanic corrosion is possible by avoiding the presence of electrolyte and by decoupling galvanic cells; hence two design principles are to respect. The first one is to insure a good drainage in fixing areas to avoid that mud and humidity get trapped. The second is to separate Magnesium from steel by the introduction of an aluminium spacer: these spacers increase the length between the anode and cathode of the galvanic cell.

This way the reduction of corrosion is obtained respecting a simple design rule of a minimum distance of 10 mm between Magnesium and steel.

5000 or 6000 series aluminium for spacers are currently used. Figure 2 shows the relative compatibility series of different metal to magnesium.

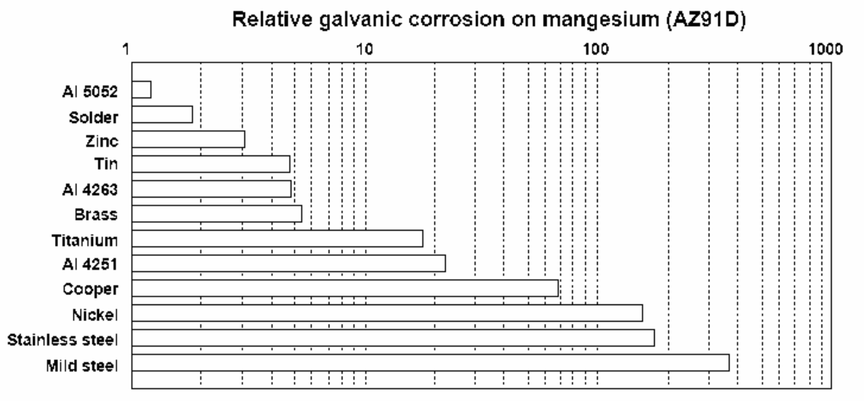

Figure 14: relative compatibility series of various metals coupled to magnesium. Galvanic assembly immersed in 5% NaCl-solution. [4]

Regarding fasteners, in recent years threadforming technology has become widely used in all magnesium component developments within Meridian Technologies Inc. including FEC's for attaching ancillary components. These fixings are fitted into blind holes which eliminates the potential for corrosion from the rear of the fastener. Examples of joint configurations are given in figure 3.

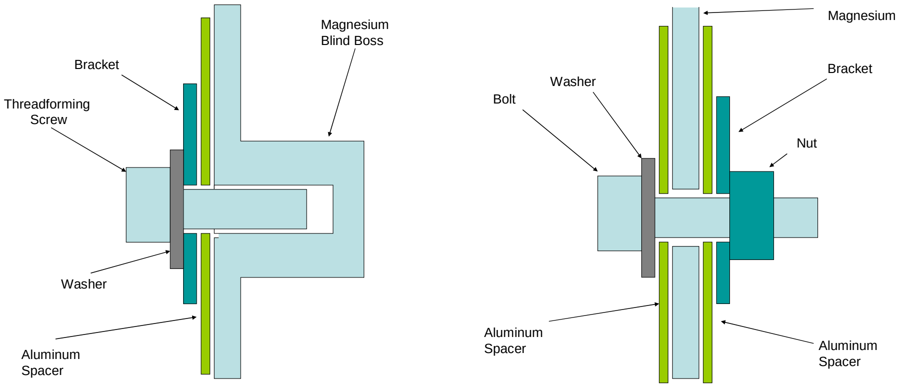

Figure 3 – Examples of Joint Configuration

If parts have a cosmetic requirement then they need to be coated. Current solution consist of an acid etch – to remove surface iron particles that may have been transferred from the die tools in casting process or during handling / transportation post process – and a chemical conversion coating to insure the adhesion of the final top coat that is an epoxy base powder coating (see figure 4). This solution is capable of 1000 hours salt spray tests of ASTM B117 and of 12 weeks humidity salt spray tests (see figure 5).

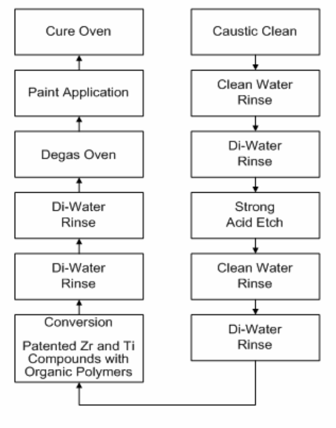

Fig. 15: Example Of current Series Production coating system process

Fig.5 Example Test Panel

5 Conclusion

The partners cooperating in this project have successfully demonstrated the high potential of magnesium in an innovative component. It was also shown that a design suitable for the material used is required in order to fulfil structural requirements. With integration of functions it is possible to design cost attractive solutions for the vehicle structure. With proper designed parts and joints corrosion protection for parts in exterior applications is possible.

6 References

[1] United States Automotive Materials Partnership (USAMP), Automotive Metals Division (AMD): “Magnesium Vision 2020: A North American Automotive Vision for Magnesium” (2004)

[2] Krusche, T.; Leyers, J.; Oehmke, T. and Parr, T.: Bewertung von Modularisierungskonzepten für unterschiedliche Fahrzeugkonzepte am Beispiel des Vorderwagens, ATZ, Vol. 10, p. 928-933, (2004)

[3] A. TIPPINGS, T. LAWSON, “Design and development of a High Pressure Die “FEC” (Front End Carrier) For Exterior Automotive Applications” 62ND Annual World Magnesium Conference, 2005

[4] Hydro Brochure “Corrosion And Finishing Of Magnesium Alloys” 10.1997.

Comparative Review of Primary Magnesium Production Technologies as Related to Global Climate Change

Eli Aghion, Ben-Gurion University of the Negev
Scott C. Bartos, U.S. EPA, Climate Change Division

While primary magnesium has been commercially produced for more than 50 years for applications in the transportation industry, its relative global climate impact is still uncertain. Regular lifecycle assessments of magnesium components for automotive applications indicate the greenhouse gas emission performance (GHGEP) of magnesium has a relative advantage compared to alternative structural materials such as aluminum and steel. However this GHGEP advantage is highly dependent on the production technology of magnesium and can be significantly reduced if the production process is not environmentally friendly.

The present study introduces and compares the principle characteristics of electrolytic production technologies and thermal reduction processes used for the production of primary magnesium. The differences between the two leading primary production technologies in terms of global climate impact (GCI) highlight the current challenge facing producers and users of magnesium, especially when one considers the dominant role of thermal reduction based processes. To simplify this comparative analysis, the authors assume the industry has achieved its 2010 climate protection goal and has eliminated emissions of sulfur hexafluoride (SF_6) in both electrolytic and thermal reduction processes. SF_6 is an extremely strong and persistent greenhouse gas. The industry will be well served by eliminating SF_6 emissions as rapidly as possible, thus allowing magnesium to meet the rapidly growing demand for climate-friendly materials in transportation applications.

1. Introduction

Magnesium's specific strength naturally motivates the transportation industry to select its use for parts manufacturing. In addition, magnesium offers the transportation industry other attractive properties such as superior castability , excellent dampening capacities, and good machining capabilities. However, the life cycle global climate impact of magnesium as a structural material is not well understood. The life cycle assessment (LCA) relates to the entire production and application chain including the primary metal production process, manufacturing and assembly of actual components, and the useful life span of these components and the vehicles. LCA also considers the use of secondary metal by the recycling process. In the case of magnesium, the energy required to produce secondary metal is less than 5 percent of the energy that is required for the production of primary magnesium. Among several attempts made to consider the LCA of magnesium, Tharamarajah and Koltum [1,2] have evaluated the environmental performance of light-weight engine blocks (V6, 3.0L) using magnesium as an alternative structural material to aluminum and cast iron. Their studies demonstrated the relative advantage of magnesium in terms of greenhouse gas emission performance (GHGEP) after driving up to 250,000 km. However, they clearly indicate magnesium's environmental advantage can diminish depending on the primary metal's energy intensity and associated emissions to the atmosphere.

The global climate impact (GCI) of primary magnesium produced in China using the Pidgeon process was evaluated by Ramakrishnan and Koltun [3] in comparison with the production of aluminum. According to this study, the estimated GCI of magnesium was 42 kg CO_2 eq/kg Mg ingot, compared to a GCI of 24.7 kg CO_2 eq/kg Al ingot produced in China and the world average impact of 12.7 kg CO_2 eq/kg Al ingot. In terms of China only, this reflects a 1.6-fold increase in the GCI of magnesium production compared to aluminum production. However, according to a late publication by Meng Shukun and Wu Xiuming in 2007 [4], China's primary magnesium producers appear to be closing the GCI gap with aluminum producers by advancing technologies related to raw material supply and energy consumption. For example, Meng and Wu report that since 2005 the consumption of dolomite was reduced by 5%, ferrosilicon was down by 1.85%, coal consumption was reduced by 35%, and the electricity consumption went down by 9%. In addition, they reported on efforts to consolidate the production facilities of magnesium in China. In fact, by 2006, China already had 10 magnesium smelters with a production capacity of over 10,000 tons/year and four smelters with a production capacity over 30,000 tons/year. The consolidation of China's small smelters has played a vital role in improving efficiencies of raw material processing and energy consumption, both contributing to an improved GCI.

Global climate change has emerged as the greatest environmental challenge facing society today. While lightweight magnesium may help mankind tackle this challenge, it is critical for the producers and consumers of magnesium to understand the environmental impact of their material and technological choices. Today more than 80% of the world's primary magnesium finds its origin in China.China's thermal reduction process has proven to be more cost competitive than the West's largely electrolytic production processes, resulting in the closure of four major production facilities over the last 10 years:

- Dow Magnesium, Freeport, TX, US – closed 1998
- Hydro Magnesium, Porsgrunn, Norway – closed 2002
- Magnola Magnesium, Pointe-Claire, Québec, Canada – closed 2003
- Hydro Magnesium, Bécancour, Canada – closed 2007

As a result, more than 200,000 tons per year of primary magnesium electrolytic production capacity has been replaced by China's thermal reduction process production. The dramatic transition in primary magnesium production technology witnessed over the last decade is illustrated in Table 1. According to this transition, the production capacity of electrolytic magnesium was reduced from 75% of the global consumption to about 20% within the last ten years.

Table 1. Production technologies transition in the last decade.

Production Technology	1997	2008
Thermal reduction	25 %	80 %
Electrolytic production	75 %	20 %

The present study aims to assess the differences between the electrolytic production process and the thermal reduction process of primary magnesium in terms of technology characteristics and GCI. As mentioned above, this study assumes that both production technologies are not using SF_6 as a protective gas atmosphere for casting magnesium ingots.

2. Raw materials for primary magnesium production

The raw materials used for the production of primary magnesium are shown in Table 2. In general, those materials can be divided into three groups. The first group relates to raw materials such as Magnesite and Dolomite that are extracted by mining. The second group includes Carnallite and Bischofite that are mainly extracted by solar evaporation of concentrated salt sea lakes. The third group relates to raw materials that are obtained as a by-product of another process. Serpentine tailing is one example of such a by-product that is obtained from the production of asbestos. Regular sea water can also be used as a source for magnesium. The magnesium content in sea water is 0.13 wt% and it is considered the third most common element in sea water after chlorine (1.95 wt %) and sodium (1.077 wt %). The process of extracting magnesium from sea water is based on the relative low solubility of salts in sea water and the use of a precipitation agent such as $Ca(OH)_2$ that can react with $MgCl_2$.

Table 2. Raw materials for the production of primary magnesium.

Raw materials (Minerals)	Chemical formula	Mg content (wt%)
Dolomite	$MgCO_3 * CaCO_3$	13.19
Magnesite	$MgCO_3$	28.8
Carnallite	$MgCl_2* KCl * 6H_2O$	8.75
Bischofite	$MgCl_2* 6H_2O$	11.96
Serpentine tailing	$3MgO * 2SiO_2 *2H_2O$	26.33
Dead sea water	Mg^{+2}	4.2
Sea water	$MgCl_2$	0.13

3. Production of primary magnesium by electrolytic process

3.1 Principles of electrolytic production

The reduction of magnesium ions in the case of electrolytic production is carried out by an electric current that is fed to the electrolysis cells. The whole electrolytic process can be divided into six major stages as follows [5]:

(1) Raw material feeding
(2) Preparation of $MgCl_2$
(3) Purification and dehydration of $MgCl_2$
(4) Electrolytic separation of $MgCl_2$ producing molten magnesium and chlorine gas
(5) Processing of chlorine gas for internal process recycling and external applications
(6) Casting pure Mg and Mg alloys ingots.

It is necessary to dehydrate $MgCl_2$ because the $MgCl_2$ contains water. Water (H_2O) has a decomposition potential of 1.8[V] compared to 2.6–2.8[V] for $MgCl_2$. Therefore, the decomposition of water in the electrolysis cell will take place prior to the decomposition of $MgCl_2$. This will result in loss of energy and damage to the electrolysis cell by the decomposition products of water. Generally, the dehydration process of $MgCl_2$ is inherently difficult mainly due to competing reactions that produce undesirable MgO according to the following reactions:

$$MgCl_2{*}6H_2O = MgCl_2{*}2H_2O + 4H_2O_{(g)}$$
$$MgCl_2{*}2H_2O = MgOHCl + HCl\ (g) + H_2O_{(g)}$$
$$MgOHCl = MgO + HCl\ (g)$$

Hence, in order to address the dehydration difficulties of $MgCl_2$, two types of technologies were developed. The first technology includes partial dehydration (with or without HCl) that is followed by a chlorination process with the presence of carbon according to the following reaction:

$$2MgO + C + 2Cl_2 = 2MgCl_2 + CO_2$$

The second technology, patented by Amundsen et al. [6], relates to the dehydration of $MgCl_2$ by preparation of magnesium chloride hexammoniate and thermal decomposition of its crystals into magnesium chloride and ammonia.

Relating to the electrolysis process, the usual operating temperature is around 700°C and is mainly monitored by the electric energy fed to the cells. However, in some advanced technologies it is also monitored by special devices such as heat exchangers that can be placed within the molten electrolyte. Although the theoretical energy value for decomposition of $MgCl_2$ is about 7 kWh/kg [7], it is evident that in practice nearly twice this energy is required, indicating that nearly 50% of the electrical energy fed to the cell is transformed into heat. Hence, in terms of energy consideration, there is still a clear potential to improve the energy efficiency of the existing electrolysis cells as well as developing practical means to use the excess heat that is being generated by the cells.

The electrolyte used by the electrolysis cells should have a low electrical resistance to improve the current efficiency of the cells.

Hence, due to the relatively low conductivity of $MgCl_2$, the common concentration of this substance in the electrolyte is between 8–25%. In addition, the electrolyte should be relatively heavy to ensure adequate separation between the electrolyte and the pure magnesium that is being produced and floating on the top. In practice, there are two types of electrolyte – "Constant electrolyte" in which only $MgCl_2$ is being renewed and "Substitute electrolyte" in which the whole electrolyte is being renewed [5]. The "Constant electrolyte" is based on NaCl (50–60%) and $CaCl_2$ (20–25%) with a balance of $MgCl_2$ (15–25%). The density of this electrolyte is around 1.75 [g/ml] and its conductivity is around 2.46 [$\Omega \bullet cm^{-1}$]. NaCl is mainly used due to its improved conductivity and affordable price, while $CaCl_2$ is used in order to increase the density of the electrolyte. The "Substitute electrolyte" is based on carallite and usually includes KCl (64–70%), NaCl (19–23%), and $MgCl_2$ (8–18%). After the extraction of magnesium from the "Substitute electrolyte", the whole electrolyte is renewed.

3.2 Industrial technologies for electrolytic production

Although the principles of electrolytic production of primary magnesium are similar, the industrial technologies are different and can be divided according to the following producers' processes:

(a) Dow magnesium
(b) Hydro magnesium
(c) USMagnesium
(d) Magnola
(e) Avisma/Dead Sea Magnesium (DSM)
(f) Australian Magnesium Corporation (AMC)

The industrial production technologies vary in terms of: electrode technology (mono-polar or multi-polar), voltage and current input, cell temperature, electrical efficiency (kWh/kg Mg), production capacity (tons per year), life span of cell (years), feeding substance and MgO content tolerances. Some of these differences may be demonstrated through closer examination of Dow's and Magnola's respective magnesium production processes.

The flow chart of Dow's magnesium production process is shown in Figure 1 [5,8–10]. According to this technology, dolomite and sea water are used as raw materials. The calcination of dolomite results in the formation of CaO*MgO and CO_2 as follow:

$$MgCO_3{*}CaCO_3 \rightarrow CaOMgO + CO_{2(g)}$$

The calcinated dolomite is then reacted with sea water to form Ca and Mg hydroxide:

$$CaOMgO + 2H_2O \text{ (sea water)} \rightarrow Ca(OH)_2 + Mg(OH)_2$$

The $Ca(OH)_2$ is washed in solution and the settled $Mg(OH)_2$ is filtered to remove impurities. To obtain the required $MgCl_2$ for the electrolysis cell, the $Mg(OH)_2$ is neutralized by HCl according to the following reaction:

$$Mg(OH)_2 + 2HCl \rightarrow MgCl_2 + 2H_2O$$

The $MgCl_2$ is then partially dehydrated from 35% to 73% and fed to the electrolytic cell to produce magnesium and chlorine. The fact that $MgCl_2$ was not fully dehydrated results in decomposition of water within the electrolysis cell. This significantly reduces the electrical efficiency to about 18–19 kWh/kg magnesium and results in graphite consumption of about 100 g per 1 kg Mg which add to the production of additional CO_2 in the process.

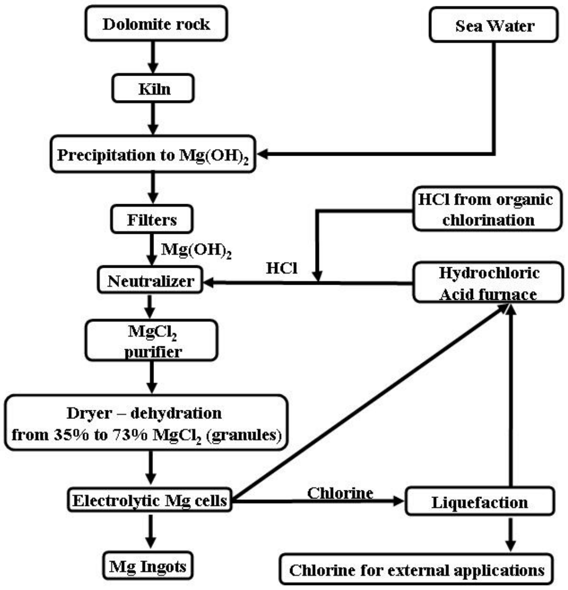

Figure 1. Dow magnesium – electrolytic production flow chart [5,8–10].

The flow chart of the advanced technology of the Magnola process is shown in Figure 2

[5,7,11]. The serpentine tailing used by this technology as a raw material is first leached with HCl to form $MgCl_2$, H_2O, and CO_2. Following this stage, the $MgCl_2$ is purified and then dehydrated using fluidized bed drier technology. To obtain the relatively very small quantity of MgO (0.03–0.1%) that is required for adequate performance of the multi-polar electrolysis technology, the $MgCl_2$ is chlorinated using a super chlorinator facility. The resulting electrical efficiency of this electrolytic technology is 10.5–11.5 kWh/kg magnesium. Hence, by comparing the Magnola technology with the Dow process, it is evident the electrical efficiency can be improved by about 40% and subsequently the GCI of this advanced technology is significantly improved. However, the relative sophistication of the Magnola technology was a disadvantage, especially when one considers the inherent requirement of the electrolysis cell to properly function only under a very small MgO content.

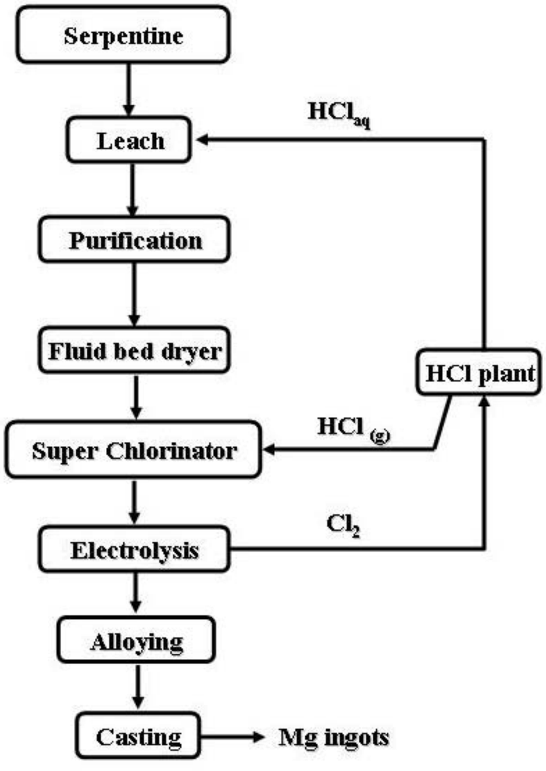

Figure 2. Magnola – electrolytic production flow chart [5,7,11].

4. Production of primary magnesium by thermal reduction process

The thermal reduction technologies for the production of primary magnesium can be divided into three categories: Silicothermic, Carbothermic, and Aluminothermic processes as shown in Table 3.

Table 3. Thermal reduction processes for the production of primary magnesium.

Silicothermic process	Carbothermic process	Aluminothermic Process
- Pidgeon - Magnetherm - Bolzano	- Coke process - CaC_2 process - Hydrocarbon gas process	- Heggie process

The flow chart of the Siliconthermic process, also known as the Pidgeon Process, is shown in Figure 3. According to this process, primary magnesium is obtained from the reaction between calcinated dolomite (MgO*CaO) and ferrosilicon (FeSi). The overall reaction can be written as follows:

$$2MgO{*}CaO_{(S)} + FeSi_{(S)} \rightarrow 2Mg_{(g)} + Ca_2SiO_4 + Fe$$

The Pidgeon reaction takes place in retorts under vacuum conditions (P = 1 mm Hg) at a temperature range of 1150–1200°C.
The cycle time of the process batch is about 8 hr for the production of a 14–23 kg magnesium crown that is being crystallized at the cool side of the retorts.

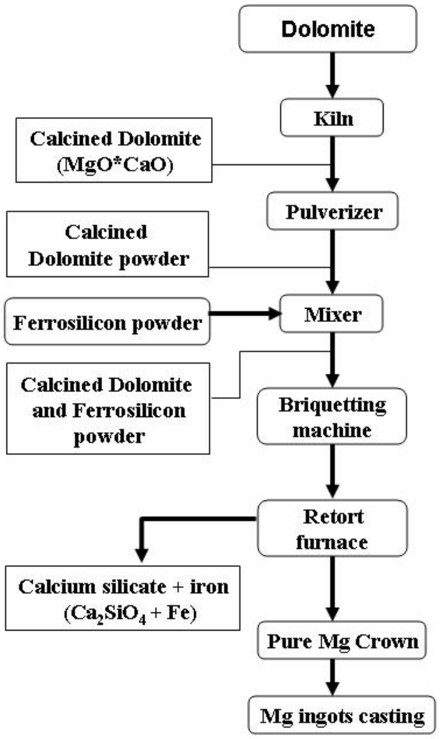

Figure 3. Siliconthermic – Pidgeon process flow chart.

The raw material consumption for the production of 1 ton magnesium by the Pidgeon Process in China since 1991 is shown in Table 4 [3, 5, 12,13]. This reveals ongoing improvements in the Pidgeon production technology that resulted in the reduction of dolomite consumption by 30%, ferrosilicon by 26%, and coal by more than 50% within the last 15 years.

Table 4. Ongoing improvements in raw material consumption by the Pidgeon Process technology in China [3,5,12,13]

Raw material consumption for 1 ton Mg	1991	2000	2004	2005	2006
Dolomite [tons]	14.11	13.0	11.6	10.5	9.98
Ferrosilicon [tons]	1.45	1.21	1.19	1.09	1.07
Coal [tons]	20.65	11.5	10.5	10.0	9.45

The magnetherm process (as well as the Bolzano process) is in fact a larger production scale Pidgeon Process [5]. The magnetherm process produces 3–8 tons of magnesium per batch. The cycle time of a batch is between 16–24 hr and the raw material to produce 1 kg magnesium includes: 6 kg calcined dolomite and 1.1 kg ferrosilicon. The magnesium production capacity of the Bolzano process is about 2 tons of magnesium per batch cycle with a running time of 20–24 hr. The Bolzano reactor operates under vacuum conditions (<3 mm Hg) and at a temperature of 1200°C.

The principle of the carbothermic processes to produce primary magnesium is based on the reaction between carbon and MgO. The MgO is usually obtained from calcinated magnesite and in the case of the "coke process" the overall reaction is as follows:

$$MgO_{(S)} + C_{(S)} \leftrightarrow Mg_{(g)} + CO_{(g)}$$

This reaction can take place at 1854°C under atmospheric pressure. In the "CaC_2 process" the CaC_2 is used as a substitute material for the carbon, and the process temperature is between 1120–1140°C under vacuum conditions (1 mm Hg). The consumption of CaC_2 is about 3 tons for the production of 1 ton magnesium. The "Hydrocarbon gas process" [14] describes the extraction of magnesium by the reaction between MgO and light hydrocarbon gas such as CH_4 at a temperature of about 1400°C. The Hydrocarbon gas process may be described as follows:

$$MgO + CH_4 \rightarrow Mg + CO + 2H_2$$

The Aluminothermic process produces magnesium by reacting calcinated magnesite or calcinated dolomite with aluminum. In the case of the "Heggie process" the aluminum is used in the form of aluminum scrap and the aluminothermic reaction is obtained at 1500°C within a plasma arc furnace. The overall reaction to produce magnesium is as follows:

$$3MgO_{(S)} + 2CaO_{(S)} + 2Al_{(l)} \rightarrow 3Mg_{(g)} + CaO^{*}\,Al_2O_{3(S)}$$

5. Global Climate Impact (GCI) for primary magnesium production

The estimated energy consumption and GCI of primary magnesium produced by Electrolytic process vs. Pidgeon process is shown in Table 5 [3,5,15]. The values related to the Pidgeon Process in China in terms of life cycle energy consumption and GCI for primary magnesium production [3] include the following processes: dolomite and coal mining, ferro-silicon production, dolomite calcination, briquette production, magnesium reduction and ingot melting, refining, and casting. The energy consumption calculated for the electrolytic technology represents the highest estimated values [5]. This includes all the energy required for mining or harvesting the raw material, producing and purifying of $MgCl_2$, dehydration in fluidized bed dryer, chlorination, electrolysis and casting of magnesium ingots. The correlated GCI for the electrolytic process assumes the electric power is generated from petroleum (1.969 pounds CO_2 per kWh) [15]. It should be pointed out that if the electric energy is produced from coal, the GCI will be slightly higher (2.095 lb CO_2 per kWh) and if it is generated from gas it will be much lower (1.321 lb CO_2 per kWh).

Table 5. Estimated energy consumption and GCI of primary Mg production [3,5,15]

Process parameters	Electrolytic process	Pidgeon process
Energy consumption MJ/Kg Mg ingot	101[(a)]	354[(b)]
Global climate impact (GCI) Kg CO_2 per Kg Mg ingot	21[(c,d)]	42[(b,d)]

(a) highest estimated value of energy consumption for electrolytic production [5].

(b) Cradle-to-gate life cycle GCI of Mg ingot produced by Pidgeon process in china [3].

(c) Electrical power generation output rate: 1.969 pound CO_2 per KWH [15].

(d) This GCI assumes no use of SF_6 as a protective gas atmosphere for magnesium ingot casting. Should a magnesium producer use and emit SF_6 at the rate of 1 Kg SF_6 / Tonne Mg, the GCI grows significantly by an additional 22.8 Kg CO_2 / Kg Mg ingot [16].

The calculated GCI values shown here indicate the electrolytic magnesium production process is more environmentally friendly than the Pidgeon Process, at least in terms of greenhouse gas emissions. In principle, this observation comes in line with the finding of Xu, et al. [17]. According to their calculations, the energy consumption for the production of 1 ton of primary magnesium by Pidgeon Process was 2.1 times higher relative to the energy consumption by electrolysis. In addition, they claimed that although the Pidgeon Process consumes more energy and produces more severe pollution than the electrolysis method, this was not a result of the method or principles of the Pidgeon Process. Xu et al reported the current disadvantage of the Pidgeon Process is a result of the lower thermal utilization efficiency of the equipment and the technology.

Hence, additional improvement of the thermal efficiency characteristics of the Pidgeon Process technology and equipment can improve the standing of this technology in terms of GCI.

Conclusions

The comparative review of this paper demonstrates that primary magnesium produced by the electrolytic process has a significantly lower GCI (21 kg CO_2 per kg Mg Ingot) compared to that of the Pidgeon Process (42 kg CO_2 per kg Mg ingot).This outcome assume that both production technologies are not using SF_6 as a protective gas atmosphere for the casting of magnesium ingots.

Relating to SF_6 it should be pointed out that the industry's first and most immediate opportunity to improve magnesium's GCI requires it to successfully fulfill its goal to eliminate SF_6 emissions. SF_6 emissions from ingot casting roughly double the climate impact of magnesium ingot produced using an electrolytic process.

The fact that currently more than 80% of global production capacity uses Pidgeon Process highlights the current drawback status of the primary magnesium production industry in terms of GCI. This status can be modified if the raw material consumption and thermal efficiency characteristics of the

Pidgeon Process are further improved. Additional strategies for the magnesium industry to improve its GCI include expanding primary production using the electrolysic process and increasing the recovery and recycling of end-of-life magnesium. All of these approaches will help magnesium compete for position and meet the growing global demand for climate-friendly (e.g., low GCI) structural materials in the transportation industry.

References

[1] Tharumarajah A. and Koltun P. “Is there an environmental advantage of using magnesium components for light-weighting cars” Journal of Cleaner Production, Vol. 15, Issues 11-12, 2007 pp. 1007-1013.

[2] Tharumarajah A. and Koltun P. “Lifecycle assessment of magnesium component supply chain” IMS 62 proceedings, 2005, pp. 69-76.

[3] Ramakrishnan S. and Koltun P. “Global warming impact of the magnesium produced in China using the Pidgeon process” Resources Conservation & Recycling, Vol. 42, 2004 pp. 49-64.

[4] Meng Shukun and Wu Xiuming “Report on China’s magnesium industry development in 2006” IMA 64 proceedings. 2007, pp. 1-11.

[5] Golub G. and Aghion E. “Production technologies of magnesium” in Friedrich H.E. and Mordike B.L. (ed.) Magnesium technology, Springer-Verlag Berlin Heidelberg 2006, pp. 29-62.

[6] Amundsen K, Eklund H.R. and Schmidt R. “Process for producing anhydrous $MgCl_2$” US Patent No. 6042794, March 2000.

[7] Stanley R.W., Berube M., Celik C., Osako Peacy Y.J. and Avedesian M. IMA 53 Proceedings, 1996 p. 58.

[8] Othmer K Encyclopedia of chemical technology, vol 15, John Wiley & Sons New York 1992.

[9] Emley B.F. Principles of magnesium technology, Pergamon, London 1966.

[10] Gilroy D. in Kuhn A.T. (Ed.) Industrial electrochemical processes, Elsevier, Amsterdam 1971 pp. 175-217.

[11] Watson K., Ficara P., Charron M., Peacey J., Chin E. and Bishop G. "The magnolia demonstration plant: a valuable investment in technology development and improvement", TMS, Magnesium Technology 2000 proceedings, Kaplan H.I., Hryn J. N. and Clow B.B. (Eds.), pp. 27 - 30

[12] Shukun M., Xieming W., Wei H. and Chunming D. “China magnesium industry development report for 2005” IMA 63 proceedings 2006 pp. 5-20.

[13] Wenfang S. and Wensheng L. “Opportunities and challenges of China’s magnesium industry” IMA 62 proceedings 2005 pp. 4-9.

[14] Howard J.B., Modestino A.J. and William A.P. US Patent 5782952 July 1998.

[15] Report by the US Department of Energy and Environmental Protection Agency “Carbon dioxide emissions from the generation of electric power in the United States” July 2000 pp. 1-12.

[16] Intergovernmental Panel on Climate Change. Climate Change 2007, Fourth Assessment Report, Cambridge University Press, 2007 p. 212. www.ipcc.ch/ipccreports/ar4-syr.htm.

[17] Xu H., Xie S. and Xia D. “A study on clean magnesium production with Pidgeon’s process” IMA 63 Proceedings 2006 pp. 120-125.

Status and potentials of magnesium production in China: Life cycle analysis focussing on CO_{2eq} emissions

Simone I. Ehrenberger
Stephan A. Schmid
Shaobo Song
Horst E. Friedrich

German Aerospace Center (DLR)

Worldwide, production technologies for magnesium differ depending on geographical situation. China produces about three quarter of primary magnesium, but the Pidgeon process as used there in the past was shown to have high CO_{2eq} emissions per kg pure Magnesium. Now, production processes in China have changed significantly in the last years, and the phase out of SF_6 is well on its way worldwide.

We analyse the present situation based on recent data for the use of producer gas/coke gas and improvements in process parameters in China and give an outlook on further improvements for the Mg production technology chains. Changing the energy carriers for heating from coal to gas can reduce the greenhouse gas emissions up to 45 %. We conclude on the break-even distance from the comparison of an A-pillar strut mounting made from Mg with a steel component.

1 Introduction

Magnesium (Mg) production and use has had an unsteady history: the yearly worldwide outputs as well as production technologies have changed many times [1]. Due to differences in feedstock, also production technologies differ worldwide, depending on the geographical situation.

During the 1990s, Chinese Mg manufacturers began to renew the thermal reduction process also known as Pidgeon process. Due to large mineral resources, cheap manpower and low investment costs, Chinese companies have been able to produce at lower prices than other market participants using electrochemical processes. As a result, China is the market leader for primary Mg today. Figure 1 shows the market shares of Mg producing countries worldwide from 1995 to 2006. During this period, China's share rose from 25 % to almost 75 %. In 2007, its production volume amounted to 627,300 t [2].

The Pidgeon process requires considerable amounts of energy for heating purposes. For reasons of economic and ecological efficiency, efforts have been made during the last years to decrease the consumption of primary energy carriers. But technological chances in the Chinese Mg industry are also driven by political guidelines. The current five-year plan provides a reduction of energy consumption of 20 % per unit gross domestic product (GDP). This moved the China Nonferrous Metals Industry Association (CNIA) to decide on specific energy reduction measures in this industry branch. For Mg production, it announced a maximum consumption of 7 t standard coal per t Mg [3].

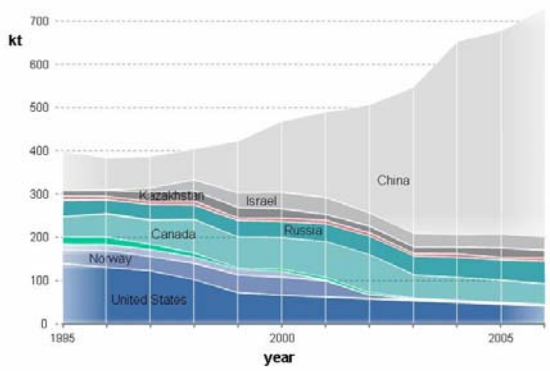

Figure 1: Primary magnesium world production

In our study we aim to assess the emissions of greenhouse gases (GHG) resulting from the Pidgeon process. Thus we modelled this technology using data from Chinese manufacturers and compared the use of coal for heating with the utilisation of gaseous fuels. Finally, we extend our study to the comparison of Mg as car component material with steel and aluminium.

2 Status of Production Technologies

2.1 Electrolysis

Electrochemical processes to make Magnesium are based on salts containing chloride which can be found naturally or are transformed from other raw materials like serpentine, magnesite, bischofite or carnallite. The magnesium chloride salts are dried with various processes in order to receive anhydrous $MgCl_2$, either in solid or molten form.

For economic reasons, several electrochemical plants have been closed down in the past. Today, there are three plants in operation in Western countries: US Magnesium (US), Dead Sea Magnesium (Israel), and Rima in Brazil. Four plants are producing in the former Soviet Union (CIS). Dismantling of Norsk Hydro Becancour magnesium plant in Quebec, Canada has started. The Magnola plant (Quebec) originally set up to recover magnesium from asbestos tailings but not operated since 2003, is also scheduled to be taken down. In contrast to this, construction of a new plant in Russia to process tailings from Uralasbest has been started in late 2007 [4].

2.2 Silicothermic Reduction

The silicothermic reduction of Mg using ferrosilicon (FeSi) as reduction agent is the only Mg production process used in China at present. It is named Pidgeon process after his inventor, the Canadian chemist Lloyd M. Pidgeon.

Figure 3 shows an overview of the process steps. Due to its abundant deposits, the raw material for Mg production in China is magnesium-calcium carbonate dolomite ($MgCO_3\cdot CaCO_3$). Thus, the first production step is the mining and transportation of dolomite to the Mg production site. In order to eliminate carbon dioxide (CO_2) from the crystal structure, the rock material is treated in continuous rotating or batch furnaces at temperatures of about 1,000 °C, which is called calcination step. The calcined material is then grounded into fine powder and mixed with reaction agents. FeSi, which is consumed in considerable amounts, is added as reduction agent, while calcium fluoride (CaF_2) works as catalyst. Calcined dolomite and agents are pressed into briquette form and put into the reduction furnace. At temperatures around 1,300 °C and under vacuum, the following chemical reaction occurs:

$$2\,MgO\cdot CaO + Si(Fe) \rightarrow 2\,Mg + Ca_2SiO_4 + Fe$$

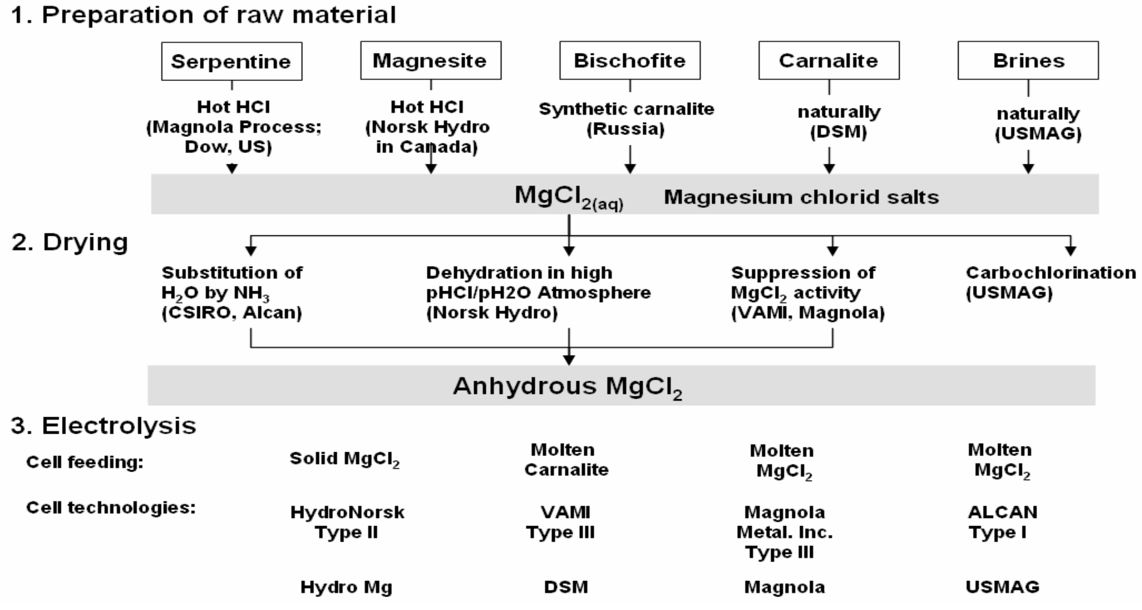

Figure 2: Different routes of the electrochemical process

The raw Mg sublimates in the water cooled part of the furnace and is removed at the end of this batch process. As these so called Mg crowns still contain certain amounts of impurities, the last step of the Pidgeon process is the refining, where the Mg crowns are melted and treated with purifying agents.

Protection agents are needed to prevent the melted Mg from burning as it is highly combustible. Formerly, sulphur hexafluoride, the most potent greenhouse gas known, has been commonly used for such purposes. Recently, its use is phasing out, as there are alternative protection agents available with lower global warming potential. Chinese Mg companies use sulphur or fluxes containing small amounts of sulphur for preventing the Mg melt from burning.

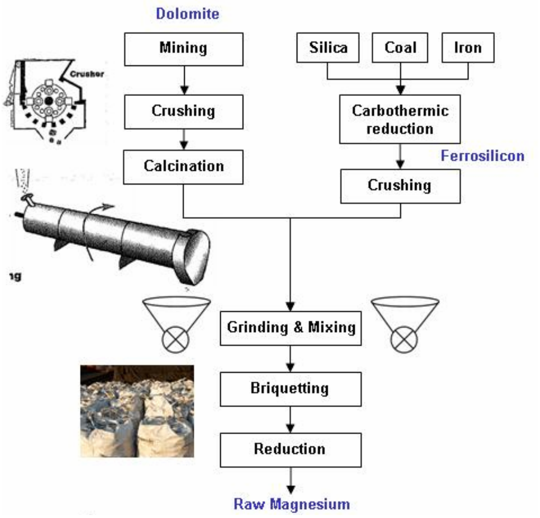

Figure 3: Overview of Pidgeon process

Though the Pidgeon process has received remarkable improvements concerning energy consumption and emissions during the last years, there is still a considerable potential for enhancing its efficiency. Subjects of study are, for instance, the performance of furnaces, the handling of retorts, the use of waste heat or the further use of production waste. Energy consumption, as addressed in our study, is of special interest and there is an obvious movement from using coal to running the process with gaseous fuels.

An overall process improvement can be achieved by integrated production of several commodities. This means, that there is no need for material transports and the possibility of using by-products from one process as input for others. Concerning the Pidgeon process, it would be favourable to install local production networks combining the production of primary energy with a FeSi and a Mg plant. Coke production, for instance, which is needed for the making of FeSi, comes along with the production of a considerable amount of coke oven gas which can be used for heating furnaces in a Mg plant.

3 Data Survey in China

There are few publications on greenhouse gas emissions for Chinese primary Mg, e.g. [5], [6], [7], [8]. As the production of Mg during the last decades has been dominated by electrochemical processing and thus first life cycle analyisis (LCA) studies on its environmental impact refer to this technology which is not representative for present Mg supply, these papers are the first to indicate the dimension of GHG or CO_2 emissions from Pidgeon process. Considering the changes mainly in energy consumption but process efficiency as well, we aim to reflect this with a new model for the Mg production process and evaluate the potential for overall CO_2 reduction.

In order to obtain an idea of how the technological improvements link to the reduction of CO_2 emissions of the entire production chain, we surveyed the 14 companies with highest primary Mg production capacity in China, most of them located in the provinces Shanxi and Ningxia. By sending them a standardized questionnaire, we ensured a consistent set of data on energy consumption and material inputs of each production step of the Pidgeon process. The questions addressed in detail qualitative as well as quantitative information on energy carriers used for each process step. Material requirements have been asked as well, specifically concerning reduction and refining agents. Additionally, we asked for possible future technology improvements concerning the use of other energy carriers than coal and the implementation of new reduction process systems. We further interviewed company employees who were in charge of the said questionnaire by telephone or via e-mail. Most of our contact persons are technicians, two work at administration offices and one is employed at the trade department. Of the 14 producers six provided us with data. These companies represent a production capacity of 178,000 t Mg per year which would be 31 % of the real annual Chinese Mg output in 2007. Some of the companies are planning or constructing new Mg facilities, so that a further increase in Mg production output can be expected. For three companies we could not find contact information.

Additional three do not produce primary Mg themselves, one company had no contact person with adequate knowledge available and another did not send the questionnaire back in time. Furthermore, we sent a similar questionnaire to two FeSi producers which provide the Mg companies with this material. Both returned us data on the energy and material demand for their product.

4 LCA models of Chinese Magnesium Production

4.1 Concept of technology evolution for energy consumption

For the cradle-to-gate assessment of Mg production in China we assume an output of 1 kg Mg ingot for each process option. We calculated the material and energy flows for the Mg production steps as well as the supply of operating and raw materials using the software tool Umberto [9]. The main process regarding the way of Mg from mining to ingot casting consists of five steps as described above. Except from the mining of dolomite, we modelled these processes according to the data we got from Chinese producers. Company data are also used for the FeSi production process. For the calculation of energy and material requirements for other processes we referred to public databases. Most of the processes calculated in our life cycle model represent present Chinese conditions. Some minor material supply processes refer to global or European average data, which have only marginal effect on the overall results. In order to show the progress of development in production technologies, we identified three technology stages:

- Solid fuel use
- Energy switch: gaseous fuel
- Integrated plants

As the thermal reduction is an energy intensive process, 51 - 57 % of the emitted GHG stem from the utilization of fossil energy carriers for fuelling issues or as electricity in plants using merely coal ([5], own calculations). Therefore, reduction of energy consumption and alternation of fuels are the most promising strategies for avoiding GHG emissions. Due to the target set by the CNIA, the utilization of gas produced from coal is seen as new technology standard and the companies we surveyed plan to implement such process improvements if not already done. The fuel gas can either be coke oven gas or producer gas. Some of the companies still use coal in addition to gas, mainly because of operational issues in the calcination step. To show some effects of implementing gaseous fuels, we compared its use to coal and evaluated the benefits for three different types: producer gas, coke oven gas and natural gas. Additionally, we assessed the effect of integrating coke and FeSi production into a Mg plant.

Solid fuel use: coal
This group represents manufacturers using coal directly as energy source for heating the furnaces. Apart from company information, we used also data from literature [5] for modelling this process version and obtained four different datasets. The coal input for fuelling for the overall process from calcination to refining varies between 8.2 and 9.5 kg per kg Mg.

Use of Producer Gas
Producer gas is the product of air and sometimes steam injection into coal. Main components are carbon monoxide (CO), hydrogen (H_2) and methane (CH_4). The amount of producer gas needed for the entire Mg production process varies from 6 to 19 m³ depending on the amount of coal used additionally. This scenario is represented by three manufacturers.

Use of Coke Oven Gas
Coke oven gas is a by-product form coke production which is obtained from pyrolysis of coal. Thus, the emissions from coke oven gas production should only take into consideration the gas itself and not to the overall coke processing. Therefore we allocated the amount of emissions to air according to the energy content of all products from coke production (coke, coke oven gas and tar) what leads to a 15 % of energy input and emissions for the gas. In our model, the Mg production requires about 5.1 m³ coke oven gas per kg Mg plus a certain amount of coal for conventional furnace heating. One company is represented in this scenario.

Integrated plant
For some plants, a reduction of the overall energy consumption is achieved by implementing waste heat utilisation. This plant version also represents a local production network combining the production of coke and coke oven gas with a FeSi and a Mg plant. From the experiences of one company, a reduction of energy consumption for fuelling of 4.5 % can be assumed. Such an integrated production is not widespread yet, but nevertheless we obtained data from one manufacturer.

Use of Natural Gas

In addition to the “real” life energy supply for Mg production, we assumed the utilization of natural gas as substitute for coke oven or producer gas. It is not used in present Chinese plants as it is significantly more expensive than the other gases mentioned. Due to its higher energy content, the amount of natural gas needed would be lower compared to other fuel gases. As this is a theoretical consideration, we calculated the amount of natural gas needed according to the information on the use of other fuel gases in an advanced Pidgeon process assuming the energy need to be equal. This reference process corresponds with the integrated process described above in terms of energy efficiency due to waste heat utilisation. Thus, the natural gas scenario does not represent present Mg production but a further and presumably best-case CO_2 reduction potential by using an alternative energy carrier.

4.2 Inputs for process steps

As the conversion rates from dolomite to calcined dolomite and from raw Mg to pure Mg hardly vary, we assumed them to be equal for each scenario. Material transport is calculated from Mg producer information and differs considerably between production sites. The data input for the main life cycle steps are explained in detail in the following.

Dolomite mining: This process is taken from the ecoinvent database [10] which is commonly used in LCA. These data present a large uncertainty, but due to the lack of alternative information they have been used in this study. The transportation of the raw material to the Mg production plant is calculated according to the average distance between dolomite mine and plant for each scenario.

Calcination: For the calcination process we used the input of 2 kg raw per kg calcined dolomite. The energy need is supplied by either coal or coke oven gas or producer gas or a combination of different energy carriers, depending on the scenario. For calcination there is still a certain amount of coal required for some production alternatives due to the specific energy feed in this process.

Briquetting: The briquetting system represents the mixing of the calcined dolomite with the additives FeSi and CaF_2. The demand of FeSi is similar for all data sources and amounts to 1.1 to 1.3 kg per kg Mg. Concerning the production of FeSi, we calculated an average production option according to the data provided by surveyed manufacturers and literature [11]. The use of CaF_2 varies from 0.01 to 0.26 kg per kg Mg and thus differs for the scenarios. Besides these additives, this process requires a certain amount of electricity ranging from 0.18 to 0.33 kWh per kg Mg.

Reduction: The reduction process is compared to all other production steps in an Mg plant the most energy intensive. It requires a considerable amount of coal, coke oven gas or producer gas for heating the reduction furnaces. Additionally, the material needs for retorts are calculated as the retort have a life time limited to a maximum of 90 days. For this study we assumed an average output for one retort of 25 kg and a life time of 60 days.

Refining: During refining the melted raw Mg is cleaned from impurities before casting the pure Mg ingot. Apart from energy for melting the Mg, flux agents are needed for refining and protection purposes. The amount of added flux agents varies from 0.08 to 0.13 kg per kg Mg.

4.3 Results for Greenhouse Gas Emissions

For the evaluation of the Pidgeon process’ environmental performance, we calculated the greenhouse gas emissions resulting from fossil resources. Figure 4 shows the results for all scenarios. As the FeSi production is associated with a considerable amount of CO_2 emissions due to its high energy consumption, the result for this material is shown separately. As for FeSi production as well as for dolomite mining, all Mg production options are based on equal input data, there is only one bar for these life cycle steps displayed. The black lines at the FeSi bar indicate the changes in emissions considering different transportation distances. A minimum of nearly 0 km is achieved in integrated plants.

Clearly, the production of FeSi, the calcination of dolomite and the reduction itself are the most emission intensive life cycle steps. The results for the coal scenario correspond with the results found in [5] and [6], where coal is the only energy input for heating as well. The overall emissions amount to 47 kg CO_{2eq} for the conventional coal using option. The uncertainty lines for the coal and producer gas scenario indicate the minimum and maximum values obtained from our calculations and represent different Mg plants and material transport distances. The emissions decrease gradually with the utilisation of producer and coke oven gas and with the implementation of an integrated plant. The lowest GHG emissions we calculated stem from the natural gas scenario and amounts to about 25 kg CO_{2eq}. Considering the decrease of emissions in the different process steps, the reduction process bears much more reduction potential than calcination. To a certain extent this is because of the CO_2 emissions from chemical reaction during calcination, which amount to 5 - 6 kg per kg Mg and which cannot be avoided. Another reason is that there have been made more efforts in increasing the efficiency of the reduction process as this directly influences recovery rate and quality of the raw Mg. This has clearly succeeded and similar efforts could lead to a further reduction of emissions from other process stages as well.

Considering the studies about Mg production by electrolysis mentioned in chapter 2.1 and taking into account the phase out of SF_6 utilisation, the GHG emission from this technology still improves our findings about the advanced Pidgeon process.

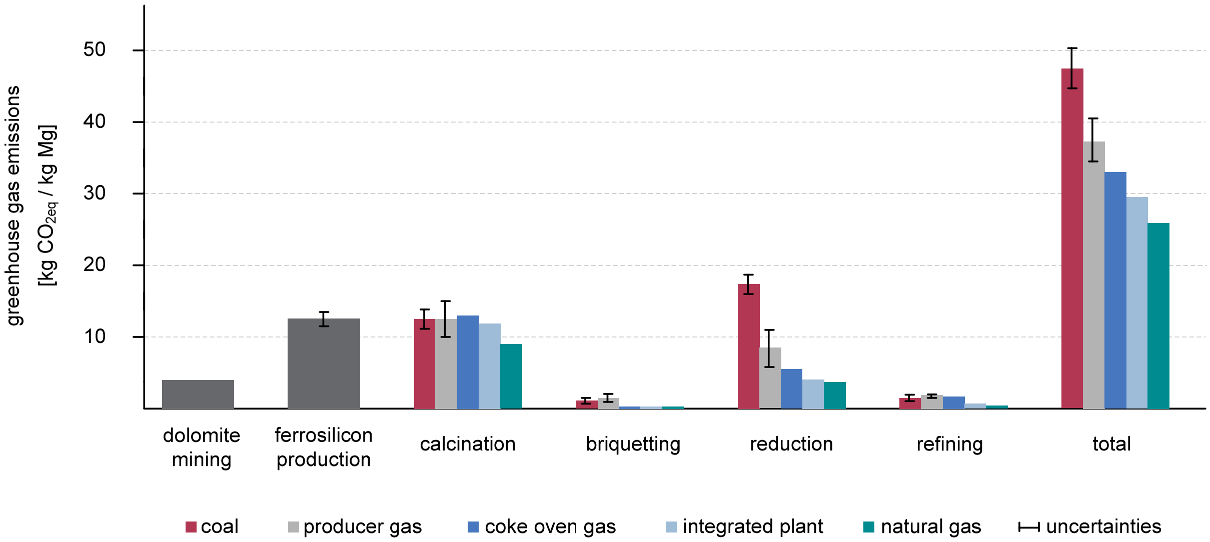

Figure 4: Greenhouse gas emissions from Pidgeon process

5 Evaluation of Magnesium application in cars – A-pillar Concept

For the assessment of the application of Mg for vehicle construction, we extended our Pidgeon process model in order to consider a car component made from Mg. Figure 5 shows images of an Mg A-pillar strut mounting.

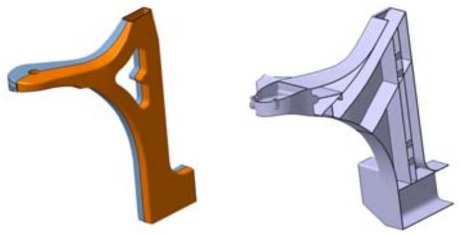

Figure 5: Examples of highly integrated A-pillar strut mountings from Mg (DLR)

For the production of this component, the Mg has to be alloyed first. For the considered automotive application, the AM50 alloy is the most appropriate. We modelled its production similar to the production of the Mg ingots, but adding Al with a share of 5 % and Mn of < 1 % (for our study, we assumed a Mn share of 0.9 %). The weight of the A-pillar is 6 kg. For modelling the production process, we took data from three Chinese companies we interviewed and which produce Mg alloy and assumed the further processing of the alloy ingots being performed in Germany. These further production steps consist mainly of material transports and of die casting which we modelled using data from the ecoinvent database. The entire production chain for the A-pillar Mg amounts to 174 kg CO_2.

For the use phase we considered an average middle class car, represented by the VW Golf, and the use of gasoline as fuel. To evaluate the potential for reducing CO_2 emissions by using this car component, we compared it with a reference part which has exactly the same function concerning its technical performance in the vehicle's construction. This reference is an A-pillar made from steel which weights 12.6 kg. The production data represent an European average and are taken from the ecoinvent database and the life cycle inventory database of the International Iron and Steel Institute. From this we calculated the CO_2 emissions from the production of the steel component (80 kg CO_2).

Apart from different production technologies for the Mg and steel components which come along with different energy and material consumptions, the weight of the car components plays a major part for the comparison of their life cycle. Approximately 0.38 l per 100 km can be saved per 100 kg weight reduction in an average middle class car [12].

For the comparison of the A-pillar from Mg and steel we first modelled its production as described above and then evaluated the fuel savings by weight reduction. As the Mg component weights 6.6 kg less than the steel one, this means a reduction of fuel consumption of 0.025 l per 100 km. We calculated the overall CO_2 emissions over the entire production chain from resource extraction to car use to assess the gross emissions for both components for a certain amount of driven km.

Figure 6 shows the CO_2 emissions for the use phase for both A-pillars up to a driving distance of 200,000 km which is a reasonable mark for a gasoline car's lifetime. Starting point of the lines is the CO_2 emissions resulting from the production itself. In chapter 4 we have discussed the GHG emissions for different Mg production options. These are represented as a best-case Mg scenario (use of natural gas). But unlike in chapter 4 we do not take into account other GHG emissions than CO_2.

The grey line represents the reference component. The vertical line marks the break-even point with the best-case Mg scenario using natural gas (green line). The point of intersection is at about 136,000 km. For the average mere coal using Pidgeon process (red line), the break-even point is beyond 200,000 km. These results show that changes in Mg production and thus its CO_2 emissions have great impact on the break-even distance, although the emissions from the use of gasoline during driving are presumed to exceed those of component manufacturing by far. In addition to decreasing the emissions from Mg production itself, there is a certain reduction potential in the component manufacturing as well. Regarding the energy requirements for melting the raw material, it would be more efficient to melt the Mg only once. For that the pure Mg and Mg alloy making as well as the die-casting process would have to take place at one single production site.

Another aspect would be the effect of end-of-life options which we do not address in this study. Regarding the fact, that Mg recycling would save more than 90 % of the energy used for its primary production [13], this would also have

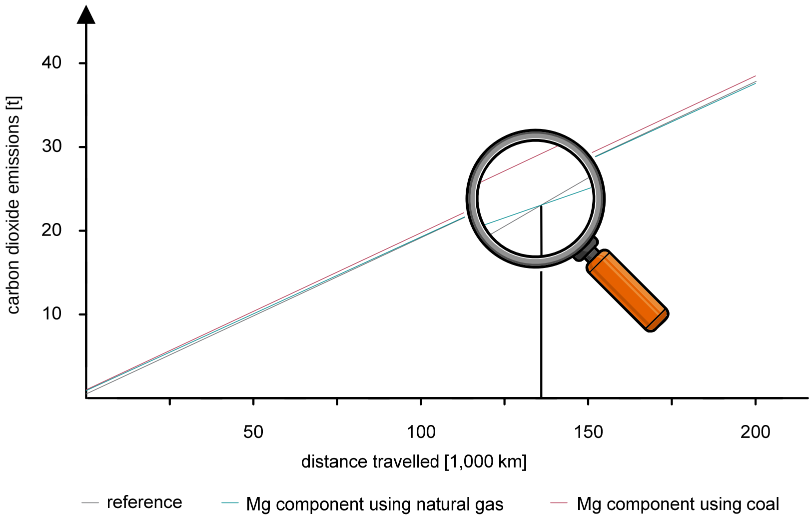

Figure 6: Break-even distance for A-pillar from steel and Mg

great impact on the CO_2 performance of the car component. The production of such components requires high quality alloy, therefore different grades of magnesium scrap become important. Nevertheless, considering further uses of Mg after its application in a vehicle would change the CO_2 emission balance and possibly improve the break-even distance for such components when compared to steel.

6 Conclusions

The examination of the present Pidgeon process in China has lead to the following basic findings:

- Compared to literature data of electrolysis using water power as energy source, the silicothermal reduction provides GHG emission rates which are up to eight-times higher (6 kg GHG per kg Mg [14] versus 47 kg in our coal scenario).
- Technological improvements alone, especially for the reduction process, can lead to significant reduction in GHG emissions as recent data from Chinese companies show.
- Changing in addition the energy carriers from coal to gas can reduce the GHG emissions by 45 % to 25 kg CO_{2eq}/kg Mg assuming a best-case scenario using natural gas in an energy efficient plant.

In our study we deal with selected points of the Pidgeon process only. It would be favourable to obtain a more comprehensive view of the Chinese average Pidgeon process.

Our calculations regarding the exemplary use of Mg as a highly integrated A-pillar strut mounting show a break-even distance of 136,000 km for the comparison with steel. Considering end-of-life options for Mg could potentially lower this distance.

The results demonstrate that magnesium can have life cycle advantages over steel, provided that its processing is developed carefully. Evidence from Chinese producers shows that important steps have been taken which need to be applied throughout the sector.

7 Literature

1. Friedrich, H.E. and B.L. Mordike, eds (2006): *Magnesium Technology. Metallurgy, Design Data, Applications*. Springer.
2. International Magnesium Association (5/2008): *Update Weekly, Newsletter*.
3. China Magnesium Association (2008): *Online Information,* *http://www.chinamagnesium.org/detail.php?id=3445*. [cited 2008 02/22].
4. USGS (2007): *MAGNESIUM IN THE THIRD QUARTER 2007*, in *Mineral Industry Surveys*, D.A. Kramer and K.K. Hermanson.
5. Ramakrishnan, S. and P. Koltun (2004): *Global warming impact of the magnesium produced in China using the Pidgeon process.* Resources, Conservation and Recycling. 42(1): p. 49-64.
6. Zang, J.C. (2001): *The Pidgeon Process in China and its Future*, in *Magnesium Technology*, Mineral, Metals and Materials Society: New Orleans, USA.
7. Gao, F., Z. Nie, Z. Wang, and T. Zuo (2006): *Resource depletion and environmental impact analysis of magnesium produced using pidgeon process in China.* Chinese Journal of Nonferrous Metals. 16(8).
8. Gao, F., Z. Nie, Z. Wang, and T. Zuo (2007): *Environmental Assessment of Magnesium Production using the Pidgeon Process in China*. in *8th International Conference of Eco-Materials*, Brunel University.
9. ifu *Umberto. Software for Process Optimisation, Material Flows and Environmental Management, and Life Cycle Assessment.*, Institute for Environmental Informatics Hamburg GmbH: Hamburg.
10. ecoinvent (2006): *Project ecoinvent data v2.0. The Life Cycle Inventory Data Version CD ROM*, Swiss Centre for Life Cycle Inventories.
11. Zulehner, W., B. Neuer, and G. Rau (2005): *Silicon*, in *Ullmann's Encyclopedia of Industrial Chemistry*, Wiley.
12. Espig, M., M. Johannaber, and R. Wohlecker (2006): *Simulation der Verbrauchsverbesserung durch Gewichtsreduzierung in Pkw.* ATZ. 108(12).
13. Hanko, G., H. Antrekowitsch, and P. Ebner *Recycling Automotive Magnesium Scrap.* Journal of Materials Processing Technology. February 2002.
14. Albright, D.L. and J.O. Haagensen (1997): *Life cycle inventory of magnesium*. in *IMA 54: Magnesium Trends*, Toronto, Canada: International Magnesium Association.

Financial benefits from SF_6 emission reductions

Presented by: Ms. Adi Dishon, CEO, EcoTraders LTD.

The Magnesium sector has been granted a golden opportunity to both participate in the global attempt to mitigate climate change and gain substantial financial benefits. Primary producers or die casters can now receive financial incentives to replace the use of SF_6 with several alternate cover gases.
A CDM baseline methodology has just recently been approved by the UN. EcoTraders as the developer of the methodology quantifying the emission reductions in the magnesium sector and Dead Sea Magnesium as developer of the first CDM project in primary production will provide valuable information regarding this new opportunity.

Financial benefits from SF_6 emission reductions

Adi Dishon
EcoTraders

Abstract:

The Magnesium sector has been granted a golden opportunity to both participate in the global attempt to mitigate climate change and gain substantial financial benefits.

Over thirty industrialized countries have committed, through their participation in the Kyoto Protocol, to significantly reduce their greenhouse gas emissions in order to mitigate climate change. The Kyoto Protocol contains within it market-based mechanisms that allow firms to benefit financially from reducing their greenhouse gas emissions by trading the reductions in the global carbon market. The use of sulfur hexafluoride (SF_6), the most potent of the climate change gases, in the Magnesium primary production and die casting process may be replaced by substitute gases. Through the Clean Development Mechanism and Joint Implementation, the Kyoto Protocol market-based mechanisms, firms can benefit financially from implementing new technology to reduce their SF_6 emissions and sell the resulting emission reductions in the global carbon market. These firms will also be able to indicate to the public that they are acting to preserve the environment and to ensure sustainable development.
A CDM baseline methodology has just recently been approved by the UN.
EcoTraders is the developer of the methodology quantifying the emission reductions in the magnesium sector and Dead Sea Magnesium is developing the first CDM project in primary production.

1. Introduction:

Kyoto Protocol

The Kyoto Protocol is an international agreement designed to reduce the total global level of greenhouse gas (GHG) emissions.

The Kyoto Protocol requires over thirty countries to reduce their GHG emissions. The required reductions constitute a serious economic challenge to these countries. To facilitate the emission reductions, the Kyoto Protocol has created a new commodity – GHG emission reductions, i.e. the absence of these emissions – and the opportunity to buy and sell these reductions.

Clean Development Mechanism and Joint Implementation

The Clean Development Mechanism (CDM) and Joint Implementation (JI) are two market-based methods established by the Kyoto Protocol to reduce global greenhouse gas (GHG) emissions and to facilitate economic and technological development.
CDM and JI are similar, though not identical:

- **CDM** projects take place in developing or newly-industrialized countries (non-Annex I) with no current targets to reduce GHG emissions such as China, India, Israel, Africa, Latin America.

- **JI** projects take place in industrialized countries (Annex I) that have committed, through Kyoto, to reduce their GHG emissions such as Russia, Ukraine, Eastern Europe.

CDM and JI both provide financial incentives for businesses to invest in GHG reduction projects because these reductions have **financial value:** they can be sold to parties that have committed to GHG reductions under the Kyoto Protocol. Investment in a CDM or a JI project is a more economically efficient way for Annex I industries to meet their Kyoto targets.

Annex I parties such as (such as German or other European plants) may finance the carbon emission reduction projects and acquire the resulting "carbon credits", or else they may purchase these "carbon credits" from the carbon market.

CDM and JI projects may include installing new technology in a facility or switching to cleaner fuels such as biogas, biomass or solar energy to reduce greenhouse gas emissions, or capturing and destroying methane. Replacement of SF_6 as a cover gas in the magnesium industry may also yield carbon credits.

CDM and JI are incentives to implement emission reduction projects now.

To be approved as eligible for CDM or JI, projects must meet certain criteria. One of the most important requirements for a CDM or a JI project is additionality. Additionality requires clear evidence that the emission reductions made possible by the project would not have otherwise occurred. Projects qualify for CDM/ JI status if:

- **Regulation**: the activity to be undertaken/greenhouse gas reduction is not required by law;
- **Financial**: There are economic barriers to implementing the project;
- **Institutional**: There are technical, institutional or other barriers that make the project difficult to implement.

In the future, the government may develop regulations that will require industries to reduce their emissions or the financial or institutional barriers may be overcome. In these cases, the project would not qualify as "additional" and could not benefit from investment under CDM or JI, nor sell the reduced emissions in the carbon market.

2. CDM in the Magnesium sector

Replacement of SF_6 as a cover gas in the magnesium industry may be eligible as a CDM project. Any plant that currently uses SF_6 as a cover gas and will substitute this gas with HFC134a/ Dilute SO_2/ Novec may receive substantial financial benefits. These benefits can cover all implementation costs resulting from the cover gas switch. A plant that will register as a CDM project will have the ability to:

- Modernize and improve magnesium production processes;
- Benefit financially from enhanced production and from incentives to reduce air pollution (greenhouse gas emissions).

How will this work in the magnesium sector?

The Seller

China (as an example) was categorized as a developing country under the Kyoto Protocol. This means that China has no emission reduction targets to date. A magnesium plant in China/ Russia switches from SF_6 to HFC134a. This environmental project releases less GHGs to the atmosphere and emissions reductions are achieved. The UN (the body governing the KP) issues the project "carbon credits" (emission reduction credits) in the amount of emission reductions actually achieved. For example, 100,000 carbon credits representing 100,000 tonnes of GHGs that were not emitted to the atmosphere.

The Buyer

A German industrial plant must reduce its GHG emissions by 100,000 tonnes a year in order to avoid heavy fines. The plant may purchase the carbon credits from the Chinese magnesium plant and submit these credits to the German government as if the plant had reduced emissions at its own facility.

The Bottom Line

Such transactions achieve global GHG emission reductions in the most cost-effective way.

The seller gains financing to implement and introduce a new and cleaner cover gas to the plant. The buyer benefits by standing to his GHG emissions quotas and avoiding heavy fines. The globe benefits as GHGs emissions are reduced to the atmosphere.

3. CDM project Cycle

In order to register a project as a CDM project with the U.N. a project must complete the following steps:

Data Collection

Collection of all quantitative and economic data required to complete project development documents.

Baseline Study

Calculation of the “carbon credit reductions” that will result from the project, based on the baseline emissions calculation and the implementation of the carbon emission reduction project, i.e., the difference between emissions that would occur without the project (“the baseline”) and the level of emission reduction from the project.

Monitoring Plan

Each project must contain a plan to monitor the amount of emission reductions throughout the project's lifetime. The monitoring plan will include: the technological information of how the emission reductions will be measured; the calibration of monitoring instruments; and the method to collect and archive the data.

National Approval

Each project must be approved by the Designated National Authority, the national body that verifies that the project meets the national sustainable development criteria.

Stakeholders’ Comments

The United Nations requires that each project includes public involvement in the project development. Therefore, information about the project must be publicized and public comments solicited as part of the project's development. Stakeholders’ comments may be gathered through a public meeting and through the internet.

Project Design Document (PDD)

The PDD is the project's main document, which includes all the project documentation and data. The United Nations draws on the PDD and the validator's comments to determine if a project should be approved as a CDM/ JI project. The PDD is also submitted to the Designated Operational Entity (DOE), who is the third-party who assesses the project before it is finally submitted to the United Nations. The PDD is a complex document that includes economic analysis, details about national regulations and quantitative data about how the project will impact the environment.

Validation

Project validation is conducted by the Designated Operational Entity (DOE), a third-party who visits the project prior to its submission to the United Nations.

Registration

The PDD and validation report are submitted to the United Nations for formal registration as a CDM/ JI project.

Carbon Commercialization

Buyers of carbon credits can be governments, banks, carbon funds or industrial facilities in Annex I countries. The process of matching the buyer to the seller requires knowledge of the different players in the carbon market. Due to the complexity of selling this unique commodity special contractial agreements must be in place such as Emission Reduction Purchase Agreements (ERPA).

If your plant uses SF_6 and you would like to benefit from this financial opportunity contact us at:
EcoTraders LTD.
email: dishon@ecotraders-global.com
Tel: +972-3-5616224
Or visit our website at:
www.ecotraders-global.com

Superplastic Forming of Magnesium Alloys

Mathias Liewald, Jens Kappes, Robert Pop

Institute for Metal Forming Technology, Stuttgart (Germany)

Abstract: Intensive investigations have been carried out at the Institute for Metal Forming Technology (IFU) Stuttgart especially with the aluminium alloy AA5083 for superplastic forming particularly with regard to the required pressure curve, pore formation, maximum attainable part height and feasibility of superplastic manufactured real components. The experience gained is presently finding application in similar investigations with magnesium alloys AZ31B and ZE10hp. The focus of these investigations is the identification of important physical characteristics for superplastic forming using high temperature uniaxial tensile tests and high temperature pneumatic bulge tests. These parameters will be further used to facilitate the robust manufacturing of complex magnesium sheet metal parts using superplastic forming.

Extensive studies on warm forming of magnesium sheets and tubes are also being carried out. Some of these investigations have shown that otherwise difficult-to-manufacture automotive magnesium alloy (AZ31) components can be manufactured by pneumatic bulging in the temperature range of 300 to 400 ℃. It has been noticed that the pressure curve over forming time is dependent on the part geometry. It is therefore suggested to investigate the superplastic behaviour of magnesium alloys in more detail. Circumferential strains up to 116 % were achieved in investigations on expansion of magnesium alloy ZM21 tubes using internal high pressure forming with axial feeding.

Keywords: Magnesium, Superplastic Forming, Internal High Pressure, AZ31, ZE10, ZM21

1. INTRODUCTION

At room temperature as also at moderately elevated temperatures, hexagonal close packed (hcp) structured magnesium (Mg) alloys have a limited number of slip systems for deformation. This results in poor formability characteristics. However, under elevated deformation conditions, prismatic and pyramidal slip systems are activated and permits plastic deformation within certain limits [1].

Superplastic sheet metal forming processes enable the production of otherwise difficult-to-manufacture or non-manufacturable complex part geometries due to their unique properties; which would otherwise require a large number of manufacturing stages or are possible only as an assembly of joined components in conventional manufacturing. Relatively low tool costs, high design complexity coupled with low forming speeds that lead to long process times make this forming process an interesting alternative especially for small lot sizes.

This paper concerns investigations on the superplastic sheet metal forming of AZ31B and ZE10hp. Results obtained with Internal High Pressure (IHP) forming of magnesium alloy ZM21 tubes at elevated temperatures are also presented.

2. SUPERPLASTIC SHEET METAL FORMING

In superplastic sheet metal forming, the sheet is clamped between two die halves. Surface increase occurs due to reduction in sheet thickness. In general, the clamped sheet is formed at elevated temperatures by pressurising with gas. The matrice forming technique represents the investigated method.

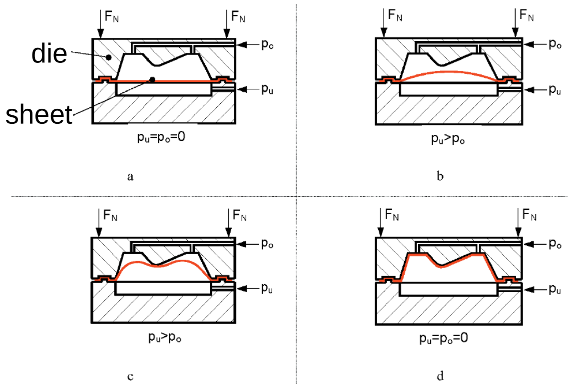

Figure 1. Schematic illustration of the matrice forming technique: a) start process; b) and c) in process; d) process finished [IFU/Vulcan]

2.1. Process Chain for Superplastic Sheet Metal Forming

Superplastic sheet metal forming is marked by an elevated forming temperature ($\vartheta_{\text{forming}} > 0.5 \cdot \vartheta_{\text{melting}}$), low strain rates ($\dot{\varepsilon} < 10^{-1}\ \text{s}^{-1}$) and very high strains. Materials with fine-grained structure and globular grain shape are preferred. Low yield stress at low strain rates and good resistance against pore formation during the forming process is desired.

The aim of the present investigations on magnesium alloy sheets is to build up the complete process chain for the superplastic forming process. This process chain should reveal a detailed perspective on the manufacturing challenges and solutions for superplastic formed components using magnesium alloy sheets.

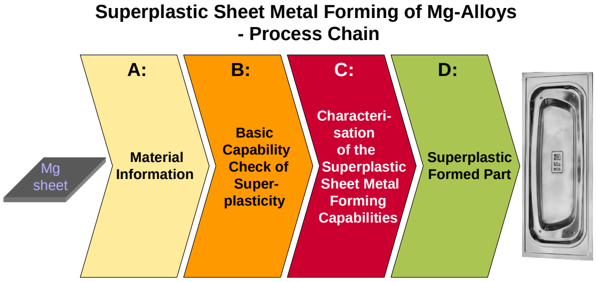

Figure 2. Process chain for superplastic forming

A: Material Information

The process chain starts with the investigation of material information of the considered magnesium alloy sheet. Information regarding the sheet metal mechanical and physical properties at room temperature is collected.

Materials for superplastic forming generally exhibit the following characteristics:

- poor formability at room temperature
- fine-grained structure and globular grain shape

Superplastic forming is not a viable option in case the sheet metal exhibits good formability at room temperature for the desired part geometry.

A fine-grained globular grain shape becomes important on account of the functional principle of superplasticity which involves grain boundary sliding.

B: Basic Capability Check of Superplasticity

The uniaxial tensile test at elevated temperatures provides one part of the Basic Capability Check of Superplasticity by determining the strain rate exponent. Superplastic forming requires $m > 0.3$ [2]. The most accurate method to determine the m-value in the uniaxial tensile test is to draw several tensile specimens at a single temperature and different constant strain rates [3].

The other part of the Basic Capability Check takes place after the uniaxial tensile tests; i.e. investigation of the grain size. This is necessary in order to prevent undesired secondary re-crystallisation (grain growth) that may occur at elevated temperatures.

C: Characterisation of the Superplastic Sheet Metal Forming Capabilities

The pneumatic bulge test takes centre stage in this step. The pressure-time paths, bulging with different counter-pressures and formation of cavities during the forming process within the material volume can be investigated using the pneumatic bulge test. A forming limit curve for the relevant state of stress can also be determined. Simultaneous numerical process simulation of the pneumatic bulge test and calculations with analytical models should be carried out in order to identify the ideal pressure-time paths; which afterwards can be confirmed in pneumatic bulge tests.

D: Superplastic Formed Part

Evaluation of the desired part design on the basis of step C forms the core of this process step. Based on the results of numerical process simulation for pneumatic bulging, it is possible to evaluate manufacturability of the desired part design. This involves identification of the maximum strain in the desired part design and comparing the same with results obtained from the pneumatic bulge test. The part design needs to be modified if the evaluation ends negative. Process numerical simulations with the considered part design are required in case the evaluation ends positive. The results of numerical process simulation should then be verified by experimental testing using the desired part design. The required tooling for manufacture of the desired part should be manufactured and magnesium alloy parts formed superplastically. This phase completes the process chain for the considered part design.

2.2. Results

Existing results of superplastic magnesium alloy sheet forming are arranged in the following; corresponding to the described process chain.

A: Material Information of AZ31B and ZE10hp

Investigations were carried out in order to provide information regarding the mechanical and physical properties of the investigated magnesium alloy sheets under initial conditions and at room temperature:

alloy:	**AZ31B**		
sheet thickness:	1.5 mm		
grain size:	8-12 µm		
mechanical properties:			
- in direction of rolling		$R_{p0,2}$	145-165 MPa
		R_m	255-270 MPa
		A_{80}	14-20 %
- transverse direction of rolling		$R_{p0,2}$	175-195 MPa
		R_m	260-270 MPa
		A_{80}	14-20 %
hardness:	53-56 HV10		source: SZMT/Juchmann

alloy:	**ZE10hp**		
sheet thickness:	1.5 mm		
grain size:	12 µm		
mechanical properties:			
- in direction of rolling		$R_{p0,2}$	148 MPa
		R_m	236 MPa
		A_{80}	18.7 %
- transverse direction of rolling		$R_{p0,2}$	100 MPa
		R_m	220 MPa
		A_{80}	24.6 %
hardness:	47 HV10		source: SZMT/Juchmann

Figure 3. Material information of AZ31B and ZE10hp

B: Basic Capability Check of Superplasticity

The strain hardening exponent can be neglected in superplatic forming [4]. The Ludwik equation then is reduced to:

$$k_f = C \cdot \dot{\varepsilon}^m$$

with k_f as yield stress, C as material constant, $\dot{\varepsilon}$ as strain rate and m as the strain rate exponent. The uniaxial tensile tests were conducted at a constant temperature and at different constant strain rates.

Yield stresses are plotted over subsequent strain rates in a double logarithmic scaled diagram. The strain rate exponent corresponds to the gradient between two measured yield stresses and as the case may be; the interpolation curve in the double logarithmic scaled diagram. Strain rate distances between two measured points should therefore be preferably small.

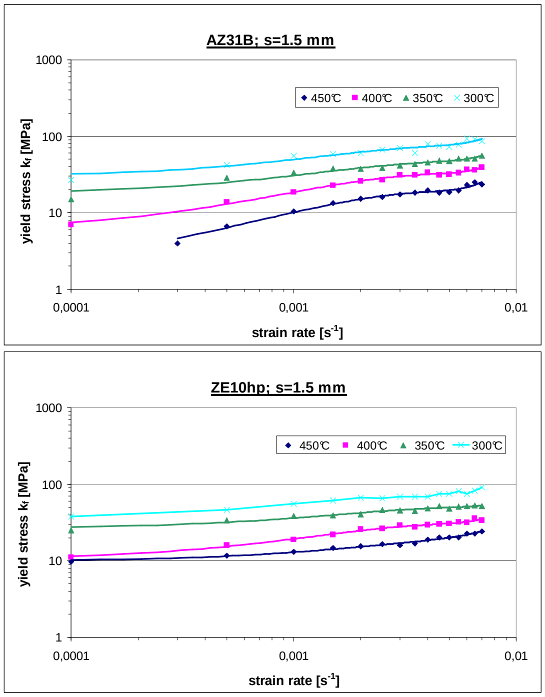

Figure 4. Yield stress diagrams

Figure 5 shows the grinding patterns of AZ31B and ZE10hp after elongation. AZ31B has an average grain size about 15 µm and ZE10hp about 18 µm.

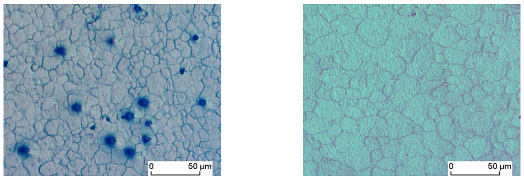
a) AZ31B (450℃; $\dot{\varepsilon}=5\cdot10^{-3}s^{-1}$) b) ZE10hp (450℃; $\dot{\varepsilon}=5\cdot10^{-3}s^{-1}$)

Figure 5. Grinding pattern of a) AZ31B, b) ZE10hp

C: Characterisation of the Superplastic Sheet Metal Forming Capabilities

Superplastic forming has been intensively investigated at the IFU in the past. Superplastic forming using especially the superplastic aluminium alloy AA5083 showed that the pneumatic bulge test is sufficiently adequate for investigation of the superplastic forming behaviour at elevated temperatures [3].

A new pneumatic bulge test tooling is presently being developed. Figure 6 shows a schematic of the same:

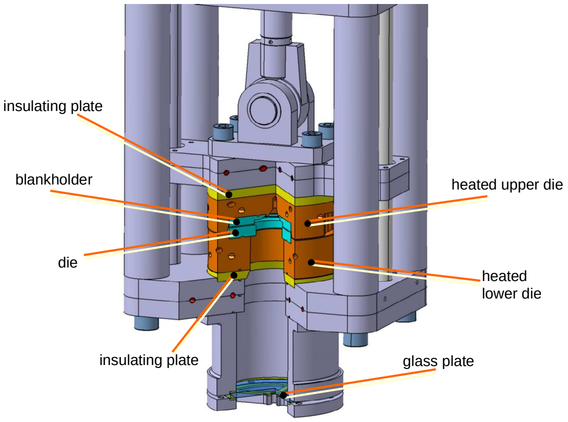

Figure 6. Schematic design of the new pneumatic bulge test

An undeformed sheet is clamped between the die on the lower side and the blankholder on the upper side so that material flow into the forming zone does not occur. Gas pressure acts on the upper side of the sheet, forcing the sheet metal to expand into the die cavity. There also exists the possibility to apply a counter-pressure on the lower side of the sheet simultaneously. Another feature is the glass plate at the bottom which allows in-process-control of the process conditions and strain measurements respectively. The tool is heated and the sheet interposed unheated, for which reason a certain time period should be allowed between clamping and pressurising in order to achieve stable working conditions. The die opening has a diameter of 100 mm and edge radius of 5 mm. Additional dies with elliptical die openings can also be used.

The magnesium alloy sheets AZ31B and ZE10hp should be tested with the new pneumatic bulge test in order to exploit the possibility of in-process-control. A tendency of the expected results can be seen out of former researches into superplastic forming of aluminium alloys at the IFU:

- Tendency of expected pressure path (Figure 7)

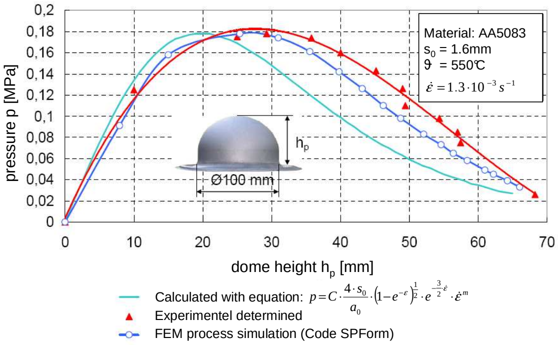

Figure 7. Pressure diagram [IFU/Vulcan]

- Tendency of expected cavities and holes within material volume after the superplastic forming process (Figure 8)

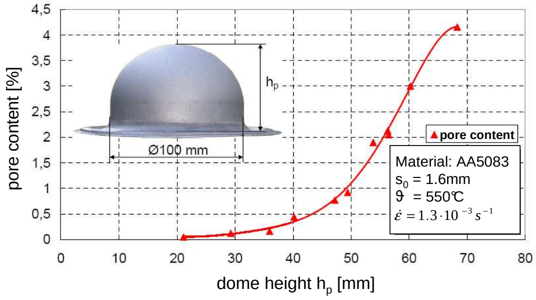

Figure 8. Pores diagram [IFU/Vulcan]

There exists the qualitative and the quantitative pores analysis method. Figure 8 shows results of the quantitative pores analysis method based on the following equation:

$$Porosity = \frac{\rho_{Al}}{\rho_W} \cdot \left(1 - \frac{m_W}{m_L}\right) - 1 \quad [\%]$$

Superplastic forming processes are often based on trial and error. Then the pneumatic bulge test is generally skipped in the process chain. Such an approach can lead to under-utilisation of the potentials of superplastic forming. A scientific approach should include the determination of process limits by using, for example, the pneumatic bulge test under superplastic conditions. The ideal temperature and ideal constant strain rate are very important for superplastic forming. Pneumatic bulge tests, numerical process simulations and analytical calculations are rudimental for selective superplastic forming in order to determine the ideal forming- and counter pressure. The flow limit curve for the relevant stress state can be determined from results of the pneumatic bulge test.

D: Superplastic Formed Part

The process chain includes the verification of step C by investigation of superplastic forming using a real part design. A superplastic formed magnesium alloy part has not yet been investigated since the present research is focused on the determination of formability using the die set described in step C. Former extensive studies at the IFU on warm forming of magnesium sheets have shown that otherwise difficult-to-manufacture automotive magnesium alloy (AZ31) components can be manufactured by pneumatic bulging in the temperature range of 300 to 400 °C. Focus has however not been laid on the determination of forming limits by using the pneumatic bulge test. Some parts manufactured using approximate pressure curves are shown in Figure 9. Future research in this area will be focused on building a robust process chain for the manufacture of complex magnesium alloy part designs.

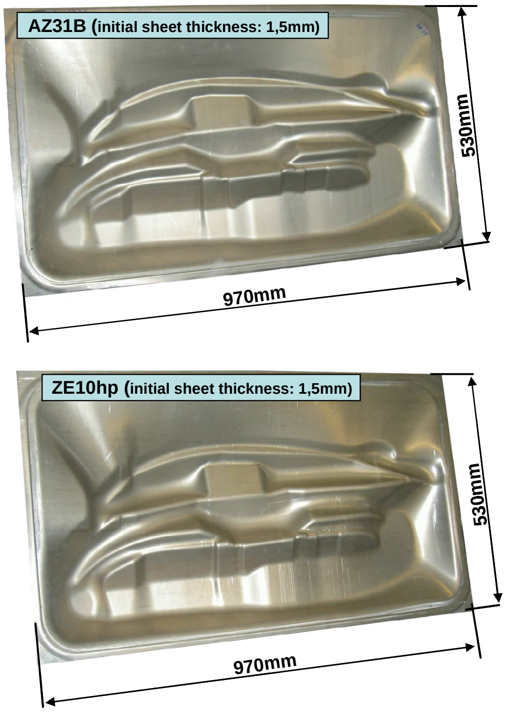

Figure 9. Pneumatic bulged parts

3. INTERNAL HIGH PRESSURE FORMING OF ZM21

Magnesium alloy ZM21 tubes extruded over a moving mandrel die are considered for IHP forming. Previous investigations have shown that welding lines e.g. in case of spider die extrusion causes failure predictably along these welding lines.

3.1. Material Characterisation

To determine the mechanical properties after extrusion, uniaxial tensile tests have been conducted for ZM21 at 20 °C, 235 °C, 300 °C, 350 °C and 400 °C with an average strain rate of $2 \cdot 10^{-2}$ s^{-1}.

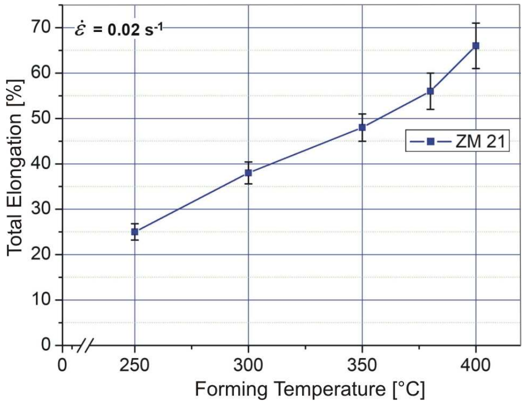

Figure 10. Total elongation versus forming temperature for ZM21

Figure 10 shows the elongations at elevated forming temperatures for milled specimens from ZM21 (seamless tubes). It can be seen that the achievable total elongation is approx. 65 % at 400 °C (as against 19 % at room temperature). For higher temperatures, secondary re-crystallisation can be detected above 380 °C; characterised by excessive grain growth and orange peel formation on the outer surface of the specimen. This incident has to be avoided by maintaining the forming temperature under a certain limit, due to the fact that the only method to eliminate these malformations is to melt the material [5, 6, 7]. The maximum elongation scatters in the range of approx. 5 % depending on the specimen. The ultimate tensile strength at elevated temperatures decreases from 125 MPa at 200 °C to approximately 30 MPa at 400 °C.

3.2. Experimental setup for IHP forming at high temperatures

Figure 11 shows the principle of the lower die for the IHP warm forming tooling designed and developed at IFU [8]. The tooling consists of two units; the clamping- and forming unit. The pressure medium (nitrogen gas) is supplied through the sealing punch.

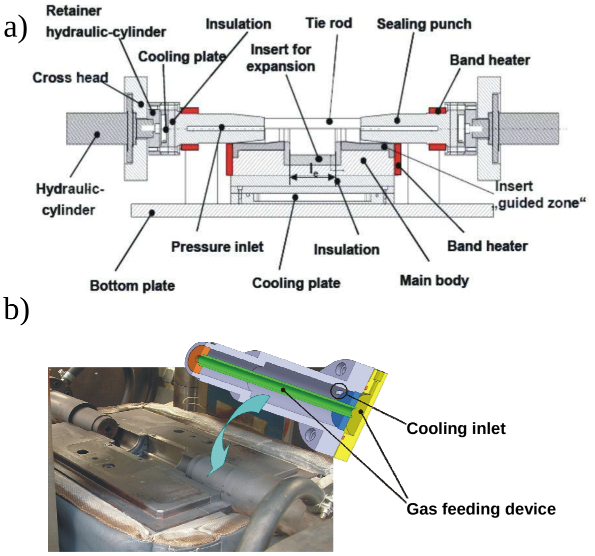

Figure 11. Principle of a tooling for IHP-forming at elevated temperatures [8] a); and lower die with cooled feeding punches for IHP-forming b)

The investigations have shown that the formability of magnesium in plane strain is limited. It is known that the formability can be improved if a compressive stress is superimposed on the material during forming. Furthermore, it is known that the range of manufacturable parts can be enlarged if the material can be fed towards the die cavity. The geometry of the sealing punches for IHP-forming with axial feeding needs to be different from the conical ones (used only for sealing). A new punch design was employed in order to avoid sticking of the tube material in the tool feeding area (Figure 11b).

3.3. Experimental results of ZM21 tubes deformed with axial feeding

IHP-bursting tests using magnesium alloy ZM21 with axial feed have been conducted at temperatures up to 350 °C. The maximum circumferential strain was measured to be 116 %. It is however to be noted that the formed part contacts the tooling in certain regions, leaving room for further extension of the mentioned limit [1].

Figure 12 shows a demonstrator part formed at 350 °C in which a maximum circumferential strain of 94 % was measured.

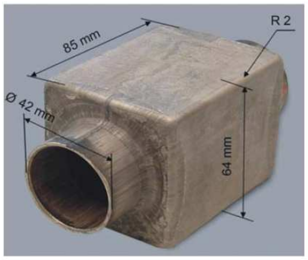

Figure 12. Magnesium alloy ZM21 part formed at 350 °C using a non-linear pressure path

Inhomogeneous re-crystallisation due to variable heat transfer from the die set to the material and the non-constant deformation degree, respectively, could be observed (Figure 13). The temperature of the die set is kept nearly constant in the forming area due to the indirect heating and the multipoint measuring temperature controlling system. During the experiments, the material contacts the tooling at an early stage in certain regions. The heat flow and the relative low deformation in these regions induce secondary re-crystallisation. The grinding patterns in the plane area (Figure 13a) and in the edges (Figure 13b) of the part are shown in Figure 13.

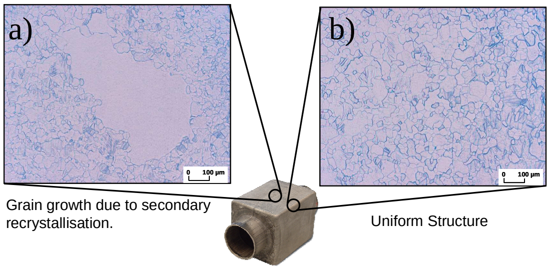

Figure 13. Grinding pattern of part

Depending on the dimensional tolerances of the extruded tubes, the wall thickness of the deformed part for all four sides along the tube axis and in the transverse direction, respectively, could be measured as shown in Figure 14. The initial wall thickness was 2 mm.

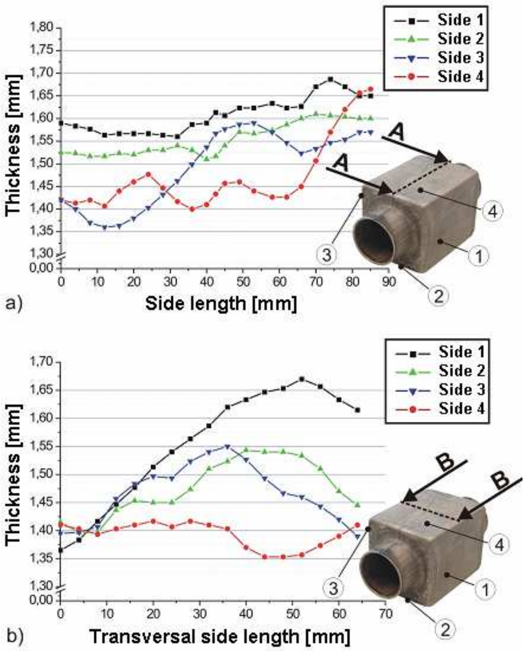

Figure 14. Wall thickness distribution of the magnesium ZM21 part: a) along the tube axis, b) in the transverse direction

A non-linear pressure curve with maximum value of 4.2 MPa has been selected in order to increase forming pressure and calibrate the small contours after the initial forming of the part geometry.

4. REFERENCES

[1] M. Liewald, R. Pop, S. Wagner, „Magnesium Tube Hydroforming“, 10th ESAFORM Conference on Material Forming, Zaragoza, Spain, 18-20 April 2007

[2] E. Roos; K. Maile: „Werkstoffkunde für Ingenieure“, 2. Auflage; Springer Verlag, Berlin Heidelberg 2002, ISBN 3-540-22034-8

[3] T. Werle: „Superplastische Aluminiumblechumformung unter besonderer Beachtung der Formänderungsgeschwindigkeit“, DGM Informationsgesellschaft Verlag, Stuttgart 1995, ISBN 3-88355214-3

[4] M. Vulcan, „Der pneumatische Tiefungsversuch und seine Anwendung in der superplastischen Aluminium-Blechumformung“, MAT INFO Werkstoff-Informationsgesellschaft mbH, Stuttgart 2006, ISBN 3-88355-356-5

[5] U. Draugelates et al., „Properties of Fine-Grained Cast Magnesium Alloys for Sheet Manufacture” in Magnesium Technology 2001, J. N. Hryn, ISBN 0-87339-481-x, Proceedings of the TMS Annual Meeting, New Orleans, Louisiana, U.S.A., February 11-15 2001, pp. 223-226

[6] A. Birkert, “Umformende Fertigungsverfahren” Lecture Notes for Mechanical Engineering Specialization, technical college Heilbronn, 2007

[7] H. Horn, “Verfestigung und Rekristallisation” Lecture Notes for Materials Science Specialization, 5th Chapter, technical college Hamburg, 2007

[8] S. Jäger and C. Wizemann, “Internal High Pressure Forming of Magnesium AZ31 Tubes”, Internal Report, Institute for Metal Forming Technology, Stuttgart, Germany, 2004

Development of the Magnesium Die-Cast Motorcycle Chassis

Takaharu Suzuki
YAMAHA-MOTOR CO.,LTD.

Junichi Inami
YAMAHA-MOTOR CO.,LTD.

Toshikatsu Koike
YAMAHA-MOTOR CO.,LTD.

ABSTRACT

The large, thin-walled magnesium die-casting technology has been developed for the purpose of motorcycle chassis production. The vacuum assisted die casting process improves not only the soundness but also the mechanical properties of the cast parts. Fatigue strength (R= - 1) of the cast pieces has been proven to have a minimum of 70MPa. The cast's minimized impurities in combination with undercoating and painting have it possible to attain a sufficient level of corrosion resistance required for use as exterior parts. The magnesium cast features a 20% weight reduction with the same stiffness compared to aluminum cast parts. Magnesium die-cast parts produced by this newly developed technology have been utilized in the rear frame of the mass produced supersport model '08 YZF-R6.

INTRODUCTION

The demand for lighter weight vehicles has become increasingly significant from the standpoint of both good drivability and low fuel consumption. The aluminum chassis have been widely used to reduce the weight of motorcycle chassis over the past twenty years. Many aluminum alloys and production processes have been developed for this purpose. To improve productivity and part cosmetics, aluminum die-casting technologies capable of producing large, thin-walled parts have also been developed and utilized for chassis parts [1]. However, in spite of those efforts, there seems to be limited possibility for additional weight reduction in today's aluminum chassis.

Magnesium is attractive as a next-stage lightweight material. However, applications of magnesium parts for motorcycles have been limited so far to covers, cases and brackets. In order to be used for motorcycle chassis parts, however, magnesium parts must not only have high strength and high ductility as structural

parts but also have sufficient corrosion resistance as external parts.

Fig.1 Magnesium rear frame in 08'YZF-R6

Reports from several studies of magnesium applications for automotive parts have been published. Large parts for automotive interiors have enabled significant weight reduction [2]. And external structural parts for attachment to other parts have also been made of magnesium [3], [4]. But there has not yet been no application of large, thin-walled parts with sufficiently high strength, ductility and corrosion resistance for the structural components that a person can ride on. For the purpose of using magnesium parts in motorcycle chassis, the mechanical properties and the corrosion characteristics of large, thin-walled vacuum die-cast AM60B parts were first investigated and compared to the conventional chassis aluminum and steel parts. Secondly, the characteristics of die-cast AM60B chassis parts with modified designs and surface coatings have been investigated and compared to conventional aluminum die-cast parts.

EXPERIMENTAL PROCEDURE

The Chemical composition of the test specimens is shown in Table1. The specimens are extracted from the H120mm x W250mm x L825mm parts cast using a horizontal cold chamber high-pressure die-casting machine. Typical wall thickness was 2mm. Table2 shows the typical casting process parameters for the production of the parts. The shot weight was about 5Kg. The Vacuum valve and censers were added in the die and control integrated by plunger position signals. In order to prepare specimens with different vacuum levels, three vacuum conditions of -0.06Mpa, -0.02MPa, and 0MPa were estimated by changing valve work time. Vacuum valve does not function at level of 0MPa.

Table 1 Chemical composition of test specimens (Wt%)

Al	Zn	Mn	Si	Fe	Cu	Ni	Be	Mg
5.8	0.02	0.293	0.0168	0.003	0.0013	0.0005	0.0004	Bal.

Table 2 Casting parameters of tensile test specimens

Metal temp.	690+ 5℃
Die temp.	200～250℃
Fill time	< 30 mm・sec
Plunger speed	7 m・sec^{-1}
Casting pressure	53MPa/ cm^{-2}
Heat treatment	F

Tensile properties

The dimensions of the specimen are shown in Fig.2. In order to examine the effect of the vacuum to the mechanical properties, three vacuum levels were chosen. Two specimens were prepared and tested for each condition. The specimens were cut from the gate area and the overflow area of the cast. The Ultimate Tensile Strength (UTS) and elongation to failure were measured. The tests were carried out using the INSTRON 5882 servo-hydraulic universal testing machine at room temperature. The cross-head speed was 1.0mm・min^{-1}. In order to compare the results, aluminum A365-F die-cast specimens (-0.06MPa Vacuum-level, gate area) were also prepared and tested. The fracture surfaces and the cross sectional views of the after tested AM60B specimens were also observed by the optical microscopy.

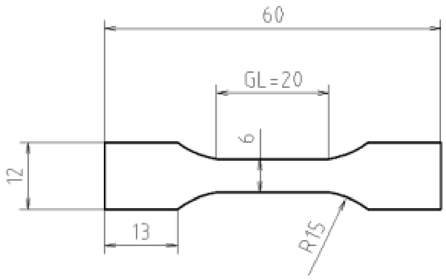

Fig.2 Dimension of the tensile test specimen (mm)

Fatigue properties

Fatigue strength tests were carried out using a Tokyo Koki Seisakusyo PWOG-L type plate bending fatigue test machine at room temperature. All the fatigue tests were performed at a stress ratio of –1 and a frequency of 25Hz. The specimens were cut from the gate area and polished with #1500 paper. The dimensions of the specimens are shown in Fig.3. In order to compare the results, aluminum A365-F die-cast specimens (-0.06MPa Vacuum-level, gate area) were also prepared and tested with the same condition.

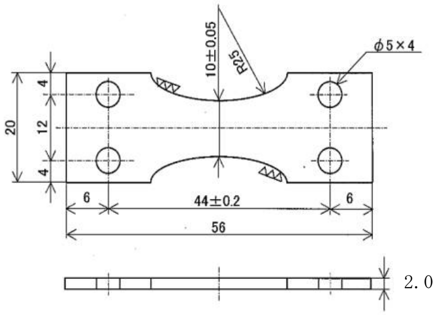

Fig.3 Dimension of the fatigue test specimen (mm)

Corrosion properties

Corrosion test was carried out using a Suga Casser-ISO-3 type test. The test was according to JIS Z 2371 Salt Splay Test (SST). The test condition is shown in Table3. The exposure time is 120Hr. In order to compare the results, JIS AC4CH aluminum gravity-cast specimen (from the conventional chassis aluminum parts) and SPHC steel specimen (from the conventional chassis steel parts) were also prepared. The all specimens were polished with #1500 paper before the test. After the test, the surfaces were observed and the weight losses were also measured.

Table 3 The conditions of corrosion test

Testing machine	SUGA CASSER-ISO-3
Standard	JIS Z 2371
Solution	50±5g/L NaCl (PH6.5～7.2)
Temp.	35±2℃
Angle of specimen	30°

RESULT

Tensile properties

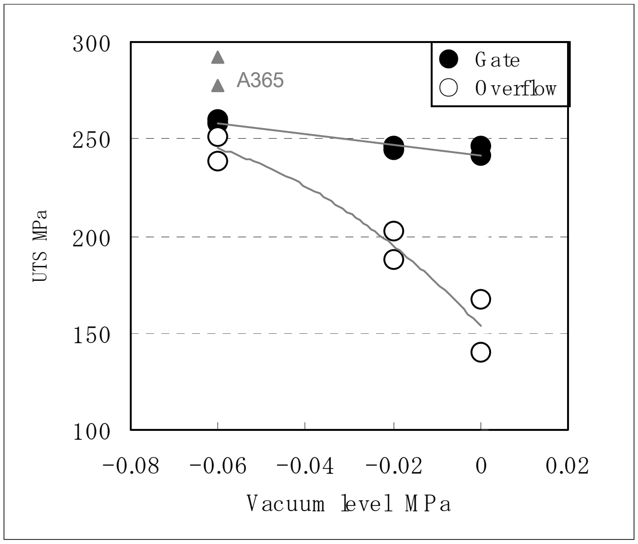

Fig.4 Relationships between UTS obtained for different vacuum level

The UTS results obtained at different vacuum level are shown in Fig.4. At vacuum level -0.06MPa, UTS of the AM60B gate area shows over 250MPa and that is a little lower than that of A356 gate area. The UTS of the AM60B gate area decreases a little bit with decreasing the vacuum level. The UTS of the AM60B overflow area shows nearly the same level as the AM60B gate area. However, the UTS of the overflow area decreases drastically with decreasing the vacuum level.

Fig.5 shows the relationships between the elongation and the vacuum levels. At vacuum level -0.06Mpa, the elongation of the AM60B gate area shows more than 15%, much higher than that of the A356 die-cast specimens. The elongation of the gate area decreases slightly with decreasing the vacuum level. The elongation of the overflow shows almost 12% at vacuum level –0.06MPa. The value is lower than that of the AM60B gate area and higher than that of the A356 gate area. The elongation of the overflow area also decreases slightly with decreasing vacuum levels.

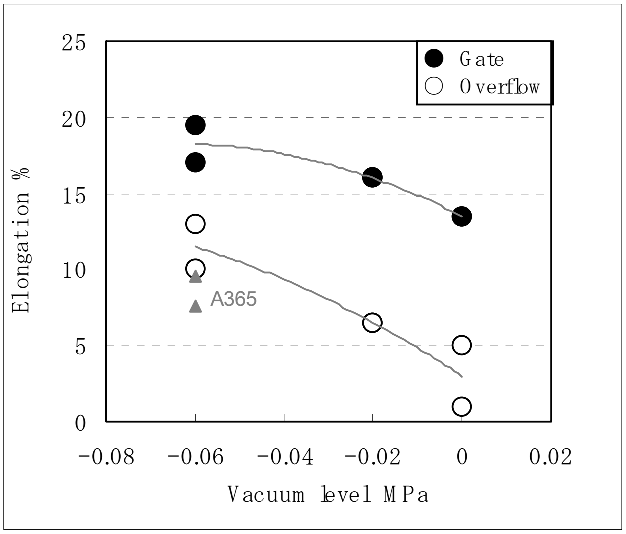

Fig.5 Relationships between elongation obtained for different vacuum level

The photographic views of the fracture surfaces are shown in Fig.6. At a vacuum level –0.06MPa, no porosity have been observed both in the gate area and in the overflow area. At a vacuum level –0.02MPa, some small porosity have been observed only in the overflow area. At a vacuum level 0MPa, some porosity was observed both in the gate area and in the overflow area, and the size and number of pores were more in the overflow area.

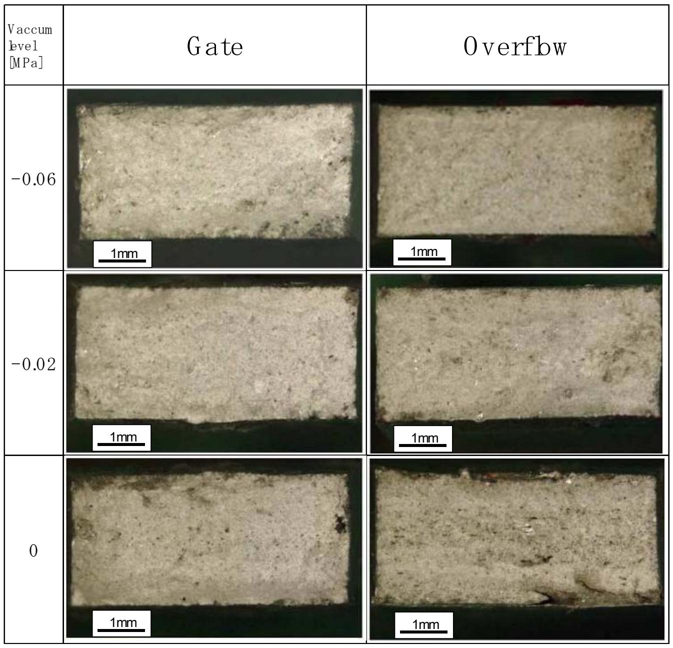

Fig.6 Photographic views of the fracture surface

Cross-sectional views of the specimens are shown in Fig.7. The grain size of the matrix and the distribution of all the precipitates are almost the same. Some porosity is observed only in the vacuum level 0MPa overflow area.

Fig.7 Cross-sectional views of the specimens

Fatigue properties

The S-N curves of the AM60B die-cast specimens and the A365 aluminum die-cast specimens are comparably shown in Fig.8.

Fatigue strength (1×10^7) of AM60B was 83MPa, that is lower than that of the A365, 93MPa.

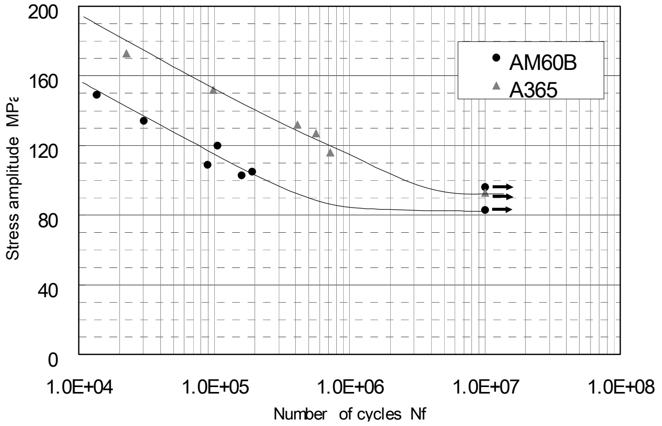

Fig.8 S-N curves of the AM60B die-cast and the A365 aluminum die-cast

The specific fatigue strength of the AM60B are shown in Fig.9. The S-N curves of the AM60B die-cast pieces and the A365 aluminum die-cast pieces are also comparably shown in Fig.8. The specific fatigue strength of the AM60B was 20% higher than that of the A356.

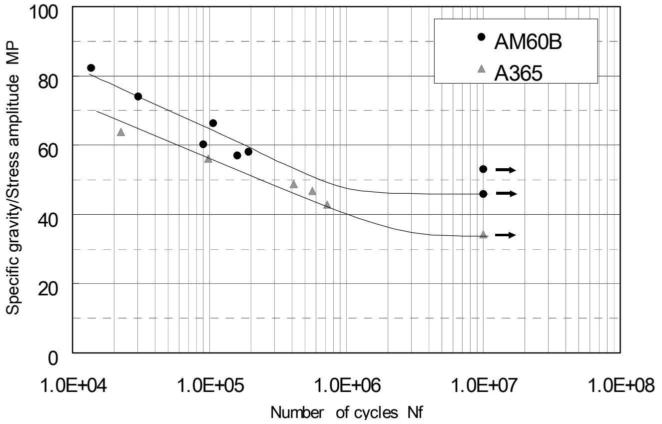

Fig.9 Specific fatigue strength of the AM60B die-cast and the A365 aluminum die-cast.

Corrosion properties

Fig.10 shows the photographic view of the surface after the SST. The surface of the AM60B die-cast turned to white. No erosion or pits have been observed at the surface. The surface of the AC4CH gravity-cast also turned to white and no erosion or pits have also been seen on it either. The surface of the SPHC steel turned to brown-black and some erosion were observed at the surface.

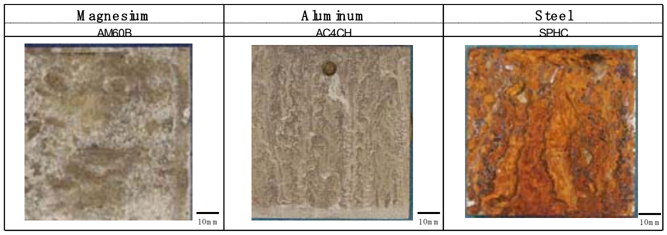

Fig.10 The photographic views of the surface after SST

Fig.11 shows the weight loss of the specimens during the SST. The results of the AM60B die-cast and the AC4CH aluminum gravity die-cast are almost the same and remarkably low level in comparison with that of the SPHC steel.

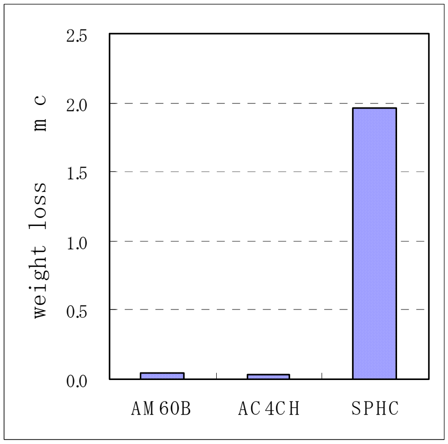

※$\text{mcd} = \text{mg}\cdot\text{cm}^{-2}\cdot\text{day}^{-1}$

Fig.11 The weight loss of the specimens during the SST

DISCUSSION

Mechanical properties

As shown in Fig.4 and Fig.5, the UTS and the elongation show the highest value with the highest vacuum(-0.06MPa) condition. This indicates the effectiveness of the vacuum to improve the tensile properties of the AM60B die-cast. The effect is most clearly observed in the UTS of the overflow area. From the results of Fig.6 and Fig.7, the porosity of the overflow area have clearly diminished in the higher vacuum level. The microstructures have not been affected with the vacuum level. Based on the above results, vacuum is concluded to improve the mechanical properties through decreasing the porosity defects in the cast. In general, die-cast process tends to take in the gas existed in the die-cavity because the flow speed is high and much turbulence occurs during the injection. The over flow area has a tendency to gather the gas inclusion more than the gate area. The vacuum is considered to take out the die-cavity-gas and decreased the opportunities of the taking in the gas into the cast, finally decreases the porosity in the cast (especially overflow area) and improves the mechanical properties of the cast. Specific fatigue results (Fig.9) indicate the possibilities to design the AM60B lighter weight die-cast parts more than the A365 aluminum die-cast parts.

Corrosion properties

The results of Fig.10 and Fig.11 indicate that AM60B die-cast has the almost same level corrosion resistance as the conventional chassis aluminum alloy JIS AC4CH. In order to ensure the good corrosion resistance of the magnesium alloy, it was known that keeping the impurities (such as Fe, Ni, Cu) at low level should be required [8]. The impurities level of the AM60B die-cast specimens (Table1) is consequently considered to be the enough low level as the applications for the exterior chassis parts.

APPLICATION

The rear frame was designed based on the above experimental results. The newly designed AM60B die-cast rear frame has achieved a 20% lighter weight with the same stiffness compared to the A365 aluminum die-cast rear frame. The designing also included the modification for avoiding the hot cracks at the die-cast. The AM60B die-cast rear frame after applying the undercoat and the paintings has also proved to have a sufficient corrosion resistance required for the exterior parts (Fig.12)

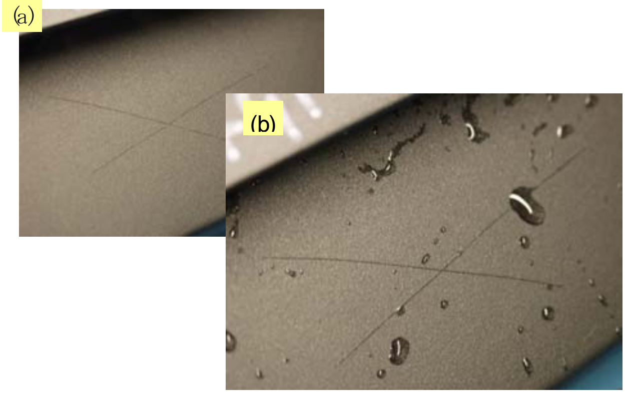

Fig.12 Photographic views of the AM60B die-cast rear frame after making the undercoat and the paintings. (a) Before salt spray test, (b) After 240Hr salt spray test

The rear frame is used for the combination with the aluminum main frame. So structures to prevent galvanic corrosion are also needed. The structures are shown in Fig.13.

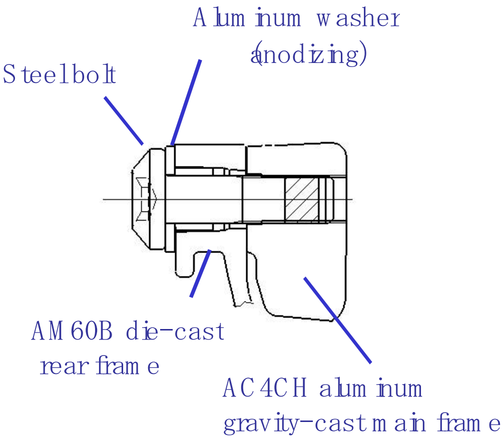

Fig.13 The Joining structures to avoid the galvanic corrosion between the AM60B die-cast rear frame and the AC4CH aluminum gravity-cast main frame.

Fig.14. shows the photographic view of the joining area after the test. No harmful corrosion has been seen at the area.

Fig.14 Photographic view of the joining area after SST

CONCLUSION

The mechanical and corrosion characteristics of the large, thin-walled and vacuum assisted die-cast AM60B parts have been investigated.

1) AM60B die-cast shows more than 250MPa UTS and more than 15% elongation under -0.06MPa vacuum level. The elongation is much higher than that of the A356 aluminum die-cast.

2) The fatigue strength of the AM60B die-cast shows 83MPa (gate area, $1x10^7$, R=-1). The specific fatigue strength is 20% higher than that of the A356 aluminum die-cast.

3) The AM60B die-cast shows almost the same level corrosion resistance as the AC4CH aluminum gravity die-cast, much lower level than the conventional chassis steel SPHC.

Based on the experimental results, motorcycle rear frame has been newly designed and evaluated.

4) Part design has been optimized to achieve a 20% weight reduction with the same stiffness compared to the aluminum die-cast.

5) The AM60B die-cast rear frame with the undercoating, paintings and the adequate joining structure shows the sufficient corrosion resistance for the exterior chassis parts.

The developed rear frame has been utilized for the mass product supersport ’08 YZF-R6 (Fig.15).

REFERENCES

1. T.kitsunai, H.yamagata, T.koike, “Light Body for Small Vehicles Using High-Quality Die Casting Component” SAE 2003-01-2869

2. S.Glen, S.Brian "Magnesium in Automobiles Application Trends and Advantages" Proc Annual Meeting International Magnesium Association Vol.63rd Page.66-72 (2006)
3. J.S.Balzer, P.K.Dellock and M.H.Maj, G.S.Cole, D.reed, T.Davis, T.Lawson, G.Simonds. "Strucural Magnesium Front End Support Assembly" SAE Technical Paper 2003-01-0186
4. C.J.Duke and S.D.Logan, "Lightweight Magnesium Spare Tire Carrier" Proc Annual Meeting International Magnesium Association Vol.64rd Page.75-80 (2007).
5. Norsk Hydro,Data Sheets for Magnesium Alloys
6. T.Kr.Aune and D.L.Albright, Hakon Westengen "Properties of Die Cast Magnesium Alloy of Varying Aluminum Content" SAE Technical Paper 1990
7. Y.Miyashita, S.A. Khan, Y.Mutoh, T.Koike, 7th International Conference on Magnesium Alloy and their application, Dresden, Germany, Nov. (2006),6-9
8. J.E.Hillis and K.N.Reichek "High Purity Magnesium AM60 Alloy: The Critical Contaminant Limits and the Salt Water Corrosion Performance" SAE Technical Paper 860288-1986
9. G.G.Wang, K.Stewart and R.Berkmortel, J.I.Skar, "Corrosion Prevention for External Magnesium Automotive Components" SAE Technical Paper 2001-01-0421
10. J.I.Skar, M.Isacsson and Z.tan, "Galvanic Corrosion of Die Cast Magnesium Exposed on Vehicles and in Acccelerated Laboratory Tests" SAE Technical Paper 2006-01-0255
11. Xiaoming C, D.A.Wangner, D.Q.Houston, R.P. Cooper, "ELONGATION VARIABILITY OF AM& DIE CAST SPECIMENS" 2004 ASME International Mechanical Engineering Congress and Exposition Nov. 13-20,2004
12. N.Moscovitch,G.Gertsberg,N.Nagar,M.Lautzker,N.Fantetti and B.Bronfin "The effect of porosity on the microstructure and mechanical properties of die cast Mg alloys" SAE Technical Paper 2006-01-0524

Fig.15 Mass product supersport '08 YZF-R6

CONTACT

Takaharu Suzuki, Materials research Dept. Research & Development Operation, YAMAHA MOTOR CO.,LTD. 2500 Shingai,Iwata,Shizuoka, 438-8501,Japan,tel.+81-538-32-1178,fax+81-538-37-9407,e-mail suzukitakaharu@yamaha-motor.co.jp,
web/ www.yamaha-motor.co.jp

Recycling of Post-Consumer Mg Scrap

Dr. Adam J. Gesing, Gesing Consultants Inc.
Dr. Alain Dubreuil, Natural Resources Canada

Mg is coming into its own as a structural parent metal. Annually, primary Mg metal production is quickly approaching one million tonnes (T), new scrap recycling and remelting 300 thousand T, and the potential availability of old post-consumer scrap is approaching 100 thousand T.

Since the EU waste directive mandates the recycling of end-of-life vehicles (ELVs), the recyclability of materials in the ELV is becoming a significant consideration that affects the penetration of magnesium-based alloys into the vehicular market.

In North America, there is still almost no recycling of post-consumer Mg. USGS statistics show a decreasing trend in the recycling of post-consumer Mg scrap with only 800 tons consumed in the US in 2005, as compared to the 10,000-20,000 tons of old Mg-alloy diecastings one already expects from shredded ELVs in the US. The Mg in the portion of the scrap that is sold directly by the shredders to the secondary smelters as Al concentrate product ends up chlorinated out of the Al foundry melt and lost in Al dross.

We explore the true global picture of Mg metal recycling, show where and how it is actually taking place, and highlight areas of current and potential use for Mg-based scrap. We describe technologies that are currently used for separation of old Mg from other scrap and waste and that may help improve Mg recovery the future. Areas where Mg losses occur in the current recycling system are described and strategies for minimization of these losses are proposed.

Global picture of Mg metal recycling

The technical feasibility of using Mg-based alloy castings, extrusions and sheet in automotive and aerospace applications was demonstrated on an industrial/commercial scale in the 1950s. The large price premium over steel and aluminium, however, prevented wide-scale commercial adoption of these products until the1980s. At that time China made a concerted effort to capture the Mg production market and drove down the price of Mg to near par with Al using a silicothermic reduction process developed in Canada in the 1940s. The return of Mg alloys to the World consumer market was spearheaded by the diecastings that started finding applications such as automotive interior components and housings for portable electronic and electrical equipment (EEE). Until recently there was not a significant amount of Mg alloy in old metal scrap. However, the first Mg-alloy components that made their way into cars in the 1980s and 1990s are now appearing in a small but ever-increasing proportion in ELVs. Until recently waste electronic and electrical equipment (WEEE) was landfilled with municipal solid waste (MSW). The regulations in EU and some parts of North America now require the manufacturers to take the responsibility for collecting and recycling their WEEE in a system separate from MSW and ELVs. The scrap recycling system is already adjusting to these new opportunities.

The challenge of enabling the recycling of post-consumer Mg alloys involves the need for collection and recycling system plus a financial profit incentive.

Until recently (~2003) there was not sufficient Mg-alloy content in the metal concentrate shredder product to warrant the separation of the Mg as separate scrap product, nor was there market demand for such a product. Any Mg present ended up as a contamination in shredded Al and was sold to secondary Al smelters where it was chlorinated out of the Al foundry alloys to be lost in Al dross residue.

Al secondary smelters now know that it is in their interest to demand that their suppliers (the ~800 shredders and ~50 media plants and metal sorters) remove free Mg from shredded scrap aluminium. (There may not be a need to remove the residual free Al from the Mg byproduct created by such a separation). Enlightened secondary Al smelter operators, in turn, share with the suppliers the benefit of reduced chlorination and improved plant throughput by paying a price premium for the low-Mg Al shred. That price premium must be sufficient to pay for the investment at the shredder for the Al-Mg sorting circuit or to induce the shredder to leave the Al in the metal concentrate sold to a dense media sink-float plant. At the sink-float plant, Mg is separated from Al and recovered in the magnetite-float fraction that contains Mg and hollow Al. This fraction is exported to Asia for handsorting.

In the case of Mg, if the metal stays at a price par with Al for the same functional component, its rate of substitution will be paced simply by the availability of the metal from prime or old scrap and the capacity of part manufacturers to produce the required shapes with the required properties.

Types of Mg-Alloy Scrap Available and its Sources

New Scrap

Diecasting dominates the fabrication of Mg-alloy components. Typically, the cast component weighs only 50% of the diecasting machine shot weight; the rest is trimmed off and recycled as scrap. In US there were 70,000 T or globally ~300,000 T of new diecasting scrap recycled in 2006 (1,2,3). Diecasters generally maintain alloy segregation at source. This allows closed-loop recycling back into the same alloy or into a compositionally more tolerant alloy.

Remelting residues: Mg can be remelted up to four times before ending up in a product component: once as primary “crown” Mg, then during alloy remelt ingot casting, then prior to diecasting and lastly as new scrap. Each of these steps generates remelt scrap and losses in the form of dross and sludge. A 3-4% melt loss in each step would be representative of a good melting and casting practice. Our estimate for 2006 in the US gives 7,000 T metal, mixed with 15,000 T of oxides and intermetallics contaminated with flux. This quantity is included in the global 40,000 T of metal with 80,000 T of oxides and intermetallics, a mixture that is sold to Mg granulation plants. There is a potential for upgrading this residue by separating the metal from its oxide by crushing, screening, eddy current separation or conceivably sensor-based sorting.

Post-Consumer Scrap

Primary Shredder Metal Concentrate: Scrap is traded on a World market where in 2006 there were ~40 million ELVs with ~2 kg of Mg diecasting each (mainly AZ91 or AM60), or 80,000 T coming back from ELVs in the Al and nonmagnetic metal concentrate (NMMC) shred streams flowing from ~800 separate shredders. In 2030 we will be scrapping the 2015 model year, which is predicted to have 0.6% Mg alloy in a 3900-pound car. There could be 70 million ELVs with 11 kg of Mg per ELV, or 770,000 T of old Mg alloy scrap, exiting the system by 2030. This assumes that these Mg components can be produced by 2015.

In total, shredder nonmagnetic metal concentrate currently contains ~100,000 T of Mg-alloy particles in ~7 million T of nonmagnetic metal shred recovered from a mixture of ~40 million ELVs, appliances, bulky consumer durables, mixed metal from demolition residue, and mixed-metal scrap yard categories shredded in 2006.

Consumer Electronics – Mg-alloy housings are penetrating the markets of 300 million cell phones and personal digital assistants (PDAs), 50 million digital cameras and video recorders, and 250 million MP3, CD and DVD players, and 200 million PCs and laptops, plus miscellaneous digital sound recorders, portable radios and TVs (4,5). EEE is already providing a major market for Mg diecastings and in the not-to-distant future, EEE will provide a major source of post-consumer Mg diecasting scrap.

These consumer electronics have a relatively short time to obsolescence (2-5 years) and are mostly non-repairable. A separate system is being set up to collect and recycle WEEE materials. This system will attempt to capture the Mg housings from WEEE. At this point, the penetration of the housing market by Mg diecastings is still limited to high-end products and the collection systems are just beginning to be set up. The majority of the collected scrap is exported to China and Africa in contravention of the Basel convention.

Forty million notebook computer housings with 750g of Mg each can bring back ~30,000 T of Mg scrap by 2010. A similar annual amount will be available soon from cell phone, PDA, and audio player housings. Mg alloys from these products, mostly Mg-AZ91D diecastings, are already in the current post-consumer scrap streams – MSW and WEEE. As Mg-alloy housings continue to penetrate this huge market, this source of old Mg alloy scrap will grow quickly.

Portable Power Tools that can benefit from Mg-AZ alloy housings are drills, saws, screw drivers, weed trimmers and lawn mowers. Plug-in electric and gas-powered tools have long lives (~15-25 years). The lives of battery-powered tools are shorter (~5 years), limited by the evolution and availability of replacement battery packs. The use of Mg housings is just beginning and significant quantities of end-of-life Mg-alloy power tools will not make it to WEEE until 2025-2030.

End-of-life electronic and electrical consumer products are supposed to be collected and processed separately as WEEE. There is battery removal and some dismantling for component and subassembly reuse, but that rarely includes housings. These are shredded for material liberation and segregation. WEEE material needs to be shredded to a finer size than vehicles and appliances to liberate individual materials.

Figure 1. Steel desulphurisation

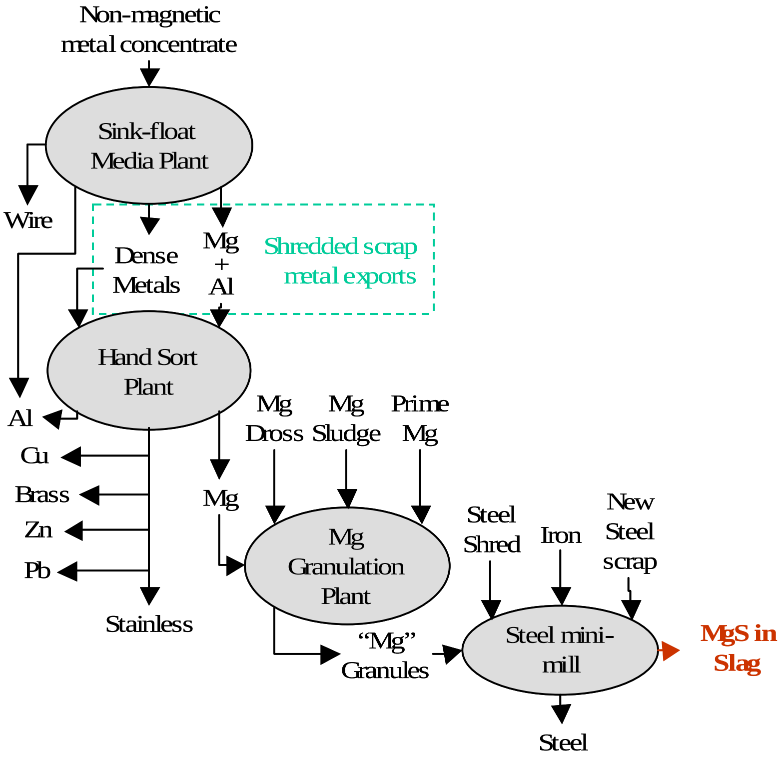

Current Markets for Post-Consumer, Mixed-Alloy, or Contaminated Mg-Alloy Scrap

There are three potential markets for old Mg scrap, either alone or in a mix with Al. These are: additives for steel and nodular iron production, Al can sheet alloys, and Mg diecasting alloys in property non-critical applications (such as housing for portable electronics, or automotive interior components such as instrument panels). These markets are all growing quickly in the developing part of the World. Whoever wants to get this scrap to feed their market will have to pay the full metal value of the scrap, which is set, as is the case with Al scrap, by comparison with the prime price on the LME or Shanghai exchange. As long as expansion in the combination of these three markets outpaces the growth of supply of old, post-consumer Mg-alloy scrap, there will be no Mg metal recycling system need to include old scrap content in property-critical applications in automotive, marine, aerospace and defence applications.

Granulates for steel desulphurisation, thermites and pyrotechnics: In 2006 these applications consumed ~8,000 T of Mg in the US, or ~75,000 T globally. Mixed-alloy machining chips, turnings and borings – always contaminated with cutting lubricants – are difficult to melt with high metal recovery. Remelting residues, including melting drosses and refining sludges, are heavily contaminated with oxides, fluxes and intermetallics. In many cases, the Mg remelt facilities are not yet equipped to deal with old, dirty, Mg-alloy scrap. Steel desulphurisation granulates, however, only require a specified Mg content which, depending on the grade, can vary between 75-90% (Fig. 1). This metal content can be supplied by the Mg scrap with no melt losses. These granulates at this time most likely consume the bulk of the post-consumer Mg-alloy scrap as well as remelting residue and mixed alloy machining chips.

Potential Markets for Post-Consumer Scrap

<u>Al alloying</u> – 3X04 can body sheet needs replacement for Mg in ~800,000 T of cans lost to litter and landfill in the US. In 2006 this required ~10,000 T of new Mg in US. Globally this amount expands to ~15,000 T of Mg, which could grow to ~40,000 T of Mg in the future if the rest of the World adopts Al cans to the extent that the US has – ~1 can per person per day. Other Al-Mg alloys could use Mg-alloy scrap for alloying element addition, if it were converted into a specification Mg hardener alloy ingot with tightly controlled composition. Total amount of prime Mg used for Al alloying globally was ~180,000 T in 2006.

At this point, Mg-alloy scrap is not used in Al alloying, in spite of the fact that UBC remelt plants could easily add Mg-alloy machining scrap or post-consumer shredded Mg-Al mix to the UBC plant feed and allow it to be cleaned and vortex sub-mergence melted with the UBC shred. In a vortex strong enough to draw Mg particles under the surface of molten Al, one would likely see a high recovery of the Mg in the melt. (Fig. 2)

The procedure in the Al industry is to use prime Mg ingot or a hardener ingot batched from prime Mg to add Mg to the melt after melting and determining the melt batch composition. In order to fit into this procedure while using Mg-alloy scrap, one would need to batch and melt Mg scrap, adjust the composition and cast Mg hardener ingot with tightly controlled composition limits. This would make economic sense only if the secondary smelter could consistently buy Mg-Al magnetite float product at a discount and sell the Mg content of the hardener ingot at the prime Mg price.

Once the Mg-Al mix is exported for handsorting, the sorted products do not return to NA or EU. Rather, the handsorted Mg scrap is used in Asia for steel desulphurisation or for batching common

Figure 2. Mg and Al Scrap for Al Alloying

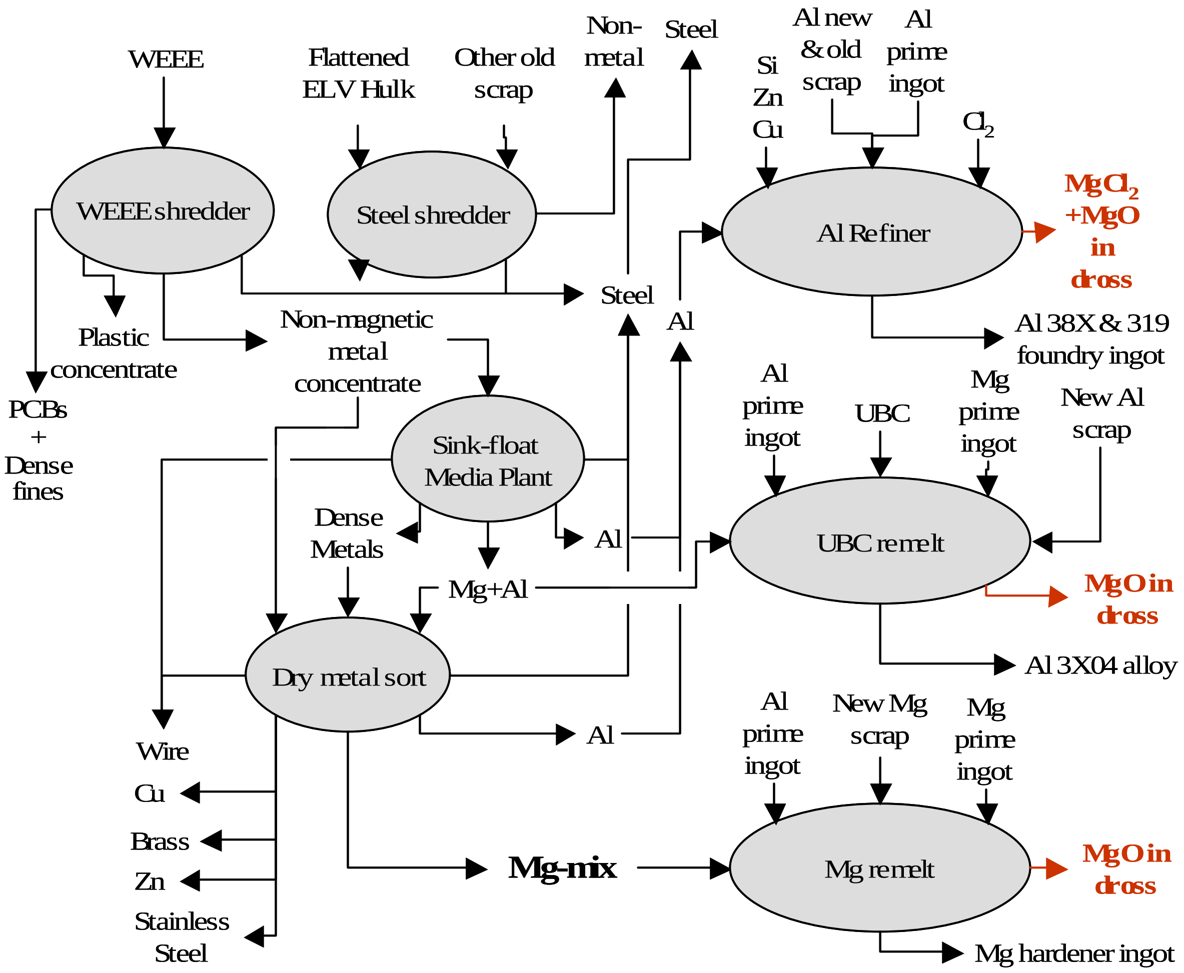

Mg diecasting alloys.

Mg alloy diecasting – Shipments in 2006 of Mg-AZ91 alloys for portable electronic and power tool housings and non-structural automotive components (e.g. instrument panel, interior brackets) were ~50,000 T in US, or ~200,000 T globally. With the price of prime Mg being at par with prime Al, and with rising oil prices making plastics more expensive, the growth of this market is limited only by the availability of competitively priced Mg.

Mg-AZ91 (Mg Al9% Zn1% Mn0.2%) has the three most common alloying elements in the generally used -AM and -AZ alloys that supply most of the diecasting alloy market. A melt of a mixture of the post-consumer diecasting scrap coming from automobiles and consumer durables is likely to end up requiring the addition of Al and Zn to satisfy the AZ91 composition requirement, while the Mn and Fe levels can be controlled by fractional precipitation of the FeMnAl intermetallics.

Auto components diecast out of old-scrap-sourced Mg AZ91-type alloys for property non-critical shapes (such as instrument panels, inner door components, sunroof and tailgate hardware) could contribute significantly to the use of Mg in automobiles. As we reach 2015, there will be about 100,000 T coming back in ELVs and another ~100,000 T from other sources of Mg diecastings. Even if the recycled metal is not used in automotive applications, each tonne of old Mg beneficially used frees up a tonne of prime Mg that could be directed to an automotive application.

Future Need for Additional Markets

Mg alloys with exotic alloying elements – Mg-AJ62 (Mg Al6% Sr2%) or Mg-AE41 (Mg Al4% RE1%), (RE = Ce, Nb, La) – have been developed for higher temperature structural applications requiring creep, fatigue and corrosion resistance. But these are composition incompatible with either Mg-AZ or -AM series of alloys. Mg-AJ62 is coming in at 20 kg/car in an R6 in-line 6-cylinder engine crankcase (300,000 units in 2006). BMW predicts that up to half of its fleet, or ~600,000 cars, could be equipped with these engines (6,7). That is 12,000 annual T that will be coming back in BMW ELVs in about 2025, a number that is likely to grow as other companies follow suit. It is likely, at least initially, that there will be a variety of mutually incompatible high-performance alloy compositions as various manufacturers battle for market share.

Where and How Old Mg Scrap Recycling is Actually Taking Place

Mg Diecastings from Automotive and Durables

End-of-life automobiles and major appliances are co-shredded with other heavy steel and mixed-metal scrap at the ~800 primary shredding plants around the world (Fig. 3). Steel is removed magnetically, nonmetals by screening, air elutriation and eddy current separation, and the Mg ends up in one of the non-ferrous shredder products. NMMC is sold to dense media sink-float plants; the Al shredder product is sold directly to Al secondary smelters. Mg alloys entering the Al secondary smelter end up in an Al foundry alloy melt, which has a low Mg alloying element specification limit. Mg is then refined out of the melt by chlorination, ending up as Mg chloride salt in the Al dross. Mg content is lost, so is some Al at the cost of productivity. There are also concerns with safety and handling of poisonous Cl_2 gas. It would be much better and cost effective to separate Mg from Al and recycle it into another product. This happens with the Al in the NMMC, and this is where sensor-based sorters could help at the secondary Al smelter.

Magnetite Slurry Float, Mg + Al Product

NMMC that reaches sink-float plants should contain up to 50,000-60,000 T of Mg alloy, ~90% of it is in the >10 mm size fraction that is floated in the magnetite slurry at a specific gravity of ~2.2 g/cm^3. Mg alloys at density of ~1.8 g/cm^3 float, but so do hollow aluminium shapes like cans, tubes and crumpled sheet. Mg recovery is highly efficient, but since it is only at ~2% of the Al in the plant feed, the product composition ends up to be a mix of ~75% Al cans and extrusions and 25% Mg diecastings. There should be ~45,000-50,000 T of Mg in this product. Its exports from NA and EU to Asia for handsorting is a loss of raw material to the EU and NA Mg remelters or granulating plants, but is not a loss globally. The Mg recovered by handsorting in Asia finds its way onto the old scrap market and is fully utilized. The most likely current uses for this material in China are granulates for steel desulphurisation and common Mg-AZxy diecasting alloys (8).

Figure 3. Light Metals in the Car Recycling System

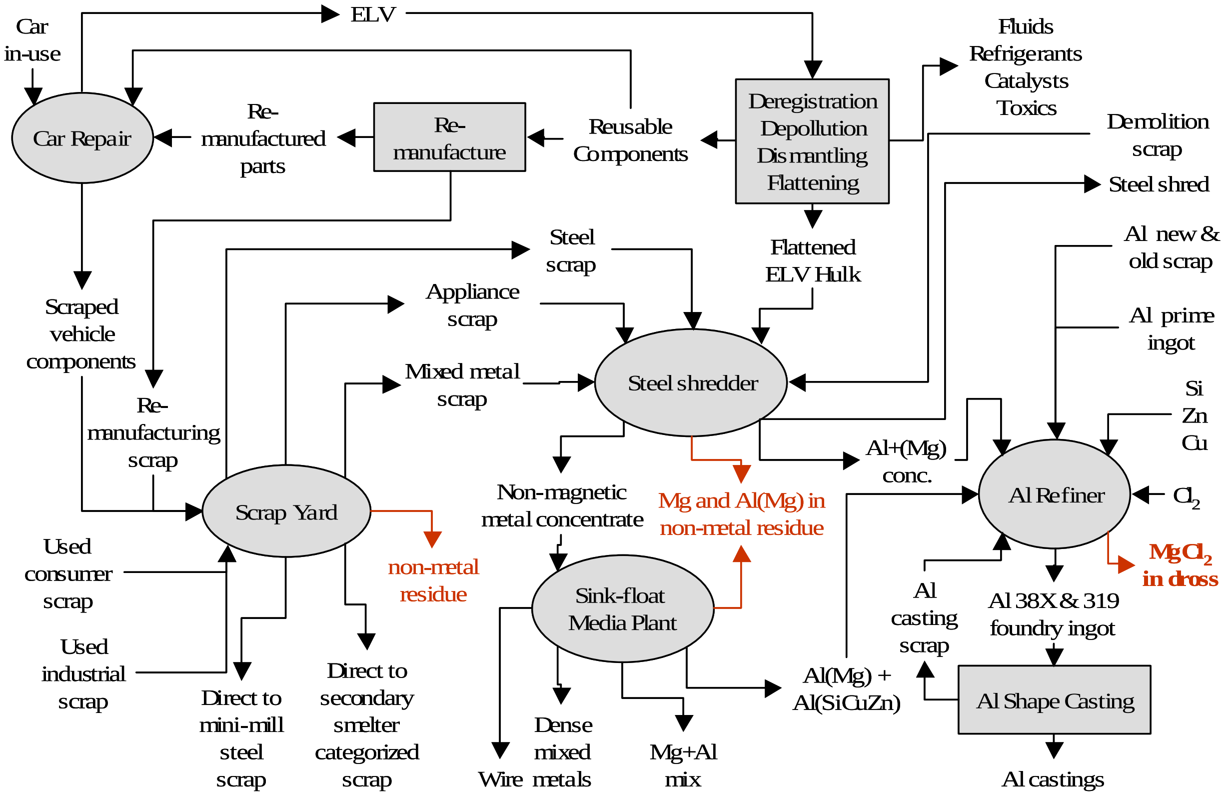

Consumer Electronics and Power Tools

End-of-life electronic and electrical products are either landfilled or are recycled through a separate WEEE system that has been set up to deal with many substances of environmental concern in these functional materials (Fig. 4). There is dismantling of batteries for material recycling and internal subassemblies for re-use, but Mg is mainly found in housings that are shredded for material liberation and segregation. In this case, the material needs to be shredded to a finer size (~1 cm) before adequate material liberation is achieved. The shredded scrap is treated in a similar sequence of bulk mechanical separations as the auto shred, albeit with equipment scaled down in proportion to the particle size. Mg is found with aluminium in the NMMC. The coarser portion of NMMC can be treated by sink-float and jig separation to produce Mg-alloy rich magnetite slurry float product.

Defence and Aerospace Scrap

Mg-alloy missile housings do not tend to survive to be recycled. However, aircraft, helicopter and vehicle and portable weapon components mostly do. These are most often specified with extremely high performance specifications with little regard to economic considerations. This spurred development of Mg alloys with exotic alloying elements, such as Ca, Sr, Li, Y, Zr, Ce, Nb and La. These alloys usually do not tolerate Zn in their make up, and common Mg-AZ alloy specifications treat these exotic elements as unwanted impurities. Hence we have an incompatibility in the Mg- alloy recycling system. As long as defence scrap is left on the battle field or is auctioned off in separate Army scrap auctions, it does not affect the bulk of the global Mg-alloy recycling system. However, the civilian transportation market is starting to adopt some of these alloys for demanding power-train applications. In time, these alloys will contaminate the main NMMC scrap stream and will open up opportunities for alloy sorting of the Mg alloys from this source.

Figure 4. Light Metals and Other Materials in WEEE Recycling

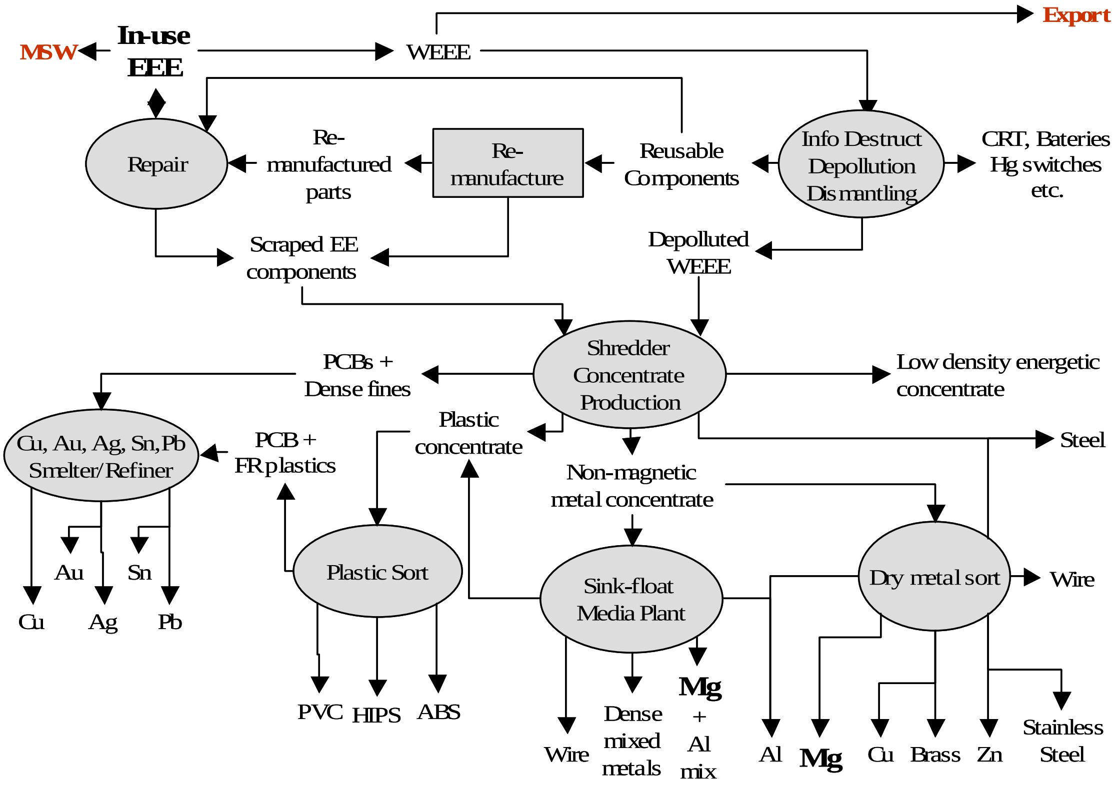

Mg Scrap Losses in the Recycling System

Shredder residue – Chunky pieces of shredded Mg diecastings are easily separated from nonmetallic residues. Hence, the Mg scrap losses in shredder plant residues are negligible.

Metal grain is 5-10 mm product of the sink-float plant and/or jig separation. Mg alloys end up in the light metal fraction currently at ~2% particle concentration. The grain output comprises ~5%-10% of the sink-float plant output, and will take with it similar proportion of Mg alloys (~5,000-6,000 T). The light metal grain is either sold to the Al secondary as Al product or exported to Asia for manual handsort clean up.

Mg in shredder Al product: Primary shredders process de-polluted, flattened ELVs, consumer durables, mixed metals from building demolition, and some even shred municipal solid waste to prepare residue derived fuel and recover the metal scrap. The ELVs at this point globally contribute ~5,000,000 T of Al and 100,000 T of Mg. Some of the light metal that is easily dismantled – Al wheels, for example – does not make it to the shredder but this deficit is more than made-up by the Al form the other scrap sources. Most of Mg scrap is from the ELVs. Some of the shredding plants installed a second splitter on the eddy current separator allowing the low density electrically conductive metals to be concentrated in a separate fraction. Without much more sophisticated procedure it is not possible to recover high proportion of the Al at the high metal grade that can be sold directly to the Secondary Al smelters, or exported to Asia. Typically less than 50% of the Al is recovered in the Al product with >95% metal content. This does not imply that half of the Al is diverted at the shredder from the nonmagnetic metal concentrate (NMMC) bound for the sink-float plants.

Not all the shredding plants are equipped with eddy current separator circuits, and fewer still have second splitters installed. Mg, having a lower density and similar electrical conductivity to Al, follows the Al and splits between the Al product and the NMMC. The Mg-alloy particles that end up in the Al product go to an Al secondary smelter. Currently there can be up to 2% Mg alloy particles in the Al shredder product, and that fraction is set to increase in parallel with the Mg-alloy content of the ELV. Unless there is an additional upgrading step at the Al smelter, Mg particles end up in the foundry alloy melt from which Mg is refined-out by chlorination to bring the Mg concentration in the Al foundry alloy down to 0.1%-0.3%. Unless some-thing is done, and as more shredders equip themselves with ECRs and second splitters, up to half of the Mg alloy particles from the >10 mm particle fraction could be lost in this way. We estimate that ~20,000 T of Mg alloy scrap were lost chlorinated out of the Al foundry alloys in 2006 (1).

The current situation of not recycling the old Mg-alloy scrap contained in Al concentrate purchased by the Al secondary smelters from the shredders is wasteful for both magnesium- and aluminium-alloy producers. This will also fuel arguments against magnesium substitution for aluminium in the automotive market. The solution is technically simple. Magnesium can be easily separated from other scrap, and the markets that could consume this separated Mg-alloy mix are already developed and operational.

Technologies Used for Separation of Old Mg from Other Scrap

Dismantling

Dismantling is justified partly by de-pollution regulations, and partly by the high value of sub-assemblies in the re-use re-manufacture market. Dalmijn and DeJong (11) quote a cost of $1,300 for each ELV that is dismantled according to Dutch requirements. Clearly this is not justified by the value of 800 kg of steel scrap (~$150), 150 kg of Al scrap (~$150) and 2 kg of Mg scrap (~$2) or the value of the prime metal replacement ($300+$450+$6=~$750). Even the Dutch are joining the rest of the world in embracing post-shred separation for material value recovery. The parallel WEEE management system in NA or EU also dismantles for de-pollution by removing CRTs, batteries and mercury or PCB-containing components, and sometimes recovers electronic chips and subassemblies for reuse. New WEEE material recovery and recycling plants are based on shredding and mechanized material separation paralleling the unit operations used for material recycling of the ELVs.

Bulk Liberation & Separation at the Shredding Plant

After de-pollution, bulky end-of-life products including ELVs are shredded followed by screening, elutriation, magnetic and eddy current rotor separation (12,13). In separate plants, de-polluted WEEE is shredded to a finer size, and is separated by smaller-scale machines in a similar sequence of unit operations. Mg alloys are recovered in the nonmagnetic metal products – Al and NMMC. The latter is further processed, usually by wet density separation.

Sensor-Based Sorting

Dry metal scrap sorting circuits are under development. They combine bulk material separation methods and sensor-based particle sorters to separate metal scrap from nonmetals, and then sort the metal scrap into parent metal categories. At this point these circuits do not include the provision for sorting or batching Mg alloys, but in theory the existing LIBS elemental analysis sensor could achieve this task.

Wet Density Sort

Wet density sort is the gold standard in the current material recycling system. It is used (separately) for both metal scrap and plastic scrap separation. For metal scrap, sink-float separation is done at three specific gravity levels: in water at ~1, in magnetite slurry at ~2+ and in ferrosilicon slurry at ~3.5. Magnesium sinks in water but floats in the magnetite slurry, but so do closed or boat shaped Al particles. This product ends up as a mixture of ~25% Mg alloy and 75% sheet and extrusion Al, adding up currently to ~5% of the total light-metal scrap output of the sink-float plant.

Handsort

China and India import large quantities of scrap for handsorting. Both the ferrosilicon sink dense metal mix and the magnetite float light-metal mix outputs of the sink-float plant are handsorted there. The light metal mix is a combination of Mg diecast particles and Al sheet and extruded shapes in 1:3 weight ratio. This is an ideal feed for visual identification by shape and hand separation. It is not practical to handsort small quantities of Mg cast shreds that are difficult to identify in a very large quantity of Al cast shreds in Al concentrate from shredding plants. Visual identification and handsorting of Mg scrap by alloy is not possible. Handsorting is a low productivity process economically enabled by a combination of geo-political and geo-economic factors. As the standard of living in Asia improves, the wage demands of the handsorters will drive the Asians to adopt the mechanized sorting methods they drove out of business in Europe and North America.

Need for Mechanized Sorting

Sink-float plants that automatically separate Mg-based alloys from the nonmagnetic shredded metal concentrate were industrially implemented in 1970s. Mg-based alloy particles report nearly exclusively to the magnetite slurry float product. This Al-Mg magnetite float product could be used in AA3X04 Al can sheet without further sorting.

In most cases, separation of metal scrap by parent metal categories is the minimum required for material recycling. Sensor-based particle sorting technology introduced in 1990s first allowed automated separation of pure Mg alloy from Mg/Al magnetite slurry float concentrate (10). Recent improvements in sensors and computing speed now allow dry separation of all common parent metals. Particle-sorting technology based on elemental chemical analysis allows for batching of specific secondary alloys from mixed-alloy post-consumer scrap.

Separation of Mg-alloy particles from shredded Al scrap products purchased directly from the shredder is an issue for the Al foundry alloy producers. Handsorting of this material is not economic by, especially in EU and NA. Colour and DE x-ray sensor-based sorters are well suited for this task. The alternative is to buy a premium (low free Mg) Al scrap product from the sink-float plants.

Currently the global market of ~75,000 T of Mg content of steel desulphurisation granulate could consume most of the post-consumer Mg scrap and Mg-containing byproducts and residues. At present, post-consumer scrap collection is not set up to be efficient, and the majority of the desulphurisation granulate is produced from prime Mg.

Other markets that could consume mixed-alloy Mg scrap include Mg-AZ diecasting alloys. The added value of the Mg-AZ91 or similar common diecasting alloy may justify batching of that alloy composition from post-consumer scrap. Initially, with post-consumer scrap dominated by Mg-AZ and -AM diecasting alloys, this should be possible by melting the Mg-alloy mix, adding Al and Zn, and refining the Mn and Fe to the required concentration levels.

As long as steel desulphurisation, aluminium alloying and common Mg diecasting markets still need input of prime Mg to satisfy the demand for Mg metal, there is no recycling system need to find other uses for the old Mg alloy scrap or to further upgrade it by sorting.

Sorting will be required when Mg alloys with exotic alloying elements become a significant fraction of post-consumer scrap. At that time, the XRF and LIBS sensor particle sorters will be able to both batch the targeted secondary diecasting alloy and group the residue by the exotic alloying element.

For the scrap streams that have a substantial content of Mg alloys with exotic alloying elements, sorting these out and then sorting among them will be justified by both incompatibility with the common AZ alloys or by the economics of recovery and recycling of the exotic alloying element content. These high-performance alloys are already beginning to penetrate auto powertrain applications. The 300,000 BMW R6 engines produced in 2006 alone will bring ~7,000 T of old Mg-AJ62 alloy scrap containing ~150 T of strontium. This strontium, diluted by 300,000 T old Mg scrap expected from ELVs in ~2020, gives ~0.05% average Sr content. This exceeds the 0.01% impurity limits for “other-each” element specification of AZ91D and AM60B alloys by a factor of 5. The situation will quickly get worse after that as other engine lines adopt high-performance Mg-alloy engine blocks. This means that the need for alloy sorting in the post-consumer scrap recycling system will become acute in about a decade.

Sorting of Mg alloys with exotic elements is not justified by the reduction of the demand for prime Mg, but rather by the recovery of the exotic elements. These are strategic since they are produced at few locations and are reasonably expensive, with prices in $10-100/kg range compared to $3-4/kg for Mg. The incentive to sort will be economic, rather than any impact on energy consumption or greenhouse gas emissions. One can expect a well-justified reluctance from engine manufacturers to include the old scrap containing exotic alloying elements in performance-critical engine applications. More likely this material will become a source for a new family of secondary alloys that will provide performance improvement over Mg-AZ91 in non-critical applications.

Recommendations for Actions to Promote and Improve Recycling of Post-Consumer Mg Scrap

The lifecycle and financial benefits of recovery of post-consumer Mg and its use in secondary Mg diecastings, or in controlled alloying of aluminium, or desulphurisation of steel need to be quantified.

The current status of post-consumer Mg-alloy recycling and the waste and negative environmental impact associated with the destruction of Mg content by chlorination should be publicized among magnesium- and aluminium-alloy producers and their suppliers (scrap shredders, sink-float plant operators and metal sorters).

The current free-Mg content of the Al concentrate product of the shredders needs to be quantified and tracked by the secondary aluminium smelters and compared to the low-Mg Al product of the sink-float plants. The price difference between these products must reflect the difference in chlorination needs, melter productivity and metal yield. This price difference economically justifies the separation of Mg from Al scrap and enables its beneficial recycling.

An optimum short-term tactic to promote and improve recycling of post-consumer Mg scrap could be to direct as much mixed-alloy Mg scrap as can be accommodated to a secondary Mg diecasting alloy without sorting and to granulate the rest for steel desulphurisation.

The Mg+Al mix and Mg-alloy mix products need to be cleaned and re-melted, refined and cast into recovered secondary ingots (RSI) to demonstrate the metal yield and its dependence on scrap cleanliness and the average composition of the product melts.

The use of these RSIs as a Mg alloying addition to Al can sheet needs to be demonstrated at aluminium can recycling remelt facilities and compared to the practice of adding Mg+Al mix shred to the UBC feed stream of the secondary can sheet remelt plant.

Granulation of post-consumer Mg and Mg+Al shredded scrap products, and use of these granulates as additives to various consumptive applications, needs to be demonstrated. These applications include steel desulphurisation, production of nodular iron, metallothermic thermite mixtures, flares and other pyrotechnics.

To improve on the current system, separation of Mg-alloy scrap from the Al concentrate shredder product by automated sensor-based particle sorting needs to be demonstrated on an industrial scale. Use of such sensor-based particle sorting should also be demonstrated for separation of Al from Mg in the magnetite slurry float fraction.

Use of post-consumer Mg and Mg+Al shredded scrap products in batching a widely used alloy with high content of common alloying elements needs to be demonstrated. The Mg AZxy alloy family used in common diecastings is a good choice for such a demonstration. The practical amount of control of the concentration for less-common alloying elements such as Ca, Sr, Li, Y, Zr, Nd and Ce needs to be determined.

The need for separation and batching of alloys with these less-common alloying elements needs to be demonstrated and quantified. This need will result from either performance degradation of the alloys that use the old mixed-alloy Mg scrap, or by the loss and non-recycling of the expensive uncommon metals.

Alloy sorting of the Mg-alloy mix designed to separate and batch Mg-RE alloy compositions needs to be demonstrated by either LIBS- or XRF- sensor-based particle sorters.

The applications that could tolerate significant post-consumer recycled content of alloy-sorted Mg-RE scrap will need to developed in the future, when the recycling of the RE alloying elements will become either required or profitable.

Conclusions

One needs to consider the World scrap market to find where the old Mg scrap is recycled. The Mg in the portion of the old scrap that is treated in the sink-float plants is recovered. At this time metal mix recovered as 2 g/cm^3 float fraction captures nearly all free Mg-alloy particles from the shredded metal concentrate treated at the sink-float plant. This float product is exclusively exported to Asia for separation by handsorting. It consists of ~75% Al cans and extrusions and ~25% Mg diecastings. The handsorted Mg is most likely granulated for use in the fast-growing Asian steel industry for desulphurisation.

The current major markets for prime Mg that can use post-consumer scrap include granulate for steel desulphurisation, Al can sheet, or a master alloy for Mg alloying element addition to other Al-based alloys and common Mg diecasting alloys. Use of the scrap containing old Mg alloys in these applications does free up a supply of prime Mg for production of new Mg alloys.

When the supply of post-consumer Mg-alloy scrap exceeds the demand for steel desulphurisation and of Al(Mg) alloys, there will be a system need to recycle Mg into Mg alloys. Following what is the case in the established Al recycling system, it is most likely that the majority of post-consumer Mg scrap will find a home in a small number of diecasting alloys. Mg-AZ91 is the most likely candidate. Chemical-analysis-based particle sorting will be useful at that time to maximize the recovery of the Mg scrap that can be batched into these target diecasting alloys.

From a global lifecycle point of view, recycling of scrap reduces the demand for the production of prime metal, which has a high cost of resources, energy and emissions. There is a large advantage to the separation of Mg-alloy particles from the Al scrap bound for refining into foundry alloys and directing this Mg scarp into steel desulphurisation, Al alloying and common diecasting applications. There is very little additional lifecycle advantage to further tightening the recycling loop and directing post-consumer Mg scrap back into production of other Mg alloys or sorting these alloys to close alloy or product loops.

The rate of penetration of Mg alloys into the transportation market is likely to be limited by the World capacity to produce prime Mg metal. Even though, as was pointed out above, there is no system need or lifecycle advantage to direct post-consumer Mg-alloy scrap to the production of Mg-alloy components for the transportation market, the importance of post-consumer scrap as a Mg metal source will be increasing with time. Also, the inclusion of old Mg scrap in batching alloys for the common Mg diecastings used in automobiles has the potential to significantly increase the rate of penetration of the Mg-alloy components into the vehicle market.

As there is a concurrent growth in the other Mg-scrap-consuming markets (steel production, and aluminium alloying), Mg scrap will continue for the foreseeable future to remain in short supply and will remain to be priced by reference to prime Mg metal replacement. Consequently, one should not expect material price reductions related to the inclusion of old scrap in the batching of Mg alloys.

Unless western Mg-alloy producers are willing to invest in automated scrap metal sorting plants, recycling of old Mg-alloy scrap will take place in China (8) and India, as they have the existing scrap handsorting plants and quickly growing steel production and Mg diecasting industries to provide ready markets for the handsorted products.

References:

1. A.J. Gesing, “Lifecycle scenarios for Mg automotive components,” report NRCan-07-03224, Nov. 2007.
2. USGS, mineral year book – Magnesium 2006, http:\\www.usgs.com\minerals\
3. International Magnesium Association, Mg production and use statistics, http://intmg.org/statistics
4. International Magnesium Association, “Magnesium Sets a New Protection Standard: Durability, Strength and Cutting-Edge Style,” Mg Showcase, Issue 3, Dec. 2007, http://intmg.org
5. Frank Czerwinski, “The 3C Market – An Opportunity for Magnesium Injection Molding,” Proceedings of 63rd World Magnesium Conference, 2006.
6. IMA, “Magnesium Fosters Rebirth of an Automotive Engine,” Mg Showcase 1, 2007, http://intmg.org
7. E. Baril, P.Labelle, A. Fischersworring-Bunk, “AJ (Mg-Al-Sr) Alloy System used for New Engine Block,” SAE 2004-01-0659, 2004.
8. HLCBeijing, “Analysis Report of the Market and Investment of Ma and Mg-Alloy in China,” HLCBeijing market report, 2007.
9. A.J. Gesing, “ELVs: How They Fit in the Global Material Recycling System and with Technologies Developed for Production or Recycling of Other Products and Materials,” IARC 2006, 15-17 March 2006, Amsterdam, The Netherlands.
10. Huron Valley Steel Corporation, Belleville, MI, USA
11. W.L. Dalmijn and T.P.R. De Jong, “The Development of Vehicle Recycling in Europe: Sorting, Shredding, and Separation,” JOM, Nov 2007, VOLUME 59, NO.11 p. 52.
12. W.L. Dalmijn and T.P.R. De Jong, “Sorting Systems for Recycling and Waste Treatment,” VUB 2004, Brussels, Belgium, 2004.
13. A.J. Gesing, “Shredder Practice for Preparation of Nonmetallic Concentrates and Potential for Particle Sorting of these Concentrates,” Sensor-Based Sorting 2006, 28-30 March, Aachen, Germany.
14. A.J. Gesing, H. Harbeck, “Need and Potential for Application of Sensor-Based Sorters to Recy-

cling of Mg-Alloy Scrap”, Sensor-Based Sorting 2008, 4-6 March, Aachen, Germany.

15. A.J. Gesing, P. Torek, R. Dalton, R. Wolanski, “Assuring Continued Recyclability of Automotive Aluminium Alloys: Chemical-Composition-Based Sorting of Magnesium Shredded Scrap,” TMS 2003 Annual Meeting: Automotive Alloys 2003, 15-24.

Page 5: [1] Deleted **Renka** **2/28/2008 6:58:00 PM**

Mg Scrap Losses in the Recycling System

Shredder residue fines consist mainly of sand, glass, crushed rock and cement, dirt and rust with some organic fibres paper and textile. These fines account for 5% of the shredder plant output and contain ~2-3% NF metal, with Mg comprising only ~1% of that fraction. Shredder light and dense nonmetallic residues consist of larger particles: plastics, rubbers, foams, textiles, paper and wood. The metal contamination of these residues consists of insulated Cu wire, Al capacitor foil and light gauge stainless steel. The chunky pieces of shredded Mg diecastings are easily separated from these residues. Mg scrap losses in shredder plant residues are thus negligible.

Metal grain is the 5-10 mm product of the sink-float plant and/or jig separation. Mg alloys end up in the light-metal fraction currently at ~1-2% particle concentration. The grain output comprises ~5-10% of the sink-float plant output and will take with it a similar proportion of Mg alloys (5,000~10,000 T in 2006). The light metal grain is either sold to the Al secondary as Al product or exported to Asia for manual handsort clean up. Since it is impractical to handsort Mg out of this product, it ends up melted with Al for foundry alloy applications (see below).

Mg in shredder Al product: Primary shredders process de-polluted, flattened ELVs, consumer durables, mixed metals from building demolition, and some even shred municipal solid waste to prepare residue-derived fuel and recover the metal scrap. ELVs globally contribute ~5,000,000 T of Al and 100,000 T of Mg. Some of the light metal that is easily dismantled (Al wheels, for example) does not make it to the shredder, but this deficit is more than made up by Al from other scrap sources. Most Mg scrap is from the ELVs. Some shredding plants have installed a second splitter on their eddy current separator allowing the low-density electrically conductive metals to be concentrated in a separate fraction. Without a much more sophisticated procedure, it is not possible to recover a high proportion of the Al at a high metal grade that can be sold directly to secondary Al smelters or exported to Asia. Typically less than 50% of the Al is recovered in Al product with >95% metal content. This does not imply that half of the Al is diverted at the shredder from the NMMC bound for sink-float plants. Not all shredding plants are equipped with eddy current separator circuits, and fewer still have second splitters installed. Mg, being lower density and similar electrical conductivity to Al, follows the Al and splits between the Al product and the NMMC. The Mg- alloy particles that end up in the Al product go to an Al secondary smelter. Currently, one could expect up to 2% Mg-alloy particles in the Al shredder product, and that fraction is set to increase in parallel with the Mg-alloy content of the ELV. Without an additional upgrading step at the Al smelter, Mg particles end up in the foundry alloy melt from which Mg is refined out by chlorination to bring the Mg concentration in the Al foundry alloy down to 0.1%-0.3%. Unless something is done, and as more shredders equip themselves with ECRs and second splitters, up to half of the Mg alloy particles from the >10 mm particle fraction could be lost in this way. We estimate that in 2006 ~20,000 T of Mg alloy scrap were lost through chlorination out of the Al foundry alloys.

Heat Treatment of Magnesium Alloys – Opportunities and Limitations

Frank Czerwinski
Husky Injection Molding Systems Ltd., Bolton, Ontario, L7E 5S5 Canada

ABSTRACT

Fundamental aspects of heat treatment of cast and wrought magnesium alloys are presented along with the role of chemical composition and specific elements. The strengthening mechanisms and key precipitates are described, explaining crystallographic limitations of their role within the hcp magnesium matrix. Examples of properties change are given for conventional alloys with trends in alloy design to magnify this effect. A particular emphasis is paid to magnesium structures produced by semisolid processing routes where a new approach to heat treatment is required. In addition, some elements of the heat treatment technology are included with the hardware and protective atmospheres against surface oxidation and ignition

INTRODUCTION

For numerous engineering alloys, heat treatment represents the effective way of further enhancement of product properties. When for ferrous and many non-ferrous alloys this step is extensively used, for magnesium alloys it is so far not fully explored. The limited strengthening response linked to the crystallographic structure of magnesium (Fig. 1) together with the low integrity of castings are seen as the major detrimental factors affecting the application scale.

Magnesium alloy components can be manufactured by all the conventional methods including casting, forging, extrusion and rolling. While solid state forming leads to generally higher properties the number of manufacturing steps and their complexity contribute to a significantly higher cost of the final product. As a result the majority of net shape products from magnesium alloys are produced at present using casting. Although there is a continuous improvement in conventional casting techniques the inherent feature of products is still not satisfactory internal integrity of cast structures. Since the alloy's porosity leads to blisters at high temperatures, such products have limited capability to be heat treatable.

A development of novel net shape manufacturing techniques which result in components having high structural integrity, e.g. semisolid processing, creates renewed interest in heat treatment [1]. The fundamental aspects of heat treatment of magnesium alloys after both the conventional and novel processing techniques are described in this report.

PROCESSES, ALLOYS, HARDWARE

There are four essential procedures of heat treatment, applicable to magnesium alloys:

(i) stress relieving;
(ii) annealing;
(iii) solution treatment;
(iv) aging.

The purpose of stress relieving is to reduce residual stress introduced at the stage of component manufacturing. It is conducted at temperatures exceeding 120 ^{o}C. The residual stress leads to dimensional distortion, stress corrosion and cracking. For wrought alloys it is required after various methods of forming, rolling, extrusion or after straightening. For castings the stress is introduced due to an interaction with the mold during solidification, frequently magnified by non-uniformity of cooling. A unique requirement of stress relieving exists for welds in cast and wrought alloys.

Annealing induces recrystallization within the material volume thus increasing substantially ductility at a cost of strength. It is typically conducted at temperatures close to 300 ^{o}C and the main objective is to facilitate certain stages of manufacturing.

The processes which benefit from internal precipitates include the solution annealing and aging. The purpose of solution annealing (T4) is to dissolve phases present in an alloy after casting or forming and create a supersaturated solid solution. It is executed by heating the alloy well above the solvus line to temperatures 380-530 ^{o}C for time periods from 4 to 24 h. The purpose of direct artificial aging (T5) is to generate precipitates from elements already present in the solid solution after casting or forming. It involves typically heating at temperatures of 130 to 230 ^{o}C for time periods from 5 to 50 h. The artificial aging frequently follows the solution annealing. In fact, a combination of solution annealing and subsequent aging, called as T6 temper, is the key

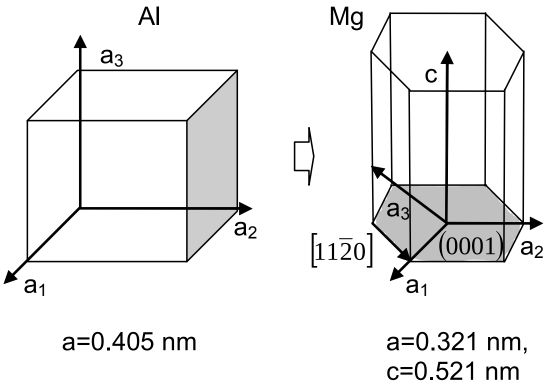

Fig. 1. The difference in crystallographic structures between aluminum and magnesium

thermal method aimed at improving mechanical properties of magnesium alloys. The practices for heat treatment of magnesium alloys are specified in ASTM B661-06 Standard. It intends to help in establishing a suitable procedure to achieve required physical and mechanical properties.

Applicable alloys

The properties of both groups of alloys, cast and wrought, may be improved by heat treatment. The cast classes include Mg-Mn-Al, Mg-Mn-Al-Zn, Mg-Mn-Zn-Cu, Mg-Zn-Zr or Mg-Zn-Zr-RE. The wrought classes include Mg-Mn-Zn, Mg-Mn-Zn-Cu, Mg-Mn-Al-Cu, Mg-Zn-Zr or Mg-Y-RE. In order to achieve useful effect during aging, certain minimum concentrations of elements forming precipitates are required. E.g. for Mg-Mn-Al system, alloys containing at least 6% of Al are considered heat treatable.

Technology and hardware

Furnaces for heat treatment are either electrically or gas heated. The furnace chamber should be tight to allow introduction and circulation of a protective gas. A high accuracy of temperature control is essential to prevent overheating and potential fire.

Quenching media. The heat treated components are typically quenched in air either still or with forced circulation. The latter is potentially applicable for treating thick wall components. There are some exceptions which require water quenching, e.g. alloy QE22 [2].

Protective atmospheres. During heat treatment, alloys are exposed to high temperatures often exceeding 400 ^{o}C for time periods longer than 20 h. The probability of ignition is increased by machining fines, casting flash or other mechanical damage. Moreover the ignition may occur when furnace exceeds the set-up temperature due to control failure. The purpose of surface protection is not only to prevent ignition and fire but also to avoid surface oxidation affecting product quality and its properties. The typical heat treatment atmospheres may include sulfur dioxide, carbon dioxide, sulfur hexafluoride or inert gases. Recently, the protective atmosphere of nitrogen gas, containing less than 2% of oxygen, was found useful for the heat treatment purpose [3].

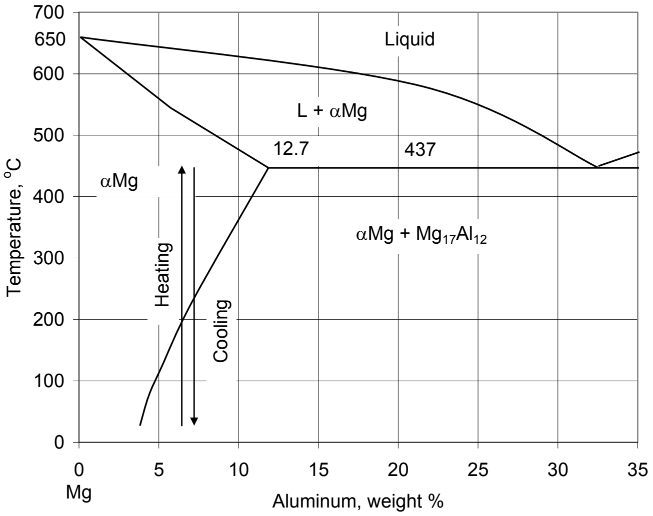

Fig. 2. The magnesium rich corner of the Mg-Al equilibrium phase diagram, emphasizing the concept of solution annealing and aging

TRANSFORMATIONS DURING AGING

The essence of precipitation hardening are certain elements that decrease their solubility with decreasing temperature, being added in amounts exceeding the equilibrium solubility at room temperatures. During aging of Mg-Al alloys, two types of precipitation take place. The discontinuous precipitation represents the cellular growth at high angle grain boundaries where $Mg_{17}Al_{12}$ phase has a form of nodules. As opposed to this, the continuous precipitation occurs within the parent grains

Role of alloying elements

Under equilibrium conditions the maximum solid solubility of *Aluminum* in Mg is rather high at 12.7 wt% (11.5 at%) at 437 ^{o}C and reduces to about 3 wt% at 90 ^{o}C (Fig. 2). In as-cast structures, however, the solid solution is enriched below 437 ^{o}C to only 3-4 at%. The precipitates present in major groups of magnesium alloys are listed in Table 1.

The additions of *Zinc* to Mg-Al alloys are expressed by reduced solid solubility of Al in Mg which increases the volume fraction of the precipitated phases, thus increasing the material's strength. The intermetallic compound $Mg_{17}Al_{12}$ transforms to $Mg_{17}(Al,Zn)_{12}$, frequently quoted as $Mg_{17}Al_{11.5}Zn_{0.5}$. According to [4], small additions of Zn to Mg-Ca alloys enhance age hardening. If the amount of Zn is excessive, the effect is detrimental since it leads to formation of $MgZn_2$ phase, known to be less effective in age hardening. A unique role of Zn is achieved when combined with rare-earth elements. A modification of Mg-2.1Gd-0.6Y-0.2Zr leads to improvement of mechanical properties with good combination of strength and elongation, e.g. 430 MPa and 12%, respectively [5].

Calcium improves oxidation resistance, hardness and creep resistance. Moreover, small amounts of Ca are effective in improving strength due to precipitation of Mg_2Ca phase. Additions of Ca to Mg-Zn system enhance age hardening response by refining the precipitates.

Rare-Earth Elements (RE) improve creep resistance of magnesium alloys. At the same time the presence of RE elements leads to substantial precipitation hardening during aging since their solubility in Mg decreases with lowering temperature. *Neodymium* leads to increasing strength especially when combined with other elements. Its content is limited by relatively low solubility limit of approximately 3.6% at 550 °C. Another element, frequently used with Neodymium is *Gadolinium*. Its solubility limit of 4% at 200 °C makes it economically not attractive since large quantities would be required of the order of 5-10% to generate a substantial effect.

Table 1. The precipitates present in major groups of magnesium alloys

System	Alloy	Precipitate	Remarks
Mg-Al Mg-Al-Zn	AM60, AZ91	$Mg_{17}Al_{12}$ $Mg_{17}(Al,Zn)_{12}$	Cubic 1.056 nm
Mg-Ca-Zn	Mg-0.3Ca-0.3Zn, Mg-0.3Ca-1.8Zn	Mg_2Ca, $Mg_2Ca(Zn)$	
Mg-Al-Si	AS21	Mg_2Si	Laves
Mg-Al-Sr	AJ52, AJ62	$Mg_{17}Sr_2$ Al_4Sr	tetragonal
Mg-Al-RE	AE42	Al_2RE	

Role of casting conditions in heat treatment

The influence of wall thickness on properties of castings is well documented. For example the yield stress increases for thinner walls. It was further suspected that casting conditions would exert an influence on properties after subsequent heat treatment. According to [6] the tensile ductility after solution treatment (T4) does not depend on the solidification rate expressed by the secondary dendrite arm spacing. However after a combination of solution annealing and aging (T6), there is a slight reduction in tensile ductility for coarser solidification structures.

EFFECT ON ALLOY PROPERTIES

Tensile data

An improvement of mechanical properties is the key objective of heat treatment. The particular effect depends on the alloy's chemistry, however, the general directions of changes are very similar for all alloys. Thus the solution treatment maximizes toughness at the cost of strength. A combination of solution treatment and aging causes maximum hardness and yield stress at the expense of ductility and toughness (Fig. 3). According to [6] the fracture mode of AZ91 alloy transfers from predominantly transgranular after T4 to predominantly intergranular after T6 treatment. As a result of T6 treatment, the crack propagates through the discontinuous precipitation regions at the grain boundaries.

Table 2. The influence of T4 and T6 heat treatments on change of selected properties of aluminum and magnesium alloys. Based on data selected from [2,7]

	UTS	YS	Elonga-tion	Hard-ness
Al 6061				
Initial O	125 MPa	55 MPa	25%	30 HV
T4/O	1.92	2.63	0.88	2.17
T6/O	2.48	5.00	0.48	3.17
AZ91 (casting)				
Initial F	160 MPa	110 MPa	2%	70HV
T4/F	1.50	1.09	3.00	1.00
T6/F	1.50	1.36	1.00	1.28
ZC71 (extrusion)				
Initial F	280 MPa	180 MPa	10%	
T4/F	1.09	1.33	0.60	
T6/F	1.29	1.89	0.40	

As mentioned earlier, the age-hardening response of magnesium alloys is lower than of heat-treatable aluminum alloys and the difference in crystallographic structure is listed as the major cause. Examples of change in properties of aluminum alloy 6061 along with

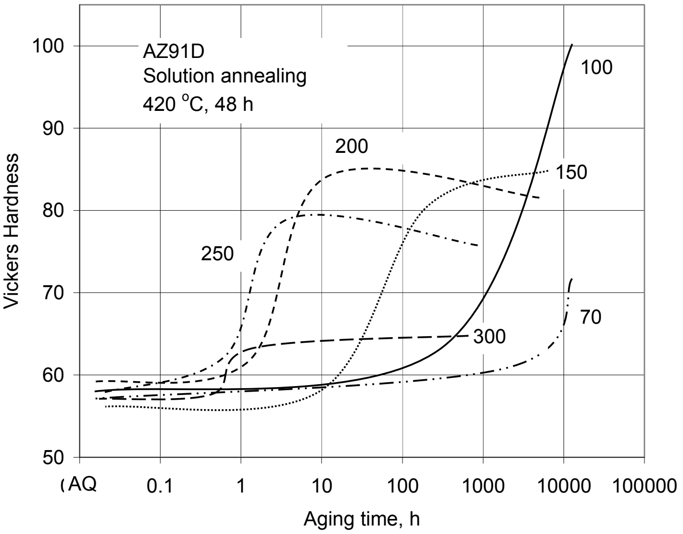

Fig. 3. The aging curves for AZ91D alloy at temperatures from 70 to 300 °C. AQ – as quenched state after solution annealing at 420 °C for 48 h [8]

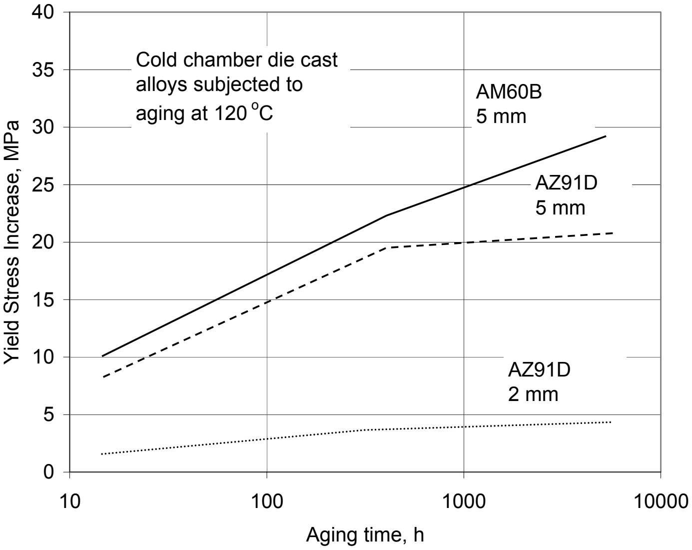

Fig. 4. The increase in yield stress of die cast AZ91D and AM60B alloys after direct aging at temperature of 120 °C [14]

cast AZ91 and wrought ZC71 alloys are listed in Table 2. The limited improvement is caused by the orientation and large size of the continuous precipitates which act as inefficient obstacles to the movement of dislocations. In the hexagonal close packed structure of magnesium, slip takes place predominantly on the close packed (0001) basal planes. The continuous precipitates with plate-like morphology, located parallel on basal planes, can easily be bypassed by dislocations which glide between them. On contrary, the high effectiveness of precipitates in Al alloys is caused in part by their location at an angle to the (111) slip planes. As a result they form more effective obstacles to the dislocation's motion.

Superplasticity

The limitations of low ductility and workability of magnesium alloys may be overcome by finding conditions for their superplastic behavior. The thermo-mechanical treatment is the attractive way to prepare superplastic alloys. It was revealed that the plasticity of the microcrystalline magnesium alloys tested at room temperature increases after heat treatment. For alloys AZ91, AE42, QE22 and ZRE1, the hot pressing following overaging at temperatures between 300 and 350 °C led to grain size between 0.7 and 6.4 µm [9]. At temperature of 420 °C and strain rate of $3x10^{-4}$ s^{-1} superplastic state was achieved with elongation of 750% for QE22 and around 260% for AZ91 and AE42.

Damping behavior

The damping capacity of magnesium alloys depends on heat treatment [10]. The solution treatment by decreasing the amount of second-phase particles distributed inside grains, weakens the strong pinning on dislocations and increases the internal friction of AZ91D. On the other hand, aging reduces the damping value due to precipitation of second-phase particles. The influence of solution treatment and aging on damping capacity of AZ91D at room temperature is the same as at 100 °C. However, the damping at 100 °C is greater than that at room temperature because of thermal activation. For commercial AZ91D the damping capacity increased with the maximum strain amplitude for all states of heat treatment.

For AZ61 alloy the strain-independent logarithmic decrement used to determine the damping capacity and being mainly composed of thermoelastic damping and dislocation damping, depends on alloy microstructure [11]. Although with increasing the annealing temperature the logarithmic increment increases the values are lower than for as cast state.

Corrosion resistance

The general factors affecting corrosion resistance of magnesium are practically the same as that important for other engineering alloys. The corrosion behavior of Mg-Al alloys is controlled by micro-galvanic cells, formed between cathodic $Mg_{17}Al_{12}$ phase and anodic αMg matrix, thus volume fraction of $Mg_{17}Al_{12}$ phase is of importance. Therefore, for AZ91D alloy the T4 heat treatment leads to improvement in corrosion resistance as compared to T6 temper [12]. The heat treatment also affects the electrochemical properties of anodic films formed on magnesium alloys. In study [13], the AZ91D alloy was solution treated at 440 °C for 20 h in N_2 atmosphere with different cooling techniques. The single-phase microstructure after air cooling formed an anodic film composed of Al_2O_3 with the highest polarization and the best protective properties.

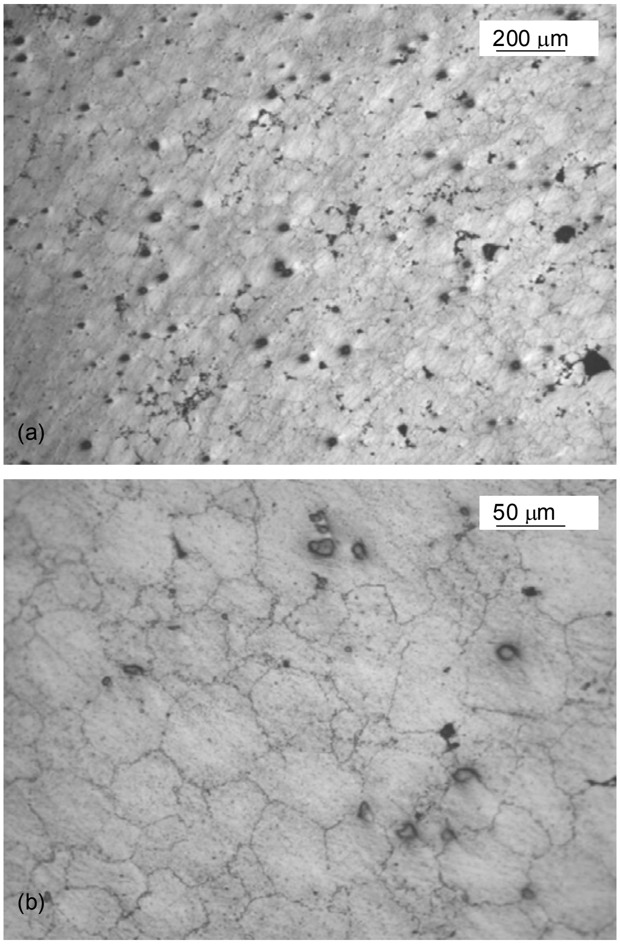

Fig. 4. The microstructure of injection molded AZ91D alloy after heating at 410 °C for 1 h

STRUCTURAL CHANGES DURING HIGH TEMPERATURE SERVICE

The unique form of heat treatment is experienced by alloys during their service at elevated temperatures. The common conditions of high temperature exposure take place for automobile engine components where temperature exceeds 100 °C and in some cases even 200 °C. The long service time, reaching hundreds of thousands of hours, is another characteristic feature of this process.

Effect of low temperature aging on die cast Mg-Al and Mg-Al-Zn alloys

An increase in yield stress and reduction in ductility of Mg-Al alloys are reported after exposure at temperatures close to 100 °C for 1,000 h. According to recent findings the moderate temperature exposure of AZ91 and AM60 alloys initially increased yield stress but for longer times of over 1,500 h reduced it by up to 40 MPa [14]. The effect depends on the casting wall thickness. For AZ91D and AM60 alloys exposures at 120 °C for time intervals up to 5,000 h resulted in substantial changes of properties. As shown in Fig. 4, for 5 mm thick castings an initial increase in strength after 300 h was the same for AZ91D and AM60. After 5,000 h the AM60 alloy experienced higher strengthening. The thin wall castings with a thickness of 2 mm had initially higher strength and although some increase was observed, the strength was generally lower than in the case of thick wall. The time interval of 5,000 h was enough to exceed the pick changes in AZ91D but for AM60 an increase in strength still continued.

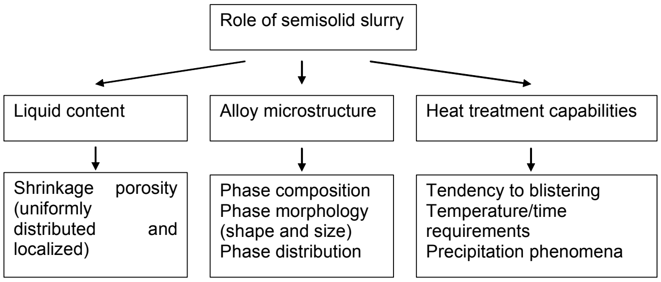

Fig. 5. The schematics explaining factors affecting heat treatment of alloys processed by semisolid methods

HEAT TREATMENT AFTER SEMISOLID PROCESSING

For semisolid processing there is insufficient distinction between the role of the microstructure and the component's integrity factors in improving properties of semisolid structures. The key feature of semisolid processing is the reduced temperature when compared to the casting of superheated melts. The commonly accepted advantages of machinery performance and energy economy, achieved due to reduced operating temperatures, are positive for all alloys and include lower energy consumption, no handling of liquid metal, longer die life, better yield from the raw material due to lower oxidation, evaporation and fewer other losses related to melt overheating. At the same time, however, the reduced processing temperature, first, replaces a molten alloy with semisolid slurry. After further reduction in temperature below the liquidus, changes the solid/liquid ratio and slurry properties which affect the final product, not only in terms of its internal integrity, but also its microstructure.

As opposed to the hardware performance and energy economy, the influence of the semisolid slurry on the component's properties is complex. First, the slurry affects product integrity throughout the reduction of porosity. The turbulent flow of a liquid alloy into a mold can result in the entrapment of air and mold gases into the melt which in turn may translate to micro and macro porosity. Smooth flow of the semisolid slurry allows for

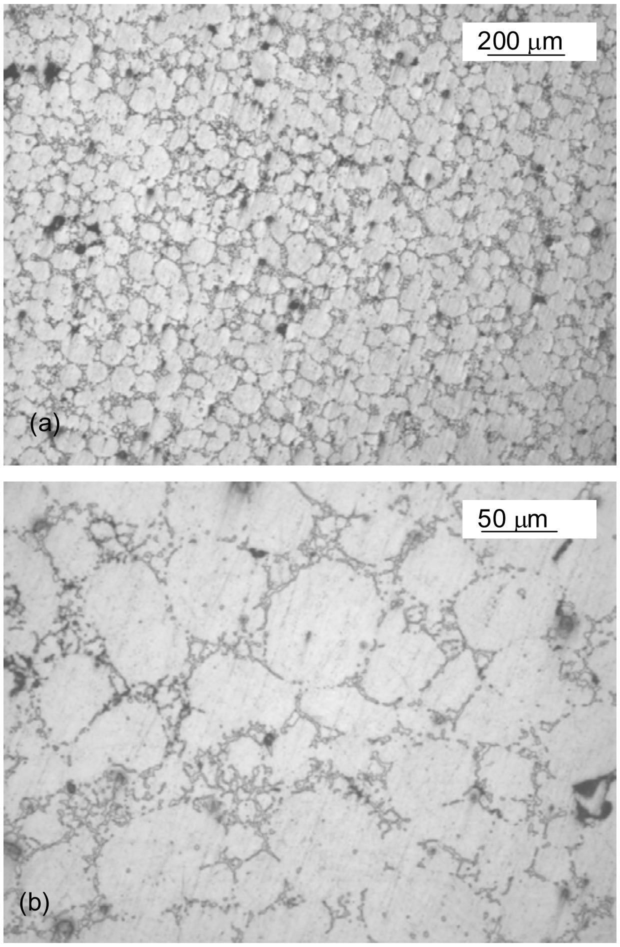

Fig. 6. The microstructure of injection molded AZ91D alloy after heating at 275 °C for 5h

minimizing these defects. Moreover, a reduced liquid content within the semisolid slurry reduces shrinkage porosity, which not only improves the material properties, but also allows achieving near-net shape capabilities. As a result of the high internal integrity a component is heat-treatable. As was the case for the general benefits specified above, the enhanced component's integrity has a universally positive effect for all alloys.

Conventional heat treatment of semisolid structures

Since the component's integrity allows conducting heat treatment by preventing blistering and other detrimental effects the semisolid structure remains as the major factor which should be considered during selecting heat treatment parameters. Exposures at temperatures higher than approximately 300 °C lead to disappearance of semisolid features. As shown in Fig. 4, heat treatment at 410 °C for 1 h transformed the microstructure to equiaxed grains. The bright contrast in Fig. 4a indicates locations of the former primary solid grains and is created by differences in chemical composition, still not homogenized by insufficient diffusion.

The conventional T4 and T6 treatments, applied to injection molded AZ91D alloy, allowed for wide modification of mechanical properties. For example, an initial strength-elongation of 275 MPa-7.5% was changed to 271MPa-11% after T4 treatment and further to 285 MPa- 5% after T6 temper [15]. It is interesting that the properties depend on an initial structure defined by the solid content which translates to the processing temperature.

Novel heat treatment of semisolid structures

It is anticipated that the heat treatment designed specifically for alloys generated by semisolid processing should take advantage of the unique thixotropic microstructure. As a result the steps which lead to formation of the homogeneous equiaxed grain structure, such as solution annealing, should be avoided. The major factors which affect the heat treatment of alloys after semisolid processing are listed in Fig. 5.

According to [16] the heat treatment of semisolid structures has following objectives: (i) it should break up the network of $Mg_{17}Al_{12}$ phase to raise ductility; (ii) temperature should be high enough to allow for phase transformations but slow down the grain growth; (iii) it should avoid precipitation of fresh $Mg_{17}Al_{12}$ phase to not reduce ductility and (iv) cost should be reduced.

An example of the microstructure of injection molded AZ91D alloy with initially ultra-high solid content, subjected to heat treatment at temperature of 275 °C, is shown in Fig. 6. This thermal exposure leads to transformation of regions with high Al content, corresponding mainly to the liquid fraction during semisolid processing. The majority of the primary solid phase is not transformed and experiences, most likely, recrystallization.

The new heat treatment, proposed by [16] for rheo-diecast structures, represents a single step process, conducted at temperatures around solvus line for shorter periods of time as compared to the conventional process Microscopically it causes a partial dissolution of non-equilibrium $Mg_{17}Al_{12}$ phase, breaking the network it forms around the primary solid phase. The treatment offers an improved combination of strength and ductility. As compared to T4 treatment it generates much higher strength with slightly reduced elongation.

CONCLUDING REMARKS

Heat treatment represents the effective way of improving properties of magnesium alloys. The internal integrity of castings along with limited strengthening, associated with the crystallographic nature of magnesium, are seen as major factors affecting the present application scale.

The new opportunities for heat treatment are created by semisolid processing through an increase in the component's integrity and its unique non-dendritic microstructure. This type of microstructure and the chemistry of phases present require novel processes of heat treatments. There is a need for new magnesium alloys which would take an advantage of semisolid processing and at the same time allow benefiting from the heat treatment which follows component forming.

REFERENCES

1. F. Czerwinski, Magnesium Injection Molding, Springer, New York, 2008.
2. Magnesium and Magnesium Alloys, edited by M. Baker and A. Avedesian, ASM International, Material Park, Ohio, 1999.
3. P.F. Stratton and E.K.Chang, Protective atmospheres for the heat treatment of magnesium alloys, in Magnesium Technology 2000 edited by H.I. Kaplan and J.N. Hryn, TMS, 2000, pp. 71-75.
4. J.C. Oh, T. Ohkubo, T. Mukai and K. Hono, TEM and 3DAP characterization of an age-hardened Mg-Ca-Zn alloy, Scripta Materialia, 53, 2005, 675-679.
5. T. Honma, T. Ohkubo, S. Kamado and K. Hono, Effect of Zn additions on the age-hardening of Mg-2.0Gd- 0.2Y-0.2Zr alloys, Acta Materialia, 55, 2007, 4137-4150
6. C.H. Caceres, C.J. Davidson, J.R. Griffiths and C.L. Newton, Effect of solidification rate and aging on the microstructure and mechanical properties of AZ91 alloy, Materials Science and Engineering, A325, 2002, 344-355.
7. Metals Handbook, vol. 2, ASM International, Materials Park, Ohio, 1990.
8. S. Celotto, TEM study of continuous precipitation in Mg-9wt%Al-1wt%Zn alloy, Acta Materialia, 48, 2000, 1775-1787.
9. F. Vesling and T. Ryspaev, Effect of heat treatment on the superplasticity of magnesium alloys, Russian Journal of Non-Ferrous Metals, 48, 1, 2007, 57-62.
10. Z. Zhang, X. Zeng and W. Ding, The influence of heat treatment on damping response of AZ91 magnesium alloys, Materials Science and Engineering, A392, 1-2, 2005, 150-155.
11. L. C. Ming, L.Z. Juan, H.B. Wen, Influence of isochronal treatment on damping behavior of AZ61 alloy, Journal of Central South University of Technology, 14, 3, 2007, 315-318.
12. N.N. Aung and W. Zhou, Effect of heat treatment on corrosion and electrochemical behavior of AZ91D magnesium alloy, Journal of Applied Electrochemistry, 32, 12, 2002, 1397-1401.
13. H.Y. Hsiao and W.T. Tsai, Effect of heat treatment on anodization and electrochemical behavior of AZ91D magnesium alloy, Journal of Materials Research, 20, 10, 2005, 2763-2771.
14. A. L. Bowles et al, The effect of low-temperature aging on the tensile properties of high-pressure die cast Mg-Al alloys, Magnesium Technology 2000, edited by H.I. Kaplan and J. Hryn, TMS, Warrendale, 2000, 295-300.
15. G. Ghosh, K. Kang, C. Bach, J.G. Roemer and C. VanSchilt, Properties and Microstructure of thixomolded and heat- treated AZ91D magnesium alloy, Proc. of The International Symposium on Recent Metallurgical Advances in Light Metals Industries, Vancouver, BC, 1995, pp. 481-492.
16. Y. Wang, G. Liu and Z. Fan, A new heat treatment procedure for rheo-diecast AZ91D magnesium alloy, Scripta Materialia, 54, 5, 2006, 903-908.